

INFORMATION TO USERS

This manuscript has been reproduced from the microfilm master. UMI films the text directly from the original or copy submitted. Thus, some thesis and dissertation copies are in typewriter face, while others may be from any type of computer printer.

The quality of this reproduction is dependent upon the quality of the copy submitted. Broken or indistinct print, colored or poor quality illustrations and photographs, print bleedthrough, substandard margins, and improper alignment can adversely affect reproduction.

In the unlikely event that the author did not send UMI a complete manuscript and there are missing pages, these will be noted. Also, if unauthorized copyright material had to be removed, a note will indicate the deletion.

Oversize materials (e.g., maps, drawings, charts) are reproduced by sectioning the original, beginning at the upper left-hand corner and continuing from left to right in equal sections with small overlaps. Each original is also photographed in one exposure and is included in reduced form at the back of the book.

Photographs included in the original manuscript have been reproduced xerographically in this copy. Higher quality 6" x 9" black and white photographic prints are available for any photographs or illustrations appearing in this copy for an additional charge. Contact UMI directly to order.

UMI

A Bell & Howell Information Company
300 North Zeeb Road, Ann Arbor MI 48106-1346 USA
313/761-4700 800/521-0600

**THE FLORIDA STATE UNIVERSITY
COLLEGE OF ARTS AND SCIENCES**

**FINITE ELEMENT APPLICATIONS AND ANALYSIS FOR
SINGULARLY PERTURBED PROBLEMS AND SHALLOW-WATER
EQUATIONS**

By

JICHUN LI

**A Dissertation submitted to the
Department of Mathematics
in partial fulfillment of the
requirements for the degree of
Doctor of Philosophy**

**Degree Awarded:
Summer Semester, 1998**

**Copyright © 1998
Jichun Li
All Rights Reserved**

UMI Number: 9903599

UMI Microform 9903599
Copyright 1998, by UMI Company. All rights reserved.

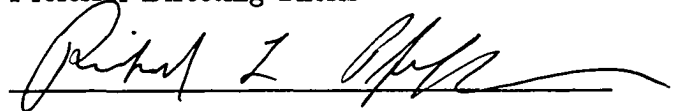
**This microform edition is protected against unauthorized
copying under Title 17, United States Code.**

UMI
300 North Zeeb Road
Ann Arbor, MI 48103

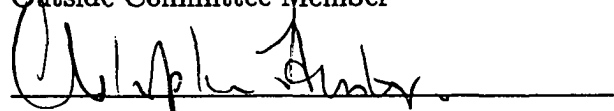
The members of the Committee approve the dissertation of Jichun Li defended on March 30, 1998.



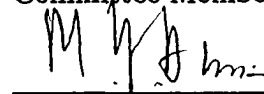
I. Michael Navon
Professor Directing Thesis



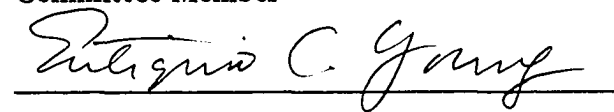
Richard L. Pfeffer
Outside Committee Member



Christopher Hunter
Committee Member



M. Yousuff Hussaini
Committee Member



Eutiquio C. Young
Committee Member

ACKNOWLEDGEMENTS

First and foremost, I wish to thank my advisor Dr. I. Michael Navon. I could never have successfully completed this work without his constant guidance, encouragement and all kinds of support. I also wish to thank Dr. Christopher Hunter, Dr. M. Yousuff Hussaini, Dr. Richard L. Pfeffer and Dr. Eutiquio C. Young for their willingness to serve on my doctorate committee.

Most of the work was carried out at the Supercomputer Computations Research Institute (SCRI) of the Florida State University (FSU). The excellent facilities, challenging environment and many people's kind help at SCRI make this work possible. I wish to thank Mimi Burbank, who provided the style file that was used to typeset this dissertation which simplified my work significantly.

I also wish to thank Dr. Gordon Erlebacher and Dr. David Kopriva for many helpful professional discussions. I also wish to thank Professors H.-G. Roos and Martin Stynes for kindly providing me with their most recent work, which makes my work as current as possible.

Thanks should also go to the department of mathematics of FSU for its continuous financial support over the years and Dr. Richard L. Pfeffer for his partial financial support through the Geophysical Fluid Dynamics Institute of FSU.

I would also like to thank all my friends and those who gave me the encouragement and help.

Finally I would like to acknowledge my parents and other family members for their love and support over the many years. Especially I feel much obliged to my wife, Tao, and my son, David, for their tolerance with my total involvement in the work.

TABLE OF CONTENTS

List of Tables	viii
List of Figures	ix
Abstract	xv
1 INTRODUCTION	1
1.1 Motivation	1
1.2 Outline	4
1.3 Generic Notations	6
2 THE ANISOTROPIC MODEL	8
2.1 Introduction	8
2.2 The Continuous Problem	8
2.3 Finite Element Methods	15
2.4 Theoretical Results	17
2.5 Numerical Results	20
3 THE REACTION-DIFFUSION MODEL	23
3.1 Introduction	23
3.2 The Asymptotic Expansion	23
3.3 Derivative Estimates of the Solution	25
3.4 Finite Element Method on Shishkin Mesh	28
3.5 Theoretical Results	31
3.6 Numerical Results	35

4	THE CONVECTION-DIFFUSION MODEL	40
4.1	Introduction	40
4.2	Exponential Boundary Layer Case	40
4.2.1	Derivative Estimates of the Solution	40
4.2.2	The Asymptotic Expansion	43
4.2.3	Finite Element Method on Shishkin Type Mesh: Case (I) . .	45
4.2.4	Uniform Convergence Analysis	47
4.2.5	Streamline Diffusion Finite Element Methods	53
4.3	Parabolic Boundary Layer Case	54
4.3.1	Derivative Estimates of the Solution	55
4.3.2	The Asymptotic Expansion	56
4.3.3	Finite Element Method on Shishkin Type Mesh: Case (II) . .	59
4.3.4	Uniform Convergence Analysis	60
4.3.5	Streamline Diffusion Finite Element Methods	64
4.4	Numerical Experiments	66
4.4.1	Example 1.	66
4.4.2	Example 2.	68
4.4.3	Conclusions	69
5	THE TWO-PARAMETER MODEL	82
5.1	Introduction	82
5.2	Derivative Estimates	82
5.3	The Asymptotic Expansion	85
5.4	Mesh and Scheme	87
5.5	Theoretical Analysis	89
5.6	Numerical Results	92

6	HIGHER-ORDER FINITE ELEMENTS	101
6.1	Introduction	101
6.2	The 2-D Linear Reaction-Diffusion Model	102
6.2.1	The Asymptotic Expansion and Derivative Estimates	102
6.2.2	The Mesh and the Finite Element Scheme	105
6.2.3	Main Results	108
6.2.4	Generalizations to Any m-th Order Tensor-Product Elements .	112
6.3	The 2-D Quasilinear Reaction-Diffusion Model	115
6.4	Numerical Experiments	118
6.5	Conclusions	120
7	SHALLOW-WATER EQUATIONS	131
7.1	Governing Equations	131
7.2	Finite Element Method	133
7.3	Finite Difference Method	134
7.4	Application to the Breaking Dam Problem	135
7.4.1	Taylor-Galerkin Method	135
7.4.2	MacCormack Scheme	136
7.5	Conclusions	136
8	CONCLUSIONS AND FUTURE DIRECTIONS	145
	REFERENCES	147
	BIOGRAPHICAL SKETCH	158

LIST OF TABLES

2.1	Errors in L^2 norm	21
2.2	Errors in L^∞ norm	21
2.3	Convergence rates R_ϵ^N in L^2 norm	22
2.4	Convergence rates \tilde{R}_ϵ^N in L^∞ norm	22
3.1	Errors in L^2 norm	37
3.2	Convergence rates R_ϵ^N in L^2 norm	37
4.1	Errors in L^2 norm for Example 1	71
4.2	Convergence rates R_ϵ^N in L^2 norm for Example 1	71
4.3	Condition numbers for Example 1	72
4.4	Errors in L^2 norm for Example 2	72
4.5	Convergence rates R_ϵ^N in L^2 norm for Example 2	73
4.6	Condition numbers for Example 2	73
5.1	Errors in L^2 norm for Example 3	95
5.2	Errors in L^∞ norm for Example 3	95
6.1	Errors in L^2 norm for Example 2 on uniform mesh	122
6.2	Errors in L^2 norm for Example 2 on piecewise uniform mesh	122
6.3	Convergence rates R in L^2 norm on uniform mesh	123
6.4	Convergence rates \tilde{R} in L^2 norm on piecewise uniform mesh	123

LIST OF FIGURES

3.1	Computed FEM solution for $\varepsilon = 1.0D - 03$: (a) N=24 (b) N=48 . . .	38
3.2	Computed FEM solution for $\varepsilon = 1.0D - 05$: (a) N=24 (b) N=48 . . .	38
3.3	Computed FEM solution for $\varepsilon = 1.0D - 07$: (a) N=24 (b) N=48 . . .	38
3.4	Pointwise error $u_h - u$ for $\varepsilon = 1.0D - 03$: (a) N=24 (b) N=48	39
3.5	Pointwise error $u_h - u$ for $\varepsilon = 1.0D - 05$: (a) N=24 (b) N=48	39
3.6	Pointwise error $u_h - u$ for $\varepsilon = 1.0D - 07$: (a) N=24 (b) N=48	39
4.1	Example 1: Standard FEM on Shishikin mesh for $\varepsilon = 10^{-3}$: (a) N=12 (b) N=24	74
4.2	Example 1: Standard FEM on Shishikin mesh for $\varepsilon = 10^{-5}$: (a) N=12 (b) N=24	74
4.3	Example 1: Standard FEM on Shishikin mesh for $\varepsilon = 10^{-7}$: (a) N=12 (b) N=24	74
4.4	Example 1: Standard FEM: (a) N=48, $\varepsilon = 10^{-3}$, Shishkin mesh (b) N=12, $\varepsilon = 10^{-3}$, Uniform mesh	75
4.5	Example 1: Standard FEM: (a) N=48, $\varepsilon = 10^{-5}$, Shishkin mesh (b) N=24, $\varepsilon = 10^{-3}$, Uniform mesh	75
4.6	Example 1: Standard FEM: (a) N=48, $\varepsilon = 10^{-7}$, Shishkin mesh (b) N=48, $\varepsilon = 10^{-3}$, Uniform mesh	75
4.7	Example 1: SD FEM on Shishikin mesh for $\varepsilon = 10^{-3}$: (a) N=12 (b) N=24	76
4.8	Example 1: SD FEM on Shishikin mesh for $\varepsilon = 10^{-7}$: (a) N=12 (b) N=24	76

4.9	Example 1: SD FEM on uniform mesh for $\varepsilon = 10^{-3}$: (a) N=12 (b) N=24	76
4.10	Example 1: SD FEM on uniform mesh for $\varepsilon = 10^{-7}$: (a) N=12 (b) N=24	77
4.11	Example 1: SD FEM for N=48, $\varepsilon = 10^{-3}$: (a) Shishkin mesh (b) Uniform mesh	77
4.12	Example 1: SD FEM for N=48, $\varepsilon = 10^{-7}$: (a) Shishkin mesh (b) Uniform mesh	77
4.13	Example 2: Standard FEM for N=12, $\varepsilon = 10^{-2}$: (a) Uniform mesh (b) Shishkin mesh	78
4.14	Example 2: Standard FEM for N=12, $\varepsilon = 10^{-6}$: (a) Uniform mesh (b) Shishkin mesh	78
4.15	Example 2: Standard FEM for N=24, $\varepsilon = 10^{-2}$: (a) Uniform mesh (b) Shishkin mesh	78
4.16	Example 2: Standard FEM for N=24, $\varepsilon = 10^{-6}$: (a) Uniform mesh (b) Shishkin mesh	79
4.17	Example 2: Standard FEM for N=48, $\varepsilon = 1.0^{-2}$: (a) Uniform mesh (b) Shishkin mesh	79
4.18	Example 2: Standard FEM for N=48, $\varepsilon = 10^{-6}$: (a) Uniform mesh (b) Shishkin mesh	79
4.19	Example 2: SD FEM for N=12, $\varepsilon = 10^{-2}$: (a) Uniform mesh (b) Shishkin mesh	80
4.20	Example 2: SD FEM for N=12, $\varepsilon = 10^{-6}$: (a) Uniform mesh (b) Shishkin mesh	80
4.21	Example 2: SD FEM for N=24, $\varepsilon = 10^{-2}$: (a) Uniform mesh (b) Shishkin mesh	80

4.22	Example 2: SD FEM for $N=24$, $\varepsilon = 10^{-6}$: (a) Uniform mesh (b) Shishkin mesh	81
4.23	Example 2: SD FEM for $N=48$, $\varepsilon = 10^{-2}$: (a) Uniform mesh (b) Shishkin mesh	81
4.24	Example 2: SD FEM for $N=48$, $\varepsilon = 10^{-6}$: (a) Uniform mesh (b) Shishkin mesh	81
5.1	Example 1: computed solution for $\varepsilon = 10^{-2}$, $N = 40$: (a) uniform mesh (b) piecewise uniform mesh	96
5.2	Example 1: computed solution for $\varepsilon = 10^{-3}$, $N = 40$: (a) uniform mesh (b) piecewise uniform mesh	96
5.3	Example 1: computed solution for $\varepsilon = 10^{-5}$, $N = 40$: (a) uniform mesh (b) piecewise uniform mesh	96
5.4	Example 2: computed solution for $\varepsilon = 10^{-2}$, $N = 40$: (a) uniform mesh (b) piecewise uniform mesh	97
5.5	Example 2: computed solution for $\varepsilon = 10^{-3}$, $N = 40$: (a) uniform mesh (b) piecewise uniform mesh	97
5.6	Example 2: computed solution for $\varepsilon = 10^{-5}$, $N = 40$: (a) uniform mesh (b) piecewise uniform mesh	97
5.7	Example 3: piecewise uniform mesh for $\varepsilon = 10^{-2}$, $N = 10$: (a) computed solution (b) pointwise error	98
5.8	Example 3: piecewise uniform mesh for $\varepsilon = 10^{-3}$, $N = 10$: (a) computed solution (b) pointwise error	98
5.9	Example 3: piecewise uniform mesh for $\varepsilon = 10^{-5}$, $N = 10$: (a) computed solution (b) pointwise error	98
5.10	Example 3: piecewise uniform mesh for $\varepsilon = 10^{-2}$, $N = 20$: (a) computed solution (b) pointwise error	99

5.11	Example 3: piecewise uniform mesh for $\varepsilon = 10^{-3}, N = 20$: (a) computed solution (b) pointwise error	99
5.12	Example 3: piecewise uniform mesh for $\varepsilon = 10^{-5}, N = 20$: (a) computed solution (b) pointwise error	99
5.13	Example 3: piecewise uniform mesh for $\varepsilon = 10^{-2}, N = 40$: (a) computed solution (b) pointwise error	100
5.14	Example 3: piecewise uniform mesh for $\varepsilon = 10^{-3}, N = 40$: (a) computed solution (b) pointwise error	100
5.15	Example 3: piecewise uniform mesh for $\varepsilon = 10^{-5}, N = 40$: (a) computed solution (b) pointwise error	100
6.1	Example 1: Computed FEM solution for $N = 12$ and $\varepsilon = 10^{-2}$: (a) uniform mesh (b) piecewise uniform mesh	124
6.2	Example 1: Computed FEM solution for $N = 12$ and $\varepsilon = 10^{-3}$: (a) uniform mesh (b) piecewise uniform mesh	124
6.3	Example 1: Computed FEM solution for $N = 12$ and $\varepsilon = 10^{-4}$: (a) uniform mesh (b) piecewise uniform mesh	124
6.4	Example 1: Computed FEM solution for $N = 24$ and $\varepsilon = 10^{-2}$: (a) uniform mesh (b) piecewise uniform mesh	125
6.5	Example 1: Computed FEM solution for $N = 24$ and $\varepsilon = 10^{-3}$: (a) uniform mesh (b) piecewise uniform mesh	125
6.6	Example 1: Computed FEM solution for $N = 24$ and $\varepsilon = 10^{-4}$: (a) uniform mesh (b) piecewise uniform mesh	125
6.7	Example 2: Standard FEM on uniform mesh with $N = 12$ and $\varepsilon = 10^{-2}$: (a) computed solution (b) pointwise error $u_h - u$	126
6.8	Example 2: Standard FEM on uniform mesh with $N = 24$ and $\varepsilon = 10^{-2}$: (a) computed solution (b) pointwise error $u_h - u$	126

6.9	Example 2: Standard FEM on uniform mesh with $N = 36$ and $\varepsilon = 10^{-2}$: (a) computed solution (b) pointwise error $u_h - u$	126
6.10	Example 2: Standard FEM on uniform mesh with $N = 12$ and $\varepsilon = 10^{-3}$: (a) computed solution (b) pointwise error $u_h - u$	127
6.11	Example 2: Standard FEM on uniform mesh with $N = 24$ and $\varepsilon = 10^{-3}$: (a) computed solution (b) pointwise error $u_h - u$	127
6.12	Example 2: Standard FEM on uniform mesh with $N = 36$ and $\varepsilon = 10^{-3}$: (a) computed solution (b) pointwise error $u_h - u$	127
6.13	Example 2: FEM on piecewise uniform mesh with $N = 12$ and $\varepsilon = 10^{-2}$: (a) computed solution (b) pointwise error $u_h - u$	128
6.14	Example 2: FEM on piecewise uniform mesh with $N = 12$ and $\varepsilon = 10^{-3}$: (a) computed solution (b) pointwise error $u_h - u$	128
6.15	Example 2: FEM on piecewise uniform mesh with $N = 12$ and $\varepsilon = 10^{-4}$: (a) computed solution (b) pointwise error $u_h - u$	128
6.16	Example 2: FEM on piecewise uniform mesh with $N = 24$ and $\varepsilon = 10^{-2}$: (a) computed solution (b) pointwise error $u_h - u$	129
6.17	Example 2: FEM on piecewise uniform mesh with $N = 24$ and $\varepsilon = 10^{-3}$: (a) computed solution (b) pointwise error $u_h - u$	129
6.18	Example 2: FEM on piecewise uniform mesh with $N = 24$ and $\varepsilon = 10^{-4}$: (a) computed solution (b) pointwise error $u_h - u$	129
6.19	Example 2: FEM on piecewise uniform mesh with $N = 36$ and $\varepsilon = 10^{-2}$: (a) computed solution (b) pointwise error $u_h - u$	130
6.20	Example 2: FEM on piecewise uniform mesh with $N = 36$ and $\varepsilon = 10^{-3}$: (a) computed solution (b) pointwise error $u_h - u$	130
6.21	Example 2: FEM on piecewise uniform mesh with $N = 36$ and $\varepsilon = 10^{-4}$: (a) computed solution (b) pointwise error $u_h - u$	130

7.1	Initial water surface	137
7.2	Water surface for FEM: (a) after 20 steps (b) after 50 steps	137
7.3	Contour plot of water surface for FEM: (a) after 20 steps (b) after 50 steps	138
7.4	Velocity field for FEM: (a) after 20 steps (b) after 50 steps	138
7.5	Water surface for FDM without artificial viscosity after 50 steps . . .	139
7.6	FDM without artificial viscosity after 50 steps: (a) Contour plot (b) Velocity field	139
7.7	Water surface for FDM with artificial viscosity after 10 steps	140
7.8	FDM with artificial viscosity after 10 steps: (a) Contour plot (b) Velocity field	140
7.9	Water surface for FDM with artificial viscosity after 20 steps	141
7.10	FDM with artificial viscosity after 20 steps: (a) Contour plot (b) Velocity field	141
7.11	Water surface for FDM with artificial viscosity after 50 steps	142
7.12	FDM with artificial viscosity after 50 steps: (a) Contour plot (b) Velocity field	142
7.13	Water surface for FDM with artificial viscosity after 75 steps	143
7.14	FDM with artificial viscosity after 75 steps: (a) Contour plot (b) Velocity field	143
7.15	Water surface for FDM with artificial viscosity after 100 steps	144
7.16	FDM with artificial viscosity after 100 steps: (a) Contour plot (b) Velocity field	144

ABSTRACT

With the development of more powerful computers, the numerical solution of partial differential equations has become a very active area of research in numerical analysis and scientific computing. The finite element method (FEM) is one of the most popular methods.

In the first part of this dissertation, we investigated the usage of FEM for the singularly perturbed problems (SPP). It is known that the classical FEM can not achieve global uniform convergence for general SPP, where the error estimate is independent of the perturbation parameter. In this work, we proposed a systematical technique for constructing global uniformly convergent finite element schemes on some piecewise uniform meshes to solve singularly perturbed elliptic problems in two space dimensions. Four model problems were considered, i.e., an anisotropic model, the reaction-diffusion model, the convection-diffusion model and a two-parameter model. Extensive numerical results are provided supporting our theoretical analysis, thus answering some open problems posed by Roos *et al.* in [1, p.278] and [2].

In the second part of the dissertation, we used FEM to simulate the more practical shallow-water equations. Here we implemented a Taylor-Galerkin FEM for a breaking dam model. For numerical comparison, the MacCormack scheme was also implemented.

[1] H.-G. Roos, M. Stynes and L. Tobiska, Numerical Methods for Singularly Perturbed Differential Equations (Springer-Verlag, Berlin, 1996).

[2] H.-G. Roos, Layer-adapted grids for singular perturbation problems, *Z. Angew. Math. Mech.* (to appear in 1998).

CHAPTER 1

INTRODUCTION

1.1 Motivation

Perturbations that occur in different problems can be formally divided into two classes: *regular perturbations* and *singular perturbations*. Consider two equations:

$$\text{Equation } A_0 : \quad L_0 u = f_0$$

$$\text{Equation } A_\varepsilon : \quad L_0 u + \varepsilon L_1 u = f_0 + \varepsilon f_1.$$

Here L_0 and L_1 are given operators, f_0 and f_1 are known functions, $0 < \varepsilon \ll 1$ is a small perturbation parameter, u is the unknown function of the independent variable x . The terms $\varepsilon L_1 u$ and εf_1 represent perturbations. Denote the solution of A_0 by $u_0(x)$, and the solution of A_ε by $u_\varepsilon(x)$ for $x \in D$, where D is the problem domain. The problem A_ε is called *regularly perturbed* in the domain D if

$$\sup_D \|u_\varepsilon(x) - u_0(x)\| \rightarrow 0 \quad \text{when } \varepsilon \rightarrow 0.$$

Otherwise, the problem A_ε is called *singularly perturbed*.

Singularly perturbed problems (SPP) appear in many branches of applied mathematics. They are often used as mathematical models describing processes in fluid mechanics [60, 128], chemical kinetics [129, 84], biochemical kinetics [76, Ch.10] and system control [77, 88, 13, 67, 65]. Such problems arise naturally when there are sudden transitions from certain physical characteristics to others. These transitions can occur either inside a very thin layer near the boundary or inside the problem domain. Such a thin layer is called the boundary layer or internal layer. These layers

make the problem very difficult to solve numerically. An extensively discussed model in fluid mechanics is the so-called "convection dominated" problem [22, 135, 57]:

$$-\nabla \cdot \varepsilon \nabla u + c \cdot \nabla u + \sigma u = f \quad \text{in } \Omega \subseteq \mathbb{R}^2 \quad (1.1)$$

$$u = 0 \quad \text{on } \partial\Omega, \quad (1.2)$$

where the diffusion coefficient ε is assumed to be very small in comparison with the other coefficients and $c \neq 0$. Corresponding to $c = 0$ is the so-called reaction-diffusion model. But "even if $c = 0$, the fact that ε can be very small in comparison with σ leads to notorious computational difficulties" [95, pp.310]. As Morton pointed in the preface of his book [86]: "Accurate modelling of the interaction between convective and diffusive processes is the most ubiquitous and challenging task in the numerical approximation of partial differential equations. This is partly because of the problems themselves, their great variety and widespread occurrence, as well as their close association with singular perturbation problems and boundary layer theory. It is also due to the fact that numerical algorithms, and the techniques used for their analysis, tend to be very different in the two limiting cases of elliptic and hyperbolic equations." Starting in early seventies, a sizable amount of work has been carried out using methods, such as *finite difference methods* (FDM) [1, 97, 14, 33, 38, 44, 66, 85], *spectral methods* [6, 40, 42, 43, 127], *finite volume methods* (FVM) [86, 56], *finite element methods* (FEM) [2, 3, 26, 29, 53, 57, 110], to name but a few. However a large number of unsolved problems still remains to be addressed, which keeps the investigation in this area still very active in both analytic [96, 64, 87, 81, 129] and numerical methods [82, 83, 85, 86, 110, 33]. In this work, we will focus only on FEM.

It is well known [58] that the standard FEM generally have the following global error estimates

$$\|u - u_h\|_{\Omega} \leq Ch^m \|u\|_{H^m(\Omega)},$$

where $H^n(\Omega)$ denotes the usual Sobolev space [16] with norm $\|\cdot\|_{H^n(\Omega)}$ and $|||\cdot|||_\Omega$ denotes an energy norm on Ω . But usually the solution u of SPP satisfies $\|u\|_{H^n(\Omega)} \leq C\varepsilon^{-k}$, where k is some positive integer. Hence to ensure global convergence, the mesh size h must be less than or equal to ε^p , where p is a positive number, which is impossible in practice, since ε can be as small as 10^{-10} . Hence many researchers switched their focus to local error estimates [59, 133, 136, 93]. But global uniformly convergent (GUC) methods, where the error between the original continuous solution u and the computed FEM solution u_h satisfies:

$$\|u - u_h\|_\varepsilon \leq Ch^m$$

for some positive constant C , that is independent of both ε and of the mesh size, are still very fascinating. The first GUC finite element scheme was obtained by Stynes and O'Riordan by using the exponential fitted FEM [122]. Some other variants of exponential fitted FEM were explored in [108, 3]. However they are complicated to use and have a very low convergence rate, which is $\|u - u_h\|_\varepsilon \leq ch^{1/2}$ for the convection-diffusion model (see Chapter 4), where $\|\cdot\|_\varepsilon$ is a variant of an energy norm. Another type of uniform convergence was achieved for the linear reaction-diffusion model (see Chapter 3) in one and two space dimensions by using hp FEM [114]. This method is also very complicated and its generalizations are still under development. Recently, almost optimal uniform convergence results were achieved by FEM on some specially designed piecewise uniform meshes, which were introduced by Shishkin [117, 118]. Such Shishkin type mesh specifies a fine uniform mesh inside part but not all of the boundary layer and coarse uniform mesh elsewhere *a priori*, yet it still yields global convergence that is uniform in ε . Such a mesh is very easy to implement, but the aforementioned studies were restricted mostly to one space dimension problems. As Roos *et al.* pointed out [108, pp. 717]: "*These meshes work well for a wide range of one-dimensional problems. In two or more dimensions, however, the analysis of*

finite element methods on Shishkin meshes is an open question;”. See also Roos *et al.* [110, pp.278]: *”Finite element methods that use Shishkin meshes in two or more dimensions have not been explored in the literature.”* The first part of this dissertation (Chapters 2-6) presents results of our research investigations in this area. By using delicate asymptotic expansions and FEM analysis, we proposed a general technique for constructing a GUC finite element scheme for solving SPP in two space dimensions, thus answering part of Roos *et al.*’s open problems. To illustrate our systematised technique, four model problems were investigated, i.e., the anisotropic model (Chapter 2), the reaction-diffusion model (Chapters 3 and 6), the convection-diffusion model (Chapter 4) and the two-parameter model (Chapter 5). During the writing of this work, some additional research advances were obtained [123, 105], however many open problems still remain in this exciting area, details of which can be found in the most recent survey by Roos [105].

In the second part of this work, we switched our interest to the shallow-water equations (SWE), which describe many practical models in hydraulic engineering, meteorology and oceanographic problems. Even though a large amount of work was carried out for meteorological and oceanographic problems using FEM[89, 90, 91, 92, 135], little work in FEM has been carried out in hydraulic engineering[25, Ch.16]. Here we attempted to solve a hypothetical breaking dam problem described by SWE by using a Taylor-Galerkin FEM and MacCormack finite difference scheme.

1.2 Outline

Chapters 2-6 constitute the first part of the dissertation. Starting with Chapter 2, we investigated an anisotropic model problem. Based on a detailed analysis of the analytic solution, we constructed a bilinear FEM on a piecewise uniform mesh. Then we proved that our FEM is almost second order GUC in L^2 norm. Finally numerical results are presented, which confirmed our theoretical analysis.

The reaction-diffusion type problem was discussed in Chapter 3. By carrying out a similar technique to that used in Chapter 2, we constructed our bilinear FEM based on another piecewise uniform mesh, and our scheme was showed to be almost second order GUC in L^2 norm. Then a numerical experiment was carried out, which supported our theoretical analysis.

Then a more widely studied convection-diffusion model was investigated in Chapter 4. Here we discussed two different cases, i.e., the exponential boundary layer case and the parabolic boundary layer case. This model is different from the previous two models in that the convergence order was proved to be one order less optimal for both cases. Numerical results were also presented for comparisons between our FEM based on some piecewise uniform meshes and the standard FEM and streamline-diffusion FEM. The results obtained showed our methods to be much better than the standard FEM.

Chapter 5 was dedicated to a two-parameter model problem. Both theoretical and numerical results showed that our bilinear FEM is GUC and performed much better than the standard FEM.

In Chapter 6, we generalized our bilinear FEM developed in Chapters 2-5 to higher-order finite element method for solving singularly perturbed elliptic problems in two space dimensions. We proved that a quasioptimal global uniform convergence rate of $O(N_x^{-(m+1)} \ln^{m+1} N_x + N_y^{-(m+1)} \ln^{m+1} N_y)$ in L^2 norm is obtained for a reaction-diffusion model by using the m -th order ($m \geq 2$) tensor-product element. Here N_x and N_y are the number of partitions in the x - and y -directions, respectively. Numerical experiments in bi-quadratic FEM were presented supporting our theoretical analysis.

As mentioned before, Chapter 7 solved a breaking dam problem. Both Taylor-Galerkin FEM and MacCormack FDM were implemented for this model.

Finally a summary of this work and some possible future research directions are presented and discussed in Chapter 8.

1.3 Generic Notations

Throughout Chapters 2-6, we will use the following notations.

Let $\varepsilon \in (0, 1]$ be a small positive number, which denotes the perturbation parameter. Let $\Omega \equiv (0, 1) \times (0, 1) \subseteq R^2$ be a square in the two-dimensional space. We assume that positive integers N_x and N_y denote the number of divisions of Ω in the x- and y-directions, respectively.

Let $k = (k_1, k_2)$ be a 2-tuple of nonnegative integers and denote $|k| = k_1 + k_2$. Also we will make frequent use of the following well-known function spaces:

$C^m(\tau)$ = the linear space consisting of all functions w with partial derivatives $D^k w$ of orders $0 \leq |k| \leq m$ continuous on τ .

$C^\infty(\tau)$ = $\cap_{k=0}^\infty C^k(\tau)$ = the linear space of functions infinitely differentiable on τ .

$C_0^m(\tau), C_0^\infty(\tau)$ = linear subspaces of $C^m(\tau)$ and $C^\infty(\tau)$, respectively, consisting of those functions that have compact support in τ .

$C^m(\bar{\tau})$ = the linear space consisting of all function w in $C^m(\tau)$ for which $D^k w$ is bounded and uniformly continuous on τ for $0 \leq |k| \leq m$.

$L^m(\tau)$ = the linear space of equivalence class of measurable functions w for which $\int_\tau |w(x, y)|^m dx dy < \infty$.

$\|w\|_{m,\tau}$ = $[\int_\tau |w(x, y)|^m dx dy]^{1/m}$ be the L^m norm on τ , where $1 \leq m \leq \infty$.

$H^m(\tau)$ = $\{w | D^k w \in L^2(\tau) \text{ for } 0 \leq |k| \leq m\}$ be the Sobolev space.

$H_0^m(\tau)$ = the closure of $C_0^\infty(\tau)$ in $H^m(\tau)$.

$$\|w\|_{m,\tau} = \left[\int_{\tau} \sum_{0 \leq |k| \leq m} |D^k w|^2 dx dy \right]^{1/2} \text{ be the norm.}$$

$$|w|_{m,\tau} = \left[\int_{\tau} \sum_{|k|=m} |D^k w|^2 dx dy \right]^{1/2} \text{ be the seminorm.}$$

Let $I_i = [x_{i-1}, x_i]$, $I = [0, 1]$, $\tilde{I}_i = I_i \times I$, $h_x = \max_{1 \leq i \leq N_x} h_i$, $K_j = [y_{j-1}, y_j]$, $\tilde{K}_j = I \times K_j$, $h_y = \max_{1 \leq j \leq N_y} k_j$ and $\|\cdot\|_{p,\tau}$ be the L^p norm on any domain τ , here $1 \leq p \leq \infty$. For simplicity, we use $\|\cdot\|$ to denote the usual L^2 norm on Ω .

Throughout Chapters 2-6, we denote the standard tensor-product finite element space as $S_h(\Omega)$. Also we express the standard tensor-product interpolation of w as Πw , and we use Π_x and Π_y to distinguish between the interpolation in the x-direction and y-direction, respectively.

CHAPTER 2

THE ANISOTROPIC MODEL

2.1 Introduction

In this chapter, we consider the following anisotropic model problem [124]:

$$L_\varepsilon u \equiv -(\varepsilon^2 \frac{\partial^2 u}{\partial x^2} + \frac{\partial^2 u}{\partial y^2}) + a(x, y)u = f(x, y) \text{ in } \Omega, \quad (2.1)$$

$$u = g(x, y) \text{ on } \partial\Omega, \quad (2.2)$$

where the functions a , f and g are assumed to be sufficiently smooth on Ω , with

$$a(x, y) \geq \alpha^2 > 0 \text{ on } \Omega.$$

For small values of ε , the solution u will vary rapidly in the elliptic boundary layers $\partial\Omega_1 \equiv \{x = 0, 0 \leq y \leq 1\}$ and $\partial\Omega_2 \equiv \{x = 1, 0 \leq y \leq 1\}$, cf. Su [124].

2.2 The Continuous Problem

In this section, we will analyze the properties of the analytic solution u of (2.1)-(2.2). Without loss of generality, we consider homogeneous boundary conditions, i.e., $g = 0$. Otherwise we can set $\tilde{u} = u - g$ as the new variable. This will give us the same equation but with a different right hand side function f .

The weak formulation of (2.1) is: find $u \in H_0^1(\Omega)$ such that

$$B(u, v) \equiv (\varepsilon^2 u_x, v_x) + (u_y, v_y) + (au, v) = (f, v), \quad \forall v \in H_0^1(\Omega), \quad (2.3)$$

where (\cdot, \cdot) denotes the usual $L^2(\Omega)$ inner product.

Denote the weighted energy norm

$$|||v||| \equiv \{\varepsilon^2 \|v_x\|^2 + \|v_y\|^2 + \|v\|^2\}^{1/2}, \quad \forall v \in H_0^1(\Omega).$$

Note that

$$\begin{aligned} B(v, v) &= \varepsilon^2 \|v_x\|^2 + \|v_y\|^2 + (av, v) \\ &\geq \min(1, \alpha^2)(\varepsilon^2 \|v_x\|^2 + \|v_y\|^2 + \|v\|^2) \\ &= \min(1, \alpha^2) |||v|||^2, \end{aligned}$$

and by the Cauchy-Schwarz inequality

$$\begin{aligned} B(v, w) &\leq \varepsilon^2 \|v_x\| \|w_x\| + \|v_y\| \|w_y\| + \left(\max_{(x,y) \in \bar{\Omega}} a \right) \|v\| \|w\| \\ &\leq \left(1 + \max_{(x,y) \in \bar{\Omega}} a \right) |||v||| |||w||| \\ &\leq C |||v||| |||w|||. \end{aligned}$$

Also the mapping $v \rightarrow (f, v)$ is a bounded functional on H_0^1 , combining this fact with the above two inequalities, the Lax-Milgram lemma [27, 16] tells us that (2.3) has a unique solution $u(x, y)$ in $H_0^1(\Omega)$.

In the following, in order to derive the pointwise estimates of the solution u of (2.1)-(2.2), we assume that u is sufficiently smooth.

In what follows we will make repeated use of the following weak maximum principle :

Theorem 2.1 *For any functions $w(x, y) \in C^2(\Omega) \cap C^0(\bar{\Omega})$, if $w \geq 0$ on $\partial\Omega$ and $L_\varepsilon w \geq 0$ on Ω , then $w \geq 0$ on $\bar{\Omega}$.*

Proof. It can be proved easily by contradiction, cf. Eckhaus [34, Lemma 6.2.1.1].

By the boundary layer correction method [124], we have

Theorem 2.2 For the solution u of (2.1)-(2.2), we have

$$u(x, y) = w_0 + v_0\left(\frac{x}{\varepsilon}, y\right) + v_1\left(\frac{1-x}{\varepsilon}, y\right) + z(x, y), \quad (2.4)$$

where w_0 , v_0 and v_1 are given in the proof. Also

$$\begin{aligned} |v_0\left(\frac{x}{\varepsilon}, y\right)| &\leq C e^{-\frac{\alpha x}{\varepsilon}} \text{ on } \bar{\Omega}, \\ |v_1\left(\frac{1-x}{\varepsilon}, y\right)| &\leq C e^{-\frac{\alpha(1-x)}{\varepsilon}} \text{ on } \bar{\Omega}, \end{aligned}$$

and

$$|z(x, y)| \leq C\varepsilon \text{ on } \bar{\Omega}.$$

Proof. Construct w_0 as a solution of the following limiting case when $\varepsilon = 0$:

$$\begin{aligned} L_0 w_0 &\equiv -w_{0yy} + a(x, y)w_0 = f(x, y), \\ w_0(x, 0) &= w_0(x, 1) = 0. \end{aligned}$$

On $\partial\Omega_1$, by introducing the local coordinate $\xi = \frac{x}{\varepsilon}$, then we construct $v_0(\xi, y)$ such that

$$-\frac{\partial^2 v_0}{\partial \xi^2} - \frac{\partial^2 v_0}{\partial y^2} + a(0, y)v_0 = 0, \quad (2.5)$$

$$v_0|_{\xi=0} = -w_0(0, y), \quad (2.6)$$

$$v_0|_{y=0} = v_0|_{y=1} = 0, \quad \lim_{\xi \rightarrow +\infty} v_0 = 0. \quad (2.7)$$

Similarly on $\partial\Omega_2$, let $\xi = \frac{1-x}{\varepsilon}$ and construct $v_1(\xi, y)$ such that

$$-\frac{\partial^2 v_1}{\partial \xi^2} - \frac{\partial^2 v_1}{\partial y^2} + a(0, y)v_1 = 0,$$

$$v_1|_{\xi=0} = -w_0(1, y),$$

$$v_1|_{y=0} = v_1|_{y=1} = 0, \quad \lim_{\xi \rightarrow +\infty} v_1 = 0.$$

We can solve this problem by Fourier method. Set $v = \psi(\xi)\varphi(y)$, then we have the following Sturm-Liouville problem:

$$\varphi''(y) - a(0, y)\varphi(y) = -\lambda\varphi(y),$$

$$\varphi(0) = \varphi(1) = 0.$$

By our assumption of $a \geq \alpha^2 > 0$, all eigenvalues λ_k ($k = 1, 2, \dots$) are positive. Let φ_k be the normal orthogonal eigenfunction corresponding to each λ_k , then the solution of (2.5)-(2.7) can be written as

$$v_0\left(\frac{x}{\varepsilon}, y\right) = v_0(\xi, y) = \sum_{k=1}^{\infty} A_k e^{-\sqrt{\lambda_k} \xi} \varphi_k(y) = \sum_{k=1}^{\infty} A_k e^{-\frac{\sqrt{\lambda_k} x}{\varepsilon}} \varphi_k(y),$$

where A_k are the coefficients of $w_0(0, y)$ expanded in $\{\varphi_k(y)\}$ and

$$\lambda_k = \frac{\int_0^1 \varphi_k'(y)^2 dy + \int_0^1 a(0, y) \varphi_k^2(y) dy}{\int_0^1 \varphi_k^2(y) dy} > \alpha^2.$$

Obviously v_0 has an exponential boundary layer at $x = 0$.

Similarly

$$v_1\left(\frac{1-x}{\varepsilon}, y\right) = \sum_{k=1}^{\infty} B_k e^{-\frac{\sqrt{\mu_k}(1-x)}{\varepsilon}} \bar{\varphi}_k(y),$$

where the eigenvalue μ_k and the corresponding eigenfunction $\bar{\varphi}_k(y)$ satisfy the following eigenvalue problem:

$$\begin{aligned} \bar{\varphi}''(y) - a(1, y) \bar{\varphi}(y) &= -\lambda \bar{\varphi}(y), \\ \bar{\varphi}(0) &= \bar{\varphi}(1) = 0. \end{aligned}$$

Consider the barrier function $\phi(x, y) = C e^{-\frac{\alpha x}{\varepsilon}}$ for (2.5)-(2.7), then by Theorem 2.1, we have

$$v_0\left(\frac{x}{\varepsilon}, y\right) \leq C e^{-\frac{\alpha x}{\varepsilon}}.$$

In the same way, we can obtain

$$v_1\left(\frac{1-x}{\varepsilon}, y\right) \leq C e^{-\frac{\alpha(1-x)}{\varepsilon}}.$$

Now we want to estimate $z(x, y)$. Let

$$z(x, y) = u(x, y) - w_0(x, y) - v_0\left(\frac{x}{\varepsilon}, y\right) - v_1\left(\frac{1-x}{\varepsilon}, y\right),$$

then

$$L_\varepsilon z = \varepsilon^2 w_{0xx} - a_x(\tilde{x}_1, y) x v_0 + a_x(\tilde{x}_2, y) x v_1 \leq C \varepsilon,$$

where \tilde{x}_1 and \tilde{x}_2 are some intermediate points between $(0, x)$ and $(x, 1)$ respectively. In the last step we used the fact that:

$$|xv_0| = \varepsilon \frac{x}{\varepsilon} |v_0| \leq C\varepsilon \frac{x}{\varepsilon} e^{-\frac{\alpha x}{\varepsilon}} \leq C\varepsilon ,$$

and

$$|(1-x)v_1| = \varepsilon \frac{(1-x)}{\varepsilon} |v_1| \leq C\varepsilon \frac{(1-x)}{\varepsilon} e^{-\frac{\alpha(1-x)}{\varepsilon}} \leq C\varepsilon .$$

By considering the barrier function $\phi(x, y) = C\varepsilon y(1-y)$, we have

$$|z(x, y)| \leq \phi(x, y) \leq C\varepsilon \quad \text{on } \bar{\Omega} ,$$

which concludes our proof.

Remark 2.1 If $a_x(x, y) = 0$, then $|z(x, y)| \leq C\varepsilon^2$ holds true on $\bar{\Omega}$.

Next we will use some elaborately chosen barrier functions [33, 103] to get our estimates for the solution u of (2.1)-(2.2).

Lemma 2.1 The following estimates hold:

- (I) $|u(x, y)| \leq Cy(1-y) \quad \text{on } \bar{\Omega} ,$
- (II) $|u(x, y)| \leq C(1 - e^{-\frac{\alpha x}{\varepsilon}}) \quad \text{on } \bar{\Omega} ,$
- (III) $|u(x, y)| \leq C(1 - e^{-\frac{\alpha(1-x)}{\varepsilon}}) \quad \text{on } \bar{\Omega} .$

Proof.(I) Use the barrier function $\phi(x, y) = Cy(1-y)$, then

$$\begin{aligned} L_\varepsilon(\phi \pm u) &= 2C + acy(1-y) \pm f , \\ &\geq 0 \quad \text{for } C \text{ sufficiently large .} \end{aligned}$$

Also note that $u|_{\partial\Omega} = 0$, hence

$$(\phi \pm u)|_{\partial\Omega} = \phi|_{\partial\Omega} \geq 0 ,$$

Thus $|u| \leq \phi$ on $\bar{\Omega}$ by Theorem 2.1.

(II) Use the barrier function $\phi(x, y) = C(1 - e^{-\frac{\alpha x}{\varepsilon}})$, then

$$\begin{aligned} L_\varepsilon(\phi \pm u) &= C\alpha^2 e^{-\frac{\alpha x}{\varepsilon}} + aC(1 - e^{-\frac{\alpha x}{\varepsilon}}) \pm f \\ &= C(\alpha^2 - a)e^{-\frac{\alpha x}{\varepsilon}} + aC \pm f. \end{aligned}$$

Note that

$$(\alpha^2 - a)(e^{-\frac{\alpha x}{\varepsilon}} - 1) \geq 0,$$

Hence

$$L_\varepsilon(\phi \pm u) \geq C\alpha^2 \pm f \geq 0 \quad \text{for } C \text{ sufficiently large,}$$

then from $(\phi \pm u)|_{\partial\Omega} \geq 0$, which concludes our proof.

(III) Use the barrier function $\phi(x, y) = C(1 - e^{-\frac{\alpha x}{\varepsilon}})$.

By Lemma 2.1, we can get the following boundary estimates:

Lemma 2.2

$$(I) \quad |u_x(x, y)|_{x=0,1} \leq C\varepsilon^{-1},$$

$$(II) \quad |u_y(x, y)| \leq C \quad \text{on } \partial\Omega.$$

Proof.(I) By Lemma 2.1(II), we have

$$\begin{aligned} |u_x(0, y)| &= \left| \lim_{x \rightarrow 0^+} \frac{u(x, y) - u(0, y)}{x} \right| \leq \lim_{x \rightarrow 0^+} \left| \frac{u(x, y) - u(0, y)}{x} \right| \\ &\leq \lim_{x \rightarrow 0^+} \frac{C(1 - e^{-\frac{\alpha x}{\varepsilon}})}{x} = C \frac{\alpha}{\varepsilon} \leq C\varepsilon^{-1}. \end{aligned}$$

By Lemma 2.1(III), we can obtain the estimate for $u_x(1, y)$ in the same way.

(II) Use Lemma 2.1(I) and the same proof in (I).

Lemma 2.3

$$(I) \quad |u_x(x, y)| \leq C(1 + \varepsilon^{-1}e^{-\frac{\alpha x}{\varepsilon}} + \varepsilon^{-1}e^{-\frac{\alpha(1-x)}{\varepsilon}}) \quad \text{on } \bar{\Omega},$$

$$(II) \quad |u_y(x, y)| \leq C \quad \text{on } \bar{\Omega}.$$

Proof.(I) Consider the barrier function

$$\phi(x, y) = C(1 + \varepsilon^{-1}e^{-\frac{\alpha x}{\varepsilon}} + \varepsilon^{-1}e^{-\frac{\alpha(1-x)}{\varepsilon}})[1 + y(1 - y)] ,$$

then

$$\begin{aligned} L_\varepsilon(\phi \pm u) &\geq 2C(1 + \varepsilon^{-1}e^{-\frac{\alpha x}{\varepsilon}} + \varepsilon^{-1}e^{-\frac{\alpha(1-x)}{\varepsilon}}) \pm (f_x - a_x u) \\ &\geq 0 \quad \text{for } C \text{ sufficiently large ,} \end{aligned}$$

and note that $(\phi \pm u)|_{\partial\Omega} > 0$, which concludes our proof of (I).

(II) To prove (II), use the barrier function $\phi(x, y) = C$.

Lemma 2.4

$$(I) \quad |u_{xx}(x, y)|_{x=0,1} \leq C\varepsilon^{-2} ,$$

$$(II) \quad |u_{yy}(x, y)| \leq C \quad \text{on } \partial\Omega .$$

Proof.(I) Set $x = 0, 1$ in (2.1) and use the fact $u = u_{yy} = 0$ on the sides of $x = 0, 1$.

(II) Let $x = 0, 1$ in (2.1) and by (I), we have $|u_{yy}|_{x=0,1} \leq C$. Then set $y = 0, 1$ in (2.1) and note that $u = u_{xx} = 0$ on the sides of $y = 0, 1$.

By Lemma 2.4, we can obtain the following estimates for the second order derivatives:

Lemma 2.5

$$(I) \quad |u_{xx}(x, y)| \leq C(1 + \varepsilon^{-2}e^{-\frac{\alpha x}{\varepsilon}} + \varepsilon^{-2}e^{-\frac{\alpha(1-x)}{\varepsilon}}) \quad \text{on } \bar{\Omega} ,$$

$$(II) \quad |u_{yy}(x, y)| \leq C \quad \text{on } \bar{\Omega} .$$

Proof.(I) Use the barrier function

$$\phi(x, y) = C(1 + \varepsilon^{-2}e^{-\frac{\alpha x}{\varepsilon}} + \varepsilon^{-2}e^{-\frac{\alpha(1-x)}{\varepsilon}})[1 + y(1 - y)] ,$$

then

$$\begin{aligned} L_\varepsilon(\phi \pm u) &\geq 2C(1 + \varepsilon^{-2}e^{-\frac{\alpha x}{\varepsilon}} + \varepsilon^{-2}e^{-\frac{\alpha(1-x)}{\varepsilon}}) \pm (f_{xx} - a_{xx}u - 2a_x u_x) , \\ &\geq 0 \quad \text{for } C \text{ sufficiently large .} \end{aligned}$$

The rest are the same as Lemma 2.3.

(II) Use the barrier function $\phi(x, y) = C$.

Remark 2.2 *From our proof, it is not difficult to see that the above estimates also hold true even if f is also a function of ε , only if*

$$|f_{x^k y^j}(x, y)| \leq C(1 + \varepsilon^{-k} e^{\frac{-\alpha x}{\varepsilon}} + \varepsilon^{-k} e^{\frac{-\alpha(1-x)}{\varepsilon}}), \quad \forall k, j \geq 0, \quad \text{on } \Omega. \quad (2.8)$$

Remark 2.3 *As for higher order estimates, we can repeat the above proofs by changing the variables. For example, by differentiating (2.1) with respect to (w.r.t.) x , we see that u_x will still have the form of (2.1) but with a different f . Generally, we can have the following estimates:*

$$|u_{x^k y^j}(x, y)| \leq C(1 + \varepsilon^{-k} e^{\frac{-\alpha x}{\varepsilon}} + \varepsilon^{-k} e^{\frac{-\alpha(1-x)}{\varepsilon}}), \quad \forall k, j \geq 0, \quad \text{on } \bar{\Omega}.$$

2.3 Finite Element Methods

Let us discretize the weak form of (2.3) by means of a finite element method [37, 7].

For simplicity, we assume that N_x is divisible by 4.

In the y -direction, we discretize $[0, 1]$ as

$$0 = y_0 < y_1 < \cdots < y_{N_y} = 1.$$

In the x -direction, first we divide the interval $[0, 1]$ into subintervals

$$[0, \sigma], \quad [\sigma, 1 - \sigma], \quad [1 - \sigma, 1].$$

Uniform meshes are then used on each subinterval, with $N_x/4$ points on each of $[0, \sigma]$ and $[1 - \sigma, 1]$, and $N_x/2$ points on $[\sigma, 1 - \sigma]$. Here σ is defined by

$$\sigma = \min\{1/4, 4\alpha^{-1}\varepsilon \ln N_x\}.$$

More explicitly, we have

$$0 = x_0 < x_1 < \cdots < x_{i_0} < \cdots < x_{N_x - i_0} < \cdots < x_{N_x} = 1 ,$$

with $i_0 = N_x/4$, $x_{i_0} = \sigma$, $x_{N_x - i_0} = 1 - \sigma$, and

$$h_i = 4\sigma N_x^{-1}, \text{ for } i = 1, \dots, i_0, N_x - i_0 + 1, \dots, N_x ,$$

$$h_i = 2(1 - 2\sigma)N_x^{-1}, \text{ for } i = i_0 + 1, \dots, N_x - i_0 ,$$

where $h_i = x_i - x_{i-1}$.

We shall assume that

$$\sigma = 4\alpha^{-1}\varepsilon \ln N_x.$$

Otherwise $\varepsilon \geq 16\alpha^{-1} \ln N_x$, which is not a singularly perturbed problem. In this case, the problem can be solved by the classical FEM.

Our finite element solution is : Find $u^h \in S_h(\Omega)$ such that

$$\overline{B}(u^h, v) \equiv (\varepsilon^2 u_x^h, v_x) + (u_y^h, v_y^h) + (\overline{a}u^h, v) = (\overline{f}, v), \quad \forall v \in S_h(\Omega) , \quad (2.9)$$

where \overline{a} and \overline{f} denote the piecewise bilinear interpolations of a and f . Here $S_h(\Omega)$ is the standard bilinear finite element space.

Now let us recall some standard interpolation error estimates from Schultz [113] which we will use in what follows.

Lemma 2.6 [113, Theorem 2.1] $\Pi u = \Pi_x \Pi_y u = \Pi_y \Pi_x u$.

Lemma 2.7 [113, Theorem 2.6] $\|u - \Pi_x u\|_{\infty, \bar{I}_i} \leq \frac{1}{8} h_i^2 \|u_{xx}\|_{\infty, \bar{I}_i}$.

Lemma 2.8 [113, Lemma 2.1]

$$\|\Pi_x u\|_{\infty, I} \leq \max_{0 \leq i \leq N} |u(x_i)| \equiv \|u\|_{\infty, I} ,$$

$$\|\Pi_x u\|_{\infty, I_i} \leq \max_{y \in I} (|u(x_{i-1}, y)|, |u(x_i, y)|) .$$

Same results hold true for the interpolation Π_y .

2.4 Theoretical Results

Let us first prove the interpolation error estimates for the solution u of (2.1)-(2.2).

Lemma 2.9

$$\|u - \Pi_x u\|_{\infty, \bar{I}_i} \leq CN_x^{-2} \ln^2 N_x, \quad \forall i = 1, \dots, N_x. \quad (2.10)$$

Proof. First, if $i = 1, \dots, i_0, N_x - i_0 + 1, \dots, N_x$, then by Lemma 2.5,

$$\begin{aligned} h_i^2 \|u_{xx}\|_{\infty, \bar{I}_i} &\leq Ch_i^2 \max_{z \in \bar{I}_i} (1 + \varepsilon^{-2} e^{\frac{-\alpha z}{\varepsilon}} + \varepsilon^{-2} e^{\frac{-\alpha(1-z)}{\varepsilon}}) \\ &\leq Ch_i^2 (1 + \varepsilon^{-2}) \leq CN_x^{-2} \ln^2 N_x, \end{aligned}$$

for $h_i = 4\sigma/N_x$ in this case. Therefore by Lemma 2.7, (2.10) holds true.

Second, if $i = i_0 + 1, \dots, N_x - i_0$, we can discuss them in two cases. Let $\sigma_\varepsilon = 2\alpha^{-1}\varepsilon |\ln \varepsilon|$ be the boundary width.

case 1: $N_x^{-2} \leq \varepsilon$. Then

$$\|u_{xx}\|_{\infty, \bar{I}_i} \leq C,$$

for x_{i-1} and $1 - x_i$ are in $[\sigma, 1 - \sigma] \subseteq [\sigma_\varepsilon, 1 - \sigma_\varepsilon]$. Hence by Lemma 2.7,

$$\|u - \Pi_x u\|_{\infty, \bar{I}_i} \leq Ch_i^2 \|u_{xx}\|_{\infty, \bar{I}_i} \leq CN_x^{-2},$$

where we used the fact

$$N_x^{-1} \leq h_i \leq 2N_x^{-1} \quad \text{for } i = i_0 + 1, \dots, N_x - i_0.$$

case 2: $N_x^{-2} \geq \varepsilon$. In this case, we have

$$[\sigma, 1 - \sigma] = [\sigma, \sigma_\varepsilon] \cup [\sigma_\varepsilon, 1 - \sigma_\varepsilon] \cup [1 - \sigma_\varepsilon, 1 - \sigma].$$

For $[\sigma_\varepsilon, 1 - \sigma_\varepsilon]$, its proof is the same as case 1.

For $[\sigma, \sigma_\varepsilon] \cup [1 - \sigma_\varepsilon, 1 - \sigma]$, by Theorem 2.2, we can write $\Pi_x u$ in the form

$$\Pi_x u = \Pi_x w_0 + \Pi_x v_0 + \Pi_x v_1 + \Pi_x z,$$

where $\Pi_x w_0, \Pi_x v_0, \Pi_x v_1$ and $\Pi_x z$ denote the linear interpolants in x-direction to w_0, v_0, v_1 and z respectively.

Note that

$$\|w_0 - \Pi_x w_0\|_{\infty, \bar{I}_i} \leq Ch_i^2 \|w_{0xx}\|_{\infty, \bar{I}_i} \leq CN_x^{-2},$$

since w_0 is a smooth function independent of ε by Theorem 2.2.

Also by Lemma 2.7, we have

$$\|v_0(\frac{x}{\varepsilon}, y) - \Pi_x v_0(\frac{x}{\varepsilon}, y)\|_{\infty, \bar{I}_i} \leq 2\|v_0(\frac{x}{\varepsilon}, y)\|_{\infty, \bar{I}_i} \quad (2.11)$$

$$\leq Ce^{-\frac{\alpha x_i - 1}{\varepsilon}} \leq Ce^{-\frac{\alpha \sigma}{\varepsilon}} \leq CN_x^{-2}. \quad (2.12)$$

$$\|v_1(\frac{x}{\varepsilon}, y) - \Pi_x v_1(\frac{x}{\varepsilon}, y)\|_{\infty, \bar{I}_i} \leq 2\|v_1(\frac{x}{\varepsilon}, y)\|_{\infty, \bar{I}_i} \quad (2.13)$$

$$\leq Ce^{-\frac{\alpha(1-x_i)}{\varepsilon}} \leq Ce^{-\frac{\alpha \sigma}{\varepsilon}} \leq CN_x^{-2}, \quad (2.14)$$

and

$$\|z(x, y) - \Pi_x z(x, y)\|_{\infty, \bar{I}_i} \leq 2\|z\|_{\infty, \bar{I}_i} \leq C\varepsilon \leq CN_x^{-2},$$

from which finishes our proof.

Thus we have:

Lemma 2.10 *For the solution u of (2.1)-(2.2), we have*

$$\|u - \Pi u\|_{\infty, \bar{\Omega}} \leq C(N_x^{-2} \ln^2 N_x + k^2).$$

Proof. Using Lemma 2.6 and Lemma 2.8, we have

$$\|u - \Pi u\|_{\infty, \bar{\Omega}} \leq \|u - \Pi_x u\|_{\infty, \bar{\Omega}} + \|\Pi_x(u - \Pi_y u)\|_{\infty, \bar{\Omega}} \quad (2.15)$$

$$\leq \|u - \Pi_x u\|_{\infty, \bar{\Omega}} + \|u - \Pi_y u\|_{\infty, \bar{\Omega}} \quad (2.16)$$

$$\leq \max_{1 \leq i \leq N_x} \|u - \Pi_x u\|_{\infty, \bar{I}_i} + \frac{1}{8}k^2 \|u_{yy}\|_{\infty, \bar{\Omega}} \quad (2.17)$$

$$\leq C(N_x^{-2} \ln^2 N_x + k^2). \quad (2.18)$$

Finally we have :

Theorem 2.3 For the solution u of (2.1)-(2.2) and the finite element solution u^h of (2.9), we have

$$\|u - u^h\| \leq C(N_x^{-2} \ln^2 N_x + k^2).$$

Proof. Note that

$$C_1 \|\Pi u - u^h\|^2 \leq \bar{B}(\Pi u - u^h, \Pi u - u^h) \quad (2.19)$$

$$= \bar{B}(\Pi u - u, \Pi u - u^h) + \bar{B}(u - u^h, \Pi u - u^h). \quad (2.20)$$

Let $\chi = \Pi u - u^h$, then

$$\bar{B}(\Pi u - u, \Pi u - u^h) = \varepsilon^2((\Pi u - u)_x, \chi_x) + ((\Pi u - u)_y, \chi_y) + (\bar{a}(\Pi u - u), \chi) \quad (2.21)$$

Due to the special properties of Π_y for piecewise bilinears, we have

$$((\Pi u - u)_y, \chi_y) = ((\Pi_y \Pi_x u - u)_y, \chi_y) = ((\Pi_x u - u)_y, \chi_y) \quad (2.22)$$

$$= (\Pi_x(u_y) - u_y, \chi_y) \quad (2.23)$$

Then by Remark 2.3 and repeating the proof of Lemma 2.9 for u_y , we have

$$((\Pi u - u)_y, \chi_y) \leq \|\Pi_x(u_y) - u_y\| \|\chi_y\| \leq C N_x^{-2} \ln^2 N_x \|(\Pi u - u^h)_y\|. \quad (2.24)$$

Similarly,

$$\varepsilon^2((\Pi u - u)_x, (\Pi u - u^h)_x) = \varepsilon^2(\Pi_y(u_x) - u_x, \chi_x) \leq C N_x^{-2} \ln^2 N_x \|\varepsilon(\Pi u - u^h)_x\|, \quad (2.25)$$

where one ε is combined into u_x . Also

$$(\bar{a}(\Pi u - u), \chi) \leq C \|\bar{a}\|_{\infty, \Omega} \|\Pi u - u\| \|\chi\| \leq C \|\Pi u - u\|_{\infty, \bar{\Omega}} \|\chi\| \quad (2.26)$$

$$\leq C N_x^{-2} \ln^2 N_x \|\Pi u - u^h\|, \quad (2.27)$$

where in the last step we used Lemma 2.10. On the other hand,

$$\begin{aligned} \bar{B}(u - u^h, \Pi u - u^h) &= (\bar{B} - B)(u, \Pi u - u^h) + B(u, \Pi u - u^h) - \bar{B}(u^h, \Pi u - u^h) \\ &= ((\bar{a} - a)u, \Pi u - u^h) + (f - \bar{f}, \Pi u - u^h) \end{aligned} \quad (2.28)$$

$$\leq C(\|\bar{a} - a\|_{\infty, \Omega} + \|f - \bar{f}\|_{\infty, \Omega}) \|\Pi u - u^h\|. \quad (2.29)$$

Combining the above inequalities, we have

$$|||\Pi u - u^h||| \leq C(N_x^{-2} \ln^2 N_x + k^2) .$$

Therefore, by the triangular inequality and Lemma 2.10,

$$\|u - u^h\| \leq \|u - \Pi u\| + \|\Pi u - u^h\| \leq \|u - \Pi u\|_{\infty, \bar{\Omega}} + C|||\Pi u - u^h||| \quad (2.30)$$

$$\leq C(N_x^{-2} \ln^2 N_x + k^2) , \quad (2.31)$$

which concludes our proof.

2.5 Numerical Results

In this section we present a numerical example applied to problem (2.1)-(2.2), where $a = 2$ and f is chosen appropriately so that the solution of (2.1)-(2.2) is given by

$$u(x, y) = \left(1 - \frac{e^{-x/\varepsilon} + e^{-(1-x)/\varepsilon}}{1 + e^{-1/\varepsilon}} + x(1-x)\right)y(1-y)$$

This u has the typical boundary layer behavior at the sides $x=0$ and $x=1$.

We choose the bilinear interpolation Πf of f as \bar{f} and $N_x = N_y = N$. Our results are shown in Table 2.1 and 2.2.

Our results present the uniform convergence rate (i.e. independent of ε) both in L^2 norm and L^∞ norm very well.

Let e_ε^N be the L^2 error between the exact solution $u(x, y)$ and the computed solution $u^h(x, y)$. The computed convergence rate can be obtained by

$$R_\varepsilon^N = (\ln e_\varepsilon^{2N} - \ln e_\varepsilon^N) / \ln\left(\frac{\ln(2N)}{2 \ln N}\right) . \quad (2.32)$$

See Table 2.3. From which we see that $u^h(x, y)$ approximates $u(x, y)$ with a uniform convergence rate of order $O(N^{-2} \ln^2 N)$ in L^2 norm, which is consistent with our theoretical analysis. The classical convergence rate $\tilde{R}_\varepsilon^N = (\ln e_\varepsilon^{2N} - \ln e_\varepsilon^N) / \ln(1/2)$ is presented in Table 2.4.

Table 2.1: Errors in L^2 norm

	N		
ϵ	12	24	48
1.0D-01	1.53773D-03	3.56846D-04	8.64822D-05
1.0D-02	3.82665D-03	1.18212D-03	3.58286D-04
1.0D-03	4.41492D-03	1.43246D-03	4.78893D-04
1.0D-04	4.49223D-03	1.47031D-03	4.99116D-04
1.0D-05	4.50080D-03	1.47433D-03	5.01235D-04
1.0D-06	4.50837D-03	1.47591D-03	5.01652D-04

Table 2.2: Errors in L^∞ norm

	N		
ϵ	12	24	48
1.0D-01	4.56598D-03	1.02124D-03	2.40876D-04
1.0D-02	1.47783D-02	6.77789D-03	2.57586D-03
1.0D-03	1.48926D-02	6.77504D-03	2.97576D-03
1.0D-04	1.49056D-02	6.77498D-03	3.14068D-03
1.0D-05	1.49069D-02	6.77498D-03	3.15773D-03
1.0D-06	1.49070D-02	6.77498D-03	3.16237D-03

Table 2.3: Convergence rates R_ϵ^N in L^2 norm

ϵ	N	
	12	24
1.0D-01	3.2672	2.8584
1.0D-02	2.6273	2.4074
1.0D-03	2.5175	2.2097
1.0D-04	2.4980	2.1789
1.0D-05	2.4962	2.1758
1.0D-06	2.4976	2.1763

Table 2.4: Convergence rates \tilde{R}_ϵ^N in L^∞ norm

ϵ	N	
	12	24
1.0D-01	2.1074	2.9132
1.0D-02	1.6947	1.9512
1.0D-03	1.6239	1.6593
1.0D-04	1.6113	1.5505
1.0D-05	1.6101	1.5395
1.0D-06	1.6110	1.5366

CHAPTER 3

THE REACTION-DIFFUSION MODEL

3.1 Introduction

In this chapter, we consider the following singularly perturbed elliptic boundary value problem:

$$L_\varepsilon u \equiv -\varepsilon^2 \left(\frac{\partial^2 u}{\partial x^2} + \frac{\partial^2 u}{\partial y^2} \right) + a(x, y)u = f(x, y) \quad \text{in } \Omega, \quad (3.1)$$

$$u = 0 \quad \text{on } \partial\Omega, \quad (3.2)$$

which is the so-called *reaction-diffusion* model problem. Here the functions a and f are assumed to be sufficiently smooth in Ω and

$$a(x, y) \geq \alpha^2 > 0 \quad \text{in } \Omega.$$

3.2 The Asymptotic Expansion

In this section, we will present the Butuzov asymptotic expansion [18, 49, 129]. This section is based mostly on Han *et al.* [49].

We start with the "outer expansion". Let $u_0(x, y) = f(x, y)/a(x, y)$, $u_1(x, y) = 0$ and $u_i(x, y) = \Delta u_{i-2}(x, y)/a(x, y)$ for $i \geq 2$. Hence $u_i = 0$ for odd i and

$$L_\varepsilon u_i = -\varepsilon^2 \Delta u_i + \Delta u_{i-2}, \quad i = 2, 4, \dots,$$

where Δ is the Laplacian operator. Let

$$U_{2n}(x, y) = \sum_{i=0}^{2n} \varepsilon^i u_i(x, y)$$

Since $u - U_{2n}$ is not small on $\partial\Omega$, we have to introduce the boundary layer functions to correct the discrepancy between the boundary data and the boundary values of the reduced problem near the four boundary sides. Han *et al.* [49, pp. 396-397] constructed the following boundary layer functions:

$$\begin{aligned} V_{2n}(x, \eta) &= \sum_{i=0}^{2n} \varepsilon^i v_i(x, \eta) \quad \text{at side } y=0, \text{ where } \eta = y/\varepsilon, \\ W_{2n}(\xi, y) &= \sum_{i=0}^{2n} \varepsilon^i w_i(\xi, y) \quad \text{at side } x=0, \text{ where } \xi = x/\varepsilon, \\ \bar{V}_{2n}(x, \bar{\eta}) &= \sum_{i=0}^{2n} \varepsilon^i v_i(x, \bar{\eta}) \quad \text{at side } y=1, \text{ where } \bar{\eta} = (1-y)/\varepsilon, \\ \bar{W}_{2n}(\bar{\xi}, y) &= \sum_{i=0}^{2n} \varepsilon^i w_i(\bar{\xi}, y) \quad \text{at side } x=1, \text{ where } \bar{\xi} = (1-x)/\varepsilon. \end{aligned}$$

Since the remainder, $u - U_{2n} - V_{2n} - W_{2n} - \bar{V}_{2n} - \bar{W}_{2n}$, is not small near the four vertices of Ω , Han *et al.* [49, pp. 397-398] introduced the following corner layer functions to correct this discrepancy in the boundary data near the four corners:

$$\begin{aligned} Z_{2n}^1(\xi, \eta) &= \sum_{i=0}^{2n} \varepsilon^i z_i^1(\xi, \eta) \quad \text{at corner } (0,0), \text{ where } \xi = x/\varepsilon, \eta = y/\varepsilon, \\ Z_{2n}^2(\bar{\xi}, \eta) &= \sum_{i=0}^{2n} \varepsilon^i z_i^2(\bar{\xi}, \eta) \quad \text{at corner } (1,0), \text{ where } \bar{\xi} = (1-x)/\varepsilon, \eta = y/\varepsilon, \\ Z_{2n}^3(\xi, \bar{\eta}) &= \sum_{i=0}^{2n} \varepsilon^i z_i^3(\xi, \bar{\eta}) \quad \text{at corner } (0,1), \text{ where } \xi = x/\varepsilon, \bar{\eta} = (1-y)/\varepsilon, \\ Z_{2n}^4(\bar{\xi}, \bar{\eta}) &= \sum_{i=0}^{2n} \varepsilon^i z_i^4(\bar{\xi}, \bar{\eta}) \quad \text{at corner } (1,1), \text{ where } \bar{\xi} = (1-x)/\varepsilon, \bar{\eta} = (1-y)/\varepsilon. \end{aligned}$$

Also they proved the following results:

Lemma 3.1 [49, (2.6c) (2.9c)] *For the boundary layer functions defined above, we have:*

$$\begin{aligned}
|V_{2n}(x, \eta)| &\leq Ce^{-\alpha\eta}, \\
|W_{2n}(\xi, y)| &\leq Ce^{-\alpha\xi}, \\
|\bar{V}_{2n}(x, \bar{\eta})| &\leq Ce^{-\alpha\bar{\eta}}, \\
|\bar{W}_{2n}(\bar{\xi}, y)| &\leq Ce^{-\alpha\bar{\xi}}, \\
|Z_{2n}^1(\xi, \eta)| &\leq Ce^{-\alpha(\xi+\eta)}, \\
|Z_{2n}^2(\bar{\xi}, \eta)| &\leq Ce^{-\alpha(\bar{\xi}+\eta)}, \\
|Z_{2n}^3(\xi, \bar{\eta})| &\leq Ce^{-\alpha(\xi+\bar{\eta})}, \\
|Z_{2n}^4(\bar{\xi}, \bar{\eta})| &\leq Ce^{-\alpha(\bar{\xi}+\bar{\eta})},
\end{aligned}$$

Theorem 3.1 [49, Theorem 2.1] *Let u solve (3.1)(3.2). There is a constant $C_n > 0$ that is independent of ε such that*

$$|R_{2n}(x, y)| \leq C_n \varepsilon^{2n+1},$$

where $R_{2n} = u - \tilde{u}_{2n}$ denote the remainder in the asymptotic expansion

$$\tilde{u}_{2n} = U_{2n} + V_{2n} + W_{2n} + \bar{V}_{2n} + \bar{W}_{2n} + \sum_{l=1}^4 Z_{2n}^l.$$

3.3 Derivative Estimates of the Solution

In this section, we will obtain some derivative estimates for the solution u of (3.1)(3.2). We assume the following compatibility conditions [103, 110]:

$$f(0, 0) = f(0, 1) = f(1, 0) = f(1, 1) = 0,$$

which ensure that the solution of (3.1)(3.2) $u(x, y) \in C^4(\Omega) \cap C^2(\bar{\Omega})$, where $\bar{\Omega} = \Omega \cup \partial\Omega$. Such compatibility conditions are necessary for the pointwise derivative estimates. Here we will make repeated use of the following weak maximum principle:

Theorem 3.2 For any functions $w(x, y) \in C^2(\Omega) \cap C^0(\bar{\Omega})$, if $w \geq 0$ on $\partial\Omega$ and $L_\varepsilon w \geq 0$ on Ω , then $w \geq 0$ on $\bar{\Omega}$.

Proof. It can be proved easily by contradiction, cf. Eckhaus [34, Lemma 6.2.1.1].

By choosing the barrier functions properly, we can obtain the following estimates for the solution u of (3.1)(3.2).

Lemma 3.2

$$\begin{aligned} (I) \quad & |u(x, y)| \leq C(1 - e^{-\frac{\alpha z}{\varepsilon}}) \quad \text{on } \bar{\Omega}, \\ (II) \quad & |u(x, y)| \leq C(1 - e^{-\frac{\alpha(1-z)}{\varepsilon}}) \quad \text{on } \bar{\Omega}, \\ (III) \quad & |u(x, y)| \leq C(1 - e^{-\frac{\alpha y}{\varepsilon}}) \quad \text{on } \bar{\Omega}, \\ (VI) \quad & |u(x, y)| \leq C(1 - e^{-\frac{\alpha(1-y)}{\varepsilon}}) \quad \text{on } \bar{\Omega}. \end{aligned}$$

Proof.(I) Use the barrier function $\phi(x, y) = C(1 - e^{-\frac{\alpha z}{\varepsilon}})$, then we have

$$\begin{aligned} L_\varepsilon(\phi \pm u) &= C\alpha^2 e^{-\frac{\alpha z}{\varepsilon}} + aC(1 - e^{-\frac{\alpha z}{\varepsilon}}) \pm f, \\ &= C(\alpha^2 - a)(e^{-\frac{\alpha z}{\varepsilon}} - 1) + C\alpha^2 \pm f. \end{aligned}$$

Note that

$$(\alpha^2 - a)(e^{-\frac{\alpha z}{\varepsilon}} - 1) \geq 0,$$

Hence

$$L_\varepsilon(\phi \pm u) \geq C\alpha^2 \pm f \geq 0 \quad \text{for } C \text{ sufficiently large,}$$

then from $(\phi \pm u)|_{\partial\Omega} \geq 0$ and Theorem 3.2 concludes our proof.

$$(II) \quad \text{Use the barrier function } \phi(x, y) = C(1 - e^{-\frac{\alpha(1-z)}{\varepsilon}}).$$

$$(III) \quad \text{Use the barrier function } \phi(x, y) = C(1 - e^{-\frac{\alpha y}{\varepsilon}}).$$

$$(VI) \quad \text{Use the barrier function } \phi(x, y) = C(1 - e^{-\frac{\alpha(1-y)}{\varepsilon}}).$$

Lemma 3.3

$$(I) \quad |u_x(x, y)| \leq C\varepsilon^{-1} \quad \text{on } \partial\Omega,$$

$$(II) \quad |u_y(x, y)| \leq C\varepsilon^{-1} \quad \text{on } \partial\Omega.$$

Proof.(I) By Lemma 3.2(I), we have

$$\begin{aligned} |u_x(0, y)| &= \left| \lim_{x \rightarrow 0^+} \frac{u(x, y) - u(0, y)}{x} \right| \leq \lim_{x \rightarrow 0^+} \left| \frac{u(x, y) - u(0, y)}{x} \right| \\ &\leq \lim_{x \rightarrow 0^+} \frac{C(1 - e^{-\frac{\alpha x}{\epsilon}})}{x} = C \frac{\alpha}{\epsilon} \leq C \epsilon^{-1}. \end{aligned}$$

By Lemma 3.2(II), we can get the estimate for $u_x(1, y)$ in a similar way.

Differentiating the given boundary conditions $u(x, y) = 0$ at $y = 0$ and $y = 1$ with respect to x gives us $u_x(x, 0) = u_x(x, 1) = 0$, which concludes our proof.

(II) Use the similar proof as (I) by Lemma 3.2(III) and (VI).

Lemma 3.4

$$(I) \quad |u_x(x, y)| \leq C(1 + \epsilon^{-1}e^{-\frac{\alpha x}{\epsilon}} + \epsilon^{-1}e^{-\frac{\alpha(1-x)}{\epsilon}}) \quad \text{on } \bar{\Omega},$$

$$(II) \quad |u_y(x, y)| \leq C(1 + \epsilon^{-1}e^{-\frac{\alpha y}{\epsilon}} + \epsilon^{-1}e^{-\frac{\alpha(1-y)}{\epsilon}}) \quad \text{on } \bar{\Omega}.$$

Proof.(I) Consider the barrier function $\phi(x, y) = C(1 + \epsilon^{-1}e^{-\frac{\alpha x}{\epsilon}} + \epsilon^{-1}e^{-\frac{\alpha(1-x)}{\epsilon}})$, then we have

$$L_\epsilon(\phi \pm u_x) \geq -\alpha^2 C(\epsilon^{-1}e^{-\frac{\alpha x}{\epsilon}} + \epsilon^{-1}e^{-\frac{\alpha(1-x)}{\epsilon}}) \quad (3.3)$$

$$+ aC(1 + \epsilon^{-1}e^{-\frac{\alpha x}{\epsilon}} + \epsilon^{-1}e^{-\frac{\alpha(1-x)}{\epsilon}}) \pm (f_x - a_x u) \quad (3.4)$$

$$\geq aC \pm (f_x - a_x u) \geq 0 \quad \text{for } C \text{ sufficiently large,} \quad (3.5)$$

and note that $(\phi \pm u_x)|_{\partial\Omega} \geq 0$, which concludes our proof of (I).

(II) To prove (II), use the barrier function $\phi(x, y) = C(1 + \epsilon^{-1}e^{-\frac{\alpha y}{\epsilon}} + \epsilon^{-1}e^{-\frac{\alpha(1-y)}{\epsilon}})$.

Lemma 3.5

$$(I) \quad |u_{xx}(x, y)| \leq C\epsilon^{-2} \quad \text{on } \partial\Omega$$

$$(II) \quad |u_{yy}(x, y)| \leq C\epsilon^{-2} \quad \text{on } \partial\Omega.$$

Proof.(I) Due to the boundary conditions $u(x, y) = 0$ at $y = 0$ and $y = 1$, we have $u_{xx} = 0$ at $y = 0$ and $y = 1$. By setting $x = 0, 1$ in (3.1) and using the fact that $u = u_{yy} = 0$ on the sides of $x = 0$ and $x = 1$, we have $u_{xx} = -f/\epsilon^2$ at $x = 0$ and $x = 1$.

(II) Use a similar proof as in (I).

Lemma 3.6

$$(I) \quad |u_{xx}(x, y)| \leq C(1 + \varepsilon^{-2}e^{\frac{-\alpha x}{\varepsilon}} + \varepsilon^{-2}e^{\frac{-\alpha(1-x)}{\varepsilon}}) \quad \text{on } \bar{\Omega},$$

$$(II) \quad |u_{yy}(x, y)| \leq C(1 + \varepsilon^{-2}e^{\frac{-\alpha y}{\varepsilon}} + \varepsilon^{-2}e^{\frac{-\alpha(1-y)}{\varepsilon}}) \quad \text{on } \bar{\Omega}.$$

Proof.(I) Use the barrier function $\phi(x, y) = C(1 + \varepsilon^{-2}e^{\frac{-\alpha x}{\varepsilon}} + \varepsilon^{-2}e^{\frac{-\alpha(1-x)}{\varepsilon}})$, then

$$\begin{aligned} L_\varepsilon(\phi \pm u_{xx}) &\geq -\alpha^2 C(\varepsilon^{-2}e^{\frac{-\alpha x}{\varepsilon}} + \varepsilon^{-2}e^{\frac{-\alpha(1-x)}{\varepsilon}}) \\ &\quad + aC(1 + \varepsilon^{-2}e^{\frac{-\alpha x}{\varepsilon}} + \varepsilon^{-2}e^{\frac{-\alpha(1-x)}{\varepsilon}}) \pm (f_{xx} - a_{xx}u - 2a_x u_x) \\ &\geq aC \pm (f_{xx} - a_{xx}u - 2a_x u_x) \geq 0 \quad \text{for } C \text{ sufficiently large.} \end{aligned}$$

then from $(\phi \pm u_{xx})|_{\partial\Omega} \geq 0$ and Theorem 3.2 concludes our proof.

(II) Use the barrier function $\phi(x, y) = C(1 + \varepsilon^{-2}e^{\frac{-\alpha y}{\varepsilon}} + \varepsilon^{-2}e^{\frac{-\alpha(1-y)}{\varepsilon}})$.

3.4 Finite Element Method on Shishkin Mesh

To construct a Shishkin mesh, we assume that the positive integers N_x and N_y are divisible by 4. In the x-direction, we first divide the interval $[0, 1]$ into subintervals

$$[0, \sigma_x], \quad [\sigma_x, 1 - \sigma_x], \quad [1 - \sigma_x, 1].$$

Uniform meshes are then used on each subinterval, with $N_x/4$ points on each of $[0, \sigma_x]$ and $[1 - \sigma_x, 1]$, and $N_x/2$ points on $[\sigma_x, 1 - \sigma_x]$. Here σ_x is defined by $\sigma_x = \min\{1/4, 2\alpha^{-1}\varepsilon \ln N_x\}$. More explicitly, we have

$$0 = x_0 < x_1 < \cdots < x_{i_0} < \cdots < x_{N_x - i_0} < \cdots < x_{N_x} = 1,$$

with $i_0 = N_x/4$, $x_{i_0} = \sigma_x$, $x_{N_x - i_0} = 1 - \sigma_x$, and

$$h_i = 4\sigma_x N_x^{-1}, \quad \text{for } i = 1, \dots, i_0, N_x - i_0 + 1, \dots, N_x,$$

$$h_i = 2(1 - 2\sigma_x)N_x^{-1}, \quad \text{for } i = i_0 + 1, \dots, N_x - i_0,$$

where $h_i = x_i - x_{i-1}$.

In the y -direction, we follow the same method described above by dividing the interval $[0, 1]$ into subintervals

$$[0, \sigma_y], \quad [\sigma_y, 1 - \sigma_y], \quad [1 - \sigma_y, 1] .$$

Uniform meshes are then used on each subinterval, with $N_y/4$ points on each of $[0, \sigma_y]$ and $[1 - \sigma_y, 1]$, and $N_y/2$ points on $[\sigma_y, 1 - \sigma_y]$. Here σ_y is defined by $\sigma_y = \min\{1/4, 2\alpha^{-1}\varepsilon \ln N_y\}$. More explicitly, we have

$$0 = y_0 < y_1 < \cdots < y_{j_0} < \cdots < y_{N_y - j_0} < \cdots < y_{N_y} = 1 ,$$

with $j_0 = N_y/4$, $y_{j_0} = \sigma_y$, $y_{N_y - j_0} = 1 - \sigma_y$, and

$$\begin{aligned} k_j &= 4\sigma_y N_y^{-1}, \quad \text{for } j = 1, \dots, j_0, N_y - j_0 + 1, \dots, N_y , \\ k_j &= 2(1 - 2\sigma_y)N_y^{-1}, \quad \text{for } j = j_0 + 1, \dots, N_y - j_0 , \end{aligned}$$

where $k_j = y_j - y_{j-1}$.

We shall assume that

$$\sigma_x = 2\alpha^{-1}\varepsilon \ln N_x \quad \sigma_y = 2\alpha^{-1}\varepsilon \ln N_y .$$

Otherwise $\varepsilon \geq \max(\frac{\alpha}{8 \ln N_x}, \frac{\alpha}{8 \ln N_y})$, which is not a singularly perturbed problem. Then the problem can be analyzed in the classical way, which is not our scope here.

The weak formulation of (3.1) is: find $u \in H_0^1(\Omega)$ such that

$$B(u, v) \equiv (\varepsilon^2 u_x, v_x) + (\varepsilon^2 u_y, v_y) + (au, v) = (f, v), \quad \forall v \in H_0^1(\Omega), \quad (3.6)$$

where (\cdot, \cdot) denotes the usual $L^2(\Omega)$ inner product.

Denote the weighted energy norm

$$|||v||| \equiv \{\varepsilon^2 \|v_x\|^2 + \varepsilon^2 \|v_y\|^2 + \|v\|^2\}^{1/2}, \quad \forall v \in H_0^1(\Omega).$$

Note that

$$\begin{aligned}
B(v, v) &= \varepsilon^2 \|v_x\|^2 + \varepsilon^2 \|v_y\|^2 + (av, v) \\
&\geq \min(1, \alpha^2) (\varepsilon^2 \|v_x\|^2 + \varepsilon^2 \|v_y\|^2 + \|v\|^2) \\
&= \min(1, \alpha^2) \|v\|^2
\end{aligned}$$

and by the Cauchy-Schwarz inequality

$$\begin{aligned}
B(v, w) &\leq \varepsilon^2 \|v_x\| \|w_x\| + \varepsilon^2 \|v_y\| \|w_y\| + (\max_{(x,y) \in \bar{\Omega}} a) \|v\| \|w\| \\
&\leq \|v\| \|w\| + \|v\| \|w\| + (\max_{(x,y) \in \bar{\Omega}} a) \|v\| \|w\| \\
&= (2 + \max_{(x,y) \in \bar{\Omega}} a) \|v\| \|w\|.
\end{aligned}$$

Note that the mapping $v \rightarrow (f, v)$ is a bounded functional on H_0^1 . Combining this fact with the above two inequalities, the Lax-Milgram lemma tells us that (3.6) has a unique solution $u(x, y)$ in $H_0^1(\Omega)$.

We seek the bilinear finite element solution $u^h \in S_h(\Omega)$ such that

$$\bar{B}(u^h, v) \equiv (\varepsilon^2 u_x^h, v_x) + (u_y^h, v_y) + (\bar{a} u^h, v) = (\bar{f}, v), \quad \forall v \in S_h(\Omega), \quad (3.7)$$

where \bar{a} and \bar{f} denote some piecewise polynomial approximation of a and f respectively such that

$$\|(\bar{a} - a)\|_{\infty, \bar{\Omega}} \leq C(h^p + k^p), \quad (3.8)$$

and

$$\|(\bar{f} - f)\|_{\infty, \bar{\Omega}} \leq C(h^p + k^p), \quad (3.9)$$

where p is the approximation order.

3.5 Theoretical Results

Let us first prove some error estimates for the solution u of (3.1)(3.2).

Lemma 3.7 *For the solution u of (3.1)(3.2) and any integer $n \geq 0$, we have*

$$(I) \quad \|u - \Pi_x u\|_{\infty, \bar{I}_i} \leq C(N_x^{-2} \ln^2 N_x + \varepsilon^{2n+1}), \quad \forall i = 1, \dots, N_x, \quad (3.10)$$

$$(II) \quad \|u - \Pi_y u\|_{\infty, \bar{K}_j} \leq C(N_y^{-2} \ln^2 N_y + \varepsilon^{2n+1}), \quad \forall j = 1, \dots, N_y. \quad (3.11)$$

Proof. First, for $i = 1, \dots, i_0, N_x - i_0 + 1, \dots, N_x$, by Lemma 3.6 and Lemma 2.7, we have

$$\begin{aligned} \|u - \Pi_x u\|_{\infty, \bar{I}_i} &\leq C h_i^2 \|u_{xx}\|_{\infty, \bar{I}_i} \leq C h_i^2 \max_{x \in \bar{I}_i} (1 + \varepsilon^{-2} e^{\frac{-\alpha x}{\varepsilon}} + \varepsilon^{-2} e^{\frac{-\alpha(1-x)}{\varepsilon}}) \\ &\leq C h_i^2 (1 + \varepsilon^{-2}) \leq C N_x^{-2} \ln^2 N_x, \end{aligned}$$

since $h_i = 4\sigma_x/N_x$ in this case. Hence (3.10) is true in this case.

Second, for $i = i_0 + 1, \dots, N_x - i_0$, in this case $[x_{i-1}, x_i] \subseteq [\sigma_x, 1 - \sigma_x]$. Use Theorem 3.1 for $n \geq 0$, we can write $\Pi_x u$ in the form

$$\Pi_x u = \Pi_x U_{2n} + \Pi_x V_{2n} + \Pi_x W_{2n} + \Pi_x \bar{V}_{2n} + \Pi_x \bar{W}_{2n} + \Pi_x \left(\sum_{l=1}^4 Z_{2n}^l \right) + \Pi_x R_{2n}$$

where $\Pi_x U_{2n}, \Pi_x V_{2n}, \Pi_x W_{2n}, \Pi_x \bar{V}_{2n}, \Pi_x \bar{W}_{2n}, \Pi_x (\sum_{l=1}^4 Z_{2n}^l)$ and $\Pi_x R_{2n}$ denote the linear interpolation in x-direction to $U_{2n}, V_{2n}, W_{2n}, \bar{V}_{2n}, \bar{W}_{2n}, \sum_{l=1}^4 Z_{2n}^l$ and R_{2n} respectively.

Note that $U_{2n}(x, y) = \sum_{i=0}^{2n} \varepsilon^i u_i(x, y)$ and $u_i(x, y)$ is independent of ε , we have

$$\|U_{2n} - \Pi_x U_{2n}\|_{\infty, \bar{I}_i} \leq C h_i^2 \|(U_{2n})_{xx}\|_{\infty, \bar{I}_i} \leq C N_x^{-2},$$

where in the last step we use the fact that $N_x^{-1} \leq h_i \leq 2N_x^{-1}$ for $i = i_0 + 1, \dots, N_x - i_0$.

By Lemma 3.1 and Lemma 2.8,

$$\begin{aligned} \|V_{2n}(x, \frac{y}{\varepsilon}) - \Pi_x V_{2n}(x, \frac{y}{\varepsilon})\|_{\infty, \bar{I}_i} &\leq C h_i^2 \|(V_{2n})_{xx}\|_{\infty, \bar{I}_i} \leq C N_x^{-2}, \\ \|\bar{V}_{2n}(x, \frac{(1-y)}{\varepsilon}) - \Pi_x \bar{V}_{2n}(x, \frac{(1-y)}{\varepsilon})\|_{\infty, \bar{I}_i} &\leq C h_i^2 \|(\bar{V}_{2n})_{xx}\|_{\infty, \bar{I}_i} \leq C N_x^{-2}, \\ \|W_{2n}(\frac{x}{\varepsilon}, y) - \Pi_x W_{2n}(\frac{x}{\varepsilon}, y)\|_{\infty, \bar{I}_i} &\leq 2 \|W_{2n}(\frac{x}{\varepsilon}, y)\|_{\infty, \bar{I}_i} \\ &\leq C e^{\frac{-\alpha x_{i-1}}{\varepsilon}} \leq C e^{\frac{-\alpha \sigma_x}{\varepsilon}} = C N_x^{-2}, \end{aligned}$$

and

$$\|\overline{W}_{2n}(\frac{1-x}{\varepsilon}, y) - \Pi_x \overline{W}_{2n}(\frac{1-x}{\varepsilon}, y)\|_{\infty, \tilde{I}_i} \quad (3.12)$$

$$\leq 2\|\overline{W}_{2n}(\frac{1-x}{\varepsilon}, y)\|_{\infty, \tilde{I}_i} \leq Ce^{\frac{-\alpha(1-x_i)}{\varepsilon}} \leq Ce^{\frac{-\alpha\sigma_x}{\varepsilon}} = CN_x^{-2}, \quad (3.13)$$

Similarly by Lemma 3.1 and Lemma 2.8, we have

$$\|Z_{2n}^1(\frac{x}{\varepsilon}, \frac{y}{\varepsilon}) - \Pi_x Z_{2n}^1(\frac{x}{\varepsilon}, \frac{y}{\varepsilon})\|_{\infty, \tilde{I}_i} \leq 2\|Z_{2n}^1(\frac{x}{\varepsilon}, \frac{y}{\varepsilon})\|_{\infty, \tilde{I}_i} \leq Ce^{\frac{-\alpha z_i - 1}{\varepsilon}} \leq Ce^{\frac{-\alpha\sigma_x}{\varepsilon}} = CN_x^{-2},$$

$$\begin{aligned} & \|Z_{2n}^2(\frac{1-x}{\varepsilon}, \frac{y}{\varepsilon}) - \Pi_x Z_{2n}^2(\frac{1-x}{\varepsilon}, \frac{y}{\varepsilon})\|_{\infty, \tilde{I}_i} \\ & \leq 2\|Z_{2n}^2(\frac{1-x}{\varepsilon}, \frac{y}{\varepsilon})\|_{\infty, \tilde{I}_i} \leq Ce^{\frac{-\alpha(1-x_i)}{\varepsilon}} \leq Ce^{\frac{-\alpha\sigma_x}{\varepsilon}} = CN_x^{-2}, \end{aligned}$$

$$\begin{aligned} & \|Z_{2n}^3(\frac{x}{\varepsilon}, \frac{1-y}{\varepsilon}) - \Pi_x Z_{2n}^3(\frac{x}{\varepsilon}, \frac{1-y}{\varepsilon})\|_{\infty, \tilde{I}_i} \\ & \leq 2\|Z_{2n}^3(\frac{x}{\varepsilon}, \frac{1-y}{\varepsilon})\|_{\infty, \tilde{I}_i} \leq Ce^{\frac{-\alpha z_i - 1}{\varepsilon}} \leq Ce^{\frac{-\alpha\sigma_x}{\varepsilon}} = CN_x^{-2}, \end{aligned}$$

$$\begin{aligned} & \|Z_{2n}^4(\frac{1-x}{\varepsilon}, \frac{1-y}{\varepsilon}) - \Pi_x Z_{2n}^4(\frac{1-x}{\varepsilon}, \frac{1-y}{\varepsilon})\|_{\infty, \tilde{I}_i} \\ & \leq 2\|Z_{2n}^4(\frac{1-x}{\varepsilon}, \frac{1-y}{\varepsilon})\|_{\infty, \tilde{I}_i} \\ & \leq Ce^{\frac{-\alpha(1-x_i)}{\varepsilon}} \leq Ce^{\frac{-\alpha\sigma_x}{\varepsilon}} = CN_x^{-2}, \end{aligned}$$

and

$$\|R_{2n}(x, y) - \Pi_x R_{2n}(x, y)\|_{\infty, \tilde{I}_i} \leq 2\|R_{2n}\|_{\infty, \tilde{I}_i} \leq C\varepsilon^{2n+1},$$

which concludes the proof of (I).

By symmetry, we can prove (II) in the same way.

Then we have:

Lemma 3.8 *For the solution u of (3.1)(3.2) and any integer $n \geq 0$, we have*

$$\|u - \Pi u\|_{\infty, \bar{\Omega}} \leq C(N_x^{-2} \ln^2 N_x + N_y^{-2} \ln^2 N_y + \varepsilon^{2n+1}).$$

Proof. Using Lemmas 2.6, 2.8 and 3.7, we have

$$\|u - \Pi u\|_{\infty, \bar{\Omega}} \leq \|u - \Pi_x u\|_{\infty, \bar{\Omega}} + \|\Pi_x(u - \Pi_y u)\|_{\infty, \bar{\Omega}} \quad (3.14)$$

$$\leq \|u - \Pi_x u\|_{\infty, \bar{\Omega}} + \|u - \Pi_y u\|_{\infty, \bar{\Omega}} \quad (3.15)$$

$$\begin{aligned} &\leq \max_{1 \leq i \leq N_x} \|u - \Pi_x u\|_{\infty, \bar{I}_i} + \max_{1 \leq j \leq N_y} \|u - \Pi_y u\|_{\infty, \bar{K}_j} \\ &\leq C(N_x^{-2} \ln^2 N_x + N_y^{-2} \ln^2 N_y + \varepsilon^{2n+1}). \end{aligned} \quad (3.16)$$

Theorem 3.3 *Let u_h be the finite element solution of (3.7) and u be the solution of (3.1)(3.2). Assume \bar{a} and \bar{f} satisfy (3.8) and (3.9), then for any integer $n \geq 0$, we have*

$$\|u - u^h\| \leq C(1 + \varepsilon N_x + \varepsilon N_y)(N_x^{-2} \ln^2 N_x + N_y^{-2} \ln^2 N_y + \varepsilon^{2n+1}) + C(h^p + k^p).$$

Proof. Note that

$$C_1 \| \Pi u - u^h \|^2 \leq \bar{B}(\Pi u - u^h, \Pi u - u^h) \quad (3.17)$$

$$= \bar{B}(\Pi u - u, \Pi u - u^h) + \bar{B}(u - u^h, \Pi u - u^h). \quad (3.18)$$

Let $\chi = \Pi u - u^h$, then from (3.7) we have

$$\bar{B}(\Pi u - u, \Pi u - u^h) = \varepsilon^2((\Pi u - u)_x, \chi_x) + \varepsilon^2((\Pi u - u)_y, \chi_y) + (\bar{a}(\Pi u - u), \chi) \quad (3.19)$$

Integrating by parts, we obtain

$$\begin{aligned} \varepsilon^2((\Pi u - u)_x, \chi_x) &= \sum_{1 \leq i \leq N_x, 1 \leq j \leq N_y} \int_{x_{i-1}}^{x_i} \int_{y_{j-1}}^{y_j} \varepsilon^2(\Pi u - u)_x \chi_x dx dy \\ &= \sum_{1 \leq i \leq N_x, 1 \leq j \leq N_y} \int_{y_{j-1}}^{y_j} \varepsilon^2(\Pi u - u)|_{x=x_{i-1}} \chi_x dy \\ &\leq \sum_{1 \leq i \leq N_x, 1 \leq j \leq N_y} \int_{y_{j-1}}^{y_j} |\varepsilon \chi_x| dy \cdot \varepsilon \|\Pi u - u\|_{\infty, \bar{\Omega}} \\ &= \sum_{1 \leq i \leq N_x} \int_0^1 |\varepsilon \chi_x| dy \cdot \varepsilon \|\Pi u - u\|_{\infty, \bar{\Omega}} \\ &= \sum_{1 \leq i \leq N_x} \int_0^1 \int_0^1 |\varepsilon \chi_x| dy dx \cdot \varepsilon \|\Pi u - u\|_{\infty, \bar{\Omega}} \end{aligned}$$

$$\begin{aligned}
&= \varepsilon N_x \|\Pi u - u\|_{\infty, \bar{\Omega}} \cdot \int_0^1 \int_0^1 |\varepsilon \chi_x| \, dy dx, \\
&\leq C \varepsilon N_x (N_x^{-2} \ln^2 N_x + N_y^{-2} \ln^2 N_y + \varepsilon^{2n+1}) \|\varepsilon \chi_x\|, \quad \text{by Lemma 3.8}
\end{aligned}$$

Similarly, we have

$$\varepsilon^2 ((\Pi u - u)_y, \chi_y) \leq C \varepsilon N_y (N_x^{-2} \ln^2 N_x + N_y^{-2} \ln^2 N_y + \varepsilon^{2n+1}) \|\varepsilon \chi_y\| \quad (3.20)$$

Also note that

$$(\bar{a}(\Pi u - u), \chi) \leq C \|\bar{a}\|_{\infty, \bar{\Omega}} \|\Pi u - u\| \|\chi\| \leq C \|\Pi u - u\|_{\infty, \bar{\Omega}} \|\chi\| \quad (3.21)$$

$$\leq C (N_x^{-2} \ln^2 N_x + N_y^{-2} \ln^2 N_y + \varepsilon^{2n+1}) \|\Pi u - u^h\|, \quad (3.22)$$

where in the last step we used Lemma 3.8. On the other hand,

$$\begin{aligned}
\bar{B}(u - u^h, \Pi u - u^h) &= (\bar{B} - B)(u, \Pi u - u^h) + B(u, \Pi u - u^h) - \bar{B}(u^h, \Pi u - u^h) \\
&= ((\bar{a} - a)u, \Pi u - u^h) + (f - \bar{f}, \Pi u - u^h)
\end{aligned} \quad (3.23)$$

$$\leq C (\|\bar{a} - a\|_{\infty, \bar{\Omega}} + \|f - \bar{f}\|_{\infty, \bar{\Omega}}) \|\Pi u - u^h\|. \quad (3.24)$$

Using (3.8)(3.9), (3.17)-(3.24) and Lemma 2.7, we have

$$\|\|\Pi u - u^h\|\| \leq C(1 + \varepsilon N_x + \varepsilon N_y)(N_x^{-2} \ln^2 N_x + N_y^{-2} \ln^2 N_y + \varepsilon^{2n+1}) + C(h^p + k^p).$$

Therefore combining this with Lemma 2.7, we obtain

$$\begin{aligned}
\|u - u^h\| &\leq \|u - \Pi u\| + \|\Pi u - u^h\| \leq \|u - \Pi u\|_{\infty, \bar{\Omega}} + \|\|\Pi u - u^h\|\| \\
&\leq C(1 + \varepsilon N_x + \varepsilon N_y)(N_x^{-2} \ln^2 N_x + N_y^{-2} \ln^2 N_y + \varepsilon^{2n+1}) + C(h^p + k^p).
\end{aligned}$$

which concludes our proof.

Since we are considering singularly perturbed problems, the parameter ε is usually very small. Without loss of generality, we can assume $\varepsilon \leq \max(N_x^{-1}, N_y^{-1})$. Then we obtain the following quasi-optimal uniform convergence result:

Lemma 3.9 *Let u_h be the finite element solution of (3.7) and u be the solution of (3.1)(3.2). Let \bar{a} and \bar{f} be the bilinear interpolation of a and f , respectively. Then we have*

$$\|u - u^h\| \leq C(N_x^{-2} \ln^2 N_x + N_y^{-2} \ln^2 N_y) .$$

Proof. Since \bar{a} and \bar{f} are the bilinear interpolates of a and f respectively, we have $p = 2$ in (3.8)(3.9). We can choose n large enough such that $\varepsilon^{2n+1} \leq \max(N_x^{-2} \ln^2 N_x, N_y^{-2} \ln^2 N_y)$ is satisfied. Using Theorem 3.3 concludes our proof.

Remark 3.1 *When f depends on ε and satisfies the assumptions in Kellogg [62, pp.128], we can see that the above results still hold true by carrying out a similar proof.*

3.6 Numerical Results

To see how our new method performs, we tested here an example problem (3.1)(3.2), where $a = 2$ and f is chosen appropriately such that the solution of (3.1)(3.2) is

$$u(x, y) = \left(1 - \frac{e^{-x/\varepsilon} + e^{-(1-x)/\varepsilon}}{1 + e^{-1/\varepsilon}}\right) \left(1 - \frac{e^{-y/\varepsilon} + e^{-(1-y)/\varepsilon}}{1 + e^{-1/\varepsilon}}\right).$$

This u has the typical boundary layer behavior. Since the exact solution is known, we can measure the errors accurately. We choose a bilinear interpolation Πf of f as \bar{f} and $N_x = N_y = N$. The numerical results of our experiments for values of ε varying from 10^{-8} to 10^{-2} and various mesh resolutions $N \in [12, 96]$ are shown in Table 3.1. They display an uniform convergence (i.e. independent of ε) in L^2 -norm.

The computed solutions u_h were plotted in Figures 3.1-3.3 for $\varepsilon = 10^{-3}, 10^{-5}, 10^{-7}$ and $N=24, 48$. The pointwise errors were plotted in Figures 3.4-3.6 for the same ε and N . From these figures, we see that our method solves this type of problems quite

well. The boundary layers are much sharper and no oscillations are observed near the boundary layers. These phenomena were also observed by Madden *et al.* [80] for FEM on Shishkin meshes for the convection-diffusion problems. But they did not present any theoretical analysis.

To see more accurately the convergence rate, let e_ϵ^N be the L^2 error between the exact solution $u(x, y)$ and the computed solution $u^h(x, y)$. The computed convergence rate can be obtained by (2.32). The results are given in Table 3.2. From Table 3.2, we see that $u^h(x, y)$ approximates $u(x, y)$ with an accuracy order of $O(N^{-2} \ln^2 N)$ in L^2 -norm, which is the same as obtained by our theoretical analysis.

Table 3.1: Errors in L^2 norm

ϵ	N			
	12	24	48	96
1.0D-02	4.08804D-02	1.13088D-02	2.48833D-03	4.14854D-04
1.0D-03	5.01689D-02	1.68489D-02	5.59478D-03	1.79468D-03
1.0D-04	5.12377D-02	1.75666D-02	6.07620D-03	2.10844D-03
1.0D-05	5.13461D-02	1.76404D-02	6.12728D-03	2.14388D-03
1.0D-06	5.13569D-02	1.76478D-02	6.13242D-03	2.14747D-03
1.0D-07	5.13580D-02	1.76486D-02	6.13293D-03	2.14783D-03
1.0D-08	5.13581D-02	1.76487D-02	6.13298D-03	2.14787D-03

Table 3.2: Convergence rates R_ϵ^N in L^2 norm

ϵ	N		
	12	24	48
1.0D-02	2.8741	3.0533	3.3901
1.0D-03	2.4403	2.2234	2.1516
1.0D-04	2.3942	2.1410	2.0029
1.0D-05	2.3895	2.1326	1.9872
1.0D-06	2.3891	2.1317	1.9857
1.0D-07	2.3890	2.1317	1.9855
1.0D-08	2.3890	2.1316	1.9855

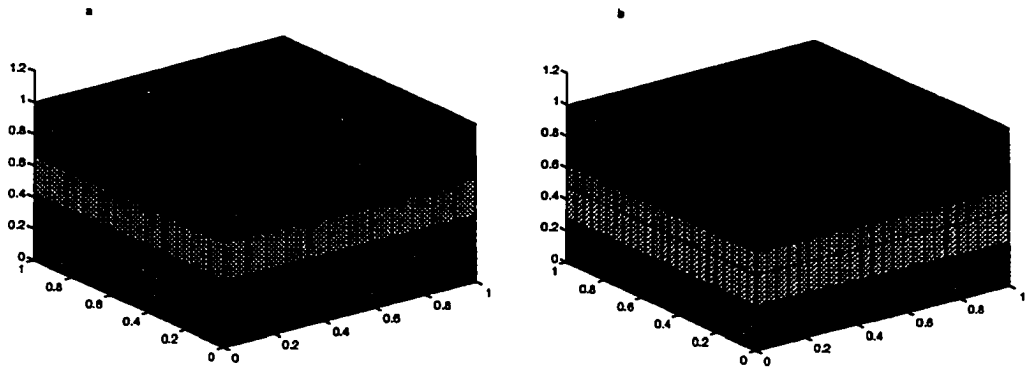


Figure 3.1: Computed FEM solution for $\varepsilon = 1.0D - 03$: (a) $N=24$ (b) $N=48$

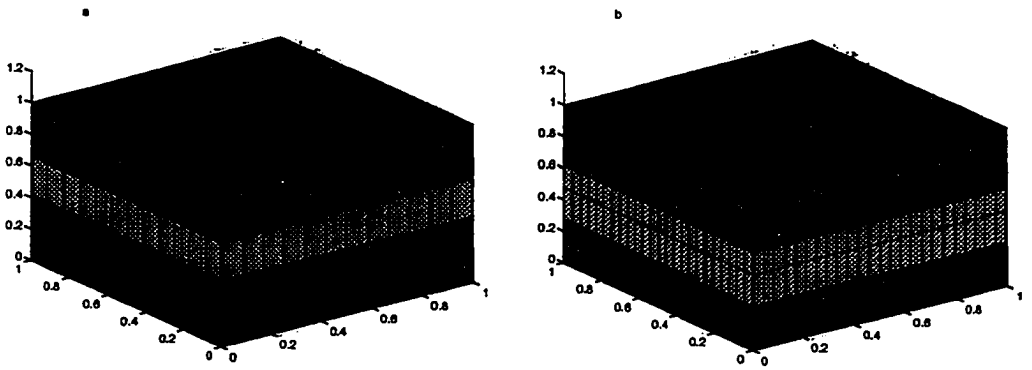


Figure 3.2: Computed FEM solution for $\varepsilon = 1.0D - 05$: (a) $N=24$ (b) $N=48$

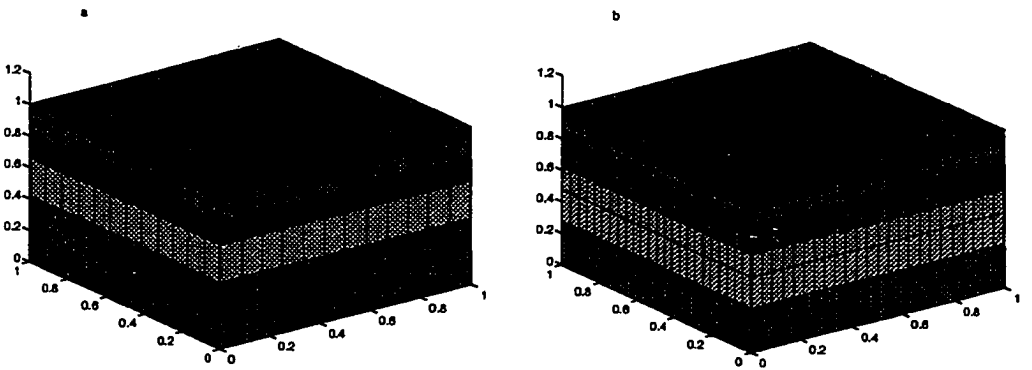


Figure 3.3: Computed FEM solution for $\varepsilon = 1.0D - 07$: (a) $N=24$ (b) $N=48$

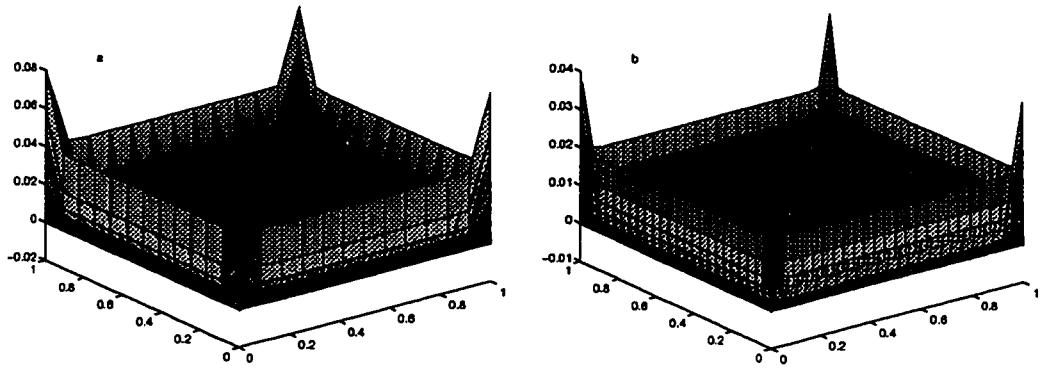


Figure 3.4: Pointwise error $u_h - u$ for $\varepsilon = 1.0D - 03$: (a) $N=24$ (b) $N=48$

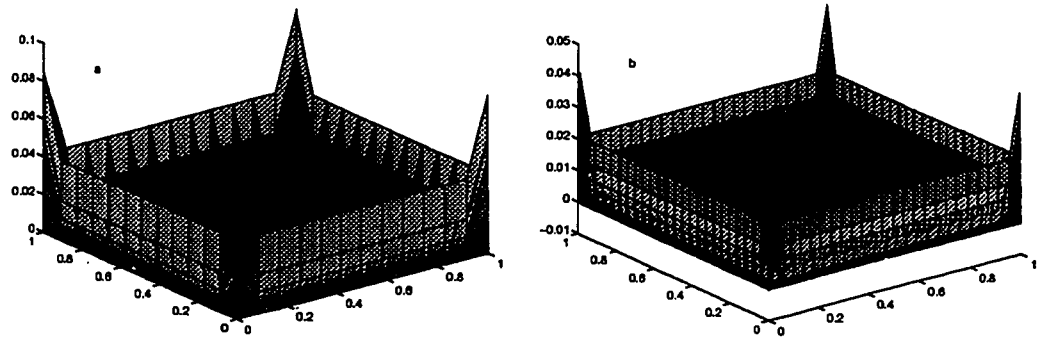


Figure 3.5: Pointwise error $u_h - u$ for $\varepsilon = 1.0D - 05$: (a) $N=24$ (b) $N=48$

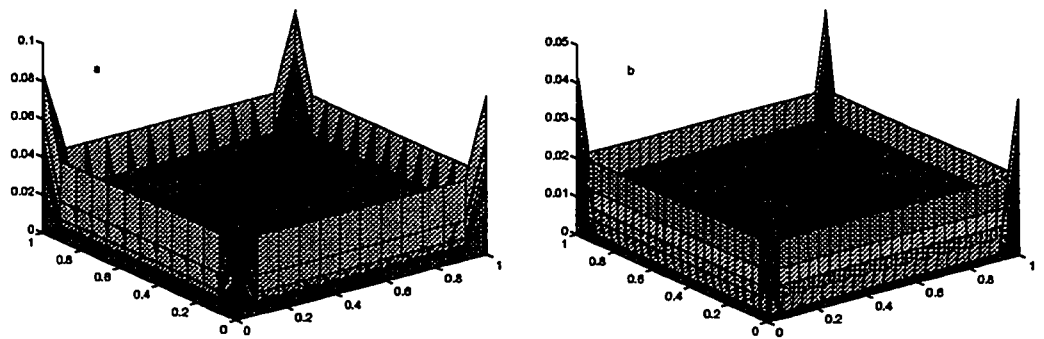


Figure 3.6: Pointwise error $u_h - u$ for $\varepsilon = 1.0D - 07$: (a) $N=24$ (b) $N=48$

CHAPTER 4
THE CONVECTION-DIFFUSION MODEL

4.1 Introduction

In this chapter, we consider the following singularly perturbed problem:

$$-\varepsilon^\alpha \left(\frac{\partial^2 u}{\partial x^2} + \frac{\partial^2 u}{\partial y^2} \right) - b(x, y) \cdot \nabla u + a^\alpha(x, y)u = f(x, y) \quad \text{in } \Omega, \quad (4.1)$$

$$u = 0 \quad \text{on } \partial\Omega, \quad (4.2)$$

which is the so-called *convection-diffusion* model problem. Here ∇u denotes the gradient of u , and $\alpha = 1$ or 2 .

4.2 Exponential Boundary Layer Case

In this section we consider the case of $\alpha = 1$ in (4.1), i.e.:

$$-\varepsilon \left(\frac{\partial^2 u}{\partial x^2} + \frac{\partial^2 u}{\partial y^2} \right) - b \cdot \nabla u + au = f(x, y) \quad \text{in } \Omega, \quad (4.3)$$

$$u = 0 \quad \text{on } \partial\Omega, \quad (4.4)$$

To avoid lengthy technicalities, we assume that the coefficients a and $b = (b_1, b_2)$ are positive constants. For variable coefficients, a similar discussion can be carried out as in Chapter 3.

4.2.1 Derivative Estimates of the Solution

In this subsection, we will obtain some derivative estimates for the solution of (4.3)(4.4) under the compatibility conditions [103, 110]:

$$(H^*) \quad f(0, 0) = f(0, 1) = f(1, 0) = f(1, 1) = 0$$

which ensure that the solution of (4.3)(4.4) $u(x, y) \in C^4(\Omega) \cap C^2(\bar{\Omega})$, where $\bar{\Omega} = \Omega \cup \partial\Omega$. O'Riordan and Stynes [103] obtained the derivative estimates for a very similar problem. Hence we will just sketch the proof here.

In this section we will make repeated use of the following weak maximum principle:

Lemma 4.1 *For any functions $w(x, y) \in C^2(\Omega) \cap C^0(\bar{\Omega})$, if $w \geq 0$ on $\partial\Omega$ and $L_\varepsilon w \geq 0$ on Ω , then $w \geq 0$ on $\bar{\Omega}$.*

Proof. It can be proved easily by contradiction, cf. Eckhaus [34, Lemma 6.2.1.1].

By choosing the barrier functions [72, 103] properly, we can obtain the following estimates for the solution u of (4.3)(4.4).

Lemma 4.2

- (I) $|u(x, y)| \leq C(1 - e^{-\frac{2b_1 x}{\varepsilon}})$ on $\bar{\Omega}$,
- (II) $|u(x, y)| \leq C(1 - x)$ on $\bar{\Omega}$,
- (III) $|u(x, y)| \leq C(1 - e^{-\frac{2b_2 y}{\varepsilon}})$ on $\bar{\Omega}$,
- (IV) $|u(x, y)| \leq C(1 - y)$ on $\bar{\Omega}$.

Proof.(I) Using the barrier function $\phi(x, y) = C(1 - e^{-\frac{2b_1 x}{\varepsilon}})$, we have

$$\begin{aligned} L_\varepsilon(\phi \pm u) &= C4b_1^2\varepsilon^{-1}e^{-\frac{2b_1 x}{\varepsilon}} - 2b_1^2C\varepsilon^{-1}e^{-\frac{2b_1 x}{\varepsilon}} + aC(1 - e^{-\frac{2b_1 x}{\varepsilon}}) \pm f, \\ &= C(2b_1^2\varepsilon^{-1} - a)e^{-\frac{2b_1 x}{\varepsilon}} + aC \pm f \\ &\geq 0, \quad \text{for sufficiently large } C, \end{aligned}$$

where we used the fact that ε is very small. Then from $(\phi \pm u)|_{\partial\Omega} \geq 0$ and Lemma 4.1 we conclude our proof.

(II) Use the barrier function $\phi(x, y) = C(1 - x)$.

(III) Use the barrier function $\phi(x, y) = C(1 - e^{-\frac{2b_2 y}{\varepsilon}})$.

(IV) Use the barrier function $\phi(x, y) = C(1 - y)$.

Lemma 4.3

$$(I) \quad |u_x(x, y)| \leq C\varepsilon^{-1} \quad \text{on } \partial\Omega,$$

$$(II) \quad |u_y(x, y)| \leq C\varepsilon^{-1} \quad \text{on } \partial\Omega.$$

Proof.(I) By Lemma 4.2(I), we have

$$\begin{aligned} |u_x(0, y)| &= \left| \lim_{x \rightarrow 0^+} \frac{u(x, y) - u(0, y)}{x} \right| \leq \lim_{x \rightarrow 0^+} \left| \frac{u(x, y) - u(0, y)}{x} \right| \\ &\leq \lim_{x \rightarrow 0^+} \frac{C(1 - e^{-\frac{2b_1 x}{\varepsilon}})}{x} = \frac{2b_1 C}{\varepsilon}. \end{aligned}$$

Similarly, by Lemma 4.2(II), we have

$$\begin{aligned} |u_x(1, y)| &= \left| \lim_{x \rightarrow 1^-} \frac{u(1, y) - u(x, y)}{(1-x)} \right| \leq \lim_{x \rightarrow 1^-} \left| \frac{u(1, y) - u(x, y)}{(1-x)} \right| \\ &\leq \lim_{x \rightarrow 1^-} \frac{C(1-x)}{(1-x)} = C. \end{aligned}$$

Using the given boundary condition (4.2), we have $u_x(x, 0) = u_x(x, 1) = 0$, which concludes our proof.

(II) Use a similar proof as in (I) by Lemma 4.2(III) and (IV).

Lemma 4.4

$$(I) \quad |u_x(x, y)| \leq C(1 + \varepsilon^{-1} e^{-\frac{b_1 x}{\varepsilon}}) \quad \text{on } \bar{\Omega},$$

$$(II) \quad |u_y(x, y)| \leq C(1 + \varepsilon^{-1} e^{-\frac{b_2 y}{\varepsilon}}) \quad \text{on } \bar{\Omega}.$$

Proof.(I) Consider the barrier function $\phi(x, y) = C(1 + \varepsilon^{-1} e^{-\frac{b_1 x}{\varepsilon}})$, then we have

$$\begin{aligned} L_\varepsilon(\phi \pm u_x) &= aC(1 + \varepsilon^{-1} e^{-\frac{b_1 x}{\varepsilon}}) \pm f_x \\ &\geq 0 \quad \text{for sufficiently large } C, \end{aligned}$$

and note that $(\phi \pm u_x)|_{\partial\Omega} \geq 0$, which concludes our proof of (I).

(II) To prove (II), we use the barrier function $\phi(x, y) = C(1 + \varepsilon^{-1} e^{-\frac{b_2 y}{\varepsilon}})$.

Lemma 4.5

$$(I) \quad |u_{xx}(x, y)| \leq C\varepsilon^{-2} \quad \text{on } \partial\Omega$$

$$(II) \quad |u_{yy}(x, y)| \leq C\varepsilon^{-2} \quad \text{on } \partial\Omega.$$

Proof.(I) From the boundary condition (4.4), we have $u_{xx}|_{y=0,1} = 0$. From equation (4.3) and boundary condition (4.2), we obtain $u_{xx}|_{x=0,1} = -\varepsilon^{-1}(f + b_1 u_x)|_{x=0,1} \leq C\varepsilon^{-2}$.

(II) Use a similar proof as in (I).

Lemma 4.6

$$(I) \quad |u_{xx}(x, y)| \leq C(1 + \varepsilon^{-2}) \text{ on } \bar{\Omega},$$

$$(II) \quad |u_{yy}(x, y)| \leq C(1 + \varepsilon^{-2}) \text{ on } \bar{\Omega}.$$

Proof.(I) Use the barrier function $\phi(x, y) = C(1 + \varepsilon^{-2})$, then

$$\begin{aligned} L_\varepsilon(\phi \pm u_{xx}) &= aC(1 + \varepsilon^{-2}) \pm f_{xx} \\ &\geq 0 \text{ for sufficiently large } C. \end{aligned}$$

then using $(\phi \pm u_{xx})|_{\partial\Omega} \geq 0$ and Lemma 4.1 concludes our proof.

(II) Use the barrier function $\phi(x, y) = C(1 + \varepsilon^{-2})$.

Remark 4.1 *From the above estimates, we can see that the solution exhibits very sharp boundary layers at $x=0$ and $y=0$, which can also be seen by carrying out an asymptotic expansion to be presented in the next subsection.*

4.2.2 The Asymptotic Expansion

In this subsection, we will use the general asymptotic expansion method developed by Vishik and Lyusternik [131] to develop an asymptotic expansion for problem (4.3)(4.4). Roos *et al.* [110, pp.183] sketched its asymptotic expansion very briefly. Here we will present a more detailed analysis by using the method of Vishik and Lyusternik.

The leading term in the regular part of the asymptotic solution $U(x, y) = \sum_{i=0}^{\infty} \varepsilon^i U_i(x, y)$ is defined by

$$-b \cdot \nabla U_0 + aU_0 = f(x, y) \text{ in } \Omega$$

$$U_0|_{x=1} = U_0|_{y=1} = 0.$$

Since the regular part of the asymptotic expansion generally does not satisfy the boundary conditions at $x=0$ and $y=0$, we have to introduce the boundary layer functions $V(\xi, y) = \sum_{i=0}^{\infty} \varepsilon^i V_i(\xi, y)$ and $W(x, \eta) = \sum_{i=0}^{\infty} \varepsilon^i W_i(x, \eta)$ to eliminate the discrepancies at $x=0$ and $y=0$ respectively, where $\xi = x/\varepsilon$ and $\eta = y/\varepsilon$.

The first two terms of V satisfy the following ordinary differential equations:

$$(V_0)_{\xi\xi} + b_1(V_0)_{\xi} = 0, \quad \text{for } \xi > 0$$

$$V_0|_{\xi=0} = -U_0(0, y), \quad V_0|_{\xi \rightarrow \infty} = 0$$

and

$$(V_1)_{\xi\xi} + b_1(V_1)_{\xi} = b_2(V_0)_y - aV_0, \quad \text{for } \xi > 0$$

$$V_1|_{\xi=0} = -U_1(0, y), \quad V_1|_{\xi \rightarrow \infty} = 0,$$

respectively. From which we obtain the solution $V_0(\xi, y) = -U_0(0, y)e^{-b_1\xi}$.

Similarly, we can obtain $W_0(x, \eta) = -U_0(x, 0)e^{-b_2\eta}$.

Note that $u - U - V - W$ is not small near the corner $(0,0)$ since the boundary layer terms overlay there. We need a corner layer function $Z(\xi, \eta) = \sum_{i=0}^{\infty} \varepsilon^i Z_i(\xi, \eta)$, to compensate for this discrepancy. The first two terms satisfy the following equations:

$$(Z_0)_{\xi\xi} + (Z_0)_{\eta\eta} + b_1(Z_0)_{\xi} + b_2(Z_0)_{\eta} = 0, \quad \forall \xi > 0, \eta > 0,$$

$$Z_0|_{\xi=0} = -(U_0 + V_0 + W_0)|_{\xi=0}, \quad Z_0|_{\eta=0} = -(U_0 + V_0 + W_0)|_{\eta=0}$$

$$Z_0 \rightarrow 0 \quad \text{as } \xi \rightarrow \infty, \eta \rightarrow \infty.$$

and

$$(Z_1)_{\xi\xi} + (Z_1)_{\eta\eta} + b_1(Z_1)_{\xi} + b_2(Z_1)_{\eta} = aZ_0, \quad \forall \xi > 0, \eta > 0,$$

$$Z_1|_{\xi=0} = -(U_1 + V_1 + W_1)|_{\xi=0}, \quad Z_1|_{\eta=0} = -(U_1 + V_1 + W_1)|_{\eta=0}$$

$$Z_1 \rightarrow 0 \quad \text{as } \xi \rightarrow \infty, \eta \rightarrow \infty$$

from which we obtain $Z_0(\xi, \eta) = U_0(0, 0)e^{-b_1\xi}e^{-b_2\eta}$.

Lemma 4.7 *Let u be the solution of (4.3)(4.4) and $U_0 \in C^2(\bar{\Omega})$, then*

$$|R(x, y)| \leq C\varepsilon, \quad \text{for all } (x, y) \in \bar{\Omega} \equiv \Omega \cup \partial\Omega,$$

where $R(x, y) = u(x, y) - u_{as}(x, y)$ denotes the remainder in the asymptotic expansion

$$u_{as}(x, y) = U_0(x, y) + V_0(\xi, y) + W_0(x, \eta) + Z_0(\xi, \eta).$$

Proof. Consider the auxiliary asymptotic expansion

$$\bar{u}_{as}(x, y) = U_0(x, y) + V_0(\xi, y) + \varepsilon V_1(\xi, y) + W_0(x, \eta) + \varepsilon W_1(x, \eta) + Z_0(\xi, \eta) + \varepsilon Z_1(\xi, \eta)$$

then from the above construction of these functions, we can find that

$$L_\varepsilon \bar{u}_{as} \leq C\varepsilon \quad \text{and} \quad |\bar{u}_{as}|_{\partial\Omega} \leq C\varepsilon.$$

Consider the barrier function $\phi = C\varepsilon$, we have

$$L_\varepsilon(\phi \pm \bar{u}_{as}) \geq 0 \quad \text{on } \Omega \quad \text{and} \quad (\phi \pm \bar{u}_{as})|_{\partial\Omega} \geq 0,$$

from Lemma 4.1 and this concludes our proof.

4.2.3 Finite Element Method on Shishkin Type Mesh: Case (I)

To construct a Shishkin type mesh, we assume that positive integers N_x and N_y are divisible by 2. In the x-direction, we can construct the Shishkin mesh by dividing the interval $[0, 1]$ into the subintervals $[0, \sigma_x]$ and $[\sigma_x, 1]$. Uniform meshes are then used on each subinterval, each with $N_x/2$ points. Here σ_x is defined by $\sigma_x = \min\{1/2, 2b_1^{-1}\varepsilon \ln N_x\}$. More explicitly, we have

$$0 = x_0 < x_1 < \cdots < x_{i_0} < \cdots < x_{N_x} = 1,$$

with $i_0 = N_x/2$, $x_{i_0} = \sigma_x$, and

$$\begin{aligned} h_i &= 2\sigma_x N_x^{-1}, \text{ for } i = 1, \dots, i_0, \\ h_i &= 2(1 - \sigma_x) N_x^{-1}, \text{ for } i = i_0 + 1, \dots, N_x, \end{aligned}$$

where $h_i = x_i - x_{i-1}$.

In the y-direction, we follow the same way above by dividing the interval $[0, 1]$ into the subintervals $[0, \sigma_y]$ and $[\sigma_y, 1]$. Uniform meshes are then used on each subinterval, each with $N_y/2$ points. Here σ_y is defined by $\sigma_y = \min\{1/2, 2b_2^{-1}\varepsilon \ln N_y\}$. More explicitly, we have

$$0 = y_0 < y_1 < \dots < y_{j_0} < \dots < y_{N_y} = 1,$$

with $j_0 = N_y/2$, $y_{j_0} = \sigma_y$, and

$$\begin{aligned} k_j &= 2\sigma_y N_y^{-1}, \text{ for } j = 1, \dots, j_0, \\ k_j &= 2(1 - \sigma_y) N_y^{-1}, \text{ for } j = j_0 + 1, \dots, N_y, \end{aligned}$$

where $k_j = y_j - y_{j-1}$.

We shall assume that $\sigma_x = 2b_1^{-1}\varepsilon \ln N_x$ and $\sigma_y = 2b_2^{-1}\varepsilon \ln N_y$. Otherwise $\varepsilon \geq \max(\frac{b_1}{4 \ln N_x}, \frac{b_2}{4 \ln N_y})$, in which case ε is not so small, allowing this problem to be analyzed in the classical way, which is not of interest here.

The weak formulation of (4.3) is: find $u \in H_0^1(\Omega)$ such that

$$B(u, v) \equiv (\varepsilon u_x, v_x) + (\varepsilon u_y, v_y) - (b \cdot \nabla u, v) + (au, v) = (f, v), \quad \forall v \in H_0^1(\Omega),$$

where (\cdot, \cdot) denotes the usual $L^2(\Omega)$ inner product.

Denote the weighted energy norm by

$$|||v||| \equiv \{\varepsilon \|v_x\|^2 + \varepsilon \|v_y\|^2 + \|v\|^2\}^{1/2}, \quad \forall v \in H_0^1(\Omega).$$

Note that for any $v \in H_0^1(\Omega)$, we have

$$\begin{aligned} B(v, v) &= (\varepsilon v_x, v_x) + (\varepsilon v_y, v_y) - (b_1 v_x, v) - (b_2 v_y, v) + (av, v) \\ &= \varepsilon \|v_x\|^2 + \varepsilon \|v_y\|^2 + a \|v\|^2 \geq \min(1, a) \|v\|^2. \end{aligned}$$

We seek the bilinear finite element solution $u^h \in S_h(\Omega)$ such that

$$B(u^h, v) \equiv (\varepsilon u_x^h, v_x) + (\varepsilon u_y^h, v_y) - (b \cdot \nabla u^h, v) + (au^h, v) = (\bar{f}, v), \quad \forall v \in S_h(\Omega), \quad (4.5)$$

where \bar{f} denotes the standard bilinear interpolation of f .

4.2.4 Uniform Convergence Analysis

In this subsection, we will use the asymptotic expansion given in subsection 4.2.2 and the technique we used in Chapter 3 to prove that our FEM is first-order uniformly convergent in L^2 norm.

Let us first prove some interpolation estimates for the solution u of (4.3)(4.4).

Lemma 4.8 *For the solution u of (4.3)(4.4), we have*

$$(I) \quad \|u - \Pi_x u\|_{\infty, \bar{I}_i} \leq C(N_x^{-2} \ln^2 N_x + \varepsilon), \quad \forall i = 1, \dots, i_0, \quad (4.6)$$

$$(II) \quad \|u - \Pi_y u\|_{\infty, \bar{K}_j} \leq C(N_y^{-2} \ln^2 N_y + \varepsilon), \quad \forall j = 1, \dots, j_0 \quad (4.7)$$

$$(I') \quad \|u - \Pi_x u\|_{\infty, \bar{I}_i} \leq C(N_x^{-2} + \varepsilon), \quad \forall i = i_0 + 1, \dots, N_x, \quad (4.8)$$

$$(II') \quad \|u - \Pi_y u\|_{\infty, \bar{K}_j} \leq C(N_y^{-2} + \varepsilon), \quad \forall j = j_0 + 1, \dots, N_y. \quad (4.9)$$

Proof. First, for $i = 1, \dots, i_0$, by Lemma 2.7 and Lemma 4.6, we obtain

$$\begin{aligned} \|u - \Pi_x u\|_{\infty, \bar{I}_i} &\leq Ch_i^2 \|u_{xx}\|_{\infty, \bar{I}_i} \\ &\leq Ch_i^2 (1 + \varepsilon^{-2}) \leq CN_x^{-2} \ln^2 N_x, \end{aligned}$$

since $h_i = 2\sigma_x/N_x$ in this case. Hence (I) is true.

Second, for $i = i_0 + 1, \dots, N_x$, in this case $[x_{i-1}, x_i] \subseteq [\sigma_x, 1]$. Use Lemma 4.7, we can write $\Pi_x u$ in the form

$$\Pi_x u = \Pi_x U_0 + \Pi_x V_0 + \Pi_x W_0 + \Pi_x Z_0 + \Pi_x R$$

where $\Pi_x U_0, \Pi_x V_0, \Pi_x W_0, \Pi_x Z_0$ and $\Pi_x R$ denote the linear interpolation in the x -direction to U_0, V_0, W_0, Z_0 and R , respectively.

Note that $U_0(x, y)$ is independent of ε , we have

$$\|U_0 - \Pi_x U_0\|_{\infty, \bar{I}_i} \leq Ch_i^2 \|(U_0)_{xx}\|_{\infty, \bar{I}_i} \leq CN_x^{-2},$$

where in the last step we used the fact that $N_x^{-1} \leq h_i \leq 2N_x^{-1}$ for $i = i_0 + 1, \dots, N_x$.

By Lemma 2.8 and the expression of V_0 , we have

$$\|V_0(\frac{x}{\varepsilon}, y) - \Pi_x V_0(\frac{x}{\varepsilon}, y)\|_{\infty, \bar{I}_i} \leq 2\|V_0(\frac{x}{\varepsilon}, y)\|_{\infty, \bar{I}_i} \leq Ce^{-\frac{b_1 x_{i-1}}{\varepsilon}} \leq Ce^{-\frac{b_1 \sigma_x}{\varepsilon}} = CN_x^{-2},$$

$$\|W_0(x, \frac{y}{\varepsilon}) - \Pi_x W_0(x, \frac{y}{\varepsilon})\|_{\infty, \bar{I}_i} \leq Ch_i^2 \|(W_0)_{xx}\|_{\infty, \bar{I}_i} \leq CN_x^{-2}, \text{ since } e^{-b_2 \eta} \leq 1,$$

$$\begin{aligned} \|Z_0(\frac{x}{\varepsilon}, \frac{y}{\varepsilon}) - \Pi_x Z_0(\frac{x}{\varepsilon}, \frac{y}{\varepsilon})\|_{\infty, \bar{I}_i} &\leq 2\|Z_0(\frac{x}{\varepsilon}, \frac{y}{\varepsilon})\|_{\infty, \bar{I}_i} \\ &\leq Ce^{-\frac{b_1 x_{i-1}}{\varepsilon}} \leq Ce^{-\frac{b_1 \sigma_x}{\varepsilon}} = CN_x^{-2}, \end{aligned}$$

and

$$\|R(x, y) - \Pi_x R(x, y)\|_{\infty, \bar{I}_i} \leq 2\|R\|_{\infty, \bar{I}_i} \leq C\varepsilon,$$

which concludes the proof of (I').

Similarly, we can prove (II) and (II') in the same way by symmetry consideration.

Then we have:

Lemma 4.9 *For the solution u of (4.3)(4.4), we have*

$$(I) \quad \|u - \Pi u\|_{\infty, \bar{\Omega}} \leq C(N_x^{-2} \ln^2 N_x + N_y^{-2} \ln^2 N_y + \varepsilon),$$

$$(II) \quad \|u - \Pi u\|_{\infty, [\sigma_x, 1] \times [\sigma_y, 1]} \leq C(N_x^{-2} + N_y^{-2} + \varepsilon).$$

Proof. Using Lemmas 2.7, 2.8 and 4.8, we have

$$\|u - \Pi u\|_{\infty, \bar{\Omega}} \leq \|u - \Pi_x u\|_{\infty, \bar{\Omega}} + \|\Pi_x(u - \Pi_y u)\|_{\infty, \bar{\Omega}} \quad (4.10)$$

$$\leq \|u - \Pi_x u\|_{\infty, \bar{\Omega}} + \|u - \Pi_y u\|_{\infty, \bar{\Omega}} \quad (4.11)$$

$$\leq \max_{1 \leq i \leq N_x} \|u - \Pi_x u\|_{\infty, \bar{I}_i} + \max_{1 \leq j \leq N_y} \|u - \Pi_y u\|_{\infty, \bar{K}_j},$$

which concludes our proof.

From now on, we denote $\chi = \Pi u - u^h$ and assume

$$(A^*) \quad 0 < C_1 N_x \leq N_y \leq C_2 N_x,$$

$$(B^*) \quad \varepsilon \leq \max(N_x^{-2} \ln^2 N_x, N_y^{-2} \ln^2 N_y),$$

where (A^*) ensures that we have a quasi-uniform mesh [16, pp. 106] away from the boundary layers.

Lemma 4.10 *Let $\tau \equiv [0, h_x] \times [0, h_y]$, then for any $v \in S_h(\Omega)$ we have*

$$(I) \quad \int_{\tau} |v_x| dx dy \leq C(h_y/h_x)^{1/2} \|v\|_{2, \tau},$$

$$(II) \quad \int_{\tau} |v_y| dx dy \leq C(h_x/h_y)^{1/2} \|v\|_{2, \tau}.$$

Proof. (I) This result can be obtained by using the standard homogeneity argument [16]. Let $\bar{\tau} \equiv [0, 1] \times [0, 1]$, so τ can be obtained by the transformation $x = h_x \bar{x}$, $y = h_y \bar{y}$, where $0 \leq \bar{x} \leq 1$, $0 \leq \bar{y} \leq 1$. Hence we have

$$\begin{aligned} \int_{\tau} |v_x| dx dy &= \int_{\bar{\tau}} |v_{\bar{x}}| \frac{1}{h_x} h_x h_y d\bar{x} d\bar{y} = h_y \int_{\bar{\tau}} |v_{\bar{x}}| d\bar{x} d\bar{y} \\ &\leq C h_y \int_{\bar{\tau}} |v| d\bar{x} d\bar{y} = C h_y \int_{\tau} |v| \frac{1}{h_x h_y} dx dy = \frac{C}{h_x} \int_{\tau} |v| dx dy \\ &\leq C h_x^{-1} \|v\|_{2, \tau} (h_x h_y)^{1/2} = C \left(\frac{h_y}{h_x}\right)^{1/2} \|v\|_{2, \tau} \end{aligned}$$

which concludes our proof.

(II) The proof is similar to (I).

Lemma 4.11 *For the solution u of (4.3)(4.4), under the assumptions of (A^*) and (B^*) , we have*

$$(I) \quad \|(b_1(\Pi u - u)_x, \chi)\| \leq C(N_x^{-1} + N_y^{-1})\|\chi\|$$

$$(II) \quad \|(b_2(\Pi u - u)_y, \chi)\| \leq C(N_x^{-1} + N_y^{-1})\|\chi\|$$

Proof. (I) Integrating by parts, we have

$$\begin{aligned} -(b_1(\Pi u - u)_x, \chi) &= (b_1(\Pi u - u), \chi_x) \\ &= \left(\int_{S_1} + \int_{S_2} + \int_{S_3} \right) b_1(\Pi u - u) \chi_x dx dy, \end{aligned}$$

where $S_1 = [0, 1] \times [0, \sigma_y]$, $S_2 = [0, \sigma_x] \times [\sigma_y, 1]$ and $S_3 = [\sigma_x, 1] \times [\sigma_y, 1]$.

Note that

$$\begin{aligned} & \left| \int_{S_1} b_1(\Pi u - u) \chi_x dx dy \right| \leq C \|\Pi u - u\|_{\infty, S_1} \int_{S_1} |\chi_x| dx dy \\ & \leq C(N_x^{-2} \ln^2 N_x + N_y^{-2} \ln^2 N_y + \varepsilon) (\text{Area } S_1)^{1/2} \|\chi_x\| \\ & \leq C(N_x^{-2} \ln^2 N_x + N_y^{-2} \ln^2 N_y + \varepsilon) \ln^{1/2} N_y \|\varepsilon^{1/2} \chi_x\|, \end{aligned}$$

and

$$\begin{aligned} & \left| \int_{S_2} b_1(\Pi u - u) \chi_x dx dy \right| \leq C \|\Pi u - u\|_{\infty, S_2} \int_{S_2} |\chi_x| dx dy \\ & \leq C(N_x^{-2} \ln^2 N_x + N_y^{-2} \ln^2 N_y + \varepsilon) (\text{Area } S_2)^{1/2} \|\chi_x\| \\ & \leq C(N_x^{-2} \ln^2 N_x + N_y^{-2} \ln^2 N_y + \varepsilon) \ln^{1/2} N_x \|\varepsilon^{1/2} \chi_x\|. \end{aligned}$$

Finally, by Lemmas 4.9 and 4.10, we have

$$\begin{aligned} & \left| \int_{S_3} b_1(\Pi u - u) \chi_x dx dy \right| \leq C \|\Pi u - u\|_{\infty, S_3} \int_{S_3} |\chi_x| dx dy \\ & \leq C(N_x^{-2} + N_y^{-2} + \varepsilon) (h_y/h_x)^{1/2} \sum_{\tau \in S_3} \|\chi\|_{2, \tau} \\ & \leq C(N_x^{-2} + N_y^{-2} + \varepsilon) (h_y/h_x)^{1/2} \left(\sum_{\tau \in S_3} \|\chi\|_{2, \tau}^2 \right)^{1/2} \left(\sum_{\tau \in S_3} 1 \right)^{1/2} \\ & \leq C(N_x^{-2} + N_y^{-2} + \varepsilon) N_x \|\chi\|_{2, S_3} \end{aligned}$$

where we used the assumption (A^*) and the fact that

$$N_x^{-1} \leq h_x \leq 2N_x^{-1} \quad \text{and} \quad N_y^{-1} \leq h_y \leq 2N_y^{-1} \quad \text{in } S_3.$$

From the above inequalities and the assumptions of (A^*) and (B^*) , we conclude our proof of (I). Here we used the fact that $0 < \frac{\ln^{2.5} N}{N} < 0.9$ for $N > 1$, since the maximum value is approximately equal to 0.8045, a value attained for $N = 12.1825$.

(II) The proof is similar to (I).

Theorem 4.1 *Let u_h be the finite element solution of (4.5) and u be the solution of (4.3)(4.4). Under the assumption of (A^*) and (B^*) , we have*

$$\|u - u^h\| \leq C(N_x^{-1} + N_y^{-1}).$$

Proof. Note that

$$C_1 \| \Pi u - u^h \|^2 \leq B(\Pi u - u^h, \Pi u - u^h) \quad (4.12)$$

$$= B(\Pi u - u, \Pi u - u^h) + B(u - u^h, \Pi u - u^h). \quad (4.13)$$

By the definition of (4.5), we have

$$B(\Pi u - u, \Pi u - u^h) = \varepsilon(\nabla(\Pi u - u), \nabla \chi) - (b \cdot \nabla(\Pi u - u), \chi) + (a(\Pi u - u), \chi)$$

Integrating by parts, we obtain

$$\begin{aligned} \varepsilon((\Pi u - u)_x, \chi_x) &= \sum_{1 \leq i \leq N_x, 1 \leq j \leq N_y} \int_{x_{i-1}}^{x_i} \int_{y_{j-1}}^{y_j} \varepsilon(\Pi u - u)_x \chi_x dx dy \\ &= \sum_{1 \leq i \leq N_x, 1 \leq j \leq N_y} \int_{y_{j-1}}^{y_j} \varepsilon(\Pi u - u) \Big|_{x=x_{i-1}}^{x=x_i} \chi_x dy, \\ &\leq \sum_{1 \leq i \leq N_x, 1 \leq j \leq N_y} \int_{y_{j-1}}^{y_j} |\varepsilon^{\frac{1}{2}} \chi_x| dy \cdot \varepsilon^{\frac{1}{2}} \|\Pi u - u\|_{\infty, \bar{\Omega}} \\ &= \sum_{1 \leq i \leq N_x} \int_0^1 |\varepsilon^{\frac{1}{2}} \chi_x| dy \cdot \varepsilon^{\frac{1}{2}} \|\Pi u - u\|_{\infty, \bar{\Omega}} \end{aligned}$$

$$\begin{aligned}
&= \sum_{1 \leq i \leq N_x} \int_0^1 \int_0^1 |\varepsilon^{\frac{1}{2}} \chi_x| \, dy dx \cdot \varepsilon^{\frac{1}{2}} \|\Pi u - u\|_{\infty, \bar{\Omega}} \\
&= \varepsilon^{\frac{1}{2}} N_x \|\Pi u - u\|_{\infty, \bar{\Omega}} \cdot \int_0^1 \int_0^1 |\varepsilon^{\frac{1}{2}} \chi_x| \, dy dx, \\
&\leq C \varepsilon^{\frac{1}{2}} N_x (N_x^{-2} \ln^2 N_x + N_y^{-2} \ln^2 N_y + \varepsilon) \|\varepsilon^{\frac{1}{2}} \chi_x\|,
\end{aligned}$$

where we use the fact that χ_x is independent of x in the above proof.

Similarly, we have

$$\varepsilon((\Pi u - u)_y, \chi_y) \leq C \varepsilon^{\frac{1}{2}} N_y (N_x^{-2} \ln^2 N_x + N_y^{-2} \ln^2 N_y + \varepsilon) \|\varepsilon^{\frac{1}{2}} \chi_y\| \quad (4.14)$$

Also note that

$$(a(\Pi u - u), \chi) \leq C \|a\|_{\infty, \bar{\Omega}} \|\Pi u - u\| \|\chi\| \leq C \|\Pi u - u\|_{\infty, \bar{\Omega}} \|\chi\| \quad (4.15)$$

$$\leq C (N_x^{-2} \ln^2 N_x + N_y^{-2} \ln^2 N_y + \varepsilon) \|\Pi u - u^h\|. \quad (4.16)$$

By Lemma 4.11, we have

$$|(b \cdot \nabla(\Pi u - u), \chi)| \leq C (N_x^{-1} + N_y^{-1}) \|\chi\| \quad (4.17)$$

Hence, combining above inequalities with assumptions of (A^*) and (B^*) , we obtain

$$|B(\Pi u - u, \Pi u - u^h)| \leq C (N_x^{-1} + N_y^{-1}) \|\chi\|$$

On the other hand,

$$B(u - u^h, \Pi u - u^h) = (f - \bar{f}, \Pi u - u^h) \quad (4.18)$$

$$\leq C \|f - \bar{f}\|_{\infty, \bar{\Omega}} \|\Pi u - u^h\| \quad (4.19)$$

$$\leq C (N_x^{-2} + N_y^{-2}) \|\Pi u - u^h\|. \quad (4.20)$$

Using (14)-(21), we have

$$\|\|\Pi u - u^h\|\| \leq C (N_x^{-1} + N_y^{-1})$$

Therefore using Lemma 4.9(I), we obtain

$$\|u - u^h\| \leq \|u - \Pi u\| + \|\Pi u - u^h\| \leq \|u - \Pi u\|_{\infty, \bar{\Omega}} + \|\Pi u - u^h\| \quad (4.21)$$

$$\leq C(N_x^{-2} \ln^2 N_x + N_y^{-2} \ln^2 N_y + \varepsilon + N_x^{-1} + N_y^{-1}). \quad (4.22)$$

which concludes our proof.

Remark 4.2 *Unlike the reaction-diffusion type problems [72], we obtain only first-order uniform convergence rate in L^2 norm for the convection-diffusion type problems. This fact was also observed in one space dimension, cf. Kellogg and Stynes [63] and Roos et al. [110]. Since we can not use duality techniques [16] to improve error estimates for singularly perturbed problems, which depend on a small parameter ε .*

4.2.5 Streamline Diffusion Finite Element Methods

In this section, we will present a brief discussion about the widely used streamline diffusion method as presented by Johnson *et al.* [58].

A description of the streamline diffusion finite element method is as follows: Find the bilinear FEM solution $u^h \in S_h(\Omega)$ such that

$$B_{SD}(u^h, v) \equiv \varepsilon(\nabla u^h, \nabla v) + (-b \cdot \nabla u^h + a u^h, v - \delta b \cdot \nabla v) = (\bar{f}, v - \delta b \cdot \nabla v),$$

for $\forall v \in S_h(\Omega)$. Here \bar{f} denotes the standard bilinear interpolation of f .

It is easy to see that for any $v \in S_h$, we have

$$B_{SD}(v, v) = \varepsilon \|\nabla v\|^2 + \delta \|b \cdot \nabla v\|^2 + a \|v\|^2 \equiv \|v\|_{SD}^2. \quad (4.23)$$

Hence

$$\begin{aligned} \|\Pi u - u^h\|_{SD}^2 &\leq B_{SD}(\Pi u - u^h, \Pi u - u^h) \\ &= B_{SD}(\Pi u - u, \chi) + B_{SD}(u - u^h, \chi) \end{aligned}$$

Note that

$$B_{SD}(\Pi u - u, \chi) = B(\Pi u - u, \chi) + (b \cdot \nabla(\Pi u - u), \delta b \cdot \nabla \chi) - (a(\Pi u - u), \delta b \cdot \nabla \chi)$$

and

$$\begin{aligned} B_{SD}(u - u^h, \chi) &= \varepsilon(\nabla u, \nabla \chi) + (-b \cdot \nabla u + au, \chi - \delta b \cdot \nabla \chi) - (\bar{f}, \chi - \delta b \cdot \nabla \chi) \\ &= -\varepsilon(\Delta u, \delta b \cdot \nabla \chi) + (f - \bar{f}, \chi - \delta b \cdot \nabla \chi) \end{aligned}$$

By carrying out a proof similar to that in last section, we can obtain uniform stability for $\|\Pi u - u^h\|_{SD}$ only when $\delta \leq C\varepsilon^n$, where $n > 1$. The different term originates in the perturbation term $\varepsilon(\Delta u, \delta b \cdot \nabla \chi)$. Since

$$|\varepsilon(\Delta u, \delta b \cdot \nabla \chi)| \leq \varepsilon \delta \|\Delta u\| \|b \cdot \nabla \chi\| \leq C\varepsilon \delta \varepsilon^{-3/2} \|b \cdot \nabla \chi\| \leq C\delta \varepsilon^{-1} \|\varepsilon^{1/2} b \cdot \nabla \chi\|,$$

we see that only when $\delta \leq C\varepsilon^n$, $n > 1$ can we obtain the uniform stability.

4.3 Parabolic Boundary Layer Case

In this section, we consider the equation

$$\bar{L}_\varepsilon u \equiv -\varepsilon^2 \left(\frac{\partial^2 u}{\partial x^2} + \frac{\partial^2 u}{\partial y^2} \right) + b \frac{\partial u}{\partial y} + a^2 u = f(x, y) \quad \text{in } \Omega \equiv (0, 1)^2, \quad (4.24)$$

$$u = 0 \quad \text{on } \partial\Omega, \quad (4.25)$$

which corresponds to the case of $\alpha = 2$ in (4.1). For simplicity, we assume that b and a are positive constants. It is easy to see that \bar{L}_ε satisfies the same weak maximum principle. This problem is different from the last one in Section 4.2 in that it has complicated parabolic boundary layers [18, 34, 116, 129, 131] at $x=0$ and $x=1$ except for the ordinary exponential boundary layer at $y=1$.

4.3.1 Derivative Estimates of the Solution

In this subsection, we will obtain some derivative estimates for the solution u of (4.24)(4.25) under compatibility conditions H^* . Since the proofs are very similar to those presented in the last problem, we will just sketch the important steps.

Lemma 4.12

- (I) $|u(x, y)| \leq C(1 - e^{-\frac{2b(1-y)}{\varepsilon^2}})$ on $\bar{\Omega}$,
- (II) $|u(x, y)| \leq Cy$ on $\bar{\Omega}$,
- (III) $|u(x, y)| \leq C(1 - e^{-\frac{a\varepsilon}{\varepsilon}})$ on $\bar{\Omega}$,
- (IV) $|u(x, y)| \leq C(1 - e^{-\frac{a(1-z)}{\varepsilon}})$ on $\bar{\Omega}$.

Proof.(I) Use the barrier function $\phi(x, y) = C(1 - e^{-\frac{2b(1-y)}{\varepsilon^2}})$.

(II) Use the barrier function $\phi(x, y) = Cy$.

(III) Use the barrier function $\phi(x, y) = C(1 - e^{-\frac{a\varepsilon}{\varepsilon}})$.

(IV) Use the barrier function $\phi(x, y) = C(1 - e^{-\frac{a(1-z)}{\varepsilon}})$.

Lemma 4.13

- (I) $|u_y(x, y)| \leq C\varepsilon^{-2}$ on $\partial\Omega$,
- (II) $|u_x(x, y)| \leq C\varepsilon^{-1}$ on $\partial\Omega$.

Proof.(I) By Lemma 4.12(I), we have

$$\begin{aligned} |u_y(x, 1)| &= \left| \lim_{y \rightarrow 1^-} \frac{u(x, 1) - u(x, y)}{(1-y)} \right| \leq \lim_{y \rightarrow 1^-} \left| \frac{u(x, 1) - u(x, y)}{(1-y)} \right| \\ &\leq \lim_{y \rightarrow 1^-} \frac{C(1 - e^{-\frac{2b(1-y)}{\varepsilon^2}})}{(1-y)} = \frac{2bC}{\varepsilon^2}. \end{aligned}$$

The rest of the proof is similar to Lemma 4.2.

Lemma 4.14

- (I) $|u_y(x, y)| \leq C(1 + \varepsilon^{-2} e^{-\frac{b(1-y)}{\varepsilon^2}})$ on $\bar{\Omega}$,
- (II) $|u_x(x, y)| \leq C(1 + \varepsilon^{-1} e^{-\frac{a\varepsilon}{\varepsilon}} + \varepsilon^{-1} e^{-\frac{a(1-z)}{\varepsilon}})$ on $\bar{\Omega}$.

Proof.(I) Consider the barrier function $\phi(x, y) = C(1 + \varepsilon^{-2}e^{-\frac{b(1-y)}{\varepsilon^2}})$.

(II) Consider the barrier function $\phi(x, y) = C(1 + \varepsilon^{-1}e^{-\frac{ax}{\varepsilon}} + \varepsilon^{-1}e^{-\frac{a(1-x)}{\varepsilon}})$.

Lemma 4.15

$$(I) \quad |u_{yy}(x, y)| \leq C\varepsilon^{-4} \quad \text{on } \partial\Omega$$

$$(II) \quad |u_{xx}(x, y)| \leq C\varepsilon^{-2} \quad \text{on } \partial\Omega .$$

Proof.(I) Using the given boundary conditions (4.25), we have $u_{yy}|_{x=0,1} = 0$.

From equation (4.24), we have $u_{yy}|_{y=0,1} = (b\frac{\partial u}{\partial y} - f)/\varepsilon^2|_{y=0,1} \leq C\varepsilon^{-4}$.

(II) Using the given boundary conditions, we obtain $u_{xx}|_{y=0,1} = 0$. From equation (4.24), we have

$$u_{xx}|_{x=0,1} = f/\varepsilon^2|_{x=0,1} \leq C\varepsilon^{-2}.$$

Lemma 4.16

$$(I) \quad |u_{yy}(x, y)| \leq C(1 + \varepsilon^{-4}) \quad \text{on } \bar{\Omega} ,$$

$$(II) \quad |u_{xx}(x, y)| \leq C(1 + \varepsilon^{-2}e^{-\frac{ax}{\varepsilon}} + \varepsilon^{-2}e^{-\frac{a(1-x)}{\varepsilon}}) \quad \text{on } \bar{\Omega} .$$

Proof.(I) Use the barrier function $\phi(x, y) = C(1 + \varepsilon^{-4})$.

(II) Use the barrier function $\phi(x, y) = C(1 + \varepsilon^{-2}e^{-\frac{ax}{\varepsilon}} + \varepsilon^{-2}e^{-\frac{a(1-x)}{\varepsilon}})$.

4.3.2 The Asymptotic Expansion

This subsection is based on the work of Butuzov [18]. Here we will use the zero order of Butuzov asymptotic expansion [18, pp.781, (5)]:

$$u_{as} = u_0(x, y) + Q_0^{(1)}(\xi_1, y) + Q_0^{(2)}(\xi_2, y) + V_0(x, \eta) \quad (4.26)$$

$$+ P_0^{(1)}(\xi_1, \eta) + P_0^{(2)}(\xi_2, \eta) + R_0^{(1)}(\zeta_1, \eta) + R_0^{(2)}(\zeta_2, \eta) , \quad (4.27)$$

where $\xi_1 = \frac{x}{\varepsilon}$, $\xi_2 = \frac{1-x}{\varepsilon}$, $\eta = \frac{1-y}{\varepsilon^2}$, $\zeta_1 = \frac{x}{\varepsilon^2}$ and $\zeta_2 = \frac{1-x}{\varepsilon^2}$.

Lemma 4.17 Assume $f(0,0) = f(1,0) = 0$, then for sufficiently small ε , we have

$$|\Delta(x,y)| \leq C\varepsilon, \quad \forall(x,y) \in \bar{\Omega},$$

where $\Delta(x,y) = u(x,y) - u_{as}(x,y)$ is the remainder of the above asymptotic expansion.

The above result corresponds to the case $n = 0$ in [18, pp.787, Theorem]. In the following we will present additional details for each term.

The regular part u_0 satisfies the following equation [18, pp.781, (6)]:

$$\begin{aligned} b \frac{\partial u_0}{\partial y} + a^2 u_0 &= f, \quad \text{in } \Omega, \\ u_0(x,0) &= 0 \end{aligned}$$

The parabolic layer function $Q_0^{(1)}(\xi_1, y)$ [18, pp.782] at $x=0$ satisfies

$$\begin{aligned} \frac{\partial^2 Q_0^{(1)}}{\partial \xi_1^2} - b \frac{\partial Q_0^{(1)}}{\partial y} - a^2 Q_0^{(1)} &= 0, \\ Q_0^{(1)}(0, y) &= -u_0(0, y), \quad Q_0^{(1)}(\xi_1, 0) = 0, \\ Q_0^{(1)}(\xi_1, y) &\rightarrow 0 \quad \text{as } \xi_1 \rightarrow \infty \end{aligned}$$

Also we have the following estimates [18, pp. 783]:

$$\begin{aligned} \left| \frac{\partial^{2m} Q_0^{(1)}(\xi_1, y)}{\partial \xi_1^{2m}} \right| &\leq C e^{-\alpha \xi_1}, \quad \text{for } \xi_1 \geq 0, 0 \leq y \leq 1, \quad m = 0, 1. \\ \left| \frac{\partial^m Q_0^{(1)}(\xi_1, y)}{\partial y^m} \right| &\leq C e^{-\alpha \xi_1}, \quad \text{for } \xi_1 \geq 0, 0 \leq y \leq 1, \quad m = 0, 1, 2. \end{aligned}$$

For the parabolic layer function $Q_0^{(2)}(\xi_2, y)$ at $x=1$ we have the similar estimates as $Q_0^{(1)}(\xi_1, y)$.

To eliminate the discrepancies introduced by $u_0(x,y)$, $Q_0^{(1)}(\xi_1, y)$ and $Q_0^{(2)}(\xi_2, y)$ at $y=1$, we need to define functions $V_0(x, \eta)$, $P_0^{(1)}(\xi_1, \eta)$ and $P_0^{(2)}(\xi_2, \eta)$ as follows:

The function $V_0(x, \eta)$ satisfies the following equation:

$$\begin{aligned}\frac{\partial^2 V_0}{\partial \eta^2} + b \frac{\partial V_0}{\partial \eta} &= 0, \quad \text{for } \eta > 0 \\ V_0(x, 0) &= -u_0(x, 1)\end{aligned}$$

From which we obtain its solution as $V_0(x, \eta) = -u_0(x, 1)e^{-b\eta}$. Hence we have

$$|V_0(x, \eta)| \leq Ce^{-\alpha\eta}, \quad \text{for } \eta \geq 0$$

The function $P_0^{(1)}(\xi_1, \eta)$ satisfies the following equation:

$$\begin{aligned}\frac{\partial^2 P_0^{(1)}}{\partial \eta^2} + b \frac{\partial P_0^{(1)}}{\partial \eta} &= 0, \quad \text{for } \eta > 0 \\ P_0^{(1)}(\xi_1, 0) &= -Q_0^{(1)}(\xi_1, 1) \\ P_0^{(1)}(\xi_1, \eta) &\rightarrow 0, \quad \text{when } \eta \rightarrow \infty\end{aligned}$$

From which we obtain its solution as $P_0^{(1)}(\xi_1, \eta) = -Q_0^{(1)}(\xi_1, 1)e^{-b\eta}$. Hence

$$|P_0^{(1)}(\xi_1, \eta)| \leq Ce^{-\alpha(\xi_1 + \eta)}, \quad \text{for } \xi_1 \geq 0, \eta \geq 0.$$

Similarly, we can find that $P_0^{(2)}(\xi_2, \eta) = -Q_0^{(2)}(\xi_2, 1)e^{-b\eta}$.

To eliminate the discrepancies introduced by functions $V_0(x, \eta) + P_0^{(1)}(\xi_1, \eta)$ and $V_0(x, \eta) + P_0^{(2)}(\xi_2, \eta)$ at the corners (0,1) and (1,1), we use the functions $R_0^{(1)}(\zeta_1, \eta)$ and $R_0^{(2)}(\zeta_2, \eta)$.

Function $R_0^{(1)}(\zeta_1, \eta)$ satisfies the following equation [18, pp. 786]:

$$\begin{aligned}\frac{\partial^2 R_0^{(1)}}{\partial \zeta_1^2} + \frac{\partial^2 R_0^{(1)}}{\partial \eta^2} + b \frac{\partial R_0^{(1)}}{\partial \eta} &= 0 \quad \text{for } \zeta_1 > 0, \eta > 0 \\ R_0^{(1)}(\zeta_1, 0) &= 0, \quad R_0^{(1)}(0, \eta) = -(V_0^{(1)}(0, \eta) + P_0^{(1)}(0, \eta)) \\ R_0^{(1)}(\zeta_1, \eta) &\rightarrow 0, \quad \text{when } \sqrt{\zeta_1^2 + \eta^2} \rightarrow \infty\end{aligned}$$

Its solution is given by [18, pp. 786, (35)]:

$$R_0^{(1)}(\zeta_1, \eta) = \tilde{R}(\xi, \eta)e^{-b\eta/2} + (V_0^{(1)}(0, \eta) + P_0^{(1)}(0, \eta))e^{-b\zeta_1/2},$$

where [18, pp.787, (41)]

$$|\tilde{R}(\zeta_1, \eta)| \leq C e^{-\alpha\sqrt{\zeta_1^2 + \eta^2}}$$

From which we obtain

$$|R_0^{(1)}(\zeta_1, \eta)| \leq C e^{-\alpha(\zeta_1 + \eta)}$$

Similar results hold true for $R_0^{(2)}(\zeta_2, \eta)$.

4.3.3 Finite Element Method on Shishkin Type Mesh: Case (II)

To construct a Shishkin type mesh, we assume that the positive integer N_x is divisible by 4 while N_y is divisible by 2. In the x-direction, we can construct the Shishkin mesh by dividing the interval $[0, 1]$ into the subintervals $[0, \sigma_x]$, $[\sigma_x, 1 - \sigma_x]$ and $[1 - \sigma_x, 1]$. Uniform meshes are then used on each subinterval, with $N_x/4$ points on each of $[0, \sigma_x]$ and $[1 - \sigma_x, 1]$ and $N_x/2$ points on $[\sigma_x, 1 - \sigma_x]$. Here σ_x is defined by $\sigma_x = \min\{1/4, 2a^{-1}\varepsilon \ln N_x\}$. More explicitly, we have

$$0 = x_0 < x_1 < \cdots < x_{i_0} < \cdots < x_{N_x - i_0} \cdots < x_{N_x} = 1 ,$$

with $i_0 = N_x/4$, $x_{i_0} = \sigma_x$, $x_{N_x - i_0} = 1 - \sigma_x$, and

$$\begin{aligned} h_i &= 4\sigma_x N_x^{-1}, \quad \text{for } i = 1, \dots, i_0, N_x - i_0 + 1, \dots, N_x, \\ h_i &= 2(1 - 2\sigma_x) N_x^{-1}, \quad \text{for } i = i_0 + 1, \dots, N_x - i_0 , \end{aligned}$$

where $h_i = x_i - x_{i-1}$.

In the y-direction, we follow a similar procedure to that outlined above by dividing the interval $[0, 1]$ into the subintervals $[0, 1 - \sigma_y]$ and $[1 - \sigma_y, 1]$. Uniform meshes are then used on each subinterval, each with $N_y/2$ points. Here σ_y is defined by $\sigma_y = \min\{1/2, 2b^{-1}\varepsilon^2 \ln N_y\}$. More explicitly, we have

$$0 = y_0 < y_1 < \cdots < y_{j_0} < \cdots < y_{N_y} = 1 ,$$

with $j_0 = N_y/2$, $y_{j_0} = 1 - \sigma_y$, and

$$\begin{aligned} k_j &= 2(1 - \sigma_y)N_y^{-1}, \quad \text{for } j = 1, \dots, j_0, \\ k_j &= 2\sigma_y N_y^{-1}, \quad \text{for } j = j_0 + 1, \dots, N_y, \end{aligned}$$

where $k_j = y_j - y_{j-1}$.

We shall assume that $\sigma_x = 2a^{-1}\varepsilon \ln N_x$, $\sigma_y = 2b^{-1}\varepsilon^2 \ln N_y$. In the following we will use the same notations as last section.

The weak formulation of (4.24) is: find $u \in H_0^1(\Omega)$ such that

$$\overline{B}(u, v) \equiv (\varepsilon^2 \nabla u, \nabla v) + (bu_y, v) + (a^2 u, v) = (f, v), \quad \forall v \in H_0^1(\Omega), \quad (4.28)$$

We seek the bilinear finite element solution $u^h \in S_h(\Omega)$ such that

$$\overline{B}(u^h, v) \equiv (\varepsilon^2 \nabla u^h, \nabla v) + (bu_y^h, v) + (a^2 u^h, v) = (\overline{f}, v), \quad \forall v \in S_h(\Omega), \quad (4.29)$$

where \overline{f} denote the standard bilinear interpolation of f .

In this section we use the following weighted energy norm

$$\|v\|_* \equiv \{\varepsilon^2 \|v_x\|^2 + \varepsilon^2 \|v_y\|^2 + \|v\|^2\}^{1/2}, \quad \forall v \in H_0^1(\Omega).$$

Note that

$$\begin{aligned} \overline{B}(v, v) &= \varepsilon^2 \|v_x\|^2 + \varepsilon^2 \|v_y\|^2 + (b \frac{\partial v}{\partial y}, v) + (a^2 v, v) \\ &\geq \min(1, a^2) (\varepsilon^2 \|v_x\|^2 + \varepsilon^2 \|v_y\|^2 + \|v\|^2) \\ &= \min(1, a^2) \|v\|_*^2 \end{aligned}$$

4.3.4 Uniform Convergence Analysis

In this section, we will prove the almost second-order uniform convergence rate in L^2 norm for the problem (4.24)(4.25). The proofs are similar to those presented for the last problem. Hence we just provide some important steps.

Lemma 4.18 For the solution u of (4.24)(4.25), we have

$$(I) \quad \|u - \Pi_x u\|_{\infty, \bar{I}_i} \leq C(N_x^{-2} \ln^2 N_x + \varepsilon), \quad \forall i = 1, \dots, i_0, N_x - i_0 + 1, \dots, N_x$$

$$(I') \quad \|u - \Pi_x u\|_{\infty, \bar{I}_i} \leq C(N_x^{-2} + \varepsilon), \quad \forall i = i_0 + 1, \dots, N_x - i_0,$$

$$(II) \quad \|u - \Pi_y u\|_{\infty, \bar{K}_j} \leq C(N_y^{-2} \ln^2 N_y + \varepsilon), \quad \forall j = j_0 + 1, \dots, N_y,$$

$$(II') \quad \|u - \Pi_y u\|_{\infty, \bar{K}_j} \leq C(N_y^{-2} + \varepsilon), \quad \forall j = 1, \dots, j_0.$$

Proof. The proof is similar to Lemma 4.8 except that here we will use the asymptotic expansion and the estimates in subsection 3.2.

By carrying out the similar proof of Lemma 4.9, we obtain

Lemma 4.19 For the solution u of (4.24)(4.25), we have

$$(I) \quad \|u - \Pi u\|_{\infty, \bar{\Omega}} \leq C(N_x^{-2} \ln^2 N_x + N_y^{-2} \ln^2 N_y + \varepsilon),$$

$$(II) \quad \|u - \Pi u\|_{\infty, [\sigma_x, 1 - \sigma_x] \times [0, 1 - \sigma_y]} \leq C(N_x^{-2} + N_y^{-2} + \varepsilon).$$

Lemma 4.20 For the solution u of (4.24)(4.25), under the assumptions of (A*) and (B*), we have

$$\|(b(\Pi u - u)_y, \chi)\| \leq C(N_x^{-1} + N_y^{-1}) \|\chi\|_*.$$

Proof. Carrying out an integration by parts,

$$\begin{aligned} (b(\Pi u - u)_y, \chi) &= -(b(\Pi u - u), \chi_y) \\ &= -\left(\int_{S_1} + \int_{S_2} + \int_{S_3} + \int_{S_4}\right) b(\Pi u - u) \chi_y dx dy, \end{aligned}$$

where $S_1 = [0, \sigma_x] \times [0, 1 - \sigma_y]$, $S_2 = [\sigma_x, 1 - \sigma_x] \times [0, 1 - \sigma_y]$, $S_3 = [1 - \sigma_x, 1] \times [0, 1 - \sigma_y]$ and $S_4 = [0, 1] \times [1 - \sigma_y, 1]$.

Note that by Lemma 4.10, we have

$$\left| \int_{S_1} b(\Pi u - u) \chi_y dx dy \right| \leq C \|\Pi u - u\|_{\infty, S_1} \int_{S_1} |\chi_y| dx dy$$

$$\begin{aligned}
&\leq C\|\Pi u - u\|_{\infty, S_1} (h_x/h_y)^{1/2} \sum_{\tau \in S_1} \|\chi\|_{2,\tau} \\
&\leq C\|\Pi u - u\|_{\infty, S_1} (h_x/h_y)^{1/2} \left(\sum_{\tau \in S_1} \|\chi\|_{2,\tau}^2 \right)^{1/2} \left(\sum_{\tau \in S_1} 1 \right)^{1/2} \\
&\leq C\|\Pi u - u\|_{\infty, S_1} (h_x/h_y)^{1/2} (N_x N_y)^{1/2} \|\chi\|_{2, S_1} \\
&\leq C(N_x^{-2} \ln^2 N_x + N_y^{-2} \ln^2 N_y + \varepsilon) \varepsilon^{1/2} N_y \ln^{1/2} N_x \|\chi\|_{2, S_1},
\end{aligned}$$

where in the last step, we used Lemma 4.19 and the fact that

$$h_x = 2a^{-1} \varepsilon N_x^{-1} \ln N_x \quad \text{and} \quad N_y^{-1} \leq h_y \leq 2N_y^{-1} \quad \text{in } S_1.$$

Similarly, we have

$$\left| \int_{S_3} b(\Pi u - u) \chi_y dx dy \right| \leq C(N_x^{-2} \ln^2 N_x + N_y^{-2} \ln^2 N_y + \varepsilon) \varepsilon^{1/2} N_y \ln^{1/2} N_x \|\chi\|_{2, S_3}.$$

and by Lemma 4.10, we have

$$\begin{aligned}
&\left| \int_{S_2} b(\Pi u - u) \chi_y dx dy \right| \leq C\|\Pi u - u\|_{\infty, S_2} \int_{S_2} |\chi_y| dx dy \\
&\leq C\|\Pi u - u\|_{\infty, S_2} (h_x/h_y)^{1/2} \sum_{\tau \in S_2} \|\chi\|_{2,\tau} \\
&\leq C\|\Pi u - u\|_{\infty, S_2} (h_x/h_y)^{1/2} \left(\sum_{\tau \in S_2} \|\chi\|_{2,\tau}^2 \right)^{1/2} \left(\sum_{\tau \in S_2} 1 \right)^{1/2} \\
&\leq C\|\Pi u - u\|_{\infty, S_2} (N_y/N_x)^{1/2} (N_x N_y)^{1/2} \|\chi\|_{2, S_2} \\
&\leq C(N_x^{-2} + N_y^{-2} + \varepsilon) N_y \|\chi\|_{2, S_2}
\end{aligned}$$

where we used the fact that

$$N_x^{-1} \leq h_x \leq 2N_x^{-1} \quad \text{and} \quad N_y^{-1} \leq h_y \leq 2N_y^{-1} \quad \text{in } S_2.$$

Finally,

$$\begin{aligned}
&\left| \int_{S_4} b(\Pi u - u) \chi_y dx dy \right| \leq C\|\Pi u - u\|_{\infty, S_4} \int_{S_4} |\chi_y| dx dy \\
&\leq C(N_x^{-2} \ln^2 N_x + N_y^{-2} \ln^2 N_y + \varepsilon) (\text{Area } S_4)^{1/2} \|\chi_y\|_{2, S_4} \\
&\leq C(N_x^{-2} \ln^2 N_x + N_y^{-2} \ln^2 N_y + \varepsilon) \ln^{1/2} N_y \|\varepsilon \chi_y\|_{2, S_4}.
\end{aligned}$$

From above inequalities and the assumptions of (A^*) and (B^*) , we conclude our proof. Here we used the fact that $0 < \frac{\ln^{2.5} N}{N} < 0.9$ for $N > 1$, since the maximum value is approximately equal to 0.8045, which is achieved at $N = 12.1825$.

Theorem 4.2 *Let u_h be the finite element solution of (4.29) and u be the solution of (4.24)(4.25). Then under the assumptions of (A^*) and (B^*) , we have*

$$\|u - u^h\| \leq C(N_x^{-1} + N_y^{-1}).$$

Proof. Note that

$$C_1 \| \Pi u - u^h \|_*^2 \leq \overline{B}(\Pi u - u^h, \Pi u - u^h) \quad (4.30)$$

$$= \overline{B}(\Pi u - u, \Pi u - u^h) + \overline{B}(u - u^h, \Pi u - u^h). \quad (4.31)$$

From (4.29) we have

$$\overline{B}(\Pi u - u, \Pi u - u^h) = \varepsilon^2(\nabla(\Pi u - u), \nabla \chi) + (b(\Pi u - u)_y, \chi) + (a^2(\Pi u - u), \chi)$$

Integrating by parts, we obtain

$$\begin{aligned} \varepsilon^2((\Pi u - u)_x, \chi_x) &= \sum_{1 \leq i \leq N_x, 1 \leq j \leq N_y} \int_{x_{i-1}}^{x_i} \int_{y_{j-1}}^{y_j} \varepsilon^2(\Pi u - u)_x \chi_x dx dy \\ &= \sum_{1 \leq i \leq N_x, 1 \leq j \leq N_y} \int_{y_{j-1}}^{y_j} \varepsilon^2(\Pi u - u) \Big|_{x=x_{i-1}}^{x=x_i} \chi_x dy, \\ &\leq \sum_{1 \leq i \leq N_x, 1 \leq j \leq N_y} \int_{y_{j-1}}^{y_j} |\varepsilon \chi_x| dy \cdot \varepsilon \|\Pi u - u\|_{\infty, \overline{\Omega}} \\ &= \sum_{1 \leq i \leq N_x} \int_0^1 |\varepsilon \chi_x| dy \cdot \varepsilon \|\Pi u - u\|_{\infty, \overline{\Omega}} \\ &= \sum_{1 \leq i \leq N_x} \int_0^1 \int_0^1 |\varepsilon \chi_x| dy dx \cdot \varepsilon \|\Pi u - u\|_{\infty, \overline{\Omega}}, \\ &= \varepsilon N_x \|\Pi u - u\|_{\infty, \overline{\Omega}} \cdot \int_0^1 \int_0^1 |\varepsilon \chi_x| dy dx, \\ &\leq C \varepsilon N_x (N_x^{-2} \ln^2 N_x + N_y^{-2} \ln^2 N_y + \varepsilon) \|\varepsilon \chi_x\|, \end{aligned}$$

where we used the fact that χ_x is independent of x in the above proof.

Similarly, we have

$$\varepsilon^2((\Pi u - u)_y, \chi_y) \leq C\varepsilon N_y(N_x^{-2} \ln^2 N_x + N_y^{-2} \ln^2 N_y + \varepsilon) \|\varepsilon \chi_y\|$$

Also note that

$$(\alpha^2(\Pi u - u), \chi) \leq C \|\alpha^2\|_{\infty, \bar{\Omega}} \|\Pi u - u\| \|\chi\| \leq C \|\Pi u - u\|_{\infty, \bar{\Omega}} \|\chi\| \quad (4.32)$$

$$\leq C(N_x^{-2} \ln^2 N_x + N_y^{-2} \ln^2 N_y + \varepsilon) \|\Pi u - u^h\|, \quad (4.33)$$

Combining with Lemma 4.20, we have

$$|\overline{B}(\Pi u - u, \Pi u - u^h)| \leq C(N_x^{-1} + N_y^{-1}).$$

On the other hand,

$$\overline{B}(u - u^h, \Pi u - u^h) = (f - \bar{f}, \Pi u - u^h) \quad (4.34)$$

$$\leq C \|f - \bar{f}\|_{\infty, \bar{\Omega}} \|\Pi u - u^h\| \leq C(N_x^{-2} + N_y^{-2}). \quad (4.35)$$

Combining (4.32)-(4.35), we have

$$\|\|\Pi u - u^h\|\| \leq C(N_x^{-1} + N_y^{-1}).$$

Therefore combining this with Lemma 4.19, we obtain

$$\begin{aligned} \|u - u^h\| &\leq \|u - \Pi u\| + \|\Pi u - u^h\| \leq \|u - \Pi u\|_{\infty, \bar{\Omega}} + \|\|\Pi u - u^h\|\| \\ &\leq C(N_x^{-1} + N_y^{-1}) \end{aligned}$$

which concludes our proof.

4.3.5 Streamline Diffusion Finite Element Methods

For the problem (4.24)(4.25), Zhou and Rannacher [136] discussed the local superconvergence property of the streamline diffusion method. Here we will show that

the streamline diffusion FEM will has the same uniform stability as the standard FEM on our Shishkin type mesh.

The streamline diffusion finite element method: Find $u^h \in S_h(\Omega)$ such that

$$\bar{B}_{SD}(u^h, v) \equiv \varepsilon^2(\nabla u^h, \nabla v) + (bu_y^h + a^2u^h, v + \delta bv_y) = (\bar{f}, v + \delta bv_y), \quad \forall v \in S_h(\Omega),$$

where \bar{f} denotes the standard bilinear interpolation of f .

Then it is easy to see that: for any $v \in S_h(\Omega)$, we have

$$\bar{B}_{SD}(v, v) = \varepsilon^2\|\nabla v\|^2 + b\delta\|v_y\|^2 + a^2\|v\|^2 \equiv \|v\|_{SD}^2.$$

Hence

$$\begin{aligned} \|\Pi u - u^h\|_{SD}^2 &\leq \bar{B}_{SD}(\Pi u - u^h, \Pi u - u^h) \\ &= \bar{B}_{SD}(\Pi u - u, \chi) + \bar{B}_{SD}(u - u^h, \chi) \end{aligned}$$

Note that

$$\bar{B}_{SD}(\Pi u - u, \chi) = \bar{B}(\Pi u - u, \chi) + (b(\Pi u - u)_y, \delta b\chi_y) + (a^2(\Pi u - u), \delta b\chi_y)$$

and

$$\begin{aligned} \bar{B}_{SD}(u - u^h, \chi) &= \bar{B}_{SD}(u, \chi) - \bar{B}_{SD}(u^h, \chi) \\ &= \varepsilon^2(\Delta u, \delta b\chi_y) + (f - \bar{f}, \chi + \delta b\chi_y) \end{aligned}$$

By carrying out a proof similar to the one in the last section, we can obtain uniform stability for $\|\Pi u - u^h\|_{SD}$ only when $\delta \leq C\varepsilon^n$, where $n > 2$. The problem originates from the perturbation term $\varepsilon^2(\Delta u, \delta b\chi_y)$. Since

$$|\varepsilon^2(\Delta u, \delta b\chi_y)| \leq C\varepsilon^2\delta\|\Delta u\|\|\chi_y\| \leq C\varepsilon^2\delta\varepsilon^{-3}\|\chi_y\| \leq C\delta\varepsilon^{-2}\|\varepsilon\chi_y\|,$$

we see that only when $\delta \leq C\varepsilon^n$, $n > 2$ can we obtain the uniform stability, where in the second inequality we used the result of Lemma 4.16.

4.4 Numerical Experiments

In this section, we will illustrate our methods with two numerical examples. The first one has only typical exponential boundary layers, while the second one has both exponential boundary layers and parabolic boundary layers.

In the following figures, we use (a) to indicate the left figure and (b) to indicate the right figure in each group, respectively. Since our problems are nonsymmetric and very ill-conditioned, we use a preconditioned ILUT-GMRES solver from the SPARSKIT package provided by Saad [111].

4.4.1 Example 1.

The first example we tested corresponds to the problem given by equations (4.3)(4.4) where $b_1 = b_2 = 1, a = 2$ and f is chosen appropriately such that the exact solution is

$$u(x, y) = (1 - e^{-x/\varepsilon})(1 - e^{-y/\varepsilon})(1 - x)(1 - y).$$

We see that this solution has typical exponential boundary layers at $x=0$ and $y=0$. We choose a bilinear interpolation Πf of f as \bar{f} and $N_x = N_y = N$. The numerical results of our experiments are presented for values of ε ranging from 10^{-8} to 10^{-2} and for mesh resolutions of $N=12, 24$ and 48 , respectively.

First we tested our standard FEM on Shishkin mesh. The computed L^2 error is provided in Table 4.1. To see more accurately the convergence order, we provide the computed convergence rate

$$R_\varepsilon^N = (\ln e_\varepsilon^N - \ln e_\varepsilon^{2N}) / \ln 2$$

in Table 4.2. Here e_ε^N is the L^2 error between the exact solution $u(x, y)$ and the computed solution $u^h(x, y)$, where $h = 1/N$. From Table 4.2, we see that $u^h(x, y)$ approximates $u(x, y)$ uniformly to almost second-order in L^2 norm, which is a better

result than predicted by our theoretical analysis. The condition numbers for the coefficient matrices resulting from the FEM discretization of this problem are provided in Table 4.3. Here we calculated the condition number by MATLAB. Using an inverse estimate [16], we can easily see that the condition number $K(A)$ of the coefficient matrix A for this FEM is bounded by $O(\varepsilon N^2 \ln^{-2} N)$, which was also shown by Roos [107]. From Table 4.3, we see that our numerical results are very consistent with the theoretical condition number. The pointwise errors $u_h - u$ are plotted in Figures 4.1-4.6 for different ε and N . The results obtained show very clearly the uniform convergence rate. They also show that the larger error originates from boundary layers, where in our case the boundary layers are located at $x=0$ and $y=0$. The error also displays some oscillations and they pollute other parts of the domain starting from the corner and boundary layers, which is normal for the standard FEM for such convection-diffusion type problems [23, 58, 135]. To compare our standard FEM with the classical standard FEM on uniform mesh, we performed same computations for the standard FEM on uniform mesh, and we present the results in Figures 4.4(b)-4.6(b) for $\varepsilon = 10^{-3}$. When ε becomes smaller, the error amplitude becomes very large. From these results we see that our standard FEM on the Shishkin type mesh performs much better than the classical standard FEM in as far as the error amplitude is concerned. The pollution range is not clear, since the plotting scale is not of the same order of magnitude.

Then we investigated the streamline diffusion (SD) FEM on our Shishkin type mesh and the standard streamline diffusion FEM [58]. Here in order to ensure global uniform convergence, we took the diffusion parameter to be $\delta = \varepsilon^2$. Unfortunately, in this case our SD FEM does not improve upon the standard FEM solution. The pointwise errors are exactly the same as the standard FEM. The reason is that the diffusion parameter δ is too small to have any sizable effect. Then we tried the widely used choice of $\delta = 1/N$. The results with the SD FEM on our Shishkin mesh

and uniform mesh are presented in Figures 4.7-4.12. Even though our SD FEM on Shishkin mesh exhibits some oscillations, both methods display a very good local uniform convergence, a fact which was proved recently by Zhou and Rannacher [136], where they also measured accurately the convergence rate for the local pointwise error.

4.4.2 Example 2.

The second example is for the problem given by equations (4.24)(4.25) where $b = 1$, $a = 1$ and f is chosen appropriately such that the exact solution is

$$u(x, y) = (1 - e^{-x/\varepsilon})(1 - e^{-(1-x)/\varepsilon})(1 - e^{-(1-y)/\varepsilon^2})y.$$

This solution has the typical exponential boundary layers at $x=0$ and $x=1$, and it has a parabolic exponential boundary layer at $y=1$. We choose a bilinear interpolation Πf of f as \bar{f} and $N_x = N_y = N$. The numerical results of our experiments are for values of ε ranging from 10^{-6} to 10^{-2} and for mesh resolutions $N=12, 24$ and 48 , respectively.

First we tested our standard FEM on Shishkin mesh. The computed L^2 norm is provided in Table 4.4. To see more accurately the convergence rate order, we provide the computed convergence rate R_ε^N in Table 4.5. From Table 4.5, we see that $u^h(x, y)$ approximates $u(x, y)$ uniformly to almost second-order in L^2 norm, which is better than expected from our theoretical analysis. The calculated condition numbers using MATLAB for this problem are provided in Table 4.6. From these results we see that the condition number is just proportional to ε^{-1} . It is better than the predicted theoretical condition number which should be proportional to ε^{-2} . For the sake of comparison, we performed the computations for standard FEM on the Shishkin mesh and uniform mesh. The pointwise errors $u_h - u$ are plotted in Figures 4.13-4.18 for different ε and N , respectively. We see that the large error also originates from boundary layers, where in our case the exponential boundary layers are located at

$x=0$ and $x=1$, and the parabolic boundary layer is located at $y=1$. The error also displays some oscillations and it polluted other regions of the computational domain by propagating from the exponential layer $y=1$. We conclude that our standard FEM on the Shishkin type mesh performs much better than the classical standard FEM in both the error amplitude and the oscillation frequency.

As for the SD FEM, our SD FEM does not improve the standard FEM as well as in example 1. This, since in order to ensure global uniform convergence, the diffusion parameter δ should satisfy $\delta \leq C\epsilon^n$, $n > 2$, a value which is too small to have any effect. We tested $\delta = \epsilon^3$, which yields almost the same solutions as the corresponding standard FEM. Then we tried the popular choice $\delta = 1/N$. The results with the SD FEM on our Shishkin mesh and uniform mesh are presented in Figures 4.19-4.24. They show that no oscillation occurs for either of the SD FEMs. Both methods display very good local uniform convergence, but the SD FEM on our Shishkin type mesh resolves the exponential boundary layers in a much better fashion than SD FEM on the uniform mesh. As N grows larger, the error is dominated only by the parabolic boundary layer.

4.4.3 Conclusions

Our numerical examples show that both SD FEMs on the Shishkin mesh and the uniform mesh with $\delta = 1/N$ provide a much better control on the error oscillations than the standard FEM. The results also show that both methods display an excellent local uniform convergence, a fact which was proved recently by Zhou and Rannacher [136] for an almost rectangular mesh, where they also measured accurately the convergence rate for the local pointwise error. For the one space dimension problem, Guo and Stynes [46] recently proved the global uniform convergence for a SD FEM on a Shishkin mesh. But it still remains an open problem [46] whether the global uniform convergence can be retained for SD FEMs in two space dimensions, which is

the reason why additional work was dedicated to local error analysis, cf. Johnson *et al.* [58], Zhou and Rannacher [136] and Wahlbin [133]. Numerical results (see Tables 4.2 and 4.5) show that our standard FEM on Shishkin type mesh is GUC to almost second-order in L^2 norm, which is better than our theoretical analysis. At present, it is still unknown if this almost second-order convergence rate can be obtained theoretically for convection-diffusion type problems (this problem is still unsolved even in one space dimension [63]), or if it is just a superconvergence phenomenon [136]. Further investigation of this topic is certainly required. Even though our standard FEM on Shishkin type mesh is GUC, it still displays some oscillations around the boundary layers. Other more stable techniques are under development, such as, the stabilized FEM and the techniques developed recently by Franca and Hughes *et al.* [17, 41], along with those discussed in Zienkiewicz and Taylor [135, Ch.12] and Carey and Oden [23, Ch.5].

Table 4.1: Errors in L^2 norm for Example 1

	N		
ϵ	12	24	48
1.0D-02	3.9353295D-03	9.5865477D-04	3.1808308D-04
1.0D-03	5.9899591D-03	1.4755047D-03	2.8507499D-04
1.0D-04	6.3435845D-03	1.7507047D-03	4.3802338D-04
1.0D-05	6.3808889D-03	1.7849438D-03	4.6954562D-04
1.0D-06	6.3848394D-03	1.7884465D-03	4.7321017D-04
1.0D-07	6.3851212D-03	1.7887975D-03	4.7356168D-04
1.0D-08	6.3851677D-03	1.7888327D-03	4.7359686D-04

Table 4.2: Convergence rates R_ϵ^N in L^2 norm for Example 1

	N	
ϵ	12	24
1.0D-02	2.0374	1.5916
1.0D-03	2.0213	2.3718
1.0D-04	1.8574	1.9989
1.0D-05	1.8379	1.9265
1.0D-06	1.8359	1.9182
1.0D-07	1.8357	1.9174
1.0D-08	1.8357	1.9173

Table 4.3: Condition numbers for Example 1

ε	N	
	12	24
1.0D-02	131.7961	393.1111
1.0D-03	1.2027e+03	3.4905e+03
1.0D-04	1.1963e+04	3.4211e+04
1.0D-05	1.1958e+05	3.4154e+05
1.0D-06	1.1958e+06	3.4148e+06
1.0D-07	1.1958e+07	3.4147e+07
1.0D-08	1.1958e+08	3.4147e+08

Table 4.4: Errors in L^2 norm for Example 2

ε	N		
	12	24	48
1.0D-02	9.3876868D-03	2.9110260D-03	8.7095706D-04
1.0D-03	7.7191053D-03	2.1519899D-03	5.8664613D-04
1.0D-04	7.5300586D-03	2.0551015D-03	5.4455535D-04
1.0D-05	7.5100947D-03	2.0453154D-03	5.4109647D-04
1.0D-06	7.5063255D-03	2.0440796D-03	5.3940714D-04

Table 4.5: Convergence rates R_ϵ^N in L^2 norm for Example 2

	N	
ϵ	12	24
1.0D-02	1.6892	1.7409
1.0D-03	1.8428	1.8751
1.0D-04	1.8735	1.9161
1.0D-05	1.8765	1.9184
1.0D-06	1.8767	1.9220

Table 4.6: Condition numbers for Example 2

	N	
ϵ	12	24
1.0D-02	513.0415	973.9048
1.0D-03	5.6629e+03	1.1022e+04
1.0D-04	5.7141e+04	1.1148e+05
1.0D-05	5.7192e+05	1.1161e+06
1.0D-06	5.7194e+06	1.1161e+07

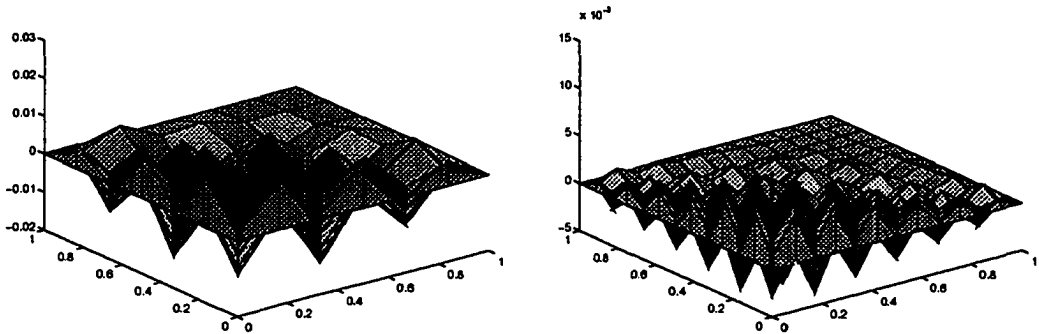


Figure 4.1: Example 1: Standard FEM on Shishikin mesh for $\varepsilon = 10^{-3}$: (a) $N=12$
 (b) $N=24$

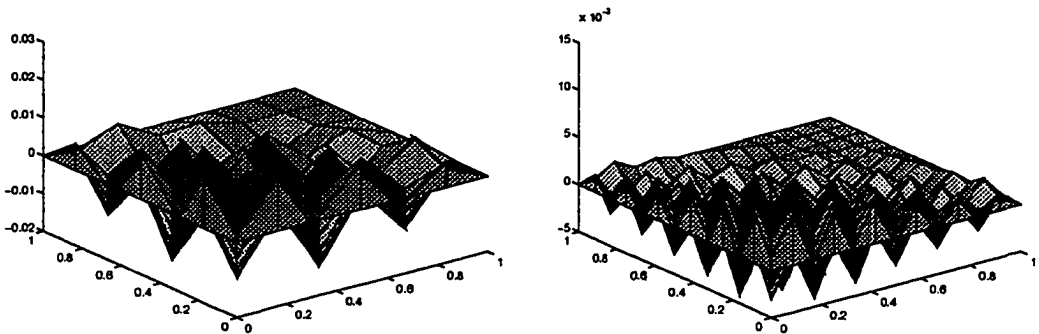


Figure 4.2: Example 1: Standard FEM on Shishikin mesh for $\varepsilon = 10^{-5}$: (a) $N=12$
 (b) $N=24$

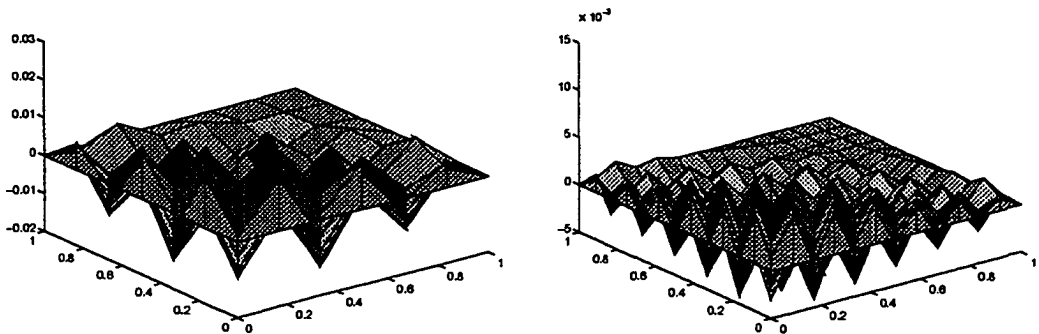


Figure 4.3: Example 1: Standard FEM on Shishikin mesh for $\varepsilon = 10^{-7}$: (a) $N=12$
 (b) $N=24$

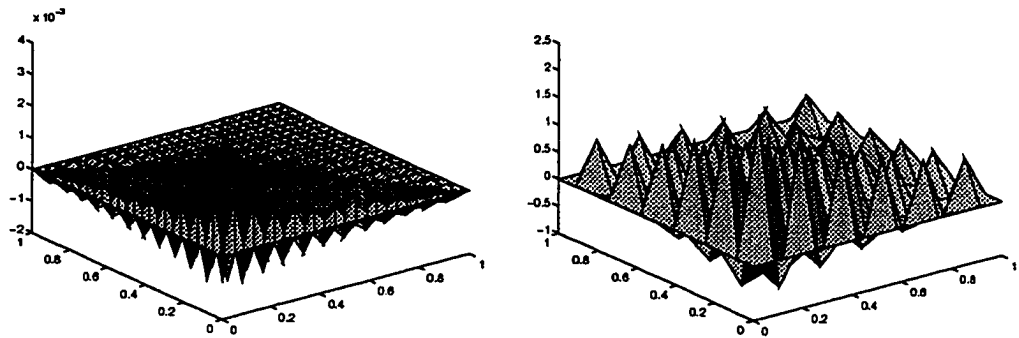


Figure 4.4: Example 1: Standard FEM: (a) $N=48$, $\varepsilon = 10^{-3}$, Shishkin mesh (b) $N=12$, $\varepsilon = 10^{-3}$, Uniform mesh

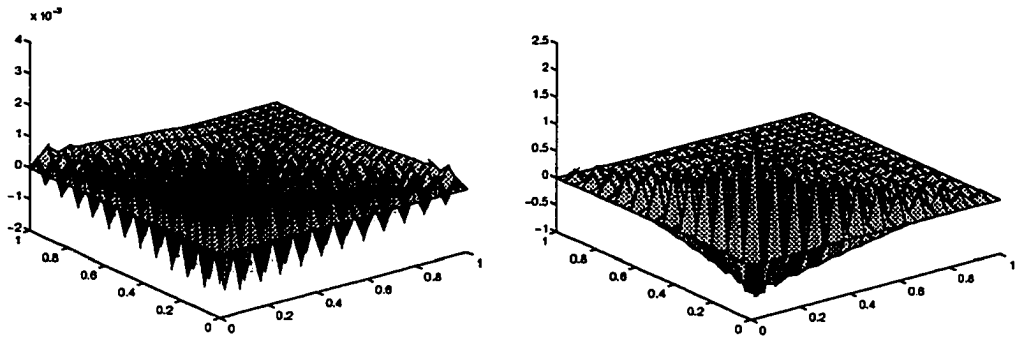


Figure 4.5: Example 1: Standard FEM: (a) $N=48$, $\varepsilon = 10^{-5}$, Shishkin mesh (b) $N=24$, $\varepsilon = 10^{-5}$, Uniform mesh

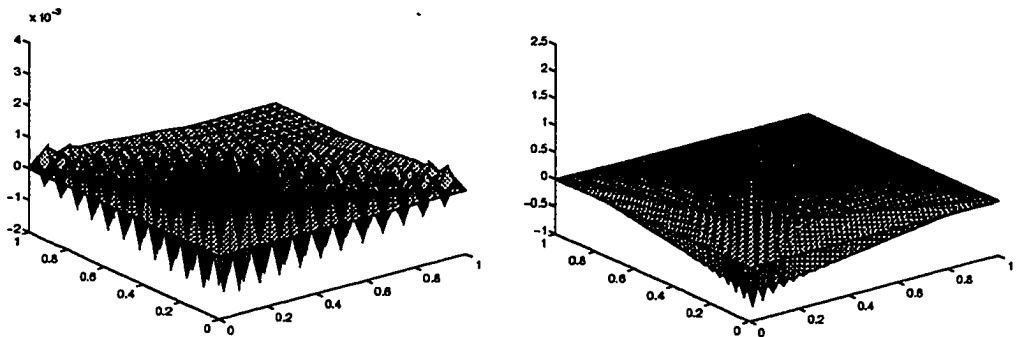


Figure 4.6: Example 1: Standard FEM: (a) $N=48$, $\varepsilon = 10^{-7}$, Shishkin mesh (b) $N=48$, $\varepsilon = 10^{-7}$, Uniform mesh

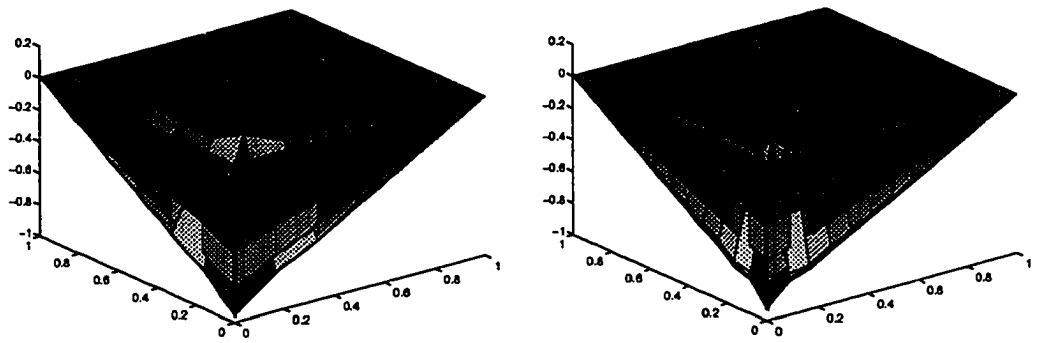


Figure 4.7: Example 1: SD FEM on Shishikin mesh for $\varepsilon = 10^{-3}$: (a) $N=12$ (b) $N=24$

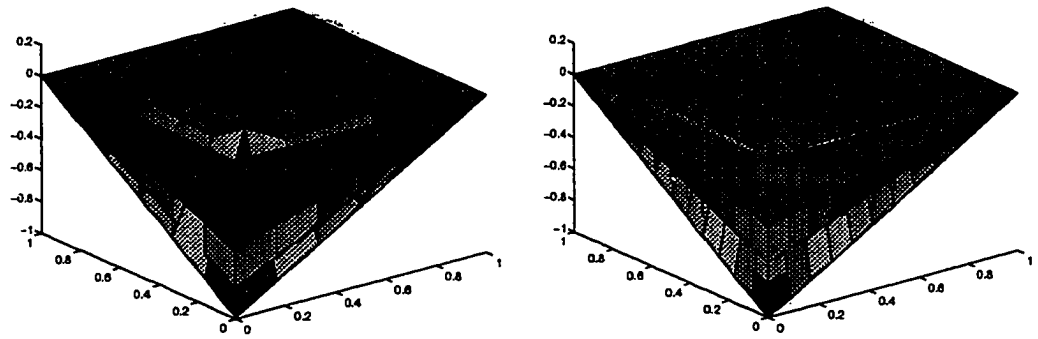


Figure 4.8: Example 1: SD FEM on Shishikin mesh for $\varepsilon = 10^{-7}$: (a) $N=12$ (b) $N=24$

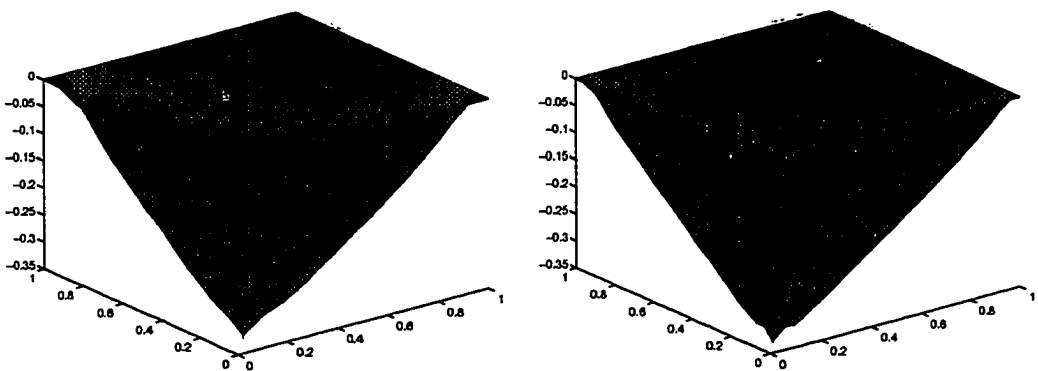


Figure 4.9: Example 1: SD FEM on uniform mesh for $\varepsilon = 10^{-3}$: (a) $N=12$ (b) $N=24$

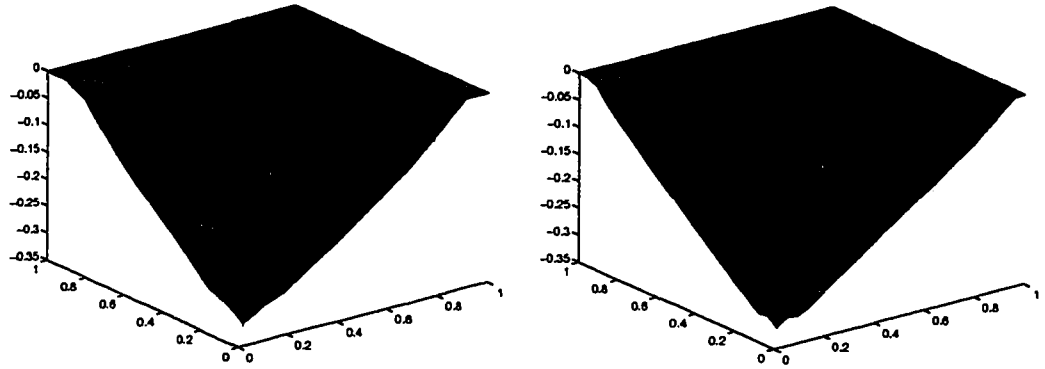


Figure 4.10: Example 1: SD FEM on uniform mesh for $\varepsilon = 10^{-7}$: (a) $N=12$ (b) $N=24$

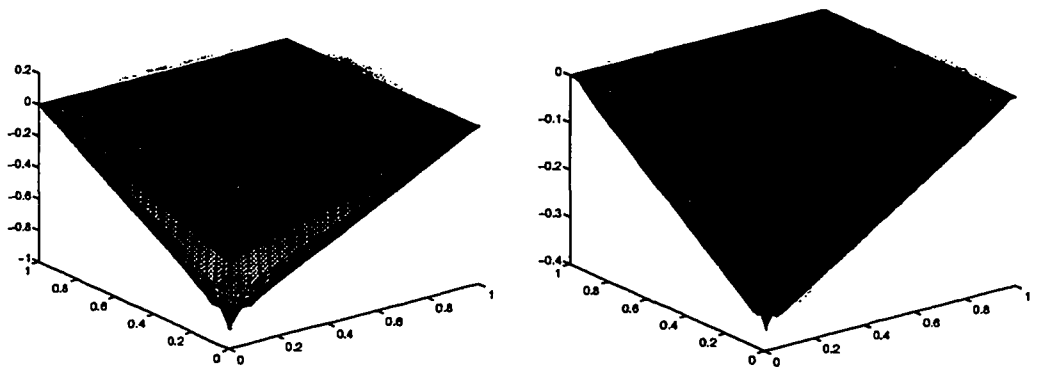


Figure 4.11: Example 1: SD FEM for $N=48$, $\varepsilon = 10^{-3}$: (a) Shishkin mesh (b) Uniform mesh

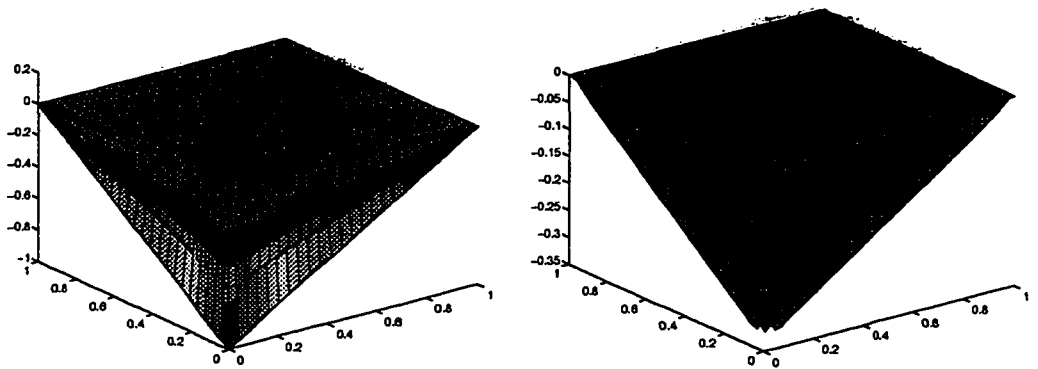


Figure 4.12: Example 1: SD FEM for $N=48$, $\varepsilon = 10^{-7}$: (a) Shishkin mesh (b) Uniform mesh

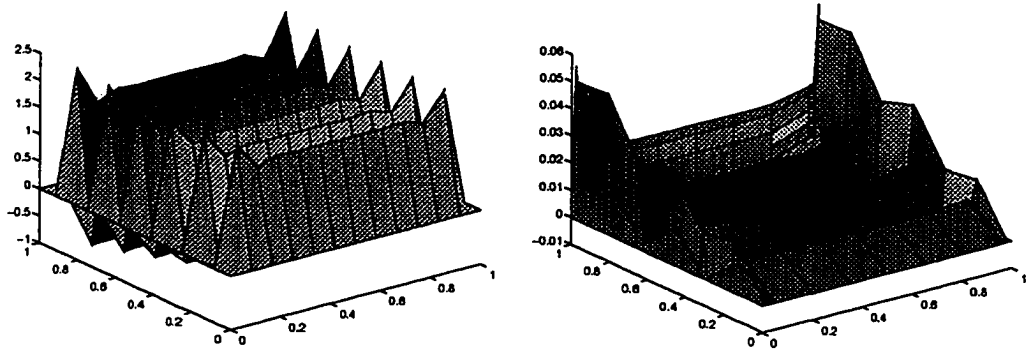


Figure 4.13: Example 2: Standard FEM for $N=12$, $\varepsilon = 10^{-2}$: (a) Uniform mesh (b) Shishkin mesh

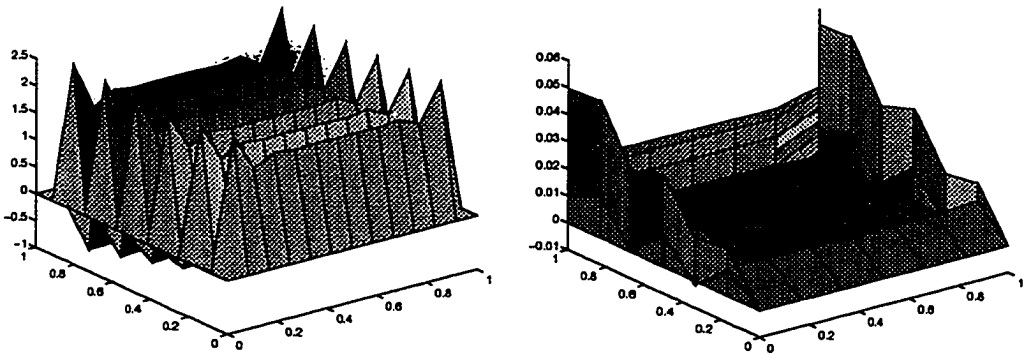


Figure 4.14: Example 2: Standard FEM for $N=12$, $\varepsilon = 10^{-6}$: (a) Uniform mesh (b) Shishkin mesh

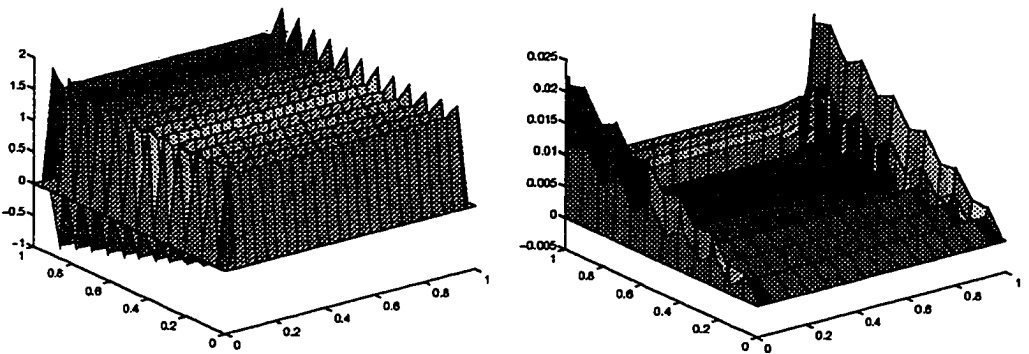


Figure 4.15: Example 2: Standard FEM for $N=24$, $\varepsilon = 10^{-2}$: (a) Uniform mesh (b) Shishkin mesh

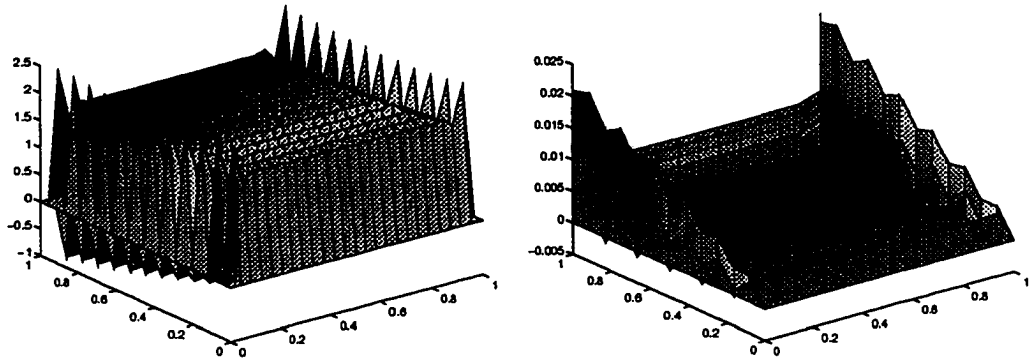


Figure 4.16: Example 2: Standard FEM for $N=24$, $\epsilon = 10^{-6}$: (a) Uniform mesh (b) Shishkin mesh

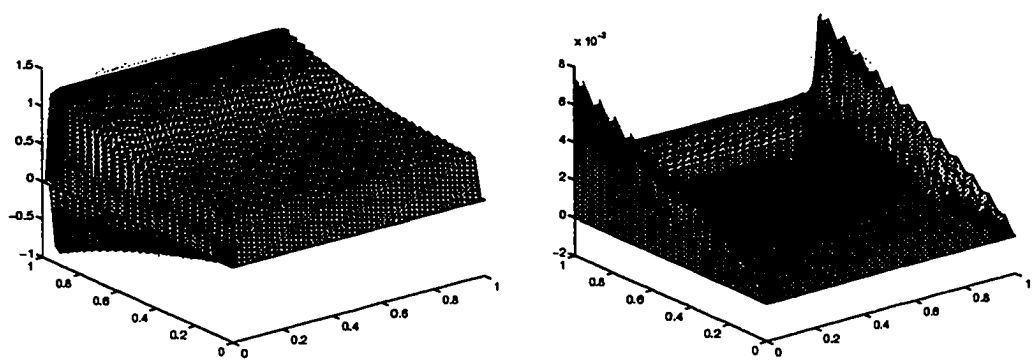


Figure 4.17: Example 2: Standard FEM for $N=48$, $\epsilon = 1.0^{-2}$: (a) Uniform mesh (b) Shishkin mesh

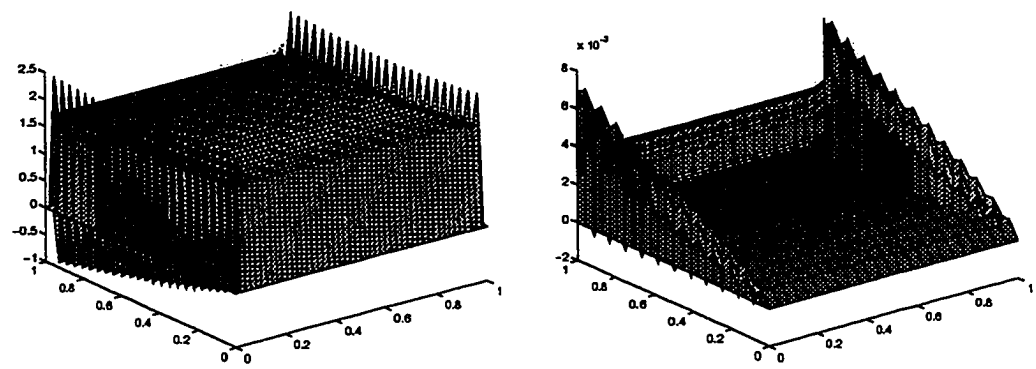


Figure 4.18: Example 2: Standard FEM for $N=48$, $\epsilon = 10^{-6}$: (a) Uniform mesh (b) Shishkin mesh

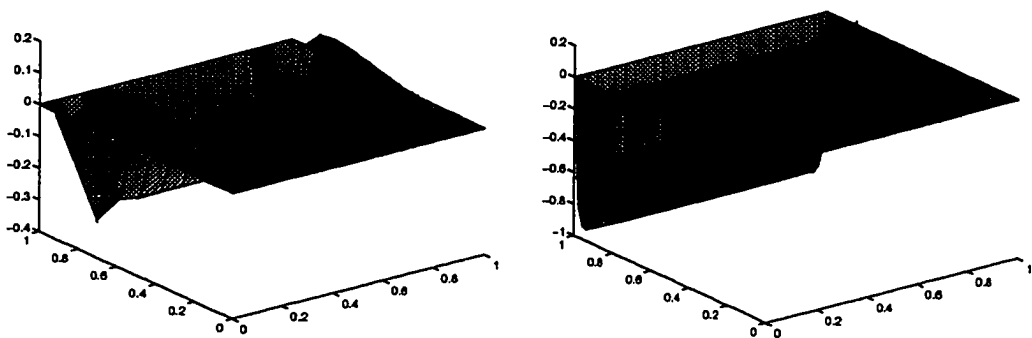


Figure 4.19: Example 2: SD FEM for $N=12$, $\varepsilon = 10^{-2}$: (a) Uniform mesh (b) Shishkin mesh

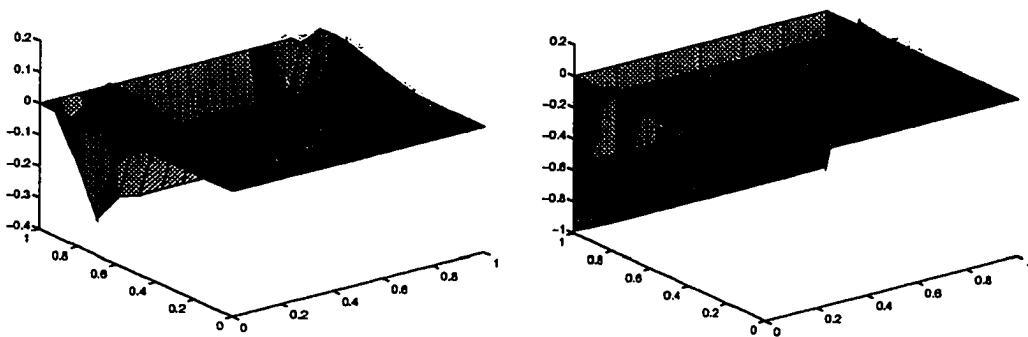


Figure 4.20: Example 2: SD FEM for $N=12$, $\varepsilon = 10^{-6}$: (a) Uniform mesh (b) Shishkin mesh

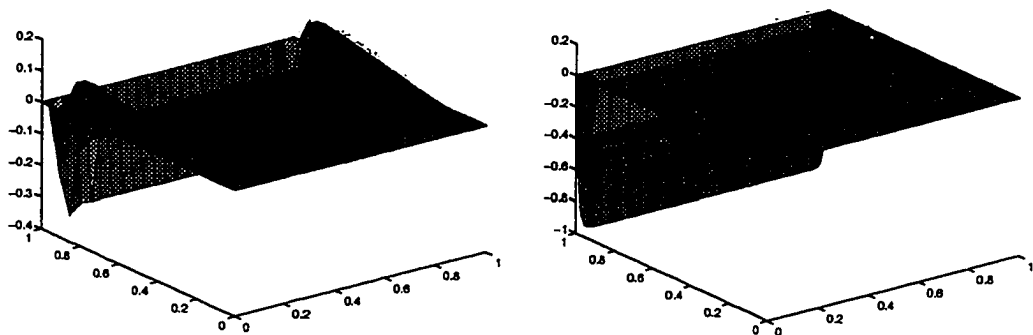


Figure 4.21: Example 2: SD FEM for $N=24$, $\varepsilon = 10^{-2}$: (a) Uniform mesh (b) Shishkin mesh

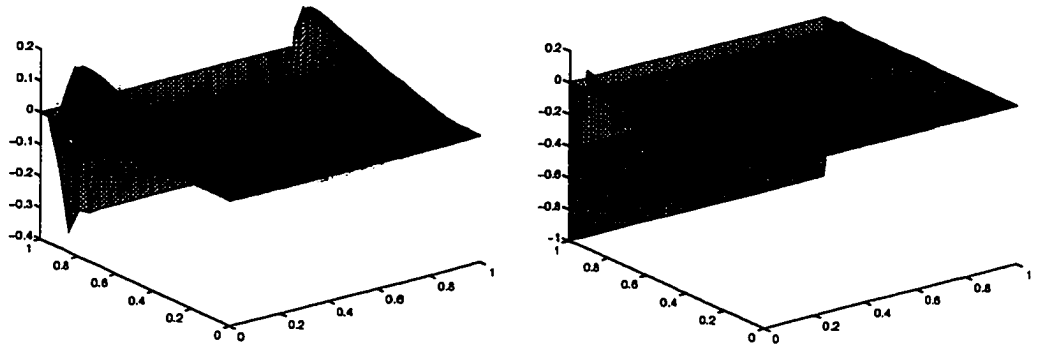


Figure 4.22: Example 2: SD FEM for $N=24$, $\varepsilon = 10^{-6}$: (a) Uniform mesh (b) Shishkin mesh

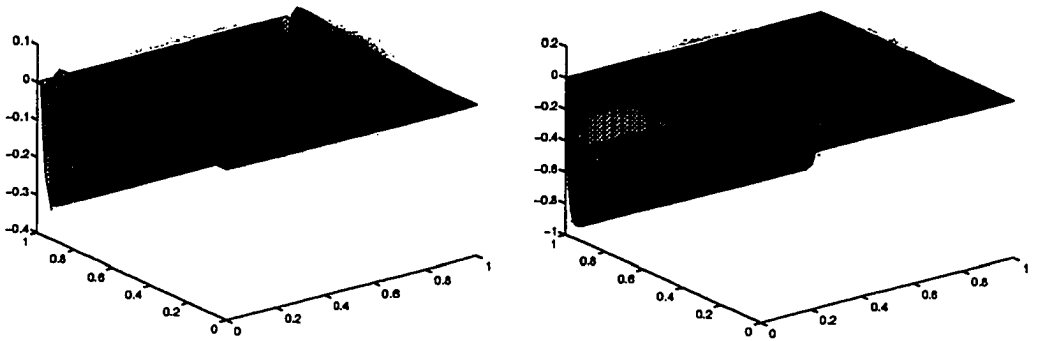


Figure 4.23: Example 2: SD FEM for $N=48$, $\varepsilon = 10^{-2}$: (a) Uniform mesh (b) Shishkin mesh

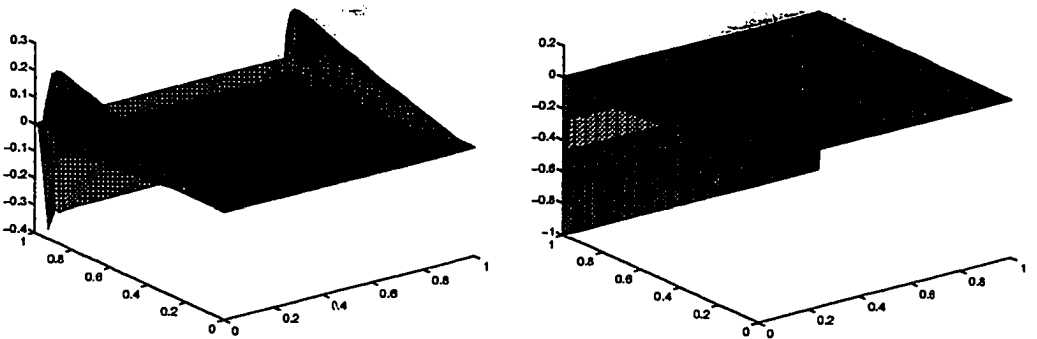


Figure 4.24: Example 2: SD FEM for $N=48$, $\varepsilon = 10^{-6}$: (a) Uniform mesh (b) Shishkin mesh

CHAPTER 5

THE TWO-PARAMETER MODEL

5.1 Introduction

In this chapter, we consider the following singularly perturbed elliptic boundary value problem:

$$L_\varepsilon u \equiv -\varepsilon^2 \mu^2 \Delta u + \varepsilon A(x, y) \frac{\partial u}{\partial y} + a^2(x, y)u = f(x, y, \varepsilon, \mu) \text{ in } \Omega, \quad (5.1)$$

$$u = 0 \text{ on } \partial\Omega, \quad (5.2)$$

where ε and μ are two small positive parameters, Δ is the Laplacian, and $\partial\Omega$ is the boundary of Ω .

5.2 Derivative Estimates

To obtain pointwise derivative estimates for the solution of (5.1)(5.2), we assume that the functions A , a and f are so smooth that $u \in C^3(\bar{\Omega})$, where $\bar{\Omega} \equiv \Omega \cup \partial\Omega$. Hence $f=0$ at the four corners is implied[108]. To avoid lengthy technicalities, we assume that A is a positive constant and $a \geq \frac{1}{2} \min(a_1, A) > 0$. When A is not a constant function, similar derivative estimates can be obtained under some restrictive assumptions[108, 103].

In this section we will make repeated use of the following weak maximum principle:

Lemma 5.1 *For any functions $w(x, y) \in C^2(\Omega) \cap C^0(\bar{\Omega})$, if $w \geq 0$ on $\partial\Omega$ and $L_\varepsilon w \geq 0$ on Ω , then $w \geq 0$ on $\bar{\Omega}$.*

Proof. It can be proved easily by contradiction, cf. Eckhaus [34, Lemma 6.2.1.1].

Lemma 5.2

- (I) $|u(x, y)| \leq C(1 - \exp(-\frac{a_1 x}{\varepsilon \mu}))$ on $\bar{\Omega}$,
- (II) $|u(x, y)| \leq C(1 - \exp(-\frac{a_1(1-x)}{\varepsilon \mu}))$ on $\bar{\Omega}$,
- (III) $|u(x, y)| \leq C(1 - \exp(-\frac{Ay}{\varepsilon}))$ on $\bar{\Omega}$,
- (IV) $|u(x, y)| \leq C(1 - \exp(-\frac{2A(1-y)}{\varepsilon \mu^2}))$ on $\bar{\Omega}$.

Proof.(I) Use the barrier function $\phi(x, y) = C(1 - \exp(-\frac{a_1 x}{\varepsilon \mu}))$, by simple calculations, we have

$$L_\varepsilon(\phi \pm u) = Ca^2[1 - (1 - \frac{a_1^2}{a^2})\exp(-\frac{a_1 x}{\varepsilon \mu})] \pm f \quad (5.3)$$

$$\geq 0, \quad \text{for sufficiently large } C. \quad (5.4)$$

Then from $(\phi \pm u)|_{\partial\Omega} \geq 0$ and Lemma 5.1 we conclude our proof.

(II) Use the barrier function $\phi(x, y) = C(1 - \exp(-\frac{a_1(1-x)}{\varepsilon \mu}))$.

(III) Use the barrier function $\phi(x, y) = C(1 - \exp(-\frac{Ay}{\varepsilon}))$. Note that

$$L_\varepsilon(\phi \pm u) = \varepsilon^2 \mu^2 C \frac{A^2}{\varepsilon^2} \exp(-\frac{Ay}{\varepsilon}) + \varepsilon AC \frac{A}{\varepsilon} \exp(-\frac{Ay}{\varepsilon}) \quad (5.5)$$

$$+ a^2 C(1 - \exp(-\frac{Ay}{\varepsilon})) \pm f \quad (5.6)$$

If $\exp(-\frac{Ay}{\varepsilon}) \geq \frac{1}{3}$, then we have

$$L_\varepsilon(\phi \pm u) \geq \frac{1}{3} A^2 C \pm f$$

otherwise, we have $1 - \exp(-\frac{Ay}{\varepsilon}) \geq \frac{2}{3}$, then we have

$$L_\varepsilon(\phi \pm u) \geq \frac{2}{3} a^2 C \pm f$$

In both cases, we can have $L_\varepsilon(\phi \pm u) \geq 0$ for sufficiently large C .

(IV) Use the barrier function $\phi(x, y) = C(1 - \exp(-\frac{2A(1-y)}{\varepsilon\mu^2}))$. Then by simple calculations, we have

$$L_\varepsilon(\phi \pm u) = \frac{2A^2C}{\mu^2} \exp(-\frac{2A(1-y)}{\varepsilon\mu^2}) + a^2C(1 - \exp(-\frac{2A(1-y)}{\varepsilon\mu^2})) \pm f \quad (5.7)$$

$$\geq 0, \quad \text{for sufficiently large } C. \quad (5.8)$$

Here we used the same procedure as (III) and the fact that $\frac{1}{\mu^2} > 1$.

Lemma 5.3

$$(I) \quad |u_x(x, y)| \leq C(\varepsilon\mu)^{-1} \quad \text{on } \partial\Omega, \quad (5.9)$$

$$(II) \quad |u_y(x, 0)| \leq C\varepsilon^{-1}, \quad |u_y(x, 1)| \leq C(\varepsilon\mu^2)^{-1} \quad \text{and} \quad |u_y(x, y)|_{x=0,1} = 0.$$

Proof. By using Lemma 5.2, the proof is all the same as [73, Lemma 2.1.3].

Lemma 5.4

$$(I) \quad |u_x(x, y)| \leq C(1 + \frac{1}{\varepsilon\mu} \exp(-\frac{a_1x}{\varepsilon\mu}) + \frac{1}{\varepsilon\mu} \exp(-\frac{a_1(1-x)}{\varepsilon\mu})) \quad \text{on } \bar{\Omega},$$

$$(II) \quad |u_y(x, y)| \leq C(1 + \frac{1}{\varepsilon} \exp(-\frac{Ay}{\varepsilon}) + \frac{1}{\varepsilon\mu^2} \exp(-\frac{A(1-y)}{\varepsilon\mu^2})) \quad \text{on } \bar{\Omega}.$$

Proof.(I) Consider the barrier function

$$\phi(x, y) = C(1 + \frac{1}{\varepsilon\mu} \exp(-\frac{a_1x}{\varepsilon\mu}) + \frac{1}{\varepsilon\mu} \exp(-\frac{a_1(1-x)}{\varepsilon\mu})),$$

then by simple calculations, we obtain

$$L_\varepsilon(\phi \pm u_x) = a^2C + \frac{C}{\varepsilon\mu}(a^2 - a_1^2)(\exp(-\frac{a_1x}{\varepsilon\mu}) + \exp(-\frac{a_1(1-x)}{\varepsilon\mu})) \pm (f_x - (a^2)_xu) \geq 0 \quad \text{for sufficiently large } C, \quad (5.10)$$

combining with Lemmas 5.1 and 5.3, concludes our proof.

(II) To prove (II), we use the barrier function

$$\phi(x, y) = C(1 + \frac{1}{\varepsilon} \exp(-\frac{Ay}{\varepsilon}) + \frac{1}{\varepsilon\mu^2} \exp(-\frac{A(1-y)}{\varepsilon\mu^2}))$$

then by simple calculations, we have

$$L_\varepsilon(\phi \pm u_y) = a^2 C + \frac{C}{\varepsilon} \exp\left(-\frac{Ay}{\varepsilon}\right)(a^2 - A^2 \mu^2 - A^2) \quad (5.11)$$

$$+ \frac{a^2 C}{\varepsilon \mu^2} \exp\left(-\frac{A(1-y)}{\varepsilon \mu^2}\right) \pm (f_y - (a^2)_y u) \quad (5.12)$$

$$\geq 0 \quad \text{for sufficiently large } C, \quad (5.13)$$

combining with Lemmas 5.1 and 5.3, concludes our proof.

Remark 5.1 *From our derivative estimates, we see that there is a boundary layer at each side, which is different from the ordinary convection-diffusion problem[73, Section 3]. There exists no boundary layer at $y=0$ when the convection term does not have a small parameter.*

Remark 5.2 *Our estimates were obtained for a generalized function $f(x, y, \varepsilon, \mu)$, which has the following boundary layer properties:*

$$|f(x, y, \varepsilon, \mu)| \leq C, \quad \forall (x, y) \in \bar{\Omega} \quad (5.14)$$

$$|f_x(x, y, \varepsilon, \mu)| \leq C\left(1 + \frac{1}{\varepsilon \mu} \exp\left(-\frac{a_1 x}{\varepsilon \mu}\right) + \frac{1}{\varepsilon \mu} \exp\left(-\frac{a_1(1-x)}{\varepsilon \mu}\right)\right), \quad \forall (x, y) \in \bar{\Omega}$$

$$|f_y(x, y, \varepsilon, \mu)| \leq C\left(1 + \frac{1}{\varepsilon} \exp\left(-\frac{Ay}{\varepsilon}\right) + \frac{1}{\varepsilon \mu^2} \exp\left(-\frac{A(1-y)}{\varepsilon \mu^2}\right)\right), \quad \forall (x, y) \in \bar{\Omega}$$

5.3 The Asymptotic Expansion

This section is based on the work of Butuzov[20]. Consider the Butuzov asymptotic expansion[20]:

$$U_0 = u_{00} + \sum_{l=1}^4 \Pi_{00}^{(l)} + \sum_{l=1}^2 (Q_{00}^{(l)} + P_{00}^{(l)}),$$

then we have

Lemma 5.5 [20, Theorem 1] *For sufficiently small ε and μ , we have*

$$|u(x, y) - U_0(x, y)| \leq C(\varepsilon + \mu), \quad \forall (x, y) \in \bar{\Omega}. \quad (5.15)$$

In the following, we will present additional details for each term.

The regular part $U_{00}(x, y) = f(x, y, 0, 0)/a^2(x, y)$.

The ordinary boundary layer function $\Pi_{00}^{(1)}(x, \eta_1)$ at $\Gamma_1(0 \leq x \leq 1, y = 0)$ satisfies:

$$A \frac{\partial \Pi_{00}^{(1)}(x, \eta_1)}{\partial \eta_1} + a^2(x, 0) \Pi_{00}^{(1)}(x, \eta_1) = 0 \quad (5.16)$$

$$\Pi_{00}^{(1)}(x, 0) = -u_{00}(x, 0), \quad \Pi_{00}^{(1)}(x, \eta_1) \rightarrow 0 \text{ as } \eta_1 \rightarrow \infty \quad (5.17)$$

from which we have

$$|\Pi_{00}^{(1)}(x, \eta_1)| \leq C \exp(-\alpha \eta_1), \quad \eta_1 \geq 0 \quad (5.18)$$

where α is a positive constant (here and in the sequel), and $\eta_1 = y/\varepsilon$.

Similar boundary layer functions can be constructed at other sides of the rectangular domain:

$$\Gamma_2(x = 0, 0 \leq y \leq 1): \quad \xi_1 = \frac{x}{\varepsilon \mu}; \quad \left(\frac{\partial^2}{\partial \xi_1^2} - a^2(0, y) \right) \Pi_{00}^{(2)} = 0 \quad (5.19)$$

$$\Gamma_3(0 \leq x \leq 1, y = 1): \quad \eta_2 = (1 - y)/(\varepsilon \mu^2); \quad \left(\frac{\partial^2}{\partial \eta_2^2} - A \frac{\partial}{\partial \eta_2} \right) \Pi_{00}^{(3)} = 0 \quad (5.20)$$

$$\Gamma_4(x = 1, 0 \leq y \leq 1): \quad \xi_2 = (1 - x)/(\varepsilon \mu); \quad \left(\frac{\partial^2}{\partial \xi_2^2} - a^2(1, y) \right) \Pi_{00}^{(4)} = 0 \quad (5.21)$$

All Π -functions have similar estimates as (5.18) [20, Section 2].

To remove the discrepancies introduced by $\Pi_{00}^{(1)}$ and $\Pi_{00}^{(2)}$ on Γ_1 and Γ_2 , $Q_{00}^{(1)}(\xi_1, \eta_1)$ is constructed:

$$\left(\frac{\partial^2}{\partial \xi_1^2} - A \frac{\partial}{\partial \eta_1} - a^2(0, 0) \right) Q_{00}^{(1)} = 0, \quad \xi_1 > 0, \eta_1 > 0 \quad (5.22)$$

$$Q_{00}^{(1)}(\xi_1, 0) = -\Pi_{00}^{(2)}(\xi_1, 0), \quad Q_{00}^{(1)}(0, \eta_1) = -\Pi_{00}^{(1)}(0, \eta_1) \quad (5.23)$$

from which we obtain

$$|Q_{00}^{(1)}(\xi_1, \eta_1)| \leq C \exp(-\alpha(\xi_1 + \eta_1)), \quad \text{for } \xi_1, \eta_1 \geq 0.$$

$Q_{00}^{(2)}(\xi_2, \eta_1)$ can be constructed in a similar way and has the following estimate

$$|Q_{00}^{(2)}(\xi_2, \eta_1)| \leq C \exp(-\alpha(\xi_2 + \eta_1)), \quad \text{for } \xi_2, \eta_1 \geq 0.$$

To remove the discrepancy introduced by $\Pi_{00}^{(2)}$ function on Γ_3 , $P_{00}^{(1)}(\xi_1, \eta_2)$ is constructed:

$$\left(\frac{\partial^2}{\partial \eta_2^2} + A \frac{\partial}{\partial \eta_2}\right) P_{00}^{(1)} = 0 \tag{5.24}$$

$$P_{00}^{(1)}(\xi_1, 0) = -\Pi_{00}^{(2)}(\xi_1, 1), \quad P_{00}^{(1)}(\xi_1, \eta_2) \rightarrow 0 \quad \text{as } \eta_2 \rightarrow \infty \tag{5.25}$$

from which we obtain

$$|P_{00}^{(1)}(\xi_1, \eta_2)| \leq C \exp(-\alpha(\xi_1 + \eta_2)), \quad \text{for } \xi_1, \eta_2 \geq 0.$$

$P_{00}^{(2)}(\xi_2, \eta_2)$ can be constructed similarly and it satisfies:

$$|P_{00}^{(2)}(\xi_2, \eta_2)| \leq C \exp(-\alpha(\xi_2 + \eta_2)), \quad \text{for } \xi_2, \eta_2 \geq 0.$$

5.4 Mesh and Scheme

To construct our piecewise uniform mesh, we assume that N_x and N_y are divisible by 10, where N_x and N_y denote the number of divisions in the x- and y-directions, respectively. Otherwise, the remaining points can be put outside the boundary layers. In the x-direction, first we divide $[0,1]$ into $[0, \sigma_x]$, $[\sigma_x, 1 - \sigma_x]$ and $[1 - \sigma_x, 1]$. Uniform meshes are then constructed on each subinterval, each with $\frac{2}{5}N_x$, $\frac{1}{5}N_x$ and $\frac{2}{5}N_x$ points, respectively. Here $\sigma_x = 2\alpha^{-1}\varepsilon\mu \ln N_x$. In the y-direction, we divide $[0,1]$ into $[0, \sigma_{y_1}]$, $[\sigma_{y_1}, \sigma_{y_2}]$ and $[\sigma_{y_2}, 1]$. Then uniform meshes are used on each subinterval,

each with $\frac{3}{10}N_y$, $\frac{2}{10}N_y$ and $\frac{5}{10}N_y$ points, respectively. Here $\sigma_{y_1} = 2\alpha^{-1}\varepsilon \ln N_y$ and $\sigma_{y_2} = 2\alpha^{-1}\varepsilon\mu^2 \ln N_y$.

More explicitly, in the x-direction, we have

$$0 = x_0 < x_1 < \cdots < x_{i_1} < \cdots < x_{i_2} < \cdots < x_{N_x} = 1,$$

with $i_1 = \frac{2}{5}N_x$, $i_2 = \frac{3}{5}N_x$, $x_{i_1} = \sigma_x$, $x_{i_2} = 1 - \sigma_x$ and the mesh size $h_i = x_i - x_{i-1}$ satisfy:

$$h_i = \sigma_x / \left(\frac{2}{5}N_x\right), \quad \text{for } i = 1, \dots, i_1, i_2 + 1, \dots, N_x \quad (5.26)$$

$$h_i = (1 - 2\sigma_x) / \left(\frac{1}{5}N_x\right), \quad \text{for } i = i_1 + 1, \dots, i_2. \quad (5.27)$$

In the y-direction, we have

$$0 = y_0 < y_1 < \cdots < y_{j_1} < \cdots < y_{j_2} < \cdots < y_{N_y} = 1,$$

with $j_1 = \frac{3}{10}N_y$, $j_2 = \frac{5}{10}N_y$, $y_{j_1} = \sigma_{y_1}$, $y_{j_2} = 1 - \sigma_{y_2}$ and the mesh size $k_j = y_j - y_{j-1}$ satisfy:

$$k_j = \sigma_{y_1} / \left(\frac{3}{10}N_y\right), \quad \text{for } j = 1, \dots, j_1, \quad (5.28)$$

$$k_j = (1 - \sigma_{y_1} - \sigma_{y_2}) / \left(\frac{2}{10}N_y\right), \quad \text{for } j = j_1 + 1, \dots, j_2 \quad (5.29)$$

$$k_j = \sigma_{y_2} / \left(\frac{5}{10}N_y\right), \quad \text{for } j = j_2 + 1, \dots, N_y. \quad (5.30)$$

The weak formulation of (5.1)(5.2) is: find $u \in H_0^1(\Omega)$ such that

$$B(u, v) \equiv \varepsilon^2 \mu^2 (\nabla u, \nabla v) + \varepsilon A(u_y, v) + (a^2 u, v) = (f, v), \quad \forall v \in H_0^1(\Omega), \quad (5.31)$$

where (\cdot, \cdot) denotes the usual $L^2(\Omega)$ inner product and $H_0^1(\Omega)$ is the usual Sobolev space[110].

Denote the weighted energy norm by

$$\|v\| \equiv \{\varepsilon^2 \mu^2 \|\nabla v\|^2 + \|v\|^2\}^{1/2}, \quad \forall v \in H_0^1(\Omega).$$

Note that for any $v \in H_0^1(\Omega)$, we have

$$B(v, v) = \varepsilon^2 \mu^2 (\nabla v, \nabla v) + \varepsilon A(v_y, v) + (a^2 v, v) \quad (5.32)$$

$$\geq \min(1, \min_{\bar{\Omega}} a^2) \|v\|^2. \quad (5.33)$$

We seek the bilinear finite element solution $u^h \in S_h(\Omega)$ such that

$$B(u^h, v) \equiv \varepsilon^2 \mu^2 (\nabla u^h, \nabla v) + \varepsilon A(u_y^h, v) + (a^2 u^h, v) = (f, v), \quad \forall v \in S_h(\Omega). \quad (5.34)$$

5.5 Theoretical Analysis

Lemma 5.6 *For the solution u of (5.1)(5.2), we have*

$$(I) \quad \|u - \Pi_x u\|_{\infty, \bar{I}_i} \leq C N_x^{-1} \ln N_x, \quad \forall i = 1, \dots, i_1, i_2 + 1, \dots, N_x,$$

$$(II) \quad \|u - \Pi_y u\|_{\infty, \bar{K}_j} \leq C N_y^{-1} \ln N_y, \quad \forall j = 1, \dots, j_1, j_2 + 1, \dots, N_y,$$

$$(I') \quad \|u - \Pi_x u\|_{\infty, \bar{I}_i} \leq C(N_x^{-2} + \varepsilon + \mu), \quad \forall i = i_1 + 1, \dots, i_2, \quad (5.35)$$

$$(II') \quad \|u - \Pi_y u\|_{\infty, \bar{K}_j} \leq C(N_y^{-2} + \varepsilon + \mu), \quad \forall j = j_1 + 1, \dots, j_2. \quad (5.36)$$

Proof. (I) For $i = 1, \dots, i_1, i_2 + 1, \dots, N_x$, by Lemmas 5.4 and 4.2, we obtain

$$\begin{aligned} \|u - \Pi_x u\|_{\infty, \bar{I}_i} &\leq C h_i \|u_x\|_{\infty, \bar{I}_i} \\ &\leq C h_i \max_{x \in \bar{I}_i} \left(1 + (\varepsilon \mu)^{-1} \exp\left(-\frac{a_1 x}{\varepsilon \mu}\right) + (\varepsilon \mu)^{-1} \exp\left(-\frac{a_1(1-x)}{\varepsilon \mu}\right) \right) \\ &\leq C h_i (1 + (\varepsilon \mu)^{-1}) \leq C N_x^{-1} \ln N_x, \end{aligned}$$

since $h_i = \sigma_x / (\frac{2}{5} N_x)$ in this case. Hence (I) is true.

(II) For $i = i_1 + 1, \dots, i_2$, in this case $x \in [\sigma_x, 1 - \sigma_x]$. We can write $\Pi_x u$ in the form

$$\Pi_x u = \Pi_x U_0 + \Pi_x (u - U_0)$$

Hence by Lemmas 5.5 and 2.8, we have

$$\|u - \Pi_x u\|_{\infty, \bar{I}_i} \leq \|U_0 - \Pi_x U_0\|_{\infty, \bar{I}_i} + \|(u - U_0) - \Pi_x(u - U_0)\|_{\infty, \bar{I}_i} \quad (5.37)$$

$$\leq \|U_0 - \Pi_x U_0\|_{\infty, \bar{I}_i} + 2\|(u - U_0)\|_{\infty, \bar{I}_i} \quad (5.38)$$

$$\leq \|U_0 - \Pi_x U_0\|_{\infty, \bar{I}_i} + C(\varepsilon + \mu). \quad (5.39)$$

The estimation of $\|U_0 - \Pi_x U_0\|_{\infty, \bar{I}_i}$ can be carried out similarly as [73, Lemma 2.4.1] by using those estimates given in Section 3.

Proof of (II) and (II') can be carried out in the same way by symmetry consideration.

Following a similar proof to that of [73, Lemma 2.4.2], we can easily obtain the following interpolation result:

Lemma 5.7 *For the solution u of (5.1)(5.2), we obtain*

$$\|u - \Pi u\|_{\infty, \bar{\Omega}} \leq C(N_x^{-1} \ln N_x + N_y^{-1} \ln N_y + \varepsilon + \mu). \quad (5.40)$$

Next we will use a result obtained in [73]:

Lemma 5.8 [73, Lemma 2.4.3] *Let $\tau \equiv [0, h_x] \times [0, h_y]$, then for any $v \in S_h(\Omega)$ we have*

$$\int_{\tau} |v_y| dx dy \leq C(h_x/h_y)^{1/2} \|v\|_{2, \tau}. \quad (5.41)$$

Theorem 5.1 *Let u_h be the finite element solution of (5.34) and u be the solution of (5.1)(5.2), then we have*

$$\|u - u^h\| \leq CC_{\varepsilon}(N_x^{-1} \ln N_x + N_y^{-1} \ln N_y + \varepsilon + \mu),$$

where $C_{\varepsilon} = 1 + \varepsilon\mu(N_x + N_y) + \varepsilon^{1/2} \ln N_y + \varepsilon^{1/2} N_y \ln^{-1/2} N_y$.

Proof. Let $\chi = \Pi u - u^h$, then by (5.32) we have

$$C_1 \| \Pi u - u^h \|^2 \leq B(\Pi u - u^h, \Pi u - u^h) = B(\Pi u - u, \Pi u - u^h). \quad (5.42)$$

By the definition of (5.31), we have

$$B(\Pi u - u, \Pi u - u^h) = \varepsilon^2 \mu^2 (\nabla(\Pi u - u), \nabla \chi) + A\varepsilon((\Pi u - u)_y, \chi) + (a^2(\Pi u - u), \chi)$$

Integrating by parts, we obtain

$$\begin{aligned} \varepsilon^2 \mu^2 ((\Pi u - u)_x, \chi_x) &= \sum_{1 \leq i \leq N_x, 1 \leq j \leq N_y} \int_{x_{i-1}}^{x_i} \int_{y_{j-1}}^{y_j} \varepsilon^2 \mu^2 (\Pi u - u)_x \chi_x dx dy \\ &= \sum_{1 \leq i \leq N_x, 1 \leq j \leq N_y} \int_{y_{j-1}}^{y_j} \varepsilon^2 \mu^2 (\Pi u - u)|_{x=x_{i-1}} \chi_x dy, \\ &\leq \sum_{1 \leq i \leq N_x, 1 \leq j \leq N_y} \int_{y_{j-1}}^{y_j} |\varepsilon \mu \chi_x| dy \cdot \varepsilon \mu \|\Pi u - u\|_{\infty, \bar{\Omega}} \\ &= \sum_{1 \leq i \leq N_x} \int_0^1 \int_0^1 |\varepsilon \mu \chi_x| dy dx \cdot \varepsilon \mu \|\Pi u - u\|_{\infty, \bar{\Omega}} \\ &\leq \varepsilon \mu N_x \|\Pi u - u\|_{\infty, \bar{\Omega}} \cdot \|\varepsilon \mu \chi_x\| \end{aligned}$$

Similarly, we have

$$\varepsilon^2 \mu^2 ((\Pi u - u)_y, \chi_y) \leq \varepsilon \mu N_y \|\Pi u - u\|_{\infty, \bar{\Omega}} \cdot \|\varepsilon \mu \chi_y\| \quad (5.43)$$

Note that

$$(a^2(\Pi u - u), \chi) \leq \|a^2\|_{\infty, \bar{\Omega}} \|\Pi u - u\| \|\chi\| \leq C \|\Pi u - u\|_{\infty, \bar{\Omega}} \|\chi\| \quad (5.44)$$

Let $S_1 = [0, 1] \times [1 - \sigma_{y_2}, 1]$ and $S_2 = [0, 1] \times [0, 1 - \sigma_{y_2}]$, then we have

$$\varepsilon A((\Pi u - u)_y, \chi) = -\varepsilon A(\Pi u - u, \chi_y) \quad (5.45)$$

$$= -\varepsilon A\left(\int_{S_1} + \int_{S_2}\right) (\Pi u - u) \chi_y dx dy \quad (5.46)$$

Note that

$$\varepsilon A \int_{S_1} (\Pi u - u) \chi_y dx dy \leq C \varepsilon \|\Pi u - u\|_{\infty, \bar{\Omega}} \int_{S_1} |\chi_y| dx dy \quad (5.47)$$

$$\leq C \varepsilon \|\Pi u - u\|_{\infty, \bar{\Omega}} (\text{meas}(S_1))^{1/2} \|\chi_y\| \quad (5.48)$$

$$\leq C \varepsilon \|\Pi u - u\|_{\infty, \bar{\Omega}} (\varepsilon \mu^2 \ln N_y)^{1/2} \|\chi_y\| \quad (5.49)$$

$$= C \varepsilon^{1/2} \ln N_y \|\Pi u - u\|_{\infty, \bar{\Omega}} \cdot \|\varepsilon \mu \chi_y\| \quad (5.50)$$

and by Lemma 5.3, we have

$$\varepsilon A \int_{S_2} (\Pi u - u) \chi_y dx dy \leq C\varepsilon \|\Pi u - u\|_{\infty, \bar{\Omega}} \int_{S_2} |\chi_y| dx dy \quad (5.51)$$

$$\leq C\varepsilon \|\Pi u - u\|_{\infty, \bar{\Omega}} \sum_{\tau \in S_2} \left(\frac{h_x}{h_y}\right)^{1/2} \|\chi\|_{2, \tau} \quad (5.52)$$

$$\leq C\varepsilon \|\Pi u - u\|_{\infty, \bar{\Omega}} \left(\frac{N_x^{-1}}{\varepsilon N_y^{-1} \ln N_y}\right)^{1/2} \sum_{\tau \in S_2} \|\chi\|_{2, \tau} \quad (5.53)$$

$$\leq C\varepsilon^{1/2} \ln^{-1/2} N_y \|\Pi u - u\|_{\infty, \bar{\Omega}} \cdot \left(\sum_{\tau \in S_2} 1^2\right)^{1/2} \left(\sum_{\tau \in S_2} \|\chi\|_{2, \tau}^2\right)^{1/2} \\ \leq C\varepsilon^{1/2} N_y \ln^{-1/2} N_y \|\Pi u - u\|_{\infty, \bar{\Omega}} \|\chi\| \quad (5.54)$$

where we used the fact that $\sum_{\tau \in S_2} 1 \leq N_x N_y$.

Combining all above inequalities, we have

$$C_1 \|\|\Pi u - u^h\|\|^2 \leq C \cdot C_\varepsilon \|\Pi u - u\|_{\infty, \bar{\Omega}} \cdot \|\|\Pi u - u^h\|\| \quad (5.55)$$

from which we obtain

$$\|\|\Pi u - u^h\|\| \leq C \cdot C_\varepsilon \|\Pi u - u\|_{\infty, \bar{\Omega}}$$

Hence by Lemma 5.2, we have

$$\|u - u^h\| \leq \|u - \Pi u\| + \|\Pi u - u^h\| \leq \|u - \Pi u\|_{\infty, \bar{\Omega}} + \|\|\Pi u - u^h\|\| \quad (5.56)$$

$$\leq C \cdot C_\varepsilon (N_x^{-1} \ln N_x + N_y^{-1} \ln N_y + \varepsilon + \mu), \quad (5.57)$$

which concludes our proof.

From Theorem 5.1, we can expect almost first-order uniform convergence rate, since practically ε and μ are small enough so that the error is dominated by $N_x^{-1} \ln N_x + N_y^{-1} \ln N_y$.

5.6 Numerical Results

For simplicity, we chose $N_x = N_y = N$ and bilinear interpolation for variable function in our numerical experiments. In Figures 5.1-5.15, we always denote (a) for the left figure and (b) for the right figure.

To test the performance of our method, we experimented with both a constant coefficient case:

$$\text{Example 1: } A = 1, a = 2, f = 16x(1-x)y(1-y) + 1$$

and a variable coefficient case:

$$\text{Example 2: } A = 1, a = 2\sqrt{1+x^2+y^2}, f = 16x(1-x)y(1-y) + 1$$

on a uniform mesh and our piecewise uniform mesh for $N=40$ with different ε and μ ranging from 10^{-7} to 10^{-2} . The computed solutions are presented in Figures 5.1-5.6. These figures clearly show that our piecewise uniform mesh performs much better than the uniform mesh. Our piecewise uniform mesh resolves the sharp boundary layers without any oscillations. Also the smaller the perturbation parameters are, the better the approximation we obtain. On the other hand, the solutions achieved on the uniform mesh become more oscillatory near the boundary layers as the perturbation parameters become larger. This is consistent with our model. Since as ε becomes smaller, the convection term (ε) becomes larger compared to the diffusion term ($\varepsilon^2\mu^2$). Note that $u_0 = 4x(1-x)y(1-y) + \frac{1}{4}$ and $u_0 = \frac{4x(1-x)y(1-y)+1/4}{1+x^2+y^2}$ are solutions of reduced problems ($\varepsilon = \mu = 0$) for Examples 1 and 2, respectively, so we know how the exact solutions should look like.

To measure the accuracy of our method, we tested another case where $A=1$, $a=2$, and f is chosen appropriately such that the exact solution is known:

$$\text{Example 3: } u = \frac{1}{4} \left(1 - \exp\left(-\frac{x}{\varepsilon\mu}\right)\right) \left(1 - \exp\left(-\frac{1-x}{\varepsilon\mu}\right)\right) \left(1 - \exp\left(-\frac{y}{\varepsilon}\right)\right) \left(1 - \exp\left(-\frac{1-y}{\varepsilon\mu^2}\right)\right)$$

The computed solution u^h and the pointwise error $u^h - u$ are shown in Figures 5.7-5.15 for $\varepsilon = \mu = 10^{-2}, 10^{-3}, 10^{-5}$ and $N=10, 20, 40$. When $\varepsilon, \mu \leq 10^{-5}$, there is almost

no distinction from $\varepsilon = \mu = 10^{-5}$. The L^2 and L^∞ error are provided in Tables 5.1 and 5.2, respectively, from which we see the uniform convergence rate in both L^2 and L^∞ norms very clearly. The estimated convergence rate $R_N = (\ln e_N - \ln e_{2N})/\ln 2$ in L^2 norm is 2.62 and 2.57 for $N=10$ and 20, respectively, which is much better than expected from our theoretical estimates. Note that our function f does not vanish at the four corners. This phenomenon has been observed in many other cases [51, 105]. Actually higher order error estimates can be proved similarly only under more restricted assumptions. We guess that the convergence rate will approach to 2 when N is large enough. But due to the heavy computational burden, such a calculation proved to be prohibitive for our computing facilities.

Another phenomenon we observed is that the error is actually independent of μ . This can be explained by Theorem 5.1 which states that the coefficient C_ε is independent of μ . Another explanation is that actually we can use an arbitrary higher order asymptotic expansion (except arbitrary small neighborhoods of corner $(0,0)$ and $(1,0)$) [20, Theorem 2] for a smooth enough solution in our proof, hence only the error resulting from the boundary layers dominates. This is shown very clearly in Figures 5.7(b)-5.15(b). As N becomes larger, the dominant error originates from those two corners $(0,0)$ and $(1,0)$, which is consistent with Butuzov asymptotic approximation [20].

Table 5.1: Errors in L^2 norm for Example 3

	N		
$\varepsilon = \mu$	10	20	40
1.0D-02	3.35145186D-03	8.54606800D-04	3.36480157D-04
1.0D-03	3.08143764D-03	5.35671619D-04	1.14297261D-04
1.0D-04	3.05463960D-03	4.98142036D-04	8.62599006D-05
1.0D-05	3.05196199D-03	4.94288340D-04	8.32021259D-05
1.0D-06	3.05169425D-03	4.93901877D-04	8.28927405D-05
1.0D-07	3.05166748D-03	4.93863219D-04	8.28617643D-05

Table 5.2: Errors in L^∞ norm for Example 3

	N		
$\varepsilon = \mu$	10	20	40
1.0D-02	2.00249517D-02	1.3875412182D-02	1.0330639906D-02
1.0D-03	2.00277257D-02	1.3875412154D-02	1.0330639789D-02
1.0D-04	2.00279914D-02	1.3875412159D-02	1.0329781808D-02
1.0D-05	2.00280178D-02	1.3875412157D-02	1.0329781808D-02
1.0D-06	2.00280205D-02	1.3875412146D-02	1.0329781808D-02
1.0D-07	2.00280207D-02	1.3875412203D-02	1.0329781840D-02

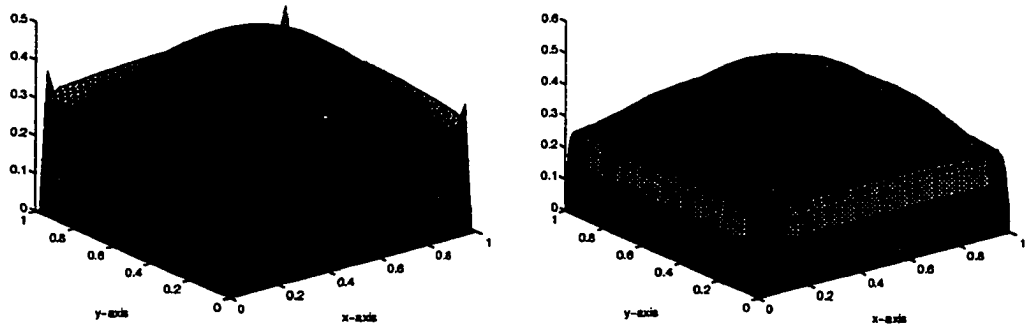


Figure 5.1: Example 1: computed solution for $\varepsilon = 10^{-2}$, $N = 40$: (a) uniform mesh (b) piecewise uniform mesh

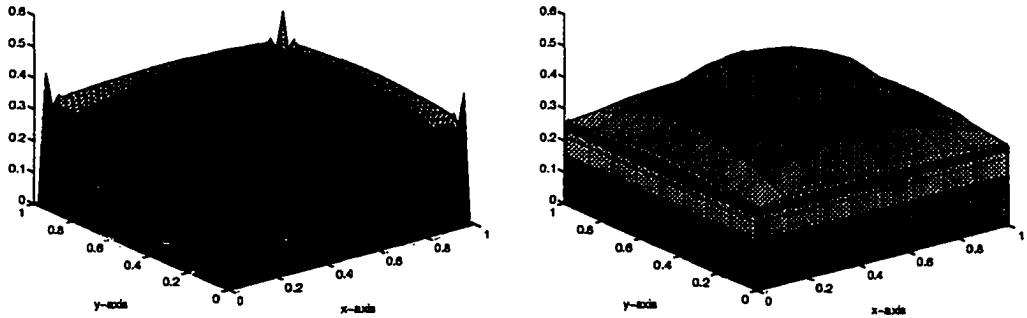


Figure 5.2: Example 1: computed solution for $\varepsilon = 10^{-3}$, $N = 40$: (a) uniform mesh (b) piecewise uniform mesh

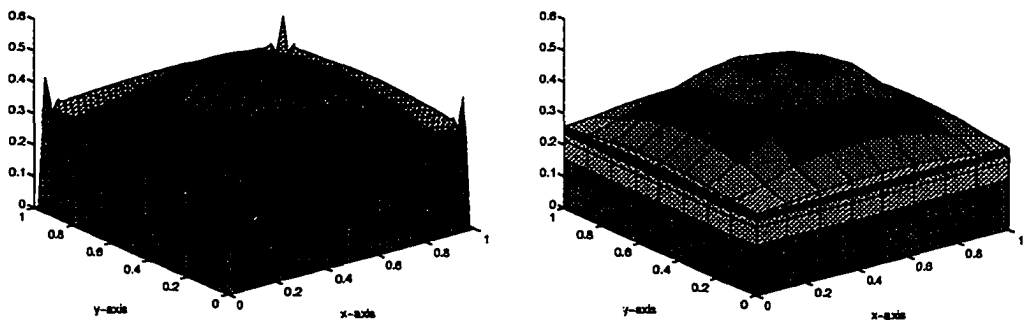


Figure 5.3: Example 1: computed solution for $\varepsilon = 10^{-5}$, $N = 40$: (a) uniform mesh (b) piecewise uniform mesh

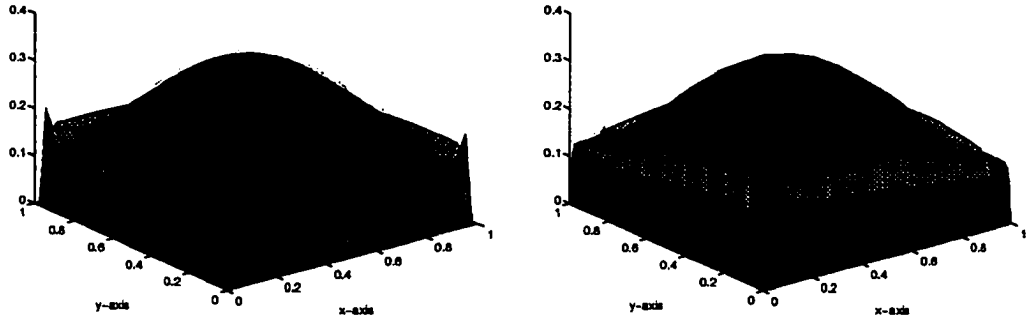


Figure 5.4: Example 2: computed solution for $\varepsilon = 10^{-2}$, $N = 40$: (a) uniform mesh
(b) piecewise uniform mesh

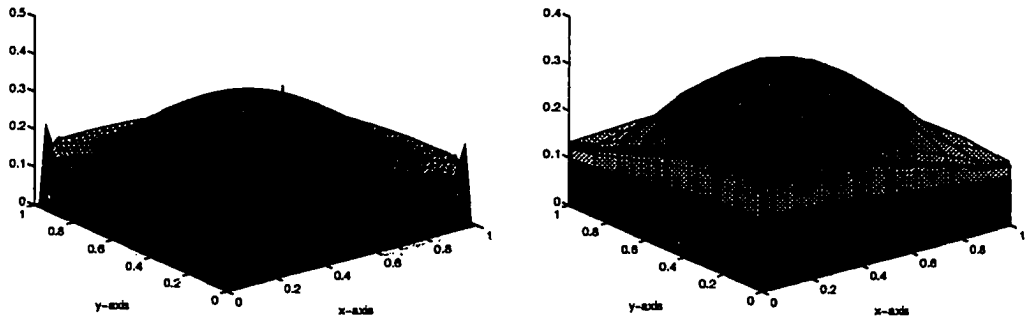


Figure 5.5: Example 2: computed solution for $\varepsilon = 10^{-3}$, $N = 40$: (a) uniform mesh
(b) piecewise uniform mesh

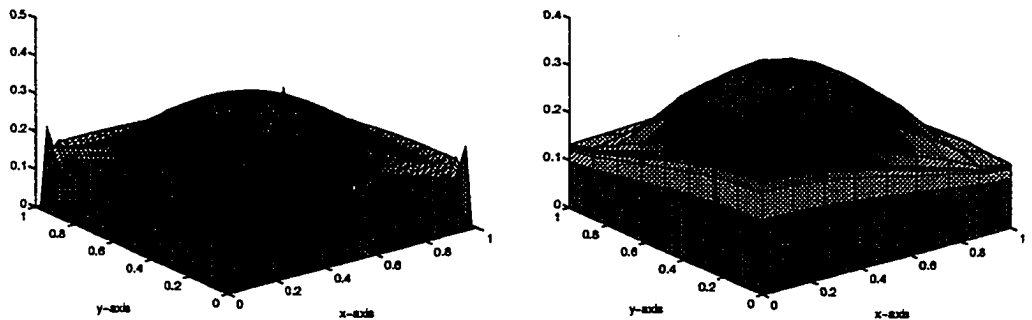


Figure 5.6: Example 2: computed solution for $\varepsilon = 10^{-5}$, $N = 40$: (a) uniform mesh
(b) piecewise uniform mesh

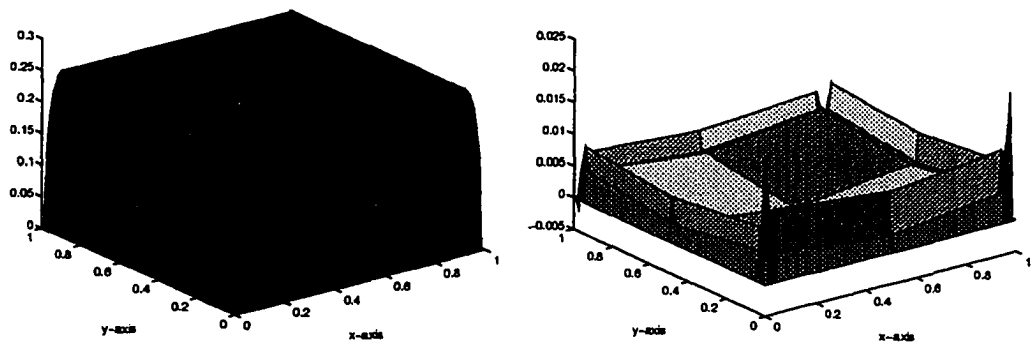


Figure 5.7: Example 3: piecewise uniform mesh for $\varepsilon = 10^{-2}$, $N = 10$: (a) computed solution (b) pointwise error

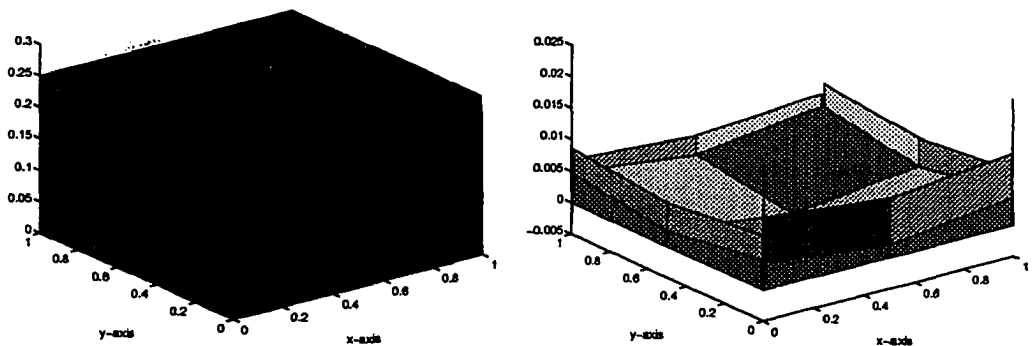


Figure 5.8: Example 3: piecewise uniform mesh for $\varepsilon = 10^{-3}$, $N = 10$: (a) computed solution (b) pointwise error

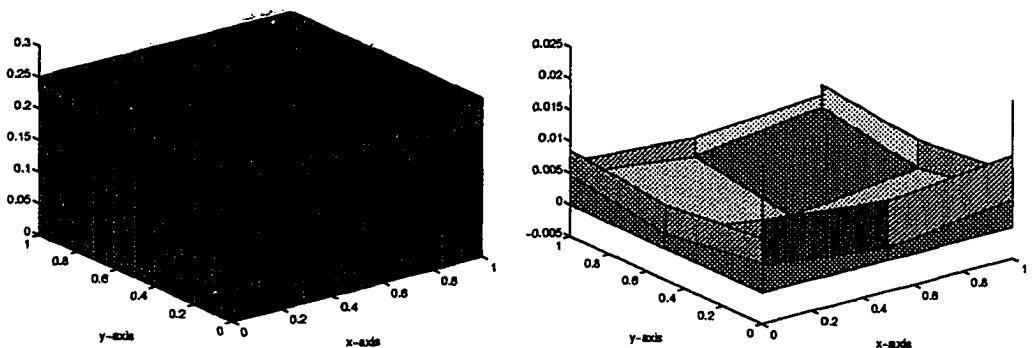


Figure 5.9: Example 3: piecewise uniform mesh for $\varepsilon = 10^{-5}$, $N = 10$: (a) computed solution (b) pointwise error

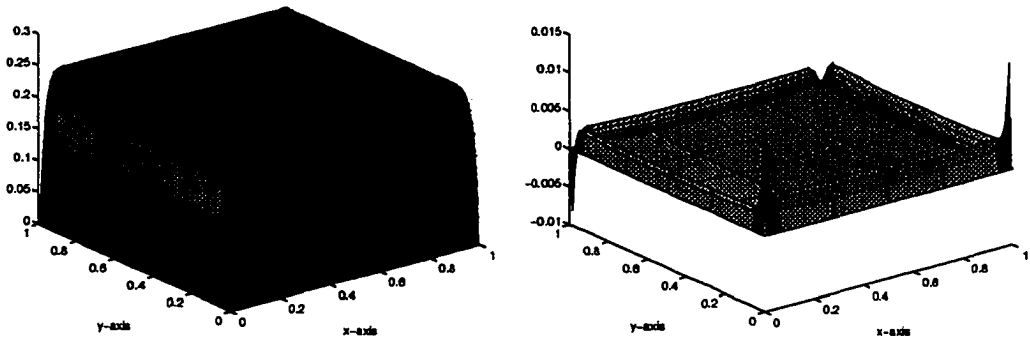


Figure 5.10: Example 3: piecewise uniform mesh for $\varepsilon = 10^{-2}$, $N = 20$: (a) computed solution (b) pointwise error

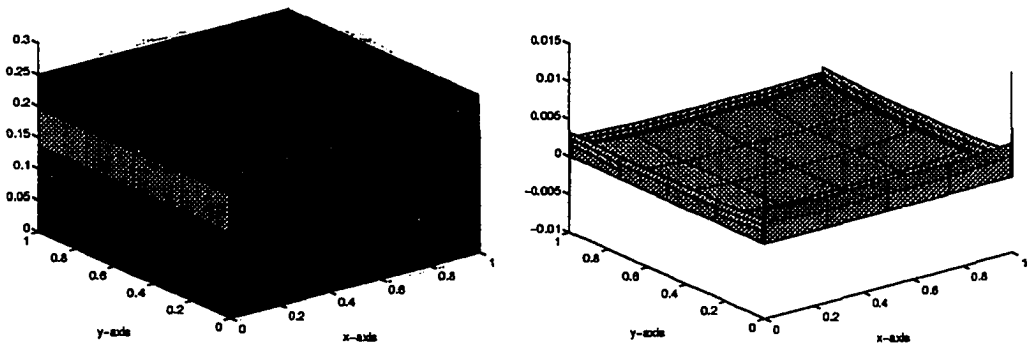


Figure 5.11: Example 3: piecewise uniform mesh for $\varepsilon = 10^{-3}$, $N = 20$: (a) computed solution (b) pointwise error

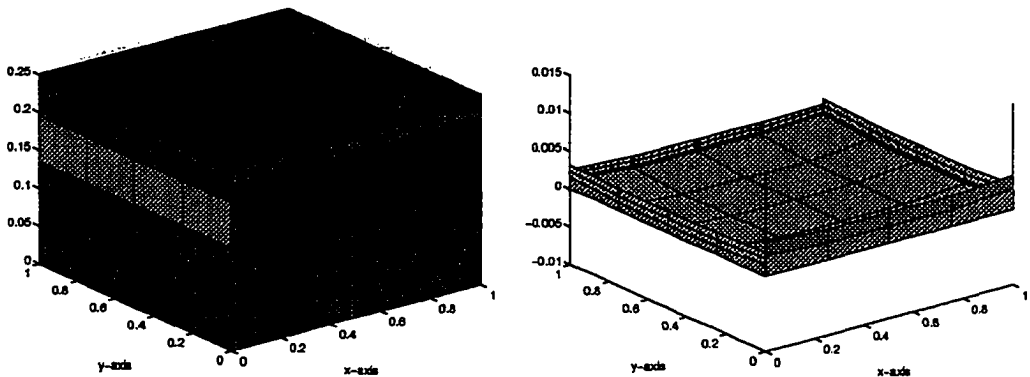


Figure 5.12: Example 3: piecewise uniform mesh for $\varepsilon = 10^{-5}$, $N = 20$: (a) computed solution (b) pointwise error

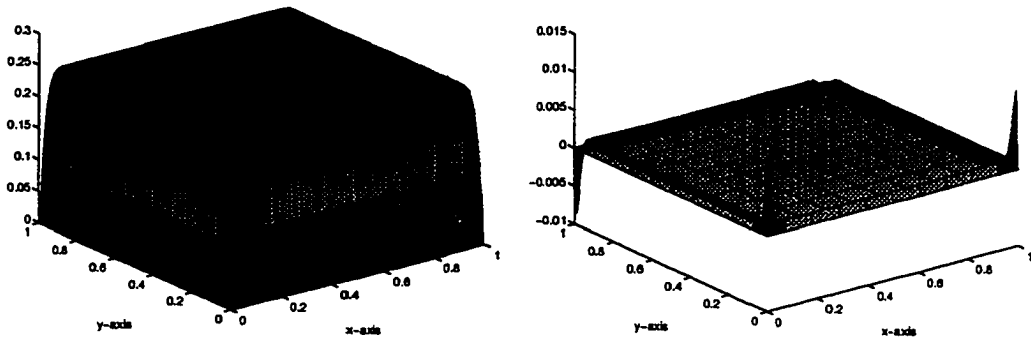


Figure 5.13: Example 3: piecewise uniform mesh for $\varepsilon = 10^{-2}$, $N = 40$: (a) computed solution (b) pointwise error

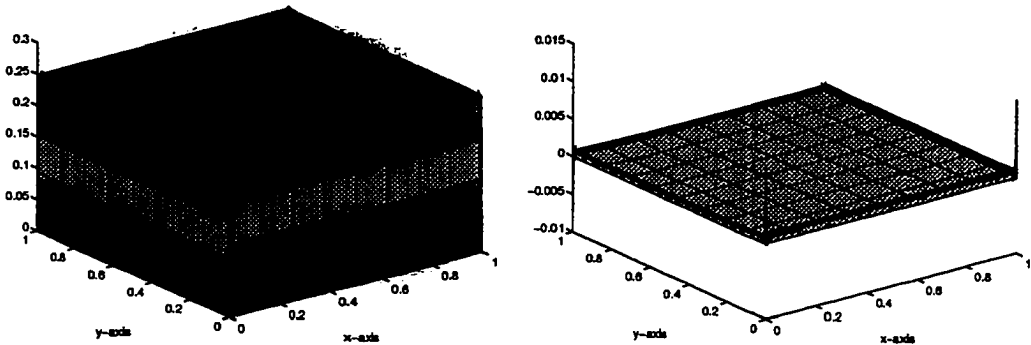


Figure 5.14: Example 3: piecewise uniform mesh for $\varepsilon = 10^{-3}$, $N = 40$: (a) computed solution (b) pointwise error

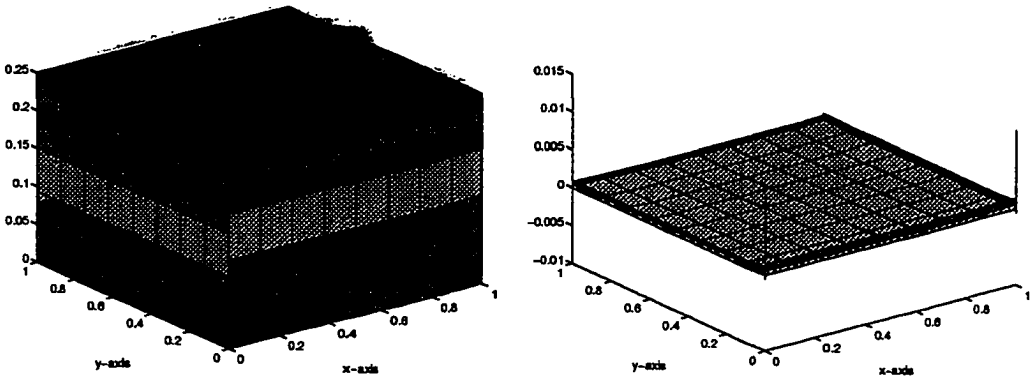


Figure 5.15: Example 3: piecewise uniform mesh for $\varepsilon = 10^{-5}$, $N = 40$: (a) computed solution (b) pointwise error

CHAPTER 6

HIGHER-ORDER FINITE ELEMENTS

6.1 Introduction

Recently, global uniform convergence was achieved by using the standard FEM on some specially constructed piecewise uniform meshes [110, 105], the so-called Shishkin mesh, which was introduced by Shishkin [117]. However, "*High-order elements seem to be more attractive than linear ones But precise error estimates for this technique on Shishkin meshes are still unavailable*" [105, pp.7]. Also "*Not much is known about Shishkin-type grids for nonlinear problems*" [105, pp.8].

Our goal in this chapter is to develop a general higher-order FEM, which is GUC, for solving the singularly perturbed elliptic boundary value problems in two space dimensions. To clarify the ideas, we first focus on a linear reaction-diffusion model by using a bi-quadratic finite element, where we show that our scheme is GUC to almost third order in L^2 norm. Then a similar discussion is carried out for a quasilinear reaction-diffusion model. Some numerical results are presented, which are consistent with our theoretical analysis. A comparison was carried out between our scheme on a piecewise uniform mesh and the standard FEM on a uniform mesh. It is shown that our method performs much better than the standard FEM on the uniform mesh. Generalizations to any m -th order tensor-product elements are also discussed, where $m \geq 3$.

6.2 The 2-D Linear Reaction-Diffusion Model

In this section, we will consider the following singularly perturbed elliptic problem:

$$L_\varepsilon u \equiv -\varepsilon^2 \left(\frac{\partial^2 u}{\partial x^2} + \frac{\partial^2 u}{\partial y^2} \right) + a(x, y)u = f(x, y) \quad \text{in } \Omega \equiv (0, 1)^2, \quad (6.1)$$

$$u = 0 \quad \text{on } \partial\Omega, \quad (6.2)$$

where $0 < \varepsilon \ll 1$. The functions a and f are assumed to be sufficiently smooth in Ω and

$$a(x, y) \geq \alpha^2 > 0 \quad \text{in } \Omega.$$

Here $\alpha > 0$ is a constant.

6.2.1 The Asymptotic Expansion and Derivative Estimates

The asymptotic expansion for (6.1)(6.2) was investigated in [49, 18], from which we have:

Lemma 6.1 [49, Theorem 2.1] *Let u solve (6.1)(6.2). There exists a constant $C_n > 0$ that is independent of ε such that*

$$|u(x, y) - \tilde{u}_{2n}(x, y)| \leq C_n \varepsilon^{2n+1},$$

where

$$\tilde{u}_{2n} = U_{2n} + V_{2n} + W_{2n} + \bar{V}_{2n} + \bar{W}_{2n} + \sum_{l=1}^4 Z_{2n}^l, \quad (6.3)$$

$$U_{2n}(x, y) \quad \text{is the regular part,} \quad (6.4)$$

$$V_{2n}(x, \eta), W_{2n}(\xi, y), \bar{V}_{2n}(x, \bar{\eta}), \bar{W}_{2n}(\bar{\xi}, y) \quad \text{are the boundary layer functions,}$$

$$Z_{2n}^1(\xi, \eta), Z_{2n}^2(\bar{\xi}, \eta), Z_{2n}^3(\xi, \bar{\eta}), Z_{2n}^4(\bar{\xi}, \bar{\eta}) \quad \text{are the corner layer functions.} \quad (6.5)$$

Here $\xi = x/\varepsilon, \eta = y/\varepsilon, \bar{\xi} = (1-x)/\varepsilon, \bar{\eta} = (1-y)/\varepsilon$. Also the estimates of Lemma 3.1 of Chapter 3 hold true.

From Lemmas 3.1, 3.3 and 3.5 of [72], we have

Lemma 6.2 For the solution u of (6.1)(6.2), we have

$$(I) \quad |u_{x^n}(x, y)| \leq C(1 + \varepsilon^{-n}e^{-\alpha x/\varepsilon} + \varepsilon^{-n}e^{-\alpha(1-x)/\varepsilon}) \quad \text{on } \bar{\Omega} \equiv \Omega \cup \partial\Omega, \quad (6.6)$$

$$(II) \quad |u_{y^n}(x, y)| \leq C(1 + \varepsilon^{-n}e^{-\alpha y/\varepsilon} + \varepsilon^{-n}e^{-\alpha(1-y)/\varepsilon}) \quad \text{on } \bar{\Omega}, \quad (6.7)$$

where $n = 0, 1, 2$.

In order to use higher-order FEM, we need to obtain higher-order derivative estimates for the solution of (6.1)(6.2). By using the boundary condition (6.2) in (6.1), we have

$$u_{xx}|_{x=0} = -\varepsilon^{-2}f(0, y), \quad u_{xx}|_{x=1} = -\varepsilon^{-2}f(1, y) \quad (6.8)$$

$$u_{xx}|_{y=0} = u_{xx}|_{y=1} = 0 \quad (6.9)$$

or in one simple form as

$$u_{xx}(x, y) = g(x, y, \varepsilon) \quad \text{on } \partial\Omega,$$

where $g(x, y, \varepsilon) = -\varepsilon^{-2}(1-x)f(0, y) - \varepsilon^{-2}xf(1, y)$. Here the compatibility conditions [49]

$$f(0, 0) = f(0, 1) = f(1, 0) = f(1, 1) = 0$$

were used.

By denoting $\tilde{u}(x, y) = u_{xx}(x, y) - g(x, y, \varepsilon)$, and differentiating (6.1) twice with respect to x , we have

$$L_\varepsilon \tilde{u} \equiv -\varepsilon^2 \Delta \tilde{u} + a\tilde{u} = \tilde{F} \quad \text{in } \Omega, \quad (6.10)$$

$$\tilde{u} = 0 \quad \text{on } \partial\Omega, \quad (6.11)$$

where $\tilde{F} = f_{xx} - 2a_x u_x - a_{xx} u + \varepsilon^2 g_{xx} + \varepsilon^2 g_{yy} - ag$.

Lemma 6.3

$$(I) \quad |\tilde{u}_x(x, y)| \leq C\varepsilon^{-3}, \quad \text{on } \partial\Omega \quad (6.12)$$

$$(II) \quad |\tilde{u}_y(x, y)| \leq C\varepsilon^{-3}, \quad \text{on } \partial\Omega \quad (6.13)$$

Proof. Using the barrier function

$$\phi = C\varepsilon^{-2}(1 - e^{-\alpha x/\varepsilon})(1 - e^{-\alpha(1-x)/\varepsilon}),$$

and after some simple calculations, we have

$$\begin{aligned} L_\varepsilon(\phi \pm \tilde{u}) &= \frac{C\alpha^2}{\varepsilon^2}[e^{-\alpha x/\varepsilon} + e^{-\alpha(1-x)/\varepsilon}] + \frac{Ca}{\varepsilon^2}(1 - e^{-\alpha x/\varepsilon})(1 - e^{-\alpha(1-x)/\varepsilon}) \pm \tilde{F} \\ &\geq \frac{C\alpha^2}{\varepsilon^2}(1 + e^{-\alpha/\varepsilon}) \pm \tilde{F} \end{aligned} \quad (6.14)$$

$$\geq 0, \quad \text{for sufficiently large } C, \quad (6.15)$$

where we used the fact that $a \geq \alpha^2$ and $|\tilde{F}| \leq C_1\varepsilon^{-2}$.

Hence, by using the maximum principle [72, Theorem 3.1] and the fact that

$$(\phi \pm \tilde{u})|_{\partial\Omega} \geq 0,$$

we obtain

$$|\tilde{u}| \leq \phi = C\varepsilon^{-2}(1 - e^{-\alpha x/\varepsilon})(1 - e^{-\alpha(1-x)/\varepsilon}), \quad \text{on } \bar{\Omega} \quad (6.16)$$

from which we have

$$|\tilde{u}_x(0, y)| = \left| \lim_{x \rightarrow 0^+} \frac{\tilde{u}(x, y) - \tilde{u}(0, y)}{x} \right| \leq \lim_{x \rightarrow 0^+} \left| \frac{\tilde{u}(x, y) - \tilde{u}(0, y)}{x} \right| \quad (6.17)$$

$$\leq \lim_{x \rightarrow 0^+} \frac{C\varepsilon^{-2}(1 - e^{-\alpha x/\varepsilon})(1 - e^{-\alpha(1-x)/\varepsilon})}{x} \leq \alpha C\varepsilon^{-3}. \quad (6.18)$$

Similarly,

$$|\tilde{u}_x(1, y)| \leq \lim_{x \rightarrow 1^-} \left| \frac{\tilde{u}(1, y) - \tilde{u}(x, y)}{1 - x} \right| \leq C\varepsilon^{-3}.$$

From the boundary condition (6.11), we have

$$\tilde{u}_x(x, 0) = 0 = \tilde{u}_x(x, 1).$$

By combining the above inequalities, we obtain

$$|\tilde{u}_x(x, y)|_{\partial\Omega} \leq C\varepsilon^{-3}. \quad (6.19)$$

By symmetry, we can easily obtain

$$|\tilde{u}_y(x, y)|_{\partial\Omega} \leq C\varepsilon^{-3}$$

which along with (6.19) concludes our proof.

Lemma 6.4

$$(I) \quad |u_{x^3}(x, y)| \leq C\varepsilon^{-3}, \quad \text{on } \bar{\Omega} \tag{6.20}$$

$$(II) \quad |u_{y^3}(x, y)| \leq C\varepsilon^{-3}, \quad \text{on } \bar{\Omega} \tag{6.21}$$

Proof. Consider the barrier function $\phi = C\varepsilon^{-3}$, then we have

$$L_\varepsilon(\phi \pm \tilde{u}_x) = aC\varepsilon^{-3} \pm (\tilde{F}_x - a_x \tilde{u}) \tag{6.22}$$

$$\geq 0, \quad \text{for sufficiently large } C. \tag{6.23}$$

By Lemma 6.3, we obtain

$$(\phi \pm \tilde{u}_x)|_{\partial\Omega} \geq 0$$

from which together with the maximum principle [72, Theorem 3.1], we have

$$|\tilde{u}_x(x, y)| \leq \phi = C\varepsilon^{-3}, \quad \text{on } \bar{\Omega}.$$

Hence by the definition of \tilde{u} , we have

$$|u_{x^3}(x, y)| = |(\tilde{u} + g)_x| \leq C\varepsilon^{-3}$$

which concludes the proof of (I).

The proof of (II) can be carried out similarly.

6.2.2 The Mesh and the Finite Element Scheme

Since our problem has boundary layers located along all sides of the rectangle Ω , our piecewise uniform mesh can be constructed in the same way as we did in [72].

Assume that the positive integers N_x and N_y are divisible by 4, where N_x and N_y denote the number of elements in the x- and y-directions, respectively. In the x-direction, we first divide the interval $[0, 1]$ into the subintervals

$$[0, \sigma_x], \quad [\sigma_x, 1 - \sigma_x], \quad [1 - \sigma_x, 1].$$

Uniform meshes are then used on each subinterval, with $N_x/4$ points on each of $[0, \sigma_x]$ and $[1 - \sigma_x, 1]$, and $N_x/2$ points on $[\sigma_x, 1 - \sigma_x]$, where $\sigma_x = 3\alpha^{-1}\varepsilon \ln N_x$. Here for simplicity, we assume that $\sigma_x \leq 1/4$, since we are considering SPP where ε is very small.

In the y-direction, we follow the same method described above by dividing the interval $[0, 1]$ into the subintervals

$$[0, \sigma_y], \quad [\sigma_y, 1 - \sigma_y], \quad [1 - \sigma_y, 1].$$

Uniform meshes are then used on each subinterval, with $N_y/4$ points on each of $[0, \sigma_y]$ and $[1 - \sigma_y, 1]$, and $N_y/2$ points on $[\sigma_y, 1 - \sigma_y]$, where $\sigma_y = 3\alpha^{-1}\varepsilon \ln N_y$.

The weak formulation of (6.1)(6.2) is: Find $u \in H_0^1(\Omega)$ such that

$$B(u, v) \equiv \varepsilon^2(\nabla u, \nabla v) + (au, v) = (f, v), \quad \forall v \in H_0^1(\Omega), \quad (6.24)$$

where (\cdot, \cdot) denotes the usual $L^2(\Omega)$ inner product and $H_0^1(\Omega)$ is the usual Sobolev space.

Denote the weighted energy norm

$$|||v||| \equiv \{\varepsilon^2\|\nabla v\|^2 + \|v\|^2\}^{1/2}, \quad \forall v \in H_0^1(\Omega).$$

Also we have

$$B(v, v) = \varepsilon^2\|\nabla v\|^2 + (av, v) \geq \min\{1, \alpha^2\}|||v|||^2. \quad (6.25)$$

Let $S_h(\Omega)$ be the ordinary tensor-product quadratic element space, and

$$\Pi w = \Pi_x \Pi_y w = \Pi_y \Pi_x w$$

be the bi-quadratic interpolation of w , where Π_x and Π_y are the interpolations in the x - and y -directions, respectively. More explicitly, the one-dimensional interpolation Π_x on $[x_{i-1}, x_i]$ can be written as

$$\Pi_x w(x) = w(x_{i-1})\psi_1(\xi) + w\left(\frac{x_{i-1} + x_i}{2}\right)\psi_2(\xi) + w(x_i)\psi_3(\xi), \quad (6.26)$$

where the shape functions are [12, pp.67]

$$\psi_1(\xi) = -\frac{1}{2}\xi(1 - \xi) \quad (6.27)$$

$$\psi_2(\xi) = (1 + \xi)(1 - \xi) \quad (6.28)$$

$$\psi_3(\xi) = \frac{1}{2}\xi(1 + \xi) \quad (6.29)$$

Here the transformation $\xi = \frac{2x - (x_{i-1} + x_i)}{x_i - x_{i-1}}$ maps $[x_{i-1}, x_i]$ to $[-1, 1]$.

From (6.26), we have

$$\|\Pi_x w\|_{\infty, I_i} \leq \|w\|_{\infty, I_i} \cdot \max_{-1 \leq \xi \leq 1} (|\psi_1(\xi)| + |\psi_2(\xi)| + |\psi_3(\xi)|) \quad (6.30)$$

$$\leq \|w\|_{\infty, I_i} \cdot \max_{-1 \leq \xi \leq 1} \left[\frac{1}{2}|\xi|(1 - \xi) + (1 - \xi^2) + \frac{1}{2}|\xi|(1 + \xi) \right] \quad (6.31)$$

$$\leq 2\|w\|_{\infty, I_i} \quad (6.32)$$

Hence, we obtain

Lemma 6.5

$$(1) \quad \Pi w = \Pi_x \Pi_y w = \Pi_y \Pi_x w \quad (6.33)$$

$$(2) \quad \|\Pi_x w\|_{\infty, \bar{I}_i} \leq 2\|w\|_{\infty, \bar{I}_i} \quad (6.34)$$

$$(3) \quad \|w - \Pi_x w\|_{\infty, \bar{I}_i} \leq \frac{1}{48}h_i^3 \|w_{x^3}\|_{\infty, \bar{I}_i} \quad (6.35)$$

Similar results hold true for the interpolation Π_y .

Proof. (1) Use the definition of the bi-quadratic interpolation.

(2) By (6.32).

(3) By [12, pp.73].

We seek the finite element solution $u_h \in S_h(\Omega)$ such that

$$B(u_h, v_h) \equiv \varepsilon^2(\nabla u_h, \nabla v_h) + (au_h, v_h) = (f, v_h), \quad \forall v_h \in S_h(\Omega). \quad (6.36)$$

6.2.3 Main Results

Using the techniques used in [71, 72, 73, 74], we can obtain the following interpolation estimates:

Lemma 6.6 *For the solution u of (6.1)(6.2) and for any integer $n \geq 0$, we have*

$$(I) \quad \|u - \Pi_x u\|_{\infty, \bar{I}_i} \leq C(N_x^{-3} \ln^3 N_x + \varepsilon^{2n+1}) \quad (6.37)$$

$$(II) \quad \|u - \Pi_y u\|_{\infty, \bar{K}_j} \leq C(N_y^{-3} \ln^3 N_y + \varepsilon^{2n+1}) \quad (6.38)$$

Proof. For $i = 1, \dots, i_0, N_x - i_0 + 1, \dots, N_x$, by Lemmas 6.5 and 6.4, we have

$$\begin{aligned} \|u - \Pi_x u\|_{\infty, \bar{I}_i} &\leq Ch_i^3 \|u_{x^3}\|_{\infty, \bar{I}_i} \leq Ch_i^3 \varepsilon^{-3} \\ &\leq CN_x^{-3} \ln^3 N_x, \end{aligned}$$

since $h_i = 4\sigma_x/N_x = 12\alpha^{-1}\varepsilon N_x^{-1} \ln N_x$ in this case. Hence (I) is true in this case.

For $i = i_0 + 1, \dots, N_x - i_0$, in this case $[x_{i-1}, x_i] \subseteq [\sigma_x, 1 - \sigma_x]$. Note that

$$u - \Pi_x u = (u - \tilde{u}_{2n}) - \Pi_x(u - \tilde{u}_{2n}) + (\tilde{u}_{2n} - \Pi_x \tilde{u}_{2n}) \quad (6.39)$$

By Lemmas 6.5 and 6.1, we obtain

$$\|(u - \tilde{u}_{2n}) - \Pi_x(u - \tilde{u}_{2n})\|_{\infty, \bar{I}_i} \leq 3\|u - \tilde{u}_{2n}\|_{\infty, \bar{I}_i} \leq C\varepsilon^{2n+1} \quad (6.40)$$

By using the asymptotic expansion and the exponentially decaying estimates of Lemma 6.1, we can obtain the estimate of $\tilde{u}_{2n} - \Pi_x \tilde{u}_{2n}$ in the same way as we did in [72, 73]. Explicitly, we have

$$\|\tilde{u}_{2n} - \Pi_x \tilde{u}_{2n}\|_{\infty, \bar{I}_i} \leq CN_x^{-3} \quad (6.41)$$

Combining (6.39)-(6.41), we see that (I) holds true in this case, which concludes our proof of (I).

The proof of (II) can be carried out in a similar manner.

Therefore, we have

Lemma 6.7 *For the solution u of (6.1)(6.2) and any integer $n \geq 0$, we have*

$$\|u - \Pi u\|_{\infty, \bar{\Omega}} \leq C(N_x^{-3} \ln^3 N_x + N_y^{-3} \ln^3 N_y + \varepsilon^{2n+1}).$$

Proof. By Lemmas 6.5 and 6.6, we have

$$\|u - \Pi u\|_{\infty, \bar{\Omega}} \leq \|u - \Pi_x u\|_{\infty, \bar{\Omega}} + \|\Pi_x(u - \Pi_y u)\|_{\infty, \bar{\Omega}} \quad (6.42)$$

$$\leq \|u - \Pi_x u\|_{\infty, \bar{\Omega}} + 2\|u - \Pi_y u\|_{\infty, \bar{\Omega}} \quad (6.43)$$

$$\leq \max_{1 \leq i \leq N_x} \|u - \Pi_x u\|_{\infty, \bar{I}_i} + 2 \max_{1 \leq j \leq N_y} \|u - \Pi_y u\|_{\infty, \bar{K}_j} \quad (6.44)$$

$$\leq \max_{1 \leq i \leq N_x} \|u - \Pi_x u\|_{\infty, \bar{I}_i} + 2 \max_{1 \leq j \leq N_y} \|u - \Pi_y u\|_{\infty, \bar{K}_j} \quad (6.45)$$

$$\leq C(N_x^{-3} \ln^3 N_x + N_y^{-3} \ln^3 N_y + \varepsilon^{2n+1})$$

which concludes our proof.

Theorem 6.1

$$\|u - u_h\| \leq C(1 + \varepsilon N_x + \varepsilon^{1/2} N_x \ln^{-1/2} N_x + \varepsilon N_y + \varepsilon^{1/2} N_y \ln^{-1/2} N_y) \|u - \Pi u\|_{\infty, \bar{\Omega}}$$

Proof. Note that

$$C_1 \| \Pi u - u_h \|^2 \leq B(\Pi u - u_h, \Pi u - u_h) = B(\Pi u - u, \Pi u - u_h) \quad (6.46)$$

$$= \varepsilon^2 (\nabla(\Pi u - u), \nabla \chi) + (a(\Pi u - u), \chi) \quad (6.47)$$

where here and in the following, we will use the notation $\chi \equiv \Pi u - u_h$.

Integrating by parts, we obtain

$$\varepsilon^2 ((\Pi u - u)_x, \chi_x) = \sum_{1 \leq i \leq N_x, 1 \leq j \leq N_y} \int_{x_{i-1}}^{x_i} \int_{y_{j-1}}^{y_j} \varepsilon^2 (\Pi u - u)_x \chi_x dx dy$$

$$\begin{aligned}
&= \sum_{1 \leq i \leq N_x, 1 \leq j \leq N_y} \int_{y_{j-1}}^{y_j} [\varepsilon^2 (\Pi u - u) \chi_x] \Big|_{x=x_{i-1}}^{x=x_i} dy - \varepsilon^2 (\Pi u - u, \chi_{xx}) \\
&\leq \varepsilon \|\Pi u - u\|_{\infty, \bar{\Omega}} \sum_{1 \leq i \leq N_x, 1 \leq j \leq N_y} \int_{y_{j-1}}^{y_j} [|\varepsilon \chi_x(x_i, y)| + |\varepsilon \chi_x(x_{i-1}, y)|] dy \\
&\quad + \sum_{1 \leq i \leq N_x, 1 \leq j \leq N_y} \int_{x_{i-1}}^{x_i} \int_{y_{j-1}}^{y_j} |\varepsilon^2 (\Pi u - u) \chi_{xx}| dy dx
\end{aligned}$$

By using the Taylor expansion and the fact that χ is a quadratic function in x , we have

$$\begin{aligned}
&\sum_{1 \leq i \leq N_x, 1 \leq j \leq N_y} \int_{y_{j-1}}^{y_j} |\varepsilon \chi_x(x_i, y)| dy \\
&= \sum_{i,j} \frac{1}{x_i - x_{i-1}} \int_{x_{i-1}}^{x_i} \int_{y_{j-1}}^{y_j} |\varepsilon \chi_x(x_i, y)| dy dx \\
&= \sum_{i,j} \frac{1}{x_i - x_{i-1}} \int_{x_{i-1}}^{x_i} \int_{y_{j-1}}^{y_j} |\varepsilon \chi_x(x, y) + (x_i - x) \varepsilon \chi_{xx}(x, y)| dy dx \\
&\leq \sum_{i,j} \left[\frac{1}{x_i - x_{i-1}} \int_{x_{i-1}}^{x_i} \int_{y_{j-1}}^{y_j} |\varepsilon \chi_x| dy dx + \int_{x_{i-1}}^{x_i} \int_{y_{j-1}}^{y_j} |\varepsilon \chi_{xx}| dy dx \right]
\end{aligned}$$

where $\sum_{i,j}$ is a short hand notation for $\sum_{1 \leq i \leq N_x, 1 \leq j \leq N_y}$.

Note that

$$\begin{aligned}
&\sum_{i,j} \frac{1}{x_i - x_{i-1}} \int_{x_{i-1}}^{x_i} \int_{y_{j-1}}^{y_j} |\varepsilon \chi_x| dy dx \\
&\leq CN_x \int_{S_1} |\varepsilon \chi_x| dy dx + \frac{CN_x}{\varepsilon \ln N_x} \int_{S_2} |\varepsilon \chi_x| dy dx \\
&\leq CN_x (\text{meas}(S_1))^{1/2} \|\varepsilon \chi_x\|_{L^2(S_1)} + \frac{CN_x}{\varepsilon \ln N_x} (\text{meas}(S_2))^{1/2} \|\varepsilon \chi_x\|_{L^2(S_2)} \\
&\leq CN_x \|\varepsilon \chi_x\|_{L^2(S_1)} + C \frac{N_x}{\varepsilon \ln N_x} (\varepsilon \ln N_x)^{1/2} \|\varepsilon \chi_x\|_{L^2(S_2)} \\
&\leq C(N_x + \varepsilon^{-1/2} N_x \ln^{-1/2} N_x) \|\varepsilon \chi_x\|
\end{aligned}$$

where $S_1 \equiv [\sigma_x, 1 - \sigma_x] \times [0, 1]$ and $S_2 \equiv \bar{\Omega} \setminus S_1$.

In the same way, we can obtain

$$\sum_{i,j} \int_{y_{j-1}}^{y_j} |\varepsilon \chi_x(x_{i-1}, y)| dy \leq C(N_x + \varepsilon^{-1/2} N_x \ln^{-1/2} N_x) \|\varepsilon \chi_x\| \quad (6.48)$$

Similarly, we have

$$\begin{aligned}
\sum_{i,j} \int_{x_{i-1}}^{x_i} \int_{y_{j-1}}^{y_j} |\varepsilon \chi_{xx}| dy dx &= \int_{S_1} |\varepsilon \chi_{xx}| dy dx + \int_{S_2} |\varepsilon \chi_{xx}| dy dx \\
&\leq (\text{meas}(S_1))^{1/2} \|\varepsilon \chi_{xx}\|_{L^2(S_1)} + (\text{meas}(S_2))^{1/2} \|\varepsilon \chi_{xx}\|_{L^2(S_2)} \\
&\leq \|\varepsilon \chi_{xx}\|_{L^2(S_1)} + C(\varepsilon \ln N_x)^{1/2} \|\varepsilon \chi_{xx}\|_{L^2(S_2)} \\
&\leq C N_x \|\varepsilon \chi_x\|_{L^2(S_1)} + C(\varepsilon \ln N_x)^{1/2} \frac{N_x}{\varepsilon \ln N_x} \|\varepsilon \chi_x\|_{L^2(S_2)} \\
&\leq C(N_x + \varepsilon^{-1/2} N_x \ln^{-1/2} N_x) \|\varepsilon \chi_x\|
\end{aligned} \tag{6.49}$$

where we used the standard inverse estimate [16, §4.5]

$$\|\chi_{xx}\| \leq C h^{-1} \|\chi_x\|, \quad \forall \chi \in S_h(\Omega)$$

and the fact that

$$h = O(N_x^{-1}) \quad \text{on } S_1 \quad \text{and} \quad h = O(\varepsilon N_x^{-1} \ln N_x) \quad \text{on } S_2.$$

On the other hand,

$$\begin{aligned}
\sum_{i,j} \int_{x_{i-1}}^{x_i} \int_{y_{j-1}}^{y_j} \varepsilon^2 (\Pi u - u) \chi_{xx} dy dx &\leq C \varepsilon \|\Pi u - u\|_{\infty, \bar{\Omega}} \left[\int_{S_1} |\varepsilon \chi_{xx}| dy dx + \int_{S_2} |\varepsilon \chi_{xx}| dy dx \right] \\
&\leq C \varepsilon \|\Pi u - u\|_{\infty, \bar{\Omega}} (N_x + \varepsilon^{-1/2} N_x \ln^{-1/2} N_x) \|\varepsilon \chi_x\|
\end{aligned}$$

where we used (6.49).

By combining the above inequalities, we have

$$\varepsilon^2 ((\Pi u - u)_x, \chi_x) \leq C(\varepsilon N_x + \varepsilon^{1/2} N_x \ln^{-1/2} N_x) \|\Pi u - u\|_{\infty, \bar{\Omega}} \|\varepsilon \chi_x\| \tag{6.50}$$

In the same way, we can obtain

$$\varepsilon^2 ((\Pi u - u)_y, \chi_y) \leq C(\varepsilon N_y + \varepsilon^{1/2} N_y \ln^{-1/2} N_y) \|\Pi u - u\|_{\infty, \bar{\Omega}} \|\varepsilon \chi_y\| \tag{6.51}$$

Finally, we have

$$|(a(\Pi u - u), \chi)| \leq C \|\Pi u - u\|_{\infty, \bar{\Omega}} \|\chi\| \tag{6.52}$$

By combining the inequalities (6.46)-(6.52), we have

$$||\Pi u - u_h|| \leq C(1 + \varepsilon N_x + \varepsilon^{1/2} N_x \ln^{-1/2} N_x + \varepsilon N_y + \varepsilon^{1/2} N_y \ln^{-1/2} N_y) ||\Pi u - u||_{\infty, \bar{\Omega}}$$

from which together with the triangular inequality, we obtain

$$\begin{aligned} ||u - u_h|| &\leq ||u - \Pi u|| + ||\Pi u - u_h|| \\ &\leq C(1 + \varepsilon N_x + \varepsilon^{1/2} N_x \ln^{-1/2} N_x + \varepsilon N_y + \varepsilon^{1/2} N_y \ln^{-1/2} N_y) ||\Pi u - u||_{\infty, \bar{\Omega}} \end{aligned}$$

which concludes our proof.

From Theorem 6.1, we see that under the assumption:

$$(A3) \quad \varepsilon \leq \max(N_x^{-2} \ln N_x, N_y^{-2} \ln N_y),$$

the error $||u - u_h||$ is bounded by the interpolation error $||u - \Pi u||_{\infty, \bar{\Omega}}$. By Lemma 6.7, if the solution u is smooth enough, then the interpolation estimate will be dominated by $N_x^{-3} \ln^3 N_x + N_y^{-3} \ln^3 N_y$, in which case we can obtain the following quasi-optimal global uniformly convergent result:

Theorem 6.2 *Let u be the solution of (6.1)(6.2), u_h be the bi-quadratic finite element solution of (6.36). Then under the assumption (A3), we have*

$$||u - u_h|| \leq C(N_x^{-3} \ln^3 N_x + N_y^{-3} \ln^3 N_y).$$

6.2.4 Generalizations to Any m-th Order Tensor-Product Elements

If the solution u of (6.1)(6.2) is smooth enough, we can use higher-order elements to find the finite element solution u_h of (6.36) in the m-th order ($m \geq 3$) tensor-product element space $S_h(\Omega)$, where $S_h(\Omega)$ can be constructed in the same way as the bi-quadratic element except that

$$\sigma_x = (m + 1)\alpha^{-1}\varepsilon \ln N_x \quad \text{and} \quad \sigma_y = (m + 1)\alpha^{-1}\varepsilon \ln N_y$$

for the m-th order tensor-product element, in which case, we have the following quasi-optimal global uniform convergence:

Theorem 6.3 *Let u be the solution of (6.1)(6.2), u_h be the finite element solution of (6.36) on the m -th order ($m \geq 3$) tensor-product element space. Then under the assumption (A3), we have*

$$\|u - u_h\| \leq C(N_x^{-(m+1)} \ln^{m+1} N_x + N_y^{-(m+1)} \ln^{m+1} N_y).$$

The proof of this theorem can be obtained by carrying out similar proofs as for the bi-quadratic case. Hence in the following, we will just sketch out some critical steps.

By carrying out the same techniques used in Lemmas 6.3 and 6.4, we can easily obtain

Lemma 6.8

$$(I) \quad |u_{x^{m+1}}(x, y)| \leq C\varepsilon^{-(m+1)}, \quad \text{on } \bar{\Omega} \quad (6.53)$$

$$(II) \quad |u_{y^{m+1}}(x, y)| \leq C\varepsilon^{-(m+1)}, \quad \text{on } \bar{\Omega} \quad (6.54)$$

Also we have

Lemma 6.9 *For the m -th order ($m \geq 3$) tensor-product interpolation Π , we have*

$$(I) \quad \Pi w = \Pi_x \Pi_y w = \Pi_y \Pi_x w \quad (6.55)$$

$$(II) \quad \|\Pi_x w\|_{\infty, \bar{I}_i} \leq C_m \|w\|_{\infty, \bar{I}_i} \quad (6.56)$$

$$(III) \quad \|w - \Pi_x w\|_{\infty, \bar{I}_i} \leq \frac{h_i^{m+1}}{2^{m+1} \cdot (m+1)!} \|w_{x^{m+1}}\|_{\infty, \bar{I}_i} \quad (6.57)$$

where C_m is a constant depending on m . Similar results hold true for the interpolation Π_y .

Proof. (I) By the definition of the tensor-product interpolation.

(II) For simplicity, hereby we just provide here the proof for the bi-cubic element, in which case the one-dimensional shape functions [12, §2.6] are

$$\psi_1(\xi) = -\frac{9}{16}(1 - \xi)\left(\frac{1}{3} - \xi\right)\left(\frac{1}{3} + \xi\right) \quad (6.58)$$

$$\psi_2(\xi) = \frac{27}{16}(1 + \xi)(1 - \xi)\left(\frac{1}{3} - \xi\right) \quad (6.59)$$

$$\psi_3(\xi) = \frac{27}{16}(1 + \xi)(1 - \xi)\left(\frac{1}{3} + \xi\right) \quad (6.60)$$

$$\psi_4(\xi) = -\frac{9}{16}(1 + \xi)\left(\frac{1}{3} - \xi\right)\left(\frac{1}{3} + \xi\right) \quad (6.61)$$

Hence we have

$$\|\Pi_x w\|_{\infty, \bar{I}_i} \leq \|w\|_{\infty, \bar{I}_i} \max_{-1 \leq \xi \leq 1} [|\psi_1(\xi)| + |\psi_2(\xi)| + |\psi_3(\xi)| + |\psi_4(\xi)|] \quad (6.62)$$

$$\leq \|w\|_{\infty, \bar{I}_i} \max_{-1 \leq \xi \leq 1} \left[\frac{9}{16}(1 - \xi^2) \left| \frac{1}{9} - \xi^2 \right| + \right. \quad (6.63)$$

$$\left. \frac{27}{16}(1 - \xi^2) \left| \frac{1}{3} - \xi \right| + \frac{27}{16}(1 - \xi^2) \left| \frac{1}{3} + \xi \right| + \frac{9}{16}(1 + \xi) \left| \frac{1}{9} - \xi^2 \right| \right]$$

$$\leq \|w\|_{\infty, \bar{I}_i} \left[\frac{9}{16} \cdot 2 \cdot \frac{8}{9} + \frac{27}{16} \cdot \frac{4}{3} + \frac{27}{16} \cdot \frac{4}{3} + \frac{9}{16} \cdot 2 \cdot \frac{8}{9} \right] \quad (6.64)$$

$$= 6.5 \|w\|_{\infty, \bar{I}_i} \quad (6.65)$$

from which we see $C_3 = 6.5$.

For the general case, $C_m = \max_{-1 \leq \xi \leq 1} \sum_{i=1}^{m+1} |\psi_i(\xi)|$, where $\{\psi_i(\xi)\}_{i=1}^{m+1}$ are the one-dimensional m-th order shape functions [12, §2.6].

(3) By [12, pp.73].

By using a similar proof of Lemmas 6.6 and 6.7, we can easily obtain

Lemma 6.10 *For the solution u of (6.1)(6.2) and any integer $n \geq 0$, we have*

$$\|u - \Pi u\|_{\infty, \bar{\Omega}} \leq C(N_x^{-(m+1)} \ln^{m+1} N_x + N_y^{-(m+1)} \ln^{m+1} N_y + \varepsilon^{2n+1}).$$

It is not difficult to see that Theorem 6.1 holds true for the m-th order ($m \geq 3$) tensor-product element. The proof is almost the same. The only difference occurs in dealing with the terms

$$\sum_{i,j} \int_{y_{j-1}}^{y_j} |\varepsilon \chi_x(x_i, y)| dy \quad \text{and} \quad \sum_{i,j} \int_{y_{j-1}}^{y_j} |\varepsilon \chi_x(x_{i-1}, y)| dy.$$

In the present case, we need a Taylor expansion up to the m -th order, since χ is a m -th order function in x . Hence we have

$$\begin{aligned}
& \sum_{i,j} \int_{y_{j-1}}^{y_j} |\varepsilon \chi_x(x_i, y)| dy \\
&= \sum_{i,j} \frac{1}{x_i - x_{i-1}} \int_{x_{i-1}}^{x_i} \int_{y_{j-1}}^{y_j} |\varepsilon \chi_x(x, y)| dy dx \\
&= \sum_{i,j} \frac{1}{x_i - x_{i-1}} \int_{x_{i-1}}^{x_i} \int_{y_{j-1}}^{y_j} |\varepsilon \chi_x(x, y) + \sum_{l=1}^{m-1} \frac{(x_i - x)^l}{l!} \varepsilon \chi_{x^{l+1}}(x, y)| dy dx \\
&\leq \sum_{i,j} \left[\frac{1}{x_i - x_{i-1}} \int_{x_{i-1}}^{x_i} \int_{y_{j-1}}^{y_j} |\varepsilon \chi_x| dy dx + C \int_{x_{i-1}}^{x_i} \int_{y_{j-1}}^{y_j} |\varepsilon \chi_{xx}| dy dx \right]
\end{aligned}$$

where in the last step, we used the standard inverse estimate

$$\|\chi_{x^{l+1}}\| \leq Ch^{1-l} \|\chi_{xx}\|, \quad \forall \chi \in S_h(\Omega).$$

By combining Lemmas 6.8-6.10 and Theorem 6.1, we conclude the proof of Theorem 6.3.

6.3 The 2-D Quasilinear Reaction-Diffusion Model

In this section, we will consider the following quasilinear singularly perturbed elliptic problem:

$$\varepsilon^2 \Delta u = F(u, x, y), \quad \text{in } \Omega = (0, 1) \times (0, 1) \quad (6.66)$$

$$u = 0 \quad \text{on } \partial\Omega. \quad (6.67)$$

The asymptotic expansion for this problem was constructed by Denisov [31], where F was assumed to be in the form of $A(u^2 + pu + q)$. For simplicity, the following conditions are assumed [31, pp.1342]:

(A1) The equation $F(u, x, y) = 0$ has a solution $u = \bar{u}_0(x, y)$ in $\bar{\Omega}$.

(A2) The derivative of F satisfies $m_2 \geq F_u(u, x, y) \geq m_1 > 0$ in $\bar{\Omega}$.

Under the above assumptions, we have:

Lemma 6.11 [31, §4] Denote the n -th order asymptotic expansion

$$U_n(x, y, \varepsilon) = \sum_{k=0}^n \varepsilon^k (\bar{u}_k + \Pi_k^{(1)} + \dots + \Pi_k^{(4)} + P_k^{(1)} + \dots + P_k^{(4)}) \quad (6.68)$$

Then we have

$$\max_{\bar{\Omega}} |u(x, y, \varepsilon) - U_n(x, y, \varepsilon)| = O(\varepsilon^{n+1}) \quad \text{as } \varepsilon \rightarrow 0, \quad (6.69)$$

where

$\bar{u}_k(x, y)$ is the regular part of the asymptotic expansion,

$\Pi^{(1)}(x, \eta), \Pi^{(2)}(\xi, y), \Pi^{(3)}(x, \eta_*), \Pi^{(4)}(\xi_*, y)$ are the boundary layer functions,

$P^{(1)}(\xi, \eta), P^{(2)}(\xi, \eta_*), P^{(3)}(\xi_*, \eta_*), P^{(4)}(\xi_*, \eta)$ are the corner layer functions.

Here $\eta = y/\varepsilon, \xi = x/\varepsilon, \eta_* = (1 - y)/\varepsilon, \xi_* = (1 - x)/\varepsilon$. Also the following estimates hold true:

$$\begin{aligned} |\Pi^{(1)}(x, \eta)| &\leq C e^{-\alpha\eta}, \\ |\Pi^{(2)}(\xi, y)| &\leq C e^{-\alpha\xi}, \\ |\Pi^{(3)}(x, \eta_*)| &\leq C e^{-\alpha\eta_*}, \\ |\Pi^{(4)}(\xi_*, y)| &\leq C e^{-\alpha\xi_*}, \\ |P^{(1)}(\xi, \eta)| &\leq C e^{-\alpha(\xi+\eta)}, \\ |P^{(2)}(\xi, \eta_*)| &\leq C e^{-\alpha(\xi+\eta_*)}, \\ |P^{(3)}(\xi_*, \eta_*)| &\leq C e^{-\alpha(\xi_*+\eta_*)}, \\ |P^{(4)}(\xi_*, \eta)| &\leq C e^{-\alpha(\xi_*+\eta)}. \end{aligned}$$

From Boglayev [15], we have the following derivative estimates:

Lemma 6.12 [15, Lemma 2] Let $u(x, y) \in C^n(\bar{\Omega}) \cap C^{n+2}(\Omega)$ be the solution of the problem (6.66) (6.67). Then the derivatives of u satisfy the following estimates:

$$\begin{aligned} (I) \quad |u_{x^n}(x, y)| &\leq C_n (1 + \varepsilon^{-n} e^{-\frac{\beta x}{\varepsilon}} + \varepsilon^{-n} e^{-\frac{\beta(1-x)}{\varepsilon}}) \quad \text{on } \bar{\Omega}, \\ (II) \quad |u_{y^n}(x, y)| &\leq C_n (1 + \varepsilon^{-n} e^{-\frac{\beta y}{\varepsilon}} + \varepsilon^{-n} e^{-\frac{\beta(1-y)}{\varepsilon}}) \quad \text{on } \bar{\Omega}, \end{aligned}$$

where $0 < \beta < m_1^{1/2}$, and $n = 1, 2, 3$.

Since the problem (6.66)(6.67) has the same boundary layers as the linear one (6.1)(6.2), we can use the same piecewise uniform mesh as we constructed for the linear case.

The weak solution of (6.66)(6.67) is: Find $u \in H_0^1(\Omega)$ such that

$$\varepsilon^2(\nabla u, \nabla v) + (F(u, x, y), v) = 0, \quad \forall v \in H_0^1(\Omega). \quad (6.70)$$

The finite element solution is: Find $u_h \in S_h(\Omega)$ such that

$$\varepsilon^2(\nabla u_h, \nabla v_h) + (F(u_h, x, y), v_h) = 0, \quad \forall v_h \in S_h(\Omega), \quad (6.71)$$

where $S_h(\Omega)$ is the tensor-product quadratic element space used in last section.

Then by carrying out the same proof as we did for the linear case, we can obtain the following interpolation estimate:

Lemma 6.13 *For the solution u of (6.66)(6.67) and any integer $n \geq 0$, we have*

$$\|u - \Pi u\|_{\infty, \Omega} \leq C(N_x^{-3} \ln^3 N_x + N_y^{-3} \ln^3 N_y + \varepsilon^{n+1}).$$

Then we have

Theorem 6.4 *Let u_h be the finite element solution of (6.71), and u be the analytic solution of (6.66)(6.67). Then we have*

$$\|u - u_h\| \leq C(1 + \varepsilon N_x + \varepsilon^{1/2} N_x \ln^{-1/2} N_x + \varepsilon N_y + \varepsilon^{1/2} N_y \ln^{-1/2} N_y) \|u - \Pi u\|_{\infty, \bar{\Omega}}.$$

Proof. By subtracting (6.71) from (6.70), we have

$$\varepsilon^2(\nabla(u - u_h), \nabla v_h) + (F(u, x, y) - F(u_h, x, y), v_h) = 0, \quad \forall v_h \in S_h(\Omega) \quad (6.72)$$

By the mean value theorem, we can rewrite (6.72) as

$$\varepsilon^2(\nabla(u - u_h), \nabla v_h) + (\tilde{F}_u \cdot (u - u_h), v_h) = 0, \quad \forall v_h \in S_h(\Omega), \quad (6.73)$$

where \tilde{F}_u denotes the value of the derivative F_u at some point $\theta u + (1-\theta)u_h$, $0 < \theta < 1$.

From (6.73), we have

$$\varepsilon^2(\nabla(\Pi u - u_h), \nabla v_h) + (\tilde{F}_u \cdot (\Pi u - u_h), v_h) \quad (6.74)$$

$$= \varepsilon^2(\nabla(\Pi u - u), \nabla v_h) + (\tilde{F}_u \cdot (\Pi u - u), v_h), \quad \forall v_h \in S_h(\Omega). \quad (6.75)$$

By denoting $\chi = \Pi u - u_h$, choosing $v_h = \chi$ in (6.74)(6.75) and using the assumption (A2), we can obtain

$$\varepsilon^2 \|\nabla \chi\|^2 + m_1 \|\chi\|^2 \leq \varepsilon^2 |(\nabla(\Pi u - u), \nabla \chi)| + |(\tilde{F}_u \cdot (\Pi u - u), \chi)| \quad (6.76)$$

The rest proof can be carried in the same way as in Theorem 6.1.

Under the assumption (A3), we can easily obtain the following quasi-optimal global uniformly convergent result:

Theorem 6.5 *Let u_h be the bi-quadratic finite element solution of (6.71) and u be the solution of (6.66)(6.67). Then under the assumptions of (A1), (A2) and (A3), we have*

$$\|u - u_h\| \leq C(N_x^{-3} \ln^3 N_x + N_y^{-3} \ln^3 N_y), \quad (6.77)$$

where the constant C is independent of the perturbation parameter ε .

Similar results can be obtained for the m -th order ($m \geq 3$) tensor-product element when there exists a smooth enough solution of (6.66)(6.67).

6.4 Numerical Experiments

For simplicity, we only carried out our experiments for a linear problem by using the bi-quadratic element. Here we chose $N_x = N_y = N$ and tensor-product quadratic interpolation for the functions a and f in our numerical experiments. In Figures 6.1-6.21, we always use (a) for the left figure and (b) for the right figure.

To see how our method performs, we first tested:

$$\text{Example 1: } a = 2, f = 20(x^2 + y^2) + 4$$

on a uniform mesh and our piecewise uniform mesh for $N=12, 24$ with different values of ε ranging from 10^{-7} to 10^{-2} . The computed solutions are presented in Figures 6.1-6.6. These figures clearly show that our piecewise uniform mesh performs much better than the uniform mesh. Our piecewise uniform mesh resolves the sharp boundary layers without any oscillations. As ε decreases, the boundary layers become sharper. However, the finite element solution on our piecewise uniform mesh captures well the sharper layer. For $\varepsilon \leq 10^{-4}$, there is almost no distinction from the case of $\varepsilon = 10^{-4}$. On the other hand, the solutions achieved on the uniform mesh display wild oscillations near the boundary layers.

Note that $u_0 = 10(x^2 + y^2) + 2$ is the solution of the reduced problem (when $\varepsilon = 0$), so we know how the solution should look like.

To measure the accuracy of our method, we tested another case where $a=2$, and f is chosen appropriately such that the exact solution is known:

$$\text{Example 2: } u(x, y) = \left(1 - \frac{e^{-x/\varepsilon} + e^{-(1-x)/\varepsilon}}{1 + e^{-1/\varepsilon}}\right) \left(1 - \frac{e^{-y/\varepsilon} + e^{-(1-y)/\varepsilon}}{1 + e^{-1/\varepsilon}}\right)$$

The computed solution u_h and the pointwise error $u_h - u$ are shown in Figures 6.7-6.12 for uniform mesh case, in Figures 6.13-6.21 for piecewise uniform mesh case, respectively. The errors in L^2 norm on both meshes are provided in Tables 6.1 and 6.2, respectively, from which the uniform convergence in both cases is displayed very clearly. The estimated convergence rates

$$R = (\ln(e_{N_1}/e_{N_2}))/\ln(N_2/N_1) \quad \text{and} \quad \tilde{R} = (\ln(e_{N_1}/e_{N_2}))/\ln((N_2 \ln N_1)/(N_1 \ln N_2))$$

are displayed in Table 6.3 and Table 6.4 for uniform mesh and piecewise uniform mesh, respectively. Here e_N is the L^2 error between the exact solution u and the

computed solution u_h on a mesh with N partitions in both the x- and y-directions. Table 6.3 shows the uniform convergence rate of $O(h^{1/2})$, which agrees with the theoretical analysis of Schatz and Wahlbin [112, Theorem A.2]. Table 6.4 shows a better uniform convergence rate than our theoretically predicted rate. Note that Figures 6.7(b)-6.12(b) show that the standard FEM on uniform mesh does not converge in L^∞ norm, while the standard FEM on our piecewise uniform mesh seems to be uniformly convergent in L^∞ norm. The pointwise error $u_h - u$ in Figures 6.13(b)-6.21(b) decreases as N increases, and the error is dominated by that occurring at the four corners of the domain.

6.5 Conclusions

In this paper, we developed a general higher-order finite element method for solving the singularly perturbed elliptic linear and quasilinear problems in two space dimensions. The quasioptimal global uniform convergence rate $O(N_x^{-(m+1)} \ln^{m+1} N_x + N_y^{-(m+1)} \ln^{m+1} N_y)$ in L^2 norm was proved for solving the reaction-diffusion model by using the m -th order ($m \geq 2$) tensor-product element, which answers part of Roos' open problems proposed in 1997 in [105] as we mentioned in the Introduction. Our numerical results also show the global uniform convergence in L^∞ norm, the proof of which is unavailable at present. Further investigation is required to address this issue.

From our proof, we can expect that our method can be directly applied to other singularly perturbed problems, which have similar asymptotic expansions and smooth enough solutions. Even though 'a posteriori' adaptive FEM sounds more promising for those SPP without an explicit asymptotic expansions, the task is more challenging. Though some effort has been carried out [126, 130, 102, 70, 29, 95, 115, 114] in this direction, "even from the practical point of view the existing adaptive

strategies so far are not completely satisfactory” [105, pp.19], since *”the construction of robust estimators is still an open problem”* [105, pp.19]. Only recently did Verfürth [130] obtain theoretically robust *a posteriori* error estimators, which are independent of the perturbation parameter, for the reaction-diffusion model, however without any implementation. Hence to solve the singularly perturbed problems, a better strategy is to start the numerical computation with such a layer-adapted piecewise uniform mesh, and then to refine the mesh adaptively based on some robust error estimators [105]. Also it would be very interesting if such a piecewise uniform mesh can be implemented with the hp-FEM [95, 115, 114].

Table 6.1: Errors in L^2 norm for Example 2 on uniform mesh

	N		
ϵ	12	24	36
1.0D-02	5.343611226D-03	1.491899416D-03	4.792132997D-04
1.0D-03	8.248501599D-03	5.681738618D-03	4.510826979D-03
1.0D-04	8.287975532D-03	5.791569840D-03	4.708982201D-03
1.0D-05	8.288371573D-03	5.792682315D-03	4.711020991D-03
1.0D-06	8.288375523D-03	5.792693454D-03	4.711041357D-03
1.0D-07	8.288375743D-03	5.792693695D-03	4.711043842D-03

Table 6.2: Errors in L^2 norm for Example 2 on piecewise uniform mesh

	N		
ϵ	12	24	36
1.0D-02	4.502200765D-04	9.529793001D-05	3.150367818D-05
1.0D-03	4.498835982D-04	9.528746525D-05	3.150143528D-05
1.0D-04	4.498482216D-04	9.539294103D-05	3.364966957D-05
1.0D-05	4.499431756D-04	9.541306516D-05	3.365684243D-05
1.0D-06	4.499855183D-04	9.546553209D-05	3.367834599D-05
1.0D-07	4.501197773D-04	9.550416942D-05	3.369497776D-05

Table 6.3: Convergence rates R in L^2 norm on uniform mesh

ϵ	N	
	12	24
1.0D-02	1.8407	2.8009
1.0D-03	0.5378	0.5692
1.0D-04	0.5171	0.5104
1.0D-05	0.5169	0.5098
1.0D-06	0.5169	0.5098
1.0D-07	0.5169	0.5098

Table 6.4: Convergence rates \tilde{R} in L^2 norm on piecewise uniform mesh

ϵ	N	
	12	24
1.0D-02	3.4728	3.8786
1.0D-03	3.4714	3.8784
1.0D-04	3.4687	3.6512
1.0D-05	3.4687	3.6512
1.0D-06	3.4677	3.6508
1.0D-07	3.4675	3.6505

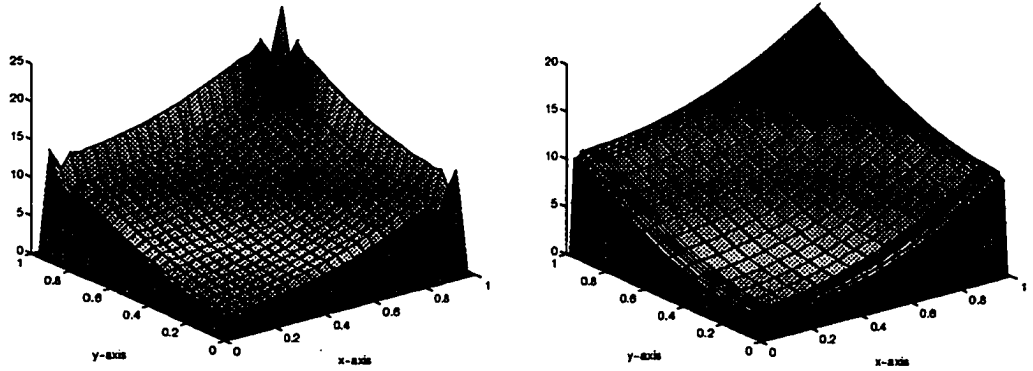


Figure 6.1: Example 1: Computed FEM solution for $N = 12$ and $\varepsilon = 10^{-2}$: (a) uniform mesh (b) piecewise uniform mesh

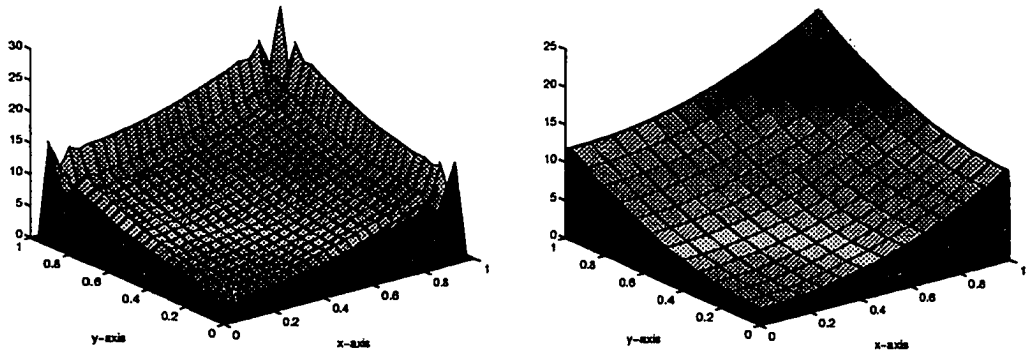


Figure 6.2: Example 1: Computed FEM solution for $N = 12$ and $\varepsilon = 10^{-3}$: (a) uniform mesh (b) piecewise uniform mesh

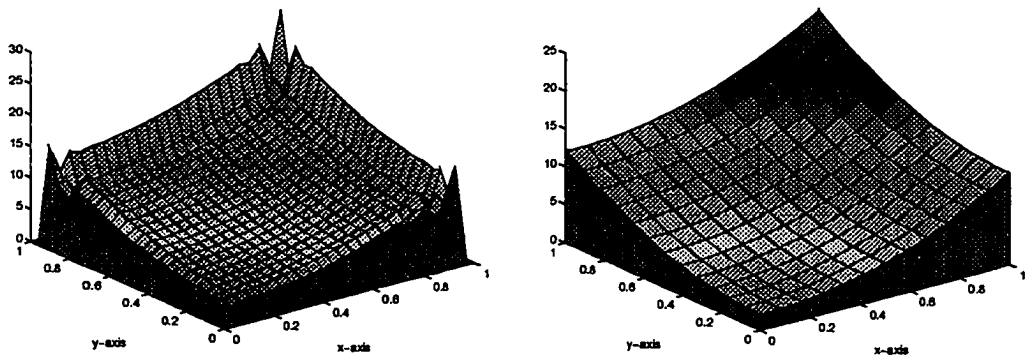


Figure 6.3: Example 1: Computed FEM solution for $N = 12$ and $\varepsilon = 10^{-4}$: (a) uniform mesh (b) piecewise uniform mesh

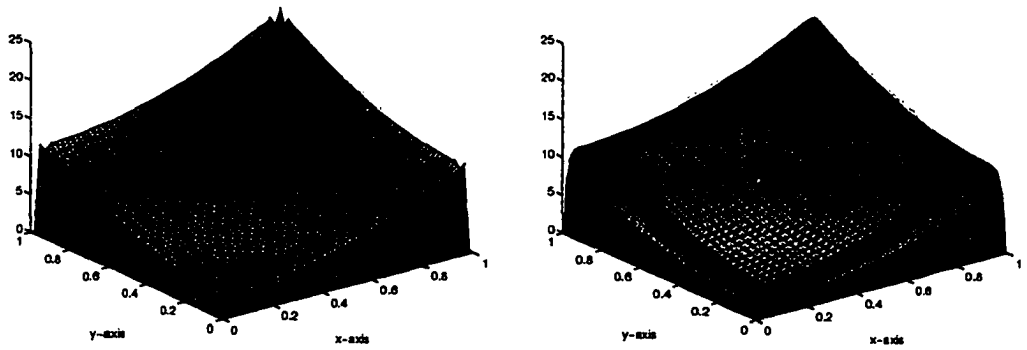


Figure 6.4: Example 1: Computed FEM solution for $N = 24$ and $\varepsilon = 10^{-2}$: (a) uniform mesh (b) piecewise uniform mesh

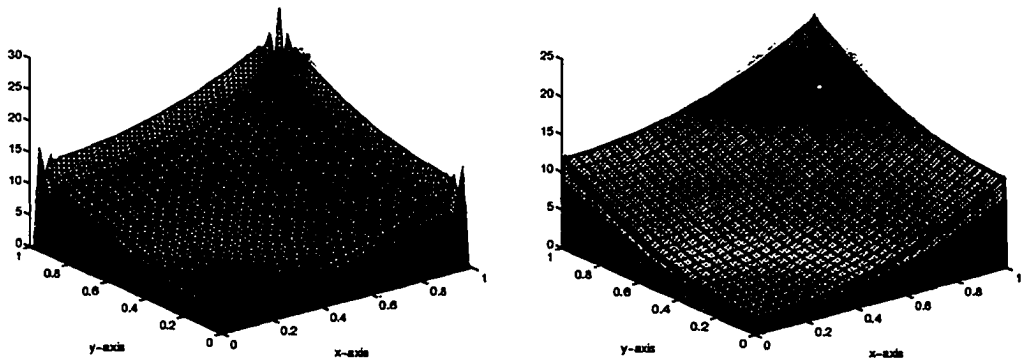


Figure 6.5: Example 1: Computed FEM solution for $N = 24$ and $\varepsilon = 10^{-3}$: (a) uniform mesh (b) piecewise uniform mesh

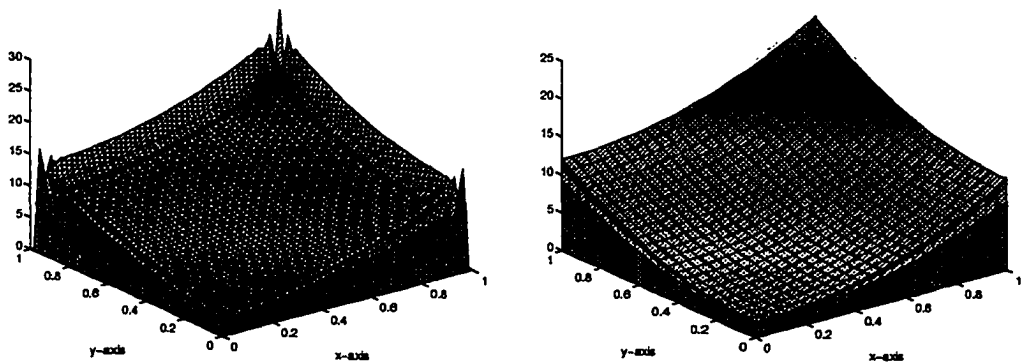


Figure 6.6: Example 1: Computed FEM solution for $N = 24$ and $\varepsilon = 10^{-4}$: (a) uniform mesh (b) piecewise uniform mesh

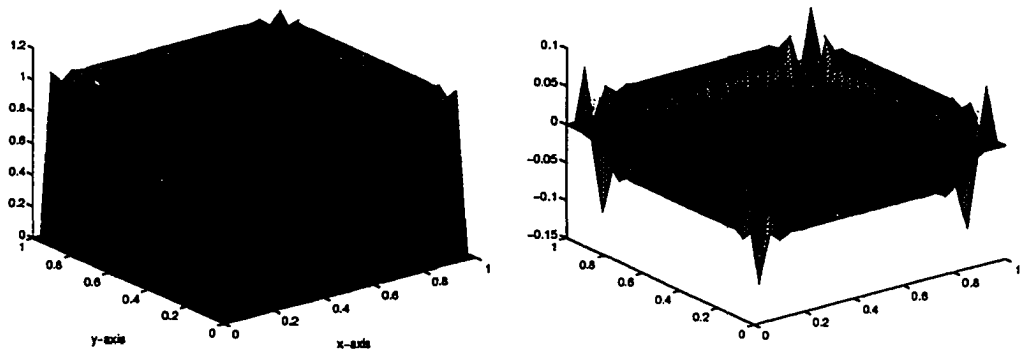


Figure 6.7: Example 2: Standard FEM on uniform mesh with $N = 12$ and $\varepsilon = 10^{-2}$:
 (a) computed solution (b) pointwise error $u_h - u$

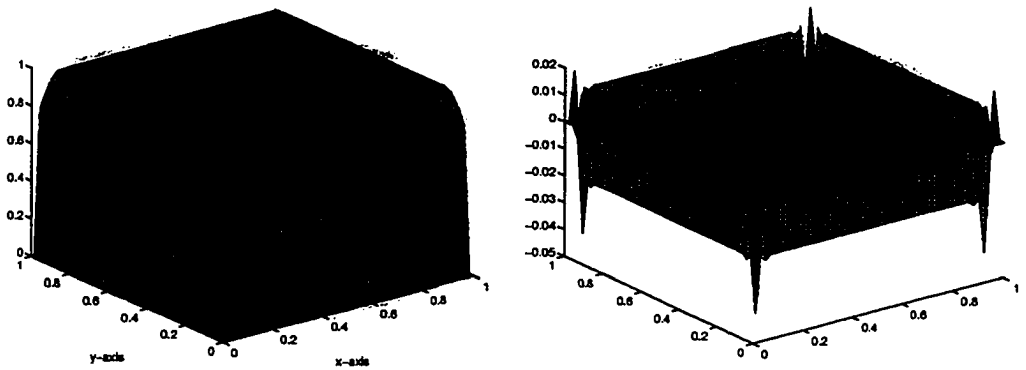


Figure 6.8: Example 2: Standard FEM on uniform mesh with $N = 24$ and $\varepsilon = 10^{-2}$:
 (a) computed solution (b) pointwise error $u_h - u$

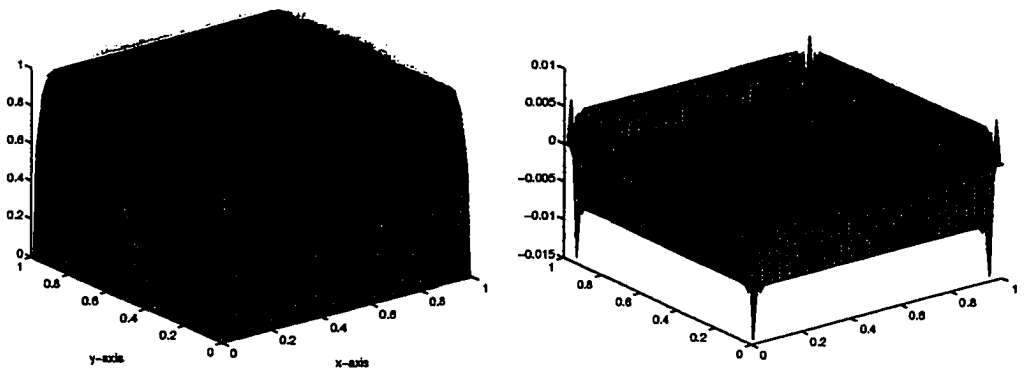


Figure 6.9: Example 2: Standard FEM on uniform mesh with $N = 36$ and $\varepsilon = 10^{-2}$:
 (a) computed solution (b) pointwise error $u_h - u$

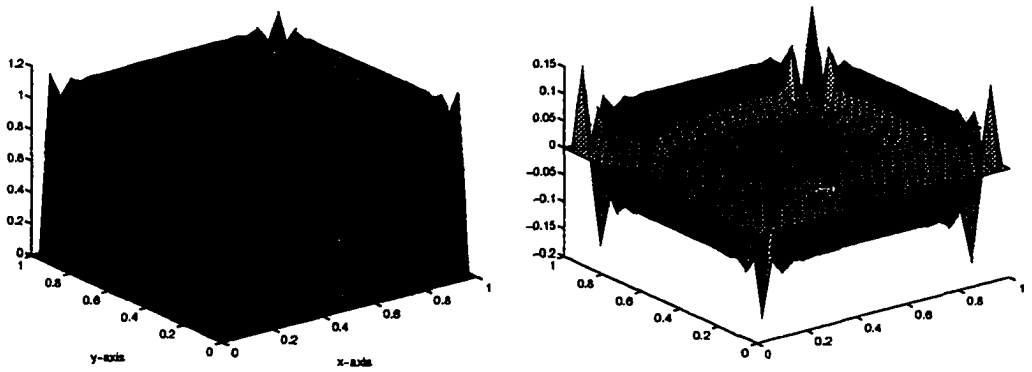


Figure 6.10: Example 2: Standard FEM on uniform mesh with $N = 12$ and $\varepsilon = 10^{-3}$:
 (a) computed solution (b) pointwise error $u_h - u$

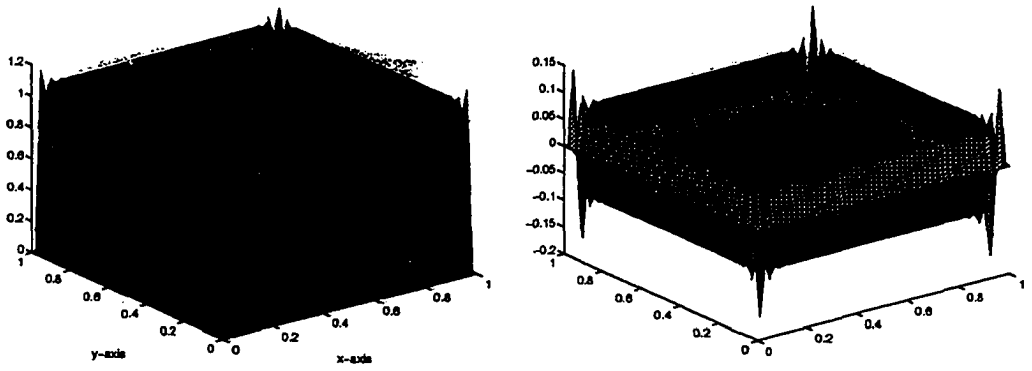


Figure 6.11: Example 2: Standard FEM on uniform mesh with $N = 24$ and $\varepsilon = 10^{-3}$:
 (a) computed solution (b) pointwise error $u_h - u$

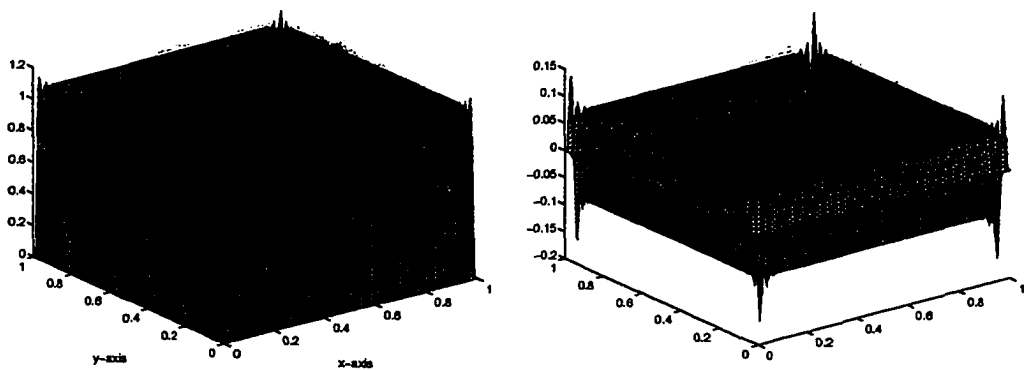


Figure 6.12: Example 2: Standard FEM on uniform mesh with $N = 36$ and $\varepsilon = 10^{-3}$:
 (a) computed solution (b) pointwise error $u_h - u$

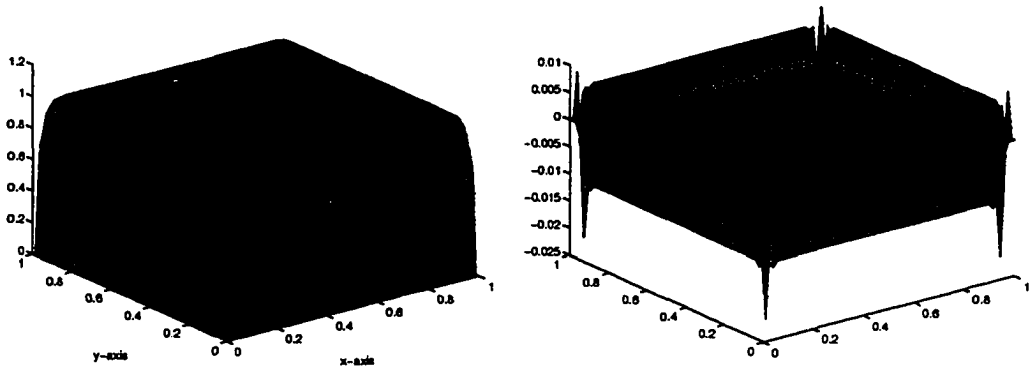


Figure 6.13: Example 2: FEM on piecewise uniform mesh with $N = 12$ and $\varepsilon = 10^{-2}$:
 (a) computed solution (b) pointwise error $u_h - u$

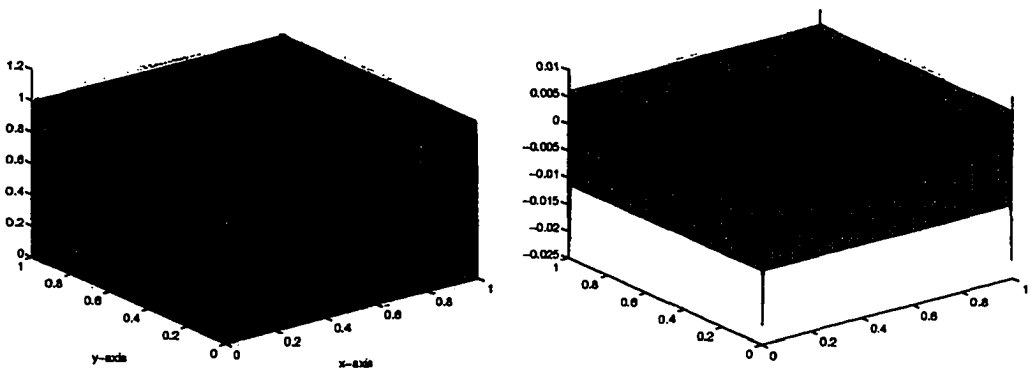


Figure 6.14: Example 2: FEM on piecewise uniform mesh with $N = 12$ and $\varepsilon = 10^{-3}$:
 (a) computed solution (b) pointwise error $u_h - u$

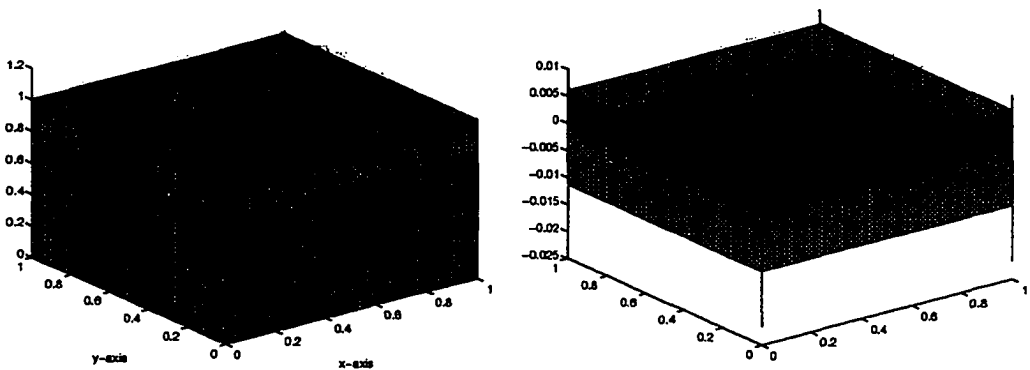


Figure 6.15: Example 2: FEM on piecewise uniform mesh with $N = 12$ and $\varepsilon = 10^{-4}$:
 (a) computed solution (b) pointwise error $u_h - u$

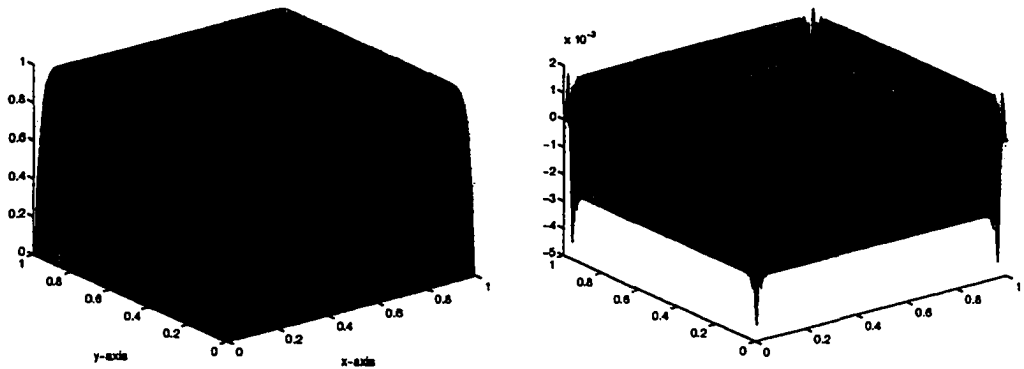


Figure 6.16: Example 2: FEM on piecewise uniform mesh with $N = 24$ and $\varepsilon = 10^{-2}$:
 (a) computed solution (b) pointwise error $u_h - u$

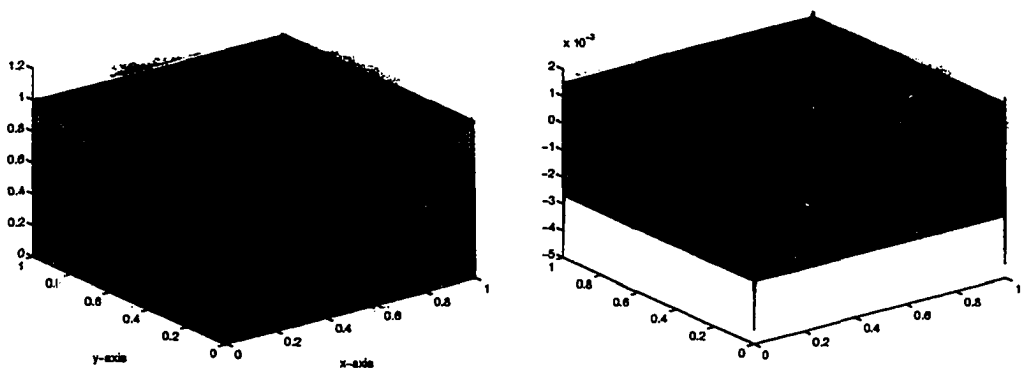


Figure 6.17: Example 2: FEM on piecewise uniform mesh with $N = 24$ and $\varepsilon = 10^{-3}$:
 (a) computed solution (b) pointwise error $u_h - u$

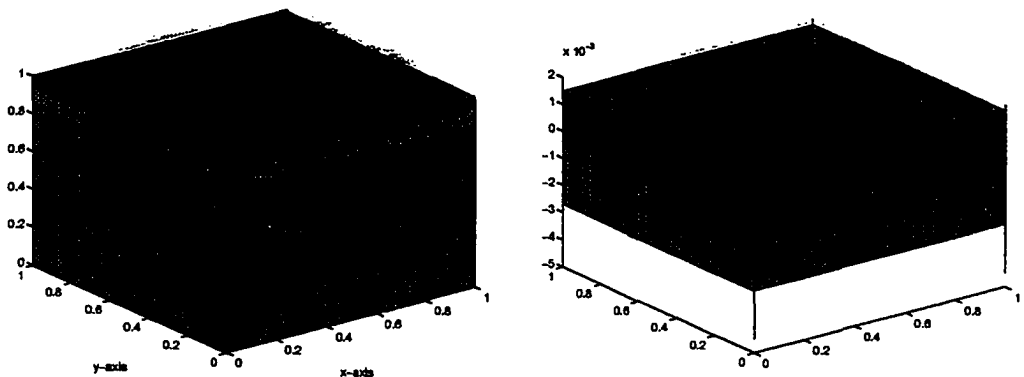


Figure 6.18: Example 2: FEM on piecewise uniform mesh with $N = 24$ and $\varepsilon = 10^{-4}$:
 (a) computed solution (b) pointwise error $u_h - u$

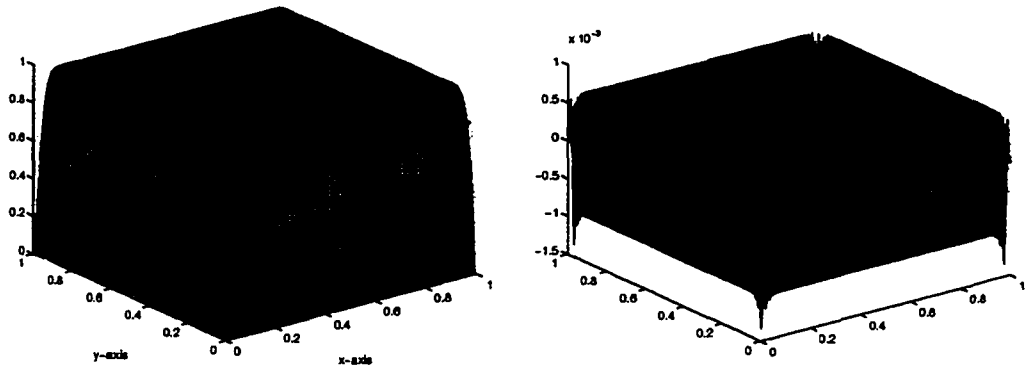


Figure 6.19: Example 2: FEM on piecewise uniform mesh with $N = 36$ and $\varepsilon = 10^{-2}$:
 (a) computed solution (b) pointwise error $u_h - u$

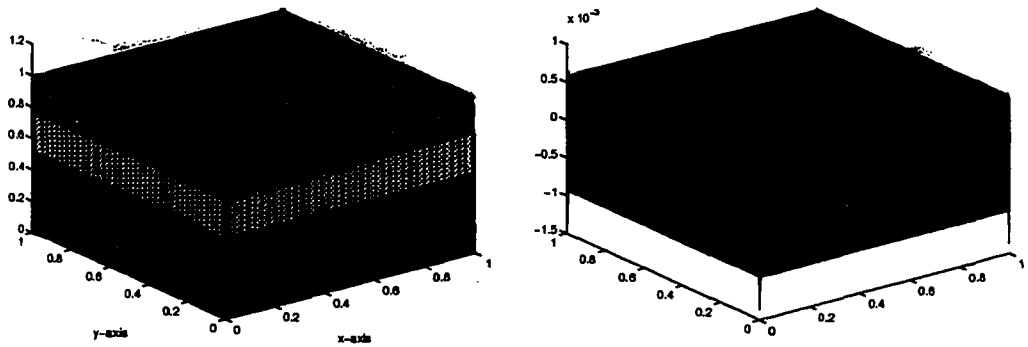


Figure 6.20: Example 2: FEM on piecewise uniform mesh with $N = 36$ and $\varepsilon = 10^{-3}$:
 (a) computed solution (b) pointwise error $u_h - u$

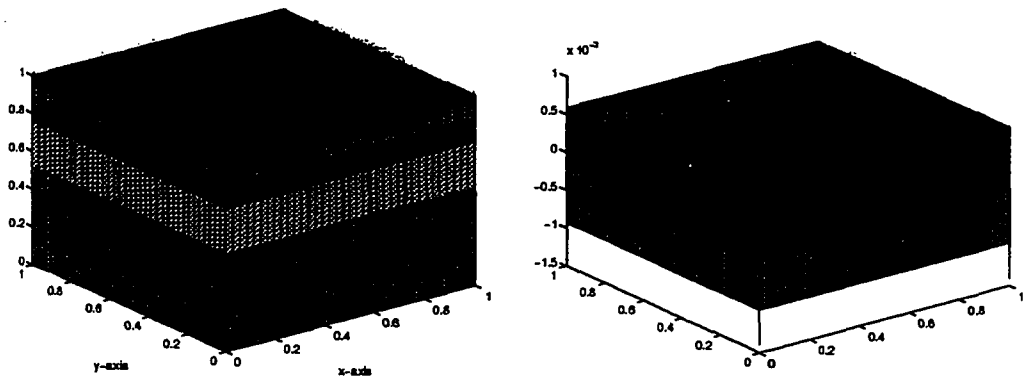


Figure 6.21: Example 2: FEM on piecewise uniform mesh with $N = 36$ and $\varepsilon = 10^{-4}$:
 (a) computed solution (b) pointwise error $u_h - u$

CHAPTER 7

SHALLOW-WATER EQUATIONS

7.1 Governing Equations

The shallow-water equations (SWE) [99], also known as the St. Venant equations, describe two-dimensional unsteady free-surface flows. These equations are derived under the assumption of hydrostatic pressure distribution. They are nonlinear first-order, hyperbolic partial differential systems for which exact solutions are not available except in some special cases. Hence the numerical computation of SWE becomes very important. As Vreugdenhil said: "The numerical solution of the SWE was one of the early applications of digital computers when these became available in the late 1940's." [132, pp.1].

Here we intend to explore the application of these equations for the analysis of tidal oscillations, flow produced by control structures such as sluice gates, pumps or turbines, and flood waves generated by storms or failure of dams, dykes, and other structures. These results can be used to estimate the arrival time and the height of flood waves at a specified downstream location.

Even though many one-dimensional numerical models have been used to simulate these events, two-dimensional models are more realistic. For open-channel flow the computation is more complicated. Some results have been obtained using finite difference methods [25, 39] and finite volume methods [4, 5]. Very few results were obtained using finite element methods [61, 78] and [25, Chap.16].

By assuming hydrostatic pressure distribution, small channel-bottom slope, and uniform velocity distribution in the vertical direction, the governing equations de-

scribing the unsteady free-surface flows can be written as

$$U_t + (F_1)_x + (F_2)_y + S = 0 \quad (7.1)$$

$$\text{where } F_1 = \begin{bmatrix} uh \\ u^2h + (1/2)gh^2 \\ uvh \end{bmatrix}, \quad F_2 = \begin{bmatrix} vh \\ uvh \\ v^2h + (1/2)gh^2 \end{bmatrix},$$

$$S = \begin{bmatrix} 0 \\ -gh(S_{0x} - S_{fx}) \\ -gh(S_{0y} - S_{fy}) \end{bmatrix}.$$

Here

$$U = (h, uh, vh)^T; \quad (7.2)$$

$$h = \text{flow depth}; \quad (7.3)$$

$$u, v = \text{flow velocity in the x- and y-directions, respectively}; \quad (7.4)$$

$$g = \text{acceleration due to gravity}; \quad (7.5)$$

$$S_{0x}, S_{0y} = \text{channel bottom slope in the x- and y-direction, respectively}; \quad (7.6)$$

$$S_{fx}, S_{fy} = \text{the hydraulic resistance slope in the x- and y-directions, respectively,}$$

computed using the steady state friction formulas

$$S_{fx} = \frac{n^2 u \sqrt{u^2 + v^2}}{C_0^2 h^{1.33}}, \quad S_{fy} = \frac{n^2 v \sqrt{u^2 + v^2}}{C_0^2 h^{1.33}}$$

where n is the Manning's roughness coefficient; and C_0 is a dimensional constant ($C_0 = 1$ for the SI units, and $C_0 = 1.49$ for the U.S. customary units).

The local Froude number ($F_r = \sqrt{u^2 + v^2} / \sqrt{gh}$) determines the correct number of boundary conditions to be applied. For two-dimensional subcritical flow (when $F_r < 1$), two external conditions must be specified at inflow boundaries, whereas only one is required at the outflow boundary. Two-dimensional supercritical flow

(when $F_r > 1$) requires the imposition of three inflow boundary conditions and none at the downstream side. For solid walls limiting the flow field, the normal velocities are set equal to zero in order to represent no flux through the solid boundary.

7.2 Finite Element Method

In this section, we will consider the widely used Taylor-Galerkin FEM [30, 32, 78, 79, 94, 135] applied in computational fluid dynamics (CFD). By carrying out a Taylor expansion in time about $t = t^n$, we have

$$U^{n+1} = U^n + \Delta t \frac{\partial U}{\partial t} \Big|_n + \frac{\Delta t^2}{2} \frac{\partial^2 U}{\partial t^2} \Big|_n \quad (7.7)$$

From (7.1), we have

$$\frac{\partial U}{\partial t} = S - \frac{\partial F_1}{\partial x} - \frac{\partial F_2}{\partial y} \quad (7.8)$$

and differentiating (7.1) gives

$$\frac{\partial^2 U}{\partial t^2} = \frac{\partial S}{\partial U} \frac{\partial U}{\partial t} - \frac{\partial}{\partial x} \left(\frac{\partial F_1}{\partial U} \frac{\partial U}{\partial t} \right) - \frac{\partial}{\partial y} \left(\frac{\partial F_2}{\partial U} \frac{\partial U}{\partial t} \right) \quad (7.9)$$

Substituting (7.8) and (7.9) into (7.7), we have

$$U^{n+1} - U^n = \Delta t \left[S - \frac{\partial F_1}{\partial x} - \frac{\partial F_2}{\partial y} \right] \quad (7.10)$$

$$+ \frac{\Delta t^2}{2} \left\{ \frac{\partial S}{\partial U} \left[S - \frac{\partial F_1}{\partial x} - \frac{\partial F_2}{\partial y} \right] - \frac{\partial}{\partial x} \left[\frac{\partial F_1}{\partial U} \left(S - \frac{\partial F_1}{\partial x} - \frac{\partial F_2}{\partial y} \right) \right] - \frac{\partial}{\partial y} \left[\frac{\partial F_2}{\partial U} \left(S - \frac{\partial F_1}{\partial x} - \frac{\partial F_2}{\partial y} \right) \right] \right\} \quad (7.11)$$

Multiplying (7.11) by a test function $\phi_i(x, y)$, integrating over domain Ω , we have the following weak formulation:

$$\int_{\Omega} (U^{n+1} - U^n) \phi_i = \Delta t \int_{\Omega} \left(S - \frac{\partial F_1}{\partial x} - \frac{\partial F_2}{\partial y} \right) \Big|_n \phi_i \quad (7.12)$$

$$+ \frac{\Delta t^2}{2} \int_{\Omega} \frac{\partial S}{\partial U} \left(S - \frac{\partial F_1}{\partial x} - \frac{\partial F_2}{\partial y} \right) \Big|_n \phi_i \quad (7.13)$$

$$+\frac{\Delta t^2}{2} \int_{\Omega} \frac{\partial F_1}{\partial U} (S - \frac{\partial F_1}{\partial x} - \frac{\partial F_2}{\partial y})|^n \frac{\partial \phi_i}{\partial x} \quad (7.14)$$

$$+\frac{\Delta t^2}{2} \int_{\Omega} \frac{\partial F_2}{\partial U} (S - \frac{\partial F_1}{\partial x} - \frac{\partial F_2}{\partial y})|^n \frac{\partial \phi_i}{\partial y} \quad (7.15)$$

$$+\text{boundary integrals} \quad (7.16)$$

Substitute the finite element solution $U^n = \sum_j U_j^n \phi_j$ at time t^n and the interpolations of the nonlinear terms S, F_1 and F_2 :

$$S^n = \sum_j S_j^n \phi_j, \quad F_1^n = \sum_j (F_1)_j^n \phi_j, \quad F_2^n = \sum_j (F_2)_j^n \phi_j \quad (7.17)$$

into (6.11)-(6.14), we have to solve the following nonlinear system at each time step:

$$M \Delta U^n = F^n \quad (7.18)$$

where M is the standard mass matrix, $\Delta U^n = U^{n+1} - U^n$.

7.3 Finite Difference Method

In this section, we consider the MacCormack scheme, which has been widely used in CFD [21, 55, 104]. This scheme consists of a two-step predictor-corrector sequence.

$$\text{Predictor:} \quad (7.19)$$

$$U_{i,j}^* = U_{i,j}^n - \frac{\Delta t}{\Delta x} \nabla_x (F_1)_{i,j}^n - \frac{\Delta t}{\Delta y} \nabla_y (F_2)_{i,j}^n - \Delta t S_{i,j}^n \quad (7.20)$$

$$\text{Corrector:} \quad (7.21)$$

$$U_{i,j}^{**} = U_{i,j}^n - \frac{\Delta t}{\Delta x} \Delta_x (F_1)_{i,j}^* - \frac{\Delta t}{\Delta y} \Delta_y (F_2)_{i,j}^* - \Delta t S_{i,j}^* \quad (7.22)$$

where U^* and U^{**} are intermediate values for U . The values for the vector U at time $n+1$ are obtained from

$$U_{i,j}^{n+1} = \frac{1}{2}(U_{i,j}^* + U_{i,j}^{**}) \quad (7.23)$$

Here the forward (Δ) and backward (∇) difference operators are defined as

$$\Delta_x U_{i,j} = U_{i+1,j} - U_{i,j} \quad (7.24)$$

$$\nabla_x U_{i,j} = U_{i,j} - U_{i-1,j} \quad (7.25)$$

where the subscript indicates the direction of differencing.

7.4 Application to the Breaking Dam Problem

An interesting test case is the breaking of a hypothetical square dam. The initial conditions consist of two regions of still water separated by a square wall of 20 meters wide. The water depth inside the dam is 10 m, whilst outside the dam it is 5 m, cf. Figure 7.1. At the instant of dam failure the square wall is assumed to be removed completely and the subsequent time evolution of the spreading waves is studied. The problem domain is assumed to be a square of 40 m wide. The computational domain was divided into 40×40 small elements.

7.4.1 Taylor-Galerkin Method

Here a Lapidus type artificial viscosity [79] has been implemented by addition of the term

$$-(C\Delta t\Delta x^2)\left|\frac{\partial h^n}{\partial x}\right|U_x - (C\Delta t\Delta y^2)\left|\frac{\partial h^n}{\partial y}\right|U_y \quad (7.26)$$

in the equation (7.1).

For simplicity, we used time step $\Delta t = 0.005$, which is small enough to ensure the CFL condition [21, 47, 55] holds true. Here we ran our problem for 20 and 50 time steps, respectively. The plot of water surface, contour plot of water surface and velocity field are provided in Figures 7.2-7.4. Unfortunately as we can see that the method did not work so well, also it took a large amount of CPU time for each time step, this since we have to solve the nonlinear system at each time step. Hence we

investigated the very popular explicit MacCormack finite difference scheme in the next section.

7.4.2 MacCormack Scheme

Here we used the antisymmetric reflection method [55, 104] in the solid wall. First we tried to use MacCormack scheme without artificial viscosity. We can see that there are wild oscillations around discontinuities, cf. Figure 7.5. To smooth the numerical oscillations near discontinuities, we implemented a smoothing procedure developed by Jameson *et al.* [39]. Artificial viscosity terms $DU = -D_x U - D_y U$ were added in the equation (7.1), where

$$D_x U = [\epsilon_{x_{i+1/2,j}}(U_{i+1,j} - U_{i,j}) - \epsilon_{x_{i-1/2,j}}(U_{i,j} - U_{i-1,j})], \quad (7.27)$$

in which

$$\nu_{x_{i,j}} = \frac{|h_{i+1,j} - 2h_{i,j} + h_{i-1,j}|}{|h_{i+1,j}| + |2h_{i,j}| + |h_{i-1,j}|} \quad (7.28)$$

$$\epsilon_{x_{i-1/2,j}} = C \frac{\Delta x}{\Delta t} \max(\nu_{x_{i-1,j}}, \nu_{x_{i,j}}). \quad (7.29)$$

With this artificial viscosity, we can see the solution was really smoothed, by comparing Figure 7.5 with Figure 7.11. Then we presented the solution at time steps 10, 20, 50, 75 and 100 in Figures 7.7-7.16, respectively, from which we saw the water moved out very clearly.

7.5 Conclusions

Our tests show that Taylor-Galerkin FEM has some difficulty simulating the discontinuous flow. Other FEM should be considered, for example, the Least-Square FEM [22], Discontinuous Galerkin FEM [28] and adaptive FEM [30, 94]. The explicit MacCormack scheme can solve the discontinuous flow very well. Also it is very

easy to implement. It would be very interesting to compare MacCormack scheme with Flux-Corrected Transport schemes [134, 36] and other high resolution schemes [50, 55, 119, 120].

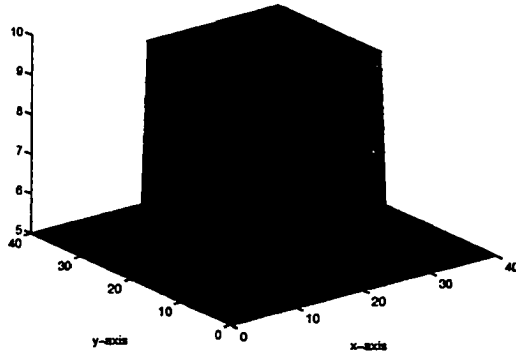


Figure 7.1: Initial water surface

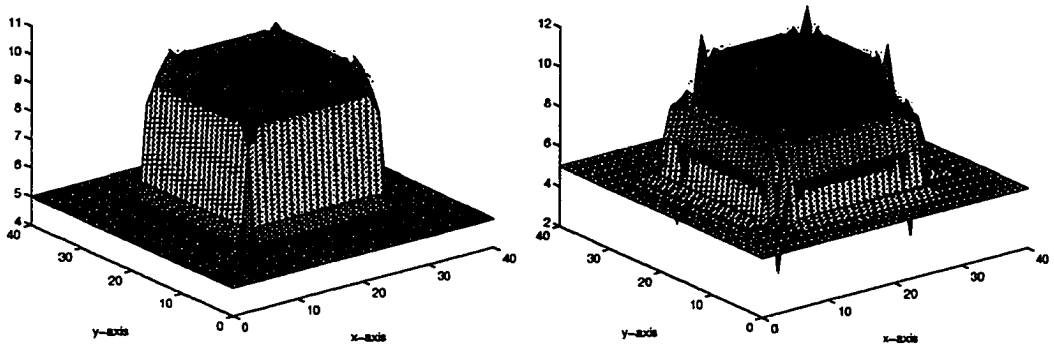


Figure 7.2: Water surface for FEM: (a) after 20 steps (b) after 50 steps

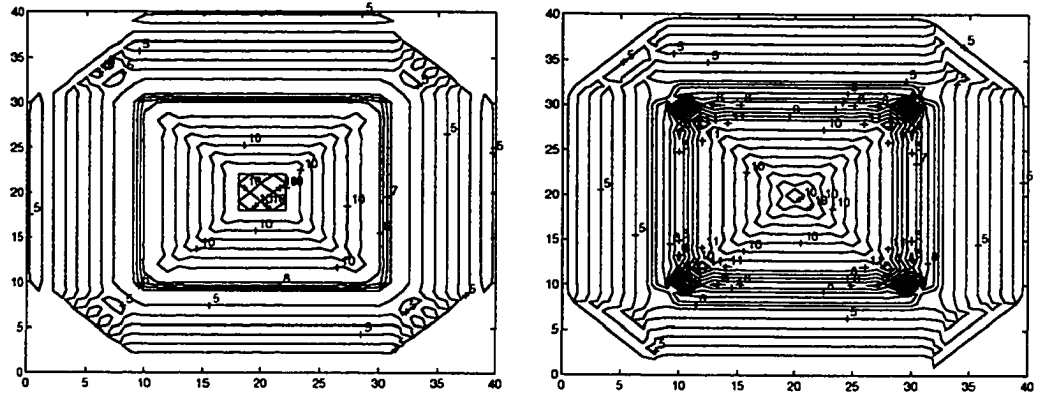


Figure 7.3: Contour plot of water surface for FEM: (a) after 20 steps (b) after 50 steps

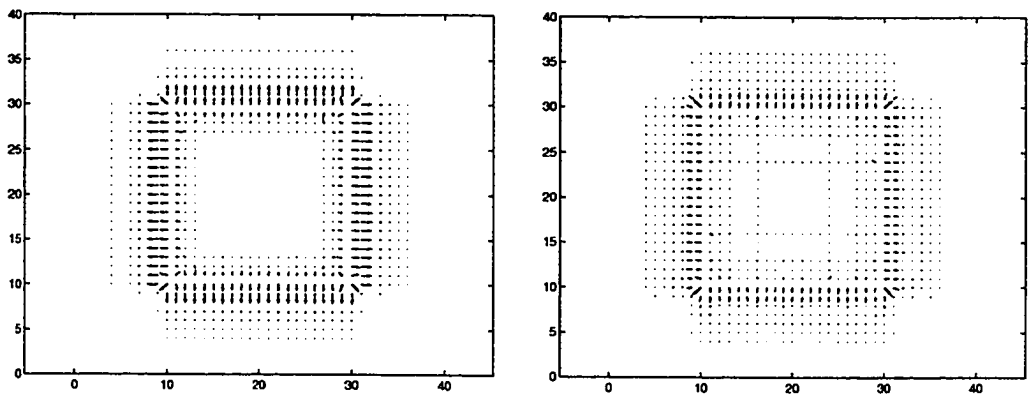


Figure 7.4: Velocity field for FEM: (a) after 20 steps (b) after 50 steps

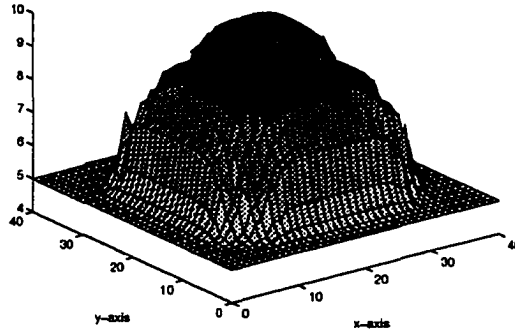


Figure 7.5: Water surface for FDM without artificial viscosity after 50 steps

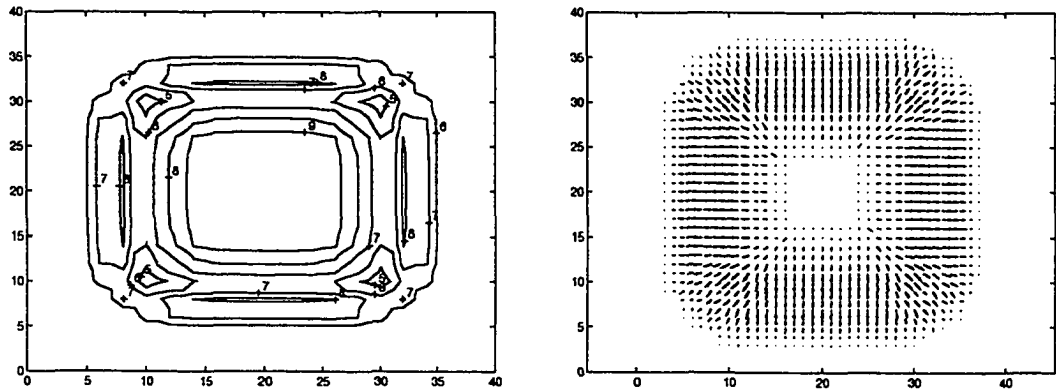


Figure 7.6: FDM without artificial viscosity after 50 steps: (a) Contour plot (b) Velocity field

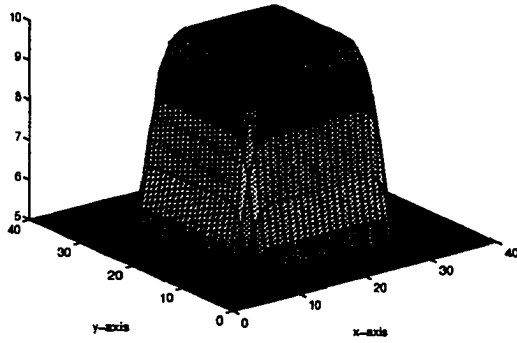


Figure 7.7: Water surface for FDM with artificial viscosity after 10 steps

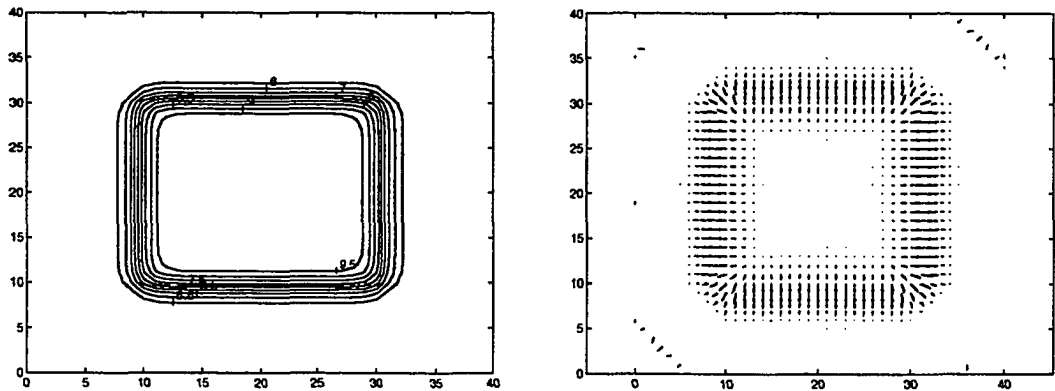


Figure 7.8: FDM with artificial viscosity after 10 steps: (a) Contour plot (b) Velocity field

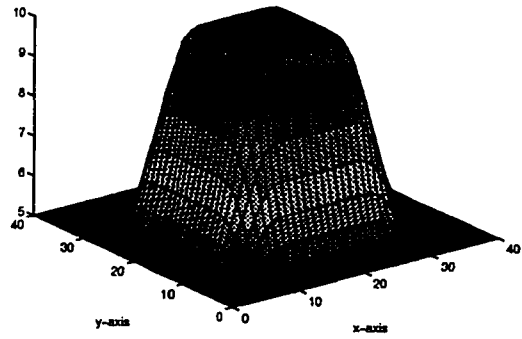


Figure 7.9: Water surface for FDM with artificial viscosity after 20 steps

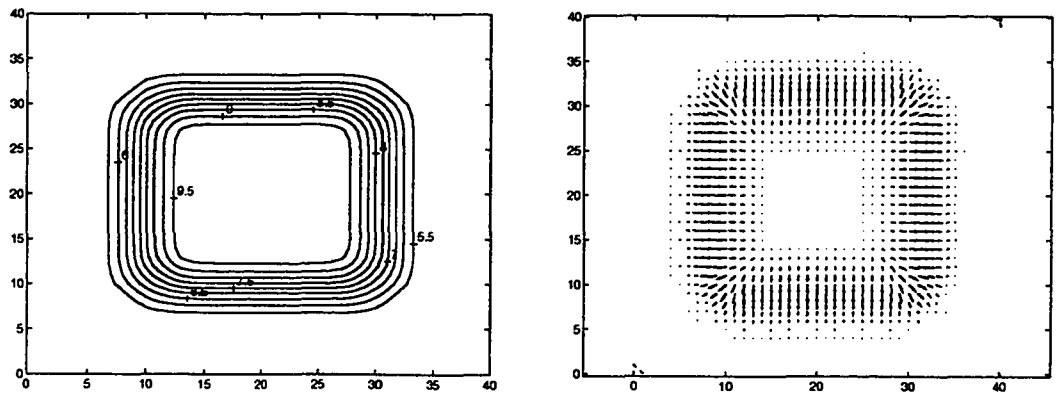


Figure 7.10: FDM with artificial viscosity after 20 steps: (a) Contour plot (b) Velocity field

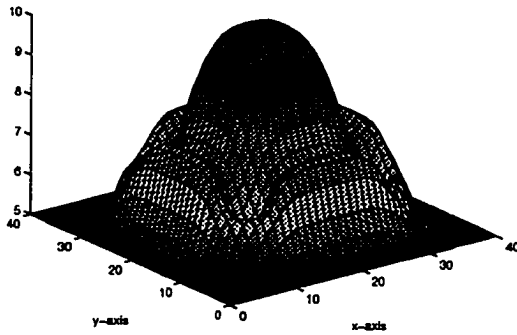


Figure 7.11: Water surface for FDM with artificial viscosity after 50 steps

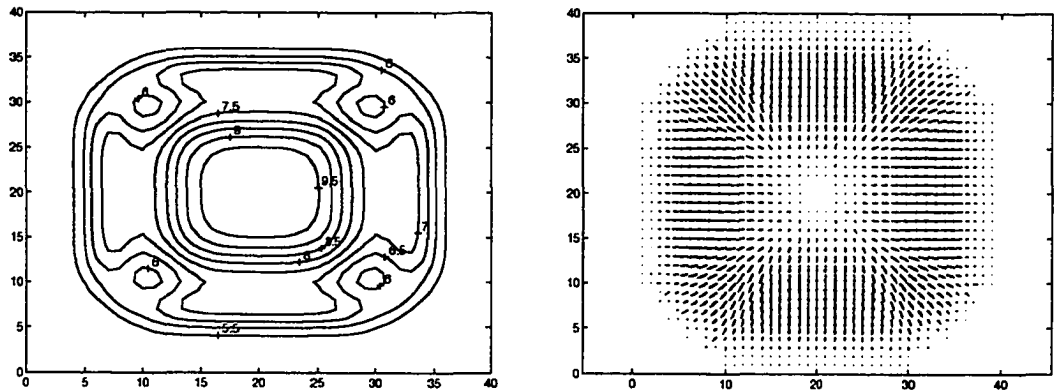


Figure 7.12: FDM with artificial viscosity after 50 steps: (a) Contour plot (b) Velocity field

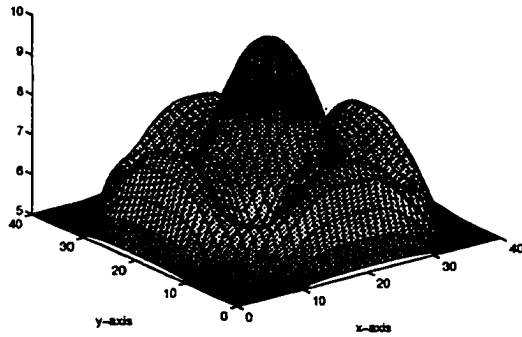


Figure 7.13: Water surface for FDM with artificial viscosity after 75 steps

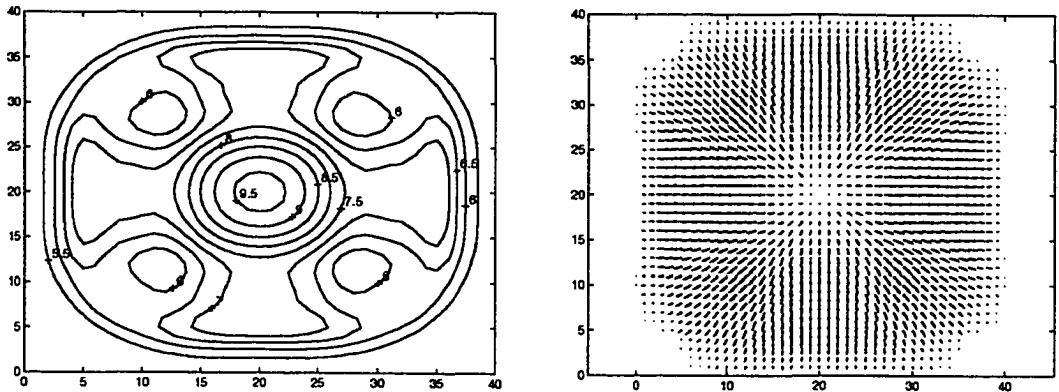


Figure 7.14: FDM with artificial viscosity after 75 steps: (a) Contour plot (b) Velocity field

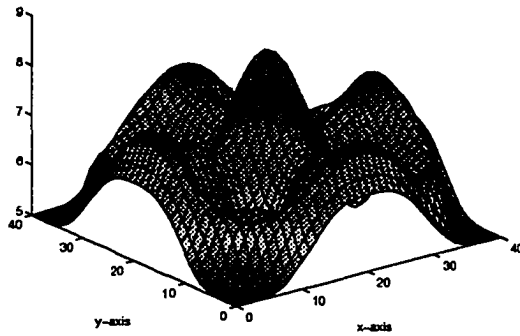


Figure 7.15: Water surface for FDM with artificial viscosity after 100 steps

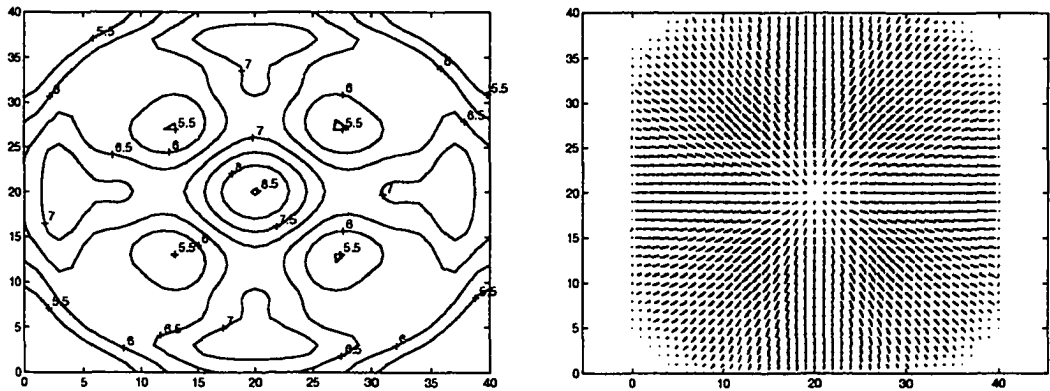


Figure 7.16: FDM with artificial viscosity after 100 steps: (a) Contour plot (b) Velocity field

CHAPTER 8

CONCLUSIONS AND FUTURE DIRECTIONS

In this thesis, we have developed a systematic finite element method to solve singularly perturbed elliptic problems. Our method is different from the traditional FEM in that our method is globally convergent independent of the perturbation parameter. Here four models were investigated. In Chapter 2, we considered the anisotropic model, where we constructed our bilinear FEM on a piecewise uniform mesh. The method was proved to be GUC in almost second order in L^2 norm. Chapter 3 was devoted to the reaction-diffusion model. Here a bilinear FEM was constructed on another type piecewise uniform mesh, and a global uniform convergence of almost second order in L^2 norm was proved. For the convection-diffusion model in Chapter 4 and the two-parameter model in Chapter 5, only first order global convergence in L^2 norm were proved for our bilinear FEM. But numerical results showed that our scheme is also almost second order in L^2 norm. Same phenomena were found in other papers [63, 123]. It is still an open question if the bilinear FEM based on such piecewise uniform mesh can be GUC in second order in L^2 norm [63, 123]. Also our numerical results showed that our scheme is GUC in L^∞ norm. But the theoretical proof is still unavailable at present. The only known result in this respect was obtained by Stynes *et al.* [123]. They obtained $O(N^{-1/2} \ln^{3/2} N)$ order pointwise error estimate near the boundary layer for the convection-diffusion model, where the total number of mesh points is $O(N^2)$. Further investigation needs to be carried in this area. In Chapter 6, we proved that the quasioptimal global uniform convergence rate of $O(N_x^{-(m+1)} \ln^{m+1} N_x + N_y^{-(m+1)} \ln^{m+1} N_y)$ in L^2 norm can be obtained for a reaction-diffusion model by using the m -th order ($m \geq 2$) tensor-product element

on some piecewise uniform meshes. More work should be carried out to see if such high-order FEM can be generalized to other SPP.

From our proofs in Chapters 2-6, we can expect that our method can be directly implemented to other general singularly perturbed problems, which have global asymptotic expansions and smooth enough solutions. Further investigation can be carried out related to these topics. Also similar methods can be considered for time dependent problems, and other more practical problems, such as those in fluid mechanics [60, 128], chemical kinetics [129, 84] and system control [77, 88, 13, 67, 65].

From Chapters 2-6, we see that our method depends strongly on the detailed analysis of the boundary layers or singularities. But such analysis would be difficult to carry out for many problems, in which case *a posteriori* adaptive FEM sounds very promising. However this approach is also more challenging. Though some effort has been done for SPP [126, 102, 121, 70, 130], "*even from the practical point of view the existing adaptive strategies so far are not completely satisfactory*" [105, pp.19], since "*the construction of robust estimators is still an open problem*" [105, pp.19]. Hence to solve SPP, it is better to start the computations with such a layer-adapted piecewise uniform mesh, and then to refine the mesh adaptively based on some robust error estimators [105]. Actually we have implemented such an idea in our two-parameter model. But a more general and systematic method needs to be developed.

Finally, we will try to develop a general multidomain [21] FEM for such SPP. Since every SPP can be naturally divided into two or more subdomains, i.e., boundary or interior layer subdomain and elsewhere. Similar ideas have been used in connection with the spectral method [43], but no work has been carried out in FEM.

Chapter 7 is our elementary exploration in the application of FEM for open-channel flow. The presented results obtained by FEM are not very promising. Further investigation needs to be carried out in this area.

REFERENCES

- [1] L.R. Abrahamsson, H.B. Keller and H.O. Kreiss, Difference Approximations for Singular Perturbations of Systems of Ordinary Differential Equations, *Numer. Math.* 22(1974) 367-391.
- [2] S. Adjerid, M. Aiffa and J.E. Flaherty, High-Order Finite Element Methods for Singularly Perturbed Elliptic and Parabolic Problems, *SIAM J. Appl. Math.* 55(1995) 520-543.
- [3] D. Adam, A. Felgenhauer, H-G. Roos and M. Stynes, A Nonconforming Finite Element Methods for a Singularly Perturbed Boundary Value Problem, *Computing* 54(1995) 1-25.
- [4] F. Alcrudo and P. Garcia-Navarro, A High-Resolution Godunov-Type Scheme in Finite Volumes for the 2D Shallow-Water Equations, *Intern. Journal Numer. Methods Fluids* 16(1993) 489-505.
- [5] K. Anastasiou and C.T. Chan, Solution of the 2D Shallow Water Equations Using the Finite Volume Method on Unstructured Triangular Meshes, *Intern. J. Numer. Methods Fluids* 24(1997) 1225-1245.
- [6] U.M. Ascher, R.M.M. Mattheij and R.D. Russell, *Numerical Solution of Boundary Value Problems for Ordinary Differential Equations* (Prentice Hall, Englewood, Cliff, 1988).
- [7] O. Axelsson and V.A. Barker, *Finite Element Solution of Boundary Value Problems - Theory and Computations* (Academic Press, London, 1984).
- [8] I. Babuska and M. Suri, On Locking and Robustness in the Finite Element Methods, *SIAM J. Numer. Anal.* 29(1992) 1261-1293.
- [9] R.E. Bank, *PLTMG: A Software Package for Solving Elliptic Partial Differential Equations, Users' Guide 7.0*, *Frontiers in Applied Mathematics*, No. 15 (SIAM, Philadelphia, 1994).
- [10] R.E. Bank and M. Benbourenane, The Hierarchical Basis Multigrid Method for Convection-Diffusion Equation, *Numer. Math.* 61(1992) 7-37.

- [11] R. Barrett, M. Berry, T.F. Chan, J. Demmel, J.M. Donato, J. Dongarra, V. Eijkhout, R. Pozo, C. Romine and H. Van der Vorst, *Templates for the Solution of Linear Systems: Building Blocks for Iterative Methods* (SIAM, Philadelphia, 1994).
- [12] E.B. Becker, G.F. Carey and J.T. Oden, *Finite Elements: An Introduction, Vol. I* (Prentice-Hall, Englewood Cliffs, N.J., 1981).
- [13] A. Bensoussan, *Perturbation Methods in Optimal Control* (Wiley, New York, 1989).
- [14] A.E. Berger, J.M. Solomon and M. Ciment, An Analysis of a Uniformly Accurate Difference Method for a Singular Perturbation Problem, *Math. Comp.* 37(1981) 79-94.
- [15] I.P. Boglayev, A Numerical Method for Solving Quasilinear Elliptic Equations with a Small Parameter for the Highest Derivatives, *Comput. Math. Math. Phys.* 28 (1988) 118-125.
- [16] S.C. Brenner and L.R. Scott, *The Mathematical Theory of Finite Element Methods, Texts in Applied Mathematics, Vol.15* (Springer-Verlag, New York, 1994).
- [17] F. Brezzi, L.P. Franca, T.J.R. Hughes and A. Russo, Stabilization techniques and subgrid scales capturing, in: *Proceeding of the Conference on the State of the Art in Numerical Analysis, York, England, April, 1996, IMA Conference Series* (Oxford University Press, to appear).
- [18] V.F. Butuzov, The Asymptotic Properties of Solutions of the Equation $\mu^2 \Delta u - k^2(x, y)u = f(x, y)$ in a Rectangle, *Differential Eqns* 9(1973) 1274-1279.
- [19] V.F. Butuzov, On Asymptotics of Solutions of Singularly Perturbed Equations of Elliptic Type in the Rectangle, *Differential Eqns* 11(1975) 780-787.
- [20] V.F. Butuzov, A Singularly Perturbed Elliptic Equation with Two Small Parameters, *Differential Eqns* 12(1976) 1261-1269.
- [21] C. Canuto, M.Y. Hussaini, A. Quarteroni and T.A. Zang, *Spectral Methods in Fluid Dynamics* (Springer-Verlag, New York, 1988).
- [22] G.F. Carey and B.N. Jiang, Least-Square Finite Elements for First-Order Hyperbolic Systems, *Intern. J. Numer. Methods Engrg.* 26(1988) 81-93.

- [23] G.F. Carey and J.T. Oden, *Finite Elements: Fluid Mechanics*, Vol. VI (Prentice-Hall, Englewood Cliffs, New Jersey, 1986).
- [24] K.W. Chang and F.A. Howes, *Nonlinear Singular Perturbation Phenomena: Theory and Application* (Springer-Verlag, New York, 1984).
- [25] M.H. Chaudhry, *Open-Channel Flow* (Prentice Hall, Englewood Cliffs, New Jersey, 1993).
- [26] I. Christie, D.F. Griffiths, A.R. Mitchell and O.C. Zienkiewicz, *Finite Element Methods for Second Order Differential Equations with Significant First Derivatives*, *Intern. J. Numer. Methods Engrg.* 10(1976) 1389-1936.
- [27] P.G. Ciarlet, *The Finite Element Method for Elliptic Problems* (North-Holland, Amsterdam, 1978).
- [28] B. Cockburn, S. Hou and C.-W. Shu, *The Runge-Kutta Local Projection Discontinuous Galerkin Finite Element Method for Conservation Laws IV: the Multidimensional Case*, *Math. Comp.* 54(1990) 545-581.
- [29] L. Demkowicz and J.T. Oden, *An Adaptive Characteristic Petrov-Galerkin Finite Element Method for Convection-Dominated Linear and Nonlinear Parabolic Problems in One Space Variable*, *J. Comp. Phys.* 67(1986) 188-213.
- [30] L. Demkowicz, J.T. Oden, W. Rachowicz and O. Hardy, *An h-p Taylor-Galerkin Finite Element Method for Compressible Euler Equations*, *Comput. Methods Appl. Mech. Engrg.* 88(1991) 363-396.
- [31] I.V. Denisov, *Quasilinear Singularly Perturbed Elliptic Equations in a Rectangle*, *Comput. Math. Math. Phys.* 35 (1995) 1341-1350.
- [32] J. Donea, *A Taylor-Galerkin Method for Convective Transport Problems*, *Intern. J. Numer. Methods Engrg.* 20(1984) 101-120.
- [33] R.P. Doolan, J.J.H. Miller and W.H.A. Schilders, *Uniform Numerical Methods for Problems with Initial and Boundary Layers* (Boole Press, Dublin, 1980).
- [34] W. Eckhaus, *Asymptotic Analysis of Singular Perturbations* (North-Holland, Amsterdam, 1979).
- [35] S.C. Eisenstat, H.C. Elman and M.H. Schultz, *Variational Iterative Methods for Nonsymmetric Systems of Linear Equations*, *SIAM J. Numer. Anal.* 20(1983) 345-357.

- [36] G. Erlebacher, Solution Adaptive Triangular Meshes with Application to the Simulation of Plasma Equilibrium, Ph.D thesis, School of Engineering and Applied Science, Columbia University, 1984.
- [37] G. Fairweather, Finite Element Galerkin Methods for Differential Equations (Marcel Dekker, New York, 1978)
- [38] P.A. Farrell, P.W. Hemker and G.I. Shishkin, Discrete Approximations for Singularly Perturbed Boundary Value Problems with Parabolic Layers, CWI Report 9502, 1995.
- [39] R.J. Fennema and M.H. Chaudhry, Explicit Methods for 2-D Transient Free-Surface Flows, Journal of Hydraulic Engineering 116(1990) 1013-1034.
- [40] J.E. Flaherty and W. Mathon, Collocation with Polynomial and Tension Splines for Singularly Perturbed Boundary Value Problems, SIAM J. Sci. Stat. Comp. 1(1980) 260-289.
- [41] L.P. Franca and C. Farhat, Bubble Functions Prompt Unusual Stabilized Finite Element Methods, Comput. Methods Appl. Mech. Engrg. 123(1995) 299-308.
- [42] D. Funaro, Some Remarks about the Collocation Method on a Modified Legendre Grid, Computers Math. Applic. 33(1997)95-103.
- [43] D. Funaro, Spectral Elements for Transport-Dominated Equations, Lecture Notes in Computational Science and Engineering Vol 1. (Springer-Verlag, Berlin, 1997).
- [44] Jr. E.C. Gartland, Graded-Mesh Difference Schemes for Singularly Perturbed Two-Point Boundary Value Problems, Math. Comp. 51(1988) 631-657.
- [45] M.D. Gunzberger, Finite Element Methods for Viscous Incompressible Flows (Academic Press, New York, 1989).
- [46] W. Guo and M. Stynes, Pointwise Error Estimates for a Streamline Diffusion Scheme on a Shishkin Mesh for a Convection-Diffusion Problem, IMA J. Numer. Anal. 17(1997) 29-59.
- [47] B. Gustafsson, H.O. Kreiss and J. Oliger, Time Dependent Problems and Difference Methods (John Wiley & Sons, New York, 1995).
- [48] W. Hackbusch, Multigrid Methods and Applications (Springer-Verlag, Berlin, 1985).

- [49] H. Han and R.B. Kellogg, Differentiability Properties of Solutions of the Equation $-\varepsilon^2 \Delta u + ru = f(x, y)$ in a Square, *SIAM J. Math. Anal.* 21(1990) 394-408.
- [50] A. Harten, B. Engquist, S. Osher and S.R. Chakravarthy, Uniformly High Order Accurate Essentially Non-Oscillatory Schemes, III, *J. Comp. Phys.* 71(1987) 231-303.
- [51] A.F. Hegarty, J.J.H. Miller, E.O'Riordan and G.I. Shishkin, Special Meshes for Finite Difference Approximations to an Advection-Diffusion Equation with Parabolic Layers, *J. Comp. Phys.* 117(1995) 47-54.
- [52] J.C. Heinrich and O.C. Zienkiewicz, Quadratic Finite Element Schemes for Two Dimensional Convective-Transport Problems, *Intern. J. Numer. Methods Engrg.* 11(1977) 1831-44.
- [53] P.W. Hemker, A Numerical Study of Stiff Two-Point Boundary Value Problems (Mathematical Center, Amsterdam, 1977).
- [54] P.W. Hemker and J.J.H. Miller, eds., Numerical and Asymptotical Methods for Singular Perturbation Problems (Academic Press, New York, 1979).
- [55] C. Hirsch, Numerical Computation of Internal and External Flows, Vol.2 (Wiley, Chichester, 1990).
- [56] X.C. Hu, T.A. Manteuffel, S. McCormick and T.F. Russell, Accurate Discretization for Singular Perturbations: the One-Dimensional Case, *SIAM J. Numer. Anal.* 32(1995) 83-109.
- [57] T.J.R. Hughes, Finite Element Methods for Convection-Dominated Flows, ASME Monograph AMD-34 (ASME, New York, 1979).
- [58] C. Johnson, U. Navert and Pitkaranta, Finite Element Methods for Linear Hyperbolic Problems, *Comput. Methods Appl. Mech. Engrg.* 45(1984)285-312.
- [59] C. Johnson, A.H. Schatz and L.B. Wahlbin, Crosswind Smear and Pointwise Errors in Streamline Diffusion Finite Element Methods, *Math. Comp.* 49(1987) 25-38.
- [60] S. Kaplun, Fluid Mechanics and Singular Perturbations, P.A. Lagerstrom, L.N. Howard and C.S. Liu (eds.) (Academic Press, New York, 1967).
- [61] N.D. Katopodes, A Dissipative Galerkin Scheme for Open-Channel Flow, *Journal of Hydraulic Engineering* 110(1984) 450-466.

- [62] R.B. Kellogg, Boundary Layers and Corner Singularities for a Self-Adjoint Problem, in: M. Costabel, ed., *Boundary Value Problems and Integral Equations in Nonsmooth Domains* (Marcel Dekker, 1995) 121-149.
- [63] R.B. Kellogg and M. Stynes, Optimal Approximability of Solutions of Singularly Perturbed Two-Point Boundary Value Problems, *SIAM J. Numer. Anal.* 34(1997) 1808-1816.
- [64] J. Kevorkian and J.D. Cole, *Multiple Scale and Singular Perturbation Methods*, Applied Mathematical Sciences, Vol.114 (Springer-Verlag, New York, 1996).
- [65] P. Kokotovic, H.K. Khalil and J. O'Reilly, *Singular Perturbation Methods in Control: Analysis and Design* (Academic Press, New York, 1986).
- [66] B. Kreiss and H.-O. Kreiss, Numerical Methods for Singular Perturbation Problems, *SIAM J. Numer. Anal.* 18(1981) 262-276.
- [67] H.J. Kushner, *Weak Convergence Methods and Singularly Perturbed Stochastic Control and Filtering Problems*, Systems & Control: Foundations & Applications, Vol.3 (Birkhauser, Boston, 1990).
- [68] P.A. Lagerstrom, *Matched Asymptotic Expansion: Ideas and Techniques*, Applied Mathematical Sciences, Vol.76 (Springer-Verlag, New York, 1988).
- [69] W. Layton and B. Polman, Oscillation Absorption Finite Element Methods for Convection-Diffusion Problems, *SIAM J. Sci. Comput.* 17(1996) 1328-1346.
- [70] J.-Y. Lee, *Adaptive Numerical Methods for Singular Perturbation Problems in One Space Dimension*, Ph.D dissertation, Courant Institute of Mathematical Sciences, 1994.
- [71] J. Li, Quasi-Optimal Uniformly Convergent Finite Element Methods for the Elliptic Boundary Layer Problem, *Computers Math. Applic.* (33)(1997) 11-22.
- [72] J. Li and I.M. Navon, Uniformly Convergent Finite Element Methods for Singularly Perturbed Elliptic Boundary Value Problems I: Reaction-Diffusion Type, *Computers Math. Applic.* (35)(1998) 57-70.
- [73] J. Li and I.M. Navon, Uniformly Convergent Finite Element Methods for Singularly Perturbed Elliptic Boundary Value Problems II: Convection-Diffusion Type, *Comput. Methods Appl. Mech. Engrg.* (to appear).

- [74] J. Li and I.M. Navon, A global uniformly convergent finite element method for a quasilinear singularly perturbed elliptic problem, *SIAM J. Numer. Anal.* (submitted)
- [75] J. Li and I.M. Navon, Global Uniformly Convergent Finite Element Methods for Singularly Perturbed Elliptic Boundary Value Problems: Higher-order Elements, *Comput. Methods Appl. Mech. Engrg.* (submitted).
- [76] C.C. Lin and L.A. Segel, *Mathematics Applied to Deterministic Problems in the Natural Sciences, Classics in Applied Mathematics, Vol.1* (SIAM, Philadelphia, 1988).
- [77] J.L. Lions, *Perturbations Singulieres dans les Problemes aux Limites et en Controle Optimal, Lecture Notes in Mathematics, No. 323* (Springer-Verlag, Berlin, 1973).
- [78] R. Lohner, K. Morgan and O.C. Zienkiewicz, The Solution of Non-linear Hyperbolic Equation Systems by the Finite Element Method, *Intern. J. Numer. Methods Fluids* 4(1984) 1043-1063.
- [79] R. Lohner, K. Morgan and T. Peraire, A Simple Extension of Multidimensional Problems of the Artificial Viscosity due to Lapidus, *Comput. Appl. Numer. Methods* 2(1985) 141-147.
- [80] N. Madden and M. Stynes, Efficient Generation of Oriented Meshes for Solving Convection-Diffusion Problem, *Intern. J. Numer. Methods Engrg.* 40(1997)565-576.
- [81] R. O'Malley, *Singular Perturbations Methods for Ordinary Differential Equations, Applied Mathematical Sciences, Vol.89* (Springer-Verlag, New York, 1991).
- [82] J.J.H. Miller(ed.), *Computational Methods for Boundary and Interior Layers in Several Dimensions* (Boole Press, Dublin, 1991).
- [83] J.J.H. Miller(ed.), *Applications of Advanced Computational Methods for Boundary and Interior Layers* (Boole Press, Dublin, 1993).
- [84] J.J.H. Miller(ed.), *Singular Perturbation Problems in Chemical Physics: Analytic and Computational Methods* (Wiley, New York, 1997).
- [85] J.J.H. Miller, E. O'Riordan and G.I. Shishkin, *Fitted Numerical Methods for Singular Perturbation Problems* (World Scientific, Singapore, 1995).

- [86] K.W. Morton, Numerical Solution of Convection-Diffusion Problems, Applied Mathematics and Mathematical Computation, Vol.12 (Chapman and Hall, 1996).
- [87] J.D. Murray, Asymptotic Analysis, Applied Mathematics Sciences, Vol.48 (Springer-Verlag, New York, 1984).
- [88] D.S. Naidu and A.K. Rao, Singular Perturbation Analysis of Discrete Control Systems, Lecture Notes in Mathematics, Vol.1154 (Springer-Verlag, New York, 1985).
- [89] I.M. Navon, Finite-Element Simulation of the Shallow-Water Equations Model on a Limited Area Domain, Appl. Math. Modelling 3(1979)337-348.
- [90] I.M. Navon, A Numerov-Galerkin Techniques Applied to a Finite-Element Shallow-Water Equations Model with Enforced Conservation of Integral Invariants and Selective Lumping, J. Comp. Phys. 52(1983)313-339.
- [91] I.M. Navon, FEUDX: a Two-Stage, High-Accuracy, Finite-Element FORTRAN Program for Solving Shallow-Water Equations, Computers and Geoscience. 13(1987) 255-285.
- [92] B. Neta, Analysis of Finite-Elements and Finite Differences for Shallow Water Equations: a Review, Math. Comput. Simul. 34(1992) 141-161.
- [93] K. Niijima, Pointwise Error Estimates for a Streamline Diffusion Finite Element Schemes, Numer. Math. 56(1990) 707-719.
- [94] J.T. Oden, T. Strouboulis and P. Devloo, Adaptive Finite Element Methods for High-Speed Compressible Flows, Intern. J. Numer. Methods Fluids 7(1987) 1211-1228.
- [95] J.T. Oden, Optimal h-p finite element methods, Comput. Methods Appl. Mech. Engrg. 112 (1994) 309-331.
- [96] O. Oleinik, Some Asymptotic Problems in the Theory of Partial Differential Equations (Cambridge University Press, Cambridge, 1996).
- [97] S. Osher, Nonlinear Singular Perturbation Problems and One Sided Difference Schemes, SIAM J. Numer. Anal. 18(1981) 129-144.
- [98] F. Pasquarelli and A. Quarteroni, Effective Spectral Approximations of Convection-Diffusion Equation, Comput. Methods Appl. Mech. Engrg. 116(1994) 39-51.

- [99] J. Pedlosky, *Geophysical Fluid Dynamics* (Springer-Verlag, New York, 1987).
- [100] O. Pironneau, *Finite Element Methods for Fluids* (John Wiley & Sons, Chichester, 1989).
- [101] Y. Qiu, D.M. Sloan and T. Tang, *Convergence Analysis for an Adaptive Finite Difference Solution of a Variable Coefficient Singular Perturbation Problem*, Strathclyde Mathematics Research Report 42, Univ. of Strathclyde, 1996.
- [102] H.-J. Reinhardt, *A Posteriori Error Estimates for the Finite Element Solution of a Singularly Perturbed Linear Ordinary Differential Equation*, *SIAM J. Numer. Anal.* 18(1981) 406-430.
- [103] E. O'Riordan and M. Stynes, *A Globally Convergent Finite Element Method for a Singularly Perturbed Elliptic Problem in Two Dimensions*, *Math. Comp.* 57(1991) 47-62.
- [104] P.J. Roache, *Computational Fluid Dynamics* (Hermosa Press, Albuquerque, 1972).
- [105] H.-G. Roos, *Layer-Adapted Grids for Singular Perturbation Problems*, *Z. Angew. Math. Mech.* (to appear).
- [106] H.-G. Roos, *Ten Ways to Generate the Π 'in and Related Schemes*, *J. Comput. Appl. Math.* 53(1994) 43-59.
- [107] H.-G. Roos, *A Note on the Conditioning of Upwind Schemes on Shishkin Meshes*, *IMA J. Numer. Anal.* 16(1996) 529-538.
- [108] H.-G. Roos, D. Adam and A. Felgenhauer, *A Novel Nonconforming Uniformly Convergent Finite Element Method in Two Dimensions*, *J. Math. Anal. Appl.* 201(1996) 715-755.
- [109] H.G. Roos and M. Stynes, *Necessary Conditions for Uniform Convergence of Finite Difference Schemes for Convection-Diffusion Problems with Exponential and Parabolic Layers*, *Appl. Math.* 41(1996) 269-280.
- [110] H.-G. Roos, M. Stynes and L. Tobiska, *Numerical Methods for Singularly Perturbed Differential Equations*, Springer Series in Computational Mathematics, Vol.24 (Springer-Verlag, Berlin, 1996).
- [111] Y. Saad, *Sparskit: a basic tool kit for sparse matrix computations*, Version 2, June 4, 1996.

- [112] A.H. Schatz and L.B. Wahlbin, On the Finite Element Method for Singularly Perturbed Reaction-Diffusion Problems in Two and One Dimensions, *Math. Comp.* 40 (1983) 47-89.
- [113] M.H. Schultz, *Spline Analysis* (Prentice-Hall, Englewood Cliffs, New Jersey, 1973).
- [114] C. Schwab and M. Suri, The p and hp Versions of the Finite Element Method for Problems with Boundary Layers, *Math. Comp.* 65(1996) 1403-1429.
- [115] C. Schwab, M. Suri and C. Xenophontos, The hp Finite Element Method for Problems in Mechanics with Boundary Layers, *Comput. Methods Appl. Engrg.* (to appear).
- [116] S. Shih and R.B. Kellogg, Asymptotic Analysis of a Singular Perturbation Problem, *SIAM J. Math. Anal.* 18(1987) 1467-1511.
- [117] G.I. Shishkin, Grid Approximation of Singularly Perturbed Parabolic Equations with Internal Layers, *Sov. J. Numer. Anal. Math. Modelling* 3(1988) 393-407.
- [118] G.I. Shishkin, Discrete Approximation of Singularly Perturbed Elliptic and Parabolic Equations, Russian Academy of Sciences, Ural Section, Ekaterinburg, 1992 (in Russian).
- [119] C.-W. Shu and S. Osher, Efficient Implementation of Essentially Non-Oscillatory Shock-Capturing Schemes, *J. Comp. Phys.* 77(1988) 439-471.
- [120] C.-W. Shu and S. Osher, Efficient Implementation of Essentially Non-Oscillatory Shock-Capturing Schemes, II, *J. Comp. Phys.* 83(1989) 32-78.
- [121] T. Skalicky, H.-G. Roos, Anisotropic mesh refinement for problems with internal and boundary layers, Preprint, MATH-NM-09-1997, Technische Universität Dresden, July, 1997.
- [122] M. Stynes and E. O'Riordan, A Finite Element Method for a Singularly Perturbed Boundary Value Problem, *Numer. Math.* 50(1986) 1-15.
- [123] M. Stynes and E. O'Riordan, A Uniformly Convergent Galerkin Method on a Shishkin Mesh for a Convection-Diffusion Problem, *J. Math. Anal. Appl.* 214(1997) 36-54.
- [124] Y. Su, *Boundary Layer Correction Method for Singularly Perturbed Problems* (Shanghai Science and Technology Press, Shanghai, 1983).

- [125] G. Sun and M. Stynes, Finite Element Methods for Singularly Perturbed High-Order Elliptic Two-Point Boundary Value Problems. I: Reaction-Diffusion-Type Problems, *IMA J. Numer. Anal.* 15(1995) 117-139.
- [126] W.G. Szymczak and I. Babuska, Adaptivity and Error Estimation for the Finite Element Method Applied to Convection Diffusion Problems, *SIAM J. Numer. Anal.* 21(1984) 910-953.
- [127] T. Tang and M.R. Trummer, Boundary Layer Resolving Pseudospectral Methods for Singular Perturbation Problems, *SIAM J. Sci. Comput.* 17(1996) 430-438.
- [128] M. Van Dyke, *Perturbation Methods in Fluid Mechanics* (Academic Press, New York, 1964).
- [129] A.B. Vasil'eva, V.F. Butuzov and L.V. Kalachev, *The Boundary Function Method for Singular Perturbation Problems*, *SIAM Studies in Applied Mathematics*, Vol.14 (SIAM, Philadelphia, 1995).
- [130] R. Verfurth, Robust a Posteriori Error Estimators for a Singularly Perturbed Reaction-Diffusion Equation, *Numer. Math.* 78(1998) 479-493.
- [131] M. Vishik and L. Lyusternik, Regular Degeneration and Boundary Layer for Linear Differential Equations with Small Parameter Multiplying the Highest Derivatives, *Amer. Math. Soc. Transl.* 20(1962) 239-364.
- [132] C.B. Vreugdenhil, *Numerical Methods for Shallow-Water Flow* (Kluwer Academic Publishers, Dordrecht, Boston, 1994).
- [133] L.B. Wahlbin, Local behavior in the finite element method, in: P.G. Ciarlet and J.L. Lions, eds., *Handbook of Numerical Analysis, Vol.II, Finite Element Methods(part 1)* (North-Holland, Amsterdam, 1991) 355-522.
- [134] S.T. Zalesak, Fully Multidimensional Flux-Corrected Transport Algorithms for Fluids, *J. Comp. Phys.* 31(1979) 335-362.
- [135] O.C. Zienkiewicz and R.L. Taylor, *The Finite Element Method, Vol.2* (McGraw-Hill Publ., New York, 1991).
- [136] G. Zhou and R. Rannacher, Pointwise Superconvergence of the Streamline Diffusion Finite Element Method, *Numer. Methods for PDEs* 12(1996) 123-145.

BIOGRAPHICAL SKETCH

Jichun Li

Education

Ph.D in Applied Mathematics, Florida State University, 1998

M.S. in Computational Mathematics, Nanjing University, Nanjing, China, 1990

B.S. in Computational Mathematics, Nanjing University, Nanjing, China, 1987

Research Experience

- 5/96–present: Visitor.
Supercomputer Computations Research Institute, Florida State University
- 9/94–2/98: Teaching assistant.
Department of Mathematics, Florida State University
- 7/19/94–7/21/94: Trainee for Cray T3D System and Emulator.
Mississippi Center for Supercomputing Research, University of Mississippi
- 8/90–8/93: Research Associate.
Institute of Systems Sciences, Chinese Academy of Sciences, Beijing, China

Other Publications

- A. Zhou and J. Li, "The Full Approximation Accuracy for the Stream Function-Vorticity-Pressure Method", *Numerische Mathematik*, Vol.68(1994), 427-435. (Math. Reviews 95k:76094).

- Q. Wu and J. Li, "Numerical Solutions for Singularly Perturbed Semi-Linear Parabolic Equations", Applied Mathematics and Mechanics(English Ed.), Vol.14, No.9(1993), 793-801. (Math. Reviews 94j:65111).
- J. Li, "A Class of Difference Schemes for the Turning Point Problem Without Resonance", Numerical Mathematics J. Chinese Univ., Vol.14, No.2(1992), 120-129. (in Chinese) (Math. Reviews 93j:65105).
- A. Zhou, J. Li and N. Yan, "On The Full Approximation Accuracy in Finite Element Methods", in: Proc. of the Symposium on Applied Mathematics for Young Chinese Scholars(F. Wu, ed.), Held at the Institute of Applied Mathematics, Academia Sinica, Beijing, 544-553 (July, 1992).
- Q. Wu and J. Li, "Numerical Methods for Parabolic Equation with a small Parameter in Time Variable", Applied Mathematics and Mechanics(English Ed.), Vol.12, No.8(1991), 733-740. (Math. Reviews 92g:65095).
- Q. Lin, J. Li and A. Zhou, "A Rectangle Test for Ciarlet-Raviart and Hermann-Miyoshi Scheme", in: Proc. Sys. Sci. & Sys. Engrg., Great Wall Culture Publ. Co., Hong Kong, 230-233 (1991) (Fully quoted in three books on Superconvergence Theory, and referred by many papers)
- X. Wu and J. Li, "On Attainable Highest Order and Stiffly Stability of Second Derivative Methods for Numerical Solution of ODE", Communication on Applied Mathematics and Computation, Vol.4, No.1(1990), 35-44. (in Chinese)

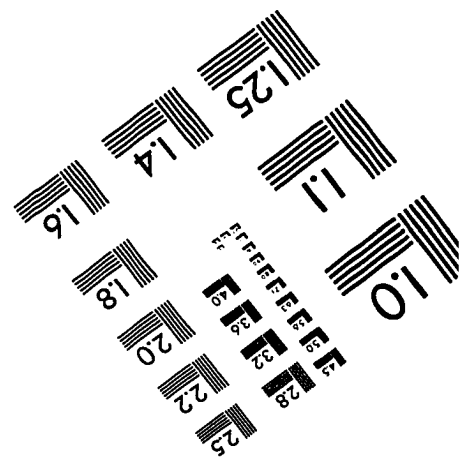
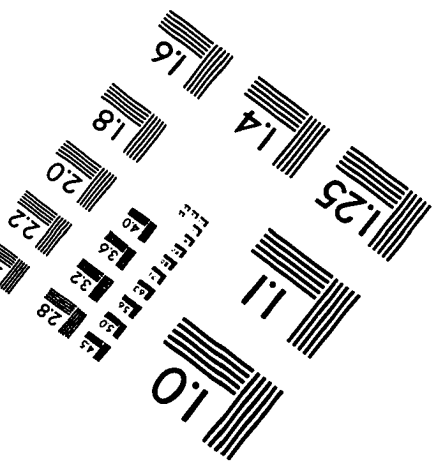
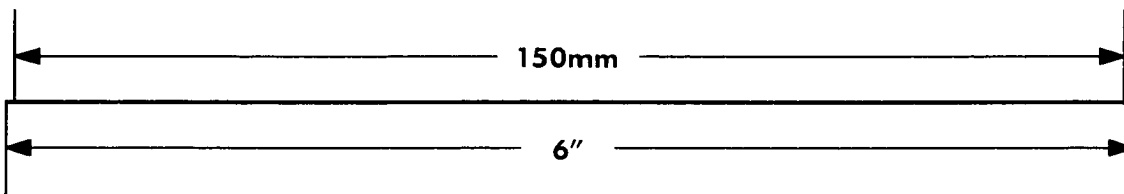
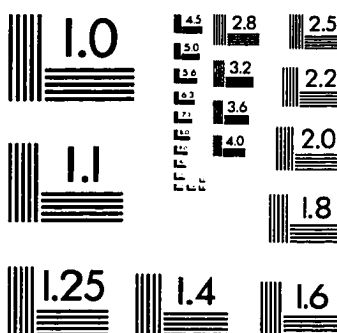
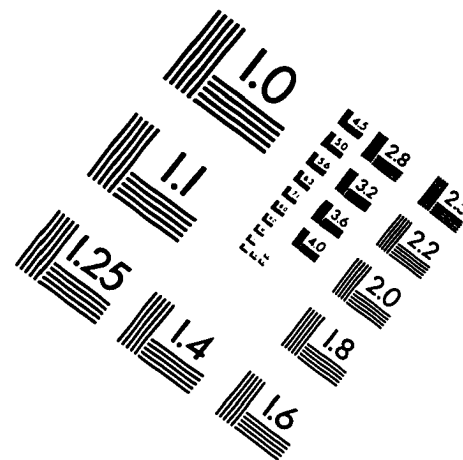
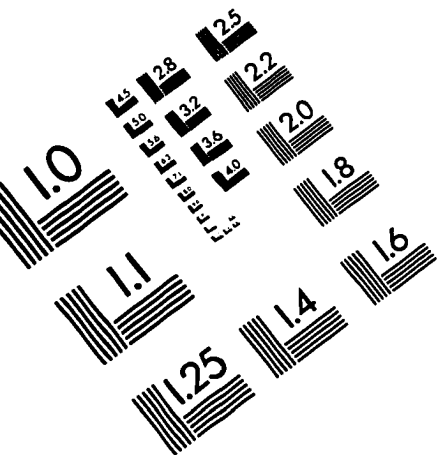
Professional Affiliations

- American Mathematical Society (AMS)
- Society for Industrial and Applied Mathematics (SIAM)

Honors

- Winner of Guanghai prize from Nanjing University in October 1990.
- Invited speaker (1 out of 20) for meeting on "Numerical Methods for Singular Perturbations" (Oberwolfach, Germany, 4/12/98-4/18/98, with full local support by Mathematisches Forschungsinstitut Oberwolfach).
- Reviewer for *Mathematical Reviews*.
- Top winner of Fellowship for "First Summer School on Numerical Analysis" (Concepcion, Chile between 1/19/98-1/30/98, with full local support plus \$500 ticket refund by Universidad de Concepcion, Chile).

IMAGE EVALUATION TEST TARGET (QA-3)



APPLIED IMAGE, Inc
1653 East Main Street
Rochester, NY 14609 USA
Phone: 716/482-0300
Fax: 716/288-5989

© 1993, Applied Image, Inc., All Rights Reserved